

BRAIN NETWORK DYNAMICS OF AUDITORY CHANGE DETECTION AND  
WORKING MEMORY IN RECREATIONAL CANNABIS USERS

by

SAMUEL P. RUMAK

BA, University of Winnipeg, 2008  
MA, The University of British Columbia, 2011

A THESIS SUBMITTED IN PARTIAL FULFILLMENT OF THE  
REQUIREMENTS FOR THE DEGREE OF

DOCTOR OF PHILOSOPHY

in

THE FACULTY OF GRADUATE AND POSTDOCTORAL STUDIES

(Psychology)

THE UNIVERSITY OF BRITISH COLUMBIA

(Vancouver)

November, 2018

© Samuel P. Rumak, 2018

The following individuals certify that they have read, and recommend to the Faculty of Graduate and Postdoctoral Studies for acceptance, the dissertation entitled:

Brain network dynamics of auditory change detection and working memory in

recreational cannabis users

Submitted by Samuel Rumak in partial fulfillment of the requirements for

the degree of Doctor of Philosophy

In Psychology

**Examining Committee:**

Lawrence Ward, Psychology

Supervisor

Wolfgang Linden, Psychology

Supervisory Committee Member

Rebecca Todd, Psychology

Supervisory Committee Member

Stan Floresco, Psychology

University Examiner

Todd Woodward, Psychiatry

University Examiner

## **Abstract**

There are concerns that cannabis use leads to increased risk of mental illness and neurocognitive impairment. However, empirical findings into the deleterious effects of cannabis use on cognition have been mixed and the underlying brain processes are poorly understood. The present research examined auditory cognitive processes putatively related to psychosis and cannabis use. Groups of cannabis users (CU) and non-users (NU) are compared on two novel tasks that examine electroencephalographic (EEG) measures of early somewhat pre-attentional (MMN) and later attentional (P300) auditory change detection and P300 response in auditory working memory. Additionally, sophisticated EEG source localization was used to interrogate underlying oscillatory activity and brain network connectivity. Chapter 2 introduced the novel roving dual oddball task, and revealed an asymmetry between easy and difficult task conditions, possibly due to increased attentional demands as evidenced by an interplay between dorsal and ventral attentional systems. Chapter 3 compared CU and NU on the same dual oddball task and revealed slower response times and increased P300 latency for CU on the more difficult condition. Theta-band network connectivity suggested that CU engaged in a stimulus driven strategy that became less effective in the more difficult condition due to a breakdown of fronto-temporal connectivity. Groups did not differ in early auditory processes (MMN). Chapter 4 unexpectedly revealed CU to have superior performance on working memory for basic auditory features (pitch and pattern), which was partially reflected in larger P300 amplitudes. Theta connectivity revealed different patterns of brain connectivity. Chapter 5 combined data from Chapters 3 and 4 to examine a local MMN effect across a larger sample along with measures putatively related to

impairments associated with heavy cannabis use and psychosis. Again, CU did not show reduced MMN and showed only small differences on various measures. As a whole, this research suggests that proposed auditory impairments due to heavy cannabis use may not generalize to all subsets of cannabis users, and additional research is needed before any definitive conclusions can be reached regarding the impact of frequent cannabis use on cognitive processes.

## **Lay Summary**

This research looks at the effects of frequent cannabis use on brain functions that relate both to automatic and to deliberate detection of changes to regularly occurring sounds, and to brain functions related to the ability to memorize basic features of those sounds (pitch and pattern). These brain functions are believed to be impaired in individuals with psychosis and may also be impacted by heavy cannabis use. We found that cannabis users have more difficulty detecting sounds under conditions that require greater conscious attention, but found no evidence for the impairments in the automatic processes that are often seen in people with psychosis. We unexpectedly found that cannabis users were better at keeping sounds in memory under difficult task conditions. Overall, this research suggests that frequent cannabis use may not impact all people in a uniform manner, and that much more research is needed to better understand how cannabis use impacts the brain.

## Preface

This dissertation will sometimes refer to a collective “we” in recognition that while I carried out the bulk of the work that went into this project, this project could not possibly be completed without the collective support of my supervisor, my graduate student colleagues, and the lab staff, all whom constitute my research group. That being said, it is understood that the purpose of a dissertation is to demonstrate my mastery over my chosen research area. As such, I am primarily responsible for the experimental design, task programming, data collection, data processing, data analysis and interpretation. Furthermore, I oversaw the recruitment of participants and designed and supervised the screening protocol that was carried out by our undergraduate research staff. It should be acknowledged that the experimental task discussed in chapters 2 and 3 was a modification and extension of work done by Elizabeth Blundon in our lab and some of the research findings discussed in chapter 2 contributed in part to a paper published by our research group (Blundon, Rumak & Ward, 2017). Also, the network analysis and subsequent pictorial representations relied heavily on modified processing scripts developed by Nicolas Bedo for his research in our lab – again, a team effort. In terms of this manuscript, I was primarily responsible for the organization, writing and literature review with recommendations and edits from my supervisor, Dr. Lawrence M. Ward, and further input from my committee members, Dr. Rebecca Todd and Dr. Wolfgang Linden. All data contributing to this dissertation was collected with the approval of the UBC Behavioural Research Ethics Board (certificate #: H15-00952). Finally, it should be emphasized that this research constitutes but a small (and narrow) part of a large (and growing) body of research regarding the effects of cannabis use on cognitive function,

and the findings ought to be interpreted in the broader context of the scientific literature. That being said, the findings presented here are not intended to inform any individual as to whether they should, or should not, consume cannabis, as it would not be reasonable to come to such a conclusion based upon such a limited amount of evidence.

## Table of Contents

<b>Abstract</b> .....	<b>iii</b>
<b>Lay Summary</b> .....	<b>v</b>
<b>Preface</b> .....	<b>vi</b>
<b>Table of Contents</b> .....	<b>viii</b>
<b>List of Tables</b> .....	<b>xii</b>
<b>List of Figures</b> .....	<b>xiv</b>
<b>Acknowledgements</b> .....	<b>xvi</b>
<b>CHAPTER 1: Cannabis Use, Auditory Cognition, and the Brain</b> .....	<b>1</b>
<b>Overview of Auditory Cognitive Processes in Context of Cannabis Use</b> .....	<b>2</b>
The Mismatch Negativity (MMN) and its Neural Underpinnings .....	2
The MMN, Psychopathology, and Cannabis Use .....	7
The P300 as an Index of Attention in Auditory Oddball Tasks .....	9
The P300 and Auditory Attention in Cannabis Users .....	11
Auditory Working Memory .....	13
Working Memory, The N-back Task, and the P300.....	14
Brain Regions and Working Memory .....	14
Oscillatory Activity, Brain Network Dynamics and Working Memory.....	15
Working Memory, Executive Function, and Cannabis Use .....	17
<b>General Overview of Methodology</b> .....	<b>19</b>
Recruitment of Cannabis Users and Non-Users .....	20
Overview of Electrophysiological Methods.....	25
<b>Overall Goals, Outline, and Predictions</b> .....	<b>38</b>
<b>CHAPTER 2: A Novel Roving Auditory Local-Global MMN/P300 Task</b> .....	<b>42</b>
<b>Introduction</b> .....	<b>42</b>
<b>Method</b> .....	<b>45</b>
Participants .....	45
Experimental Procedures.....	46
Behavioural Analysis .....	48
EEG Acquisition .....	49
Offline Processing.....	49
Channel Level ERP Analysis.....	50
Local MMN ERP Measurement .....	51
Measurement of Feature Present and Feature Absent MMNs.....	52
P300 ERP measurement .....	52
Dipole Fitting (Source Localization) and ROI Selection via Cluster Analysis.....	53
Event-Related Potentials (ERPs) for Independent Component Clusters .....	56
Event related spectral perturbation .....	56
Phase synchrony.....	58
<b>Results</b> .....	<b>62</b>
Accuracy and Reaction Time.....	62
Channel Level ERP Analysis.....	62
ROI Cluster Analysis.....	67
ROI Cluster ERPs .....	68

ERSP Results .....	72
Phase Synchrony Results.....	78
<b>Discussion.....</b>	<b>87</b>
Behavioural Asymmetry.....	87
MMN Asymmetry: Local vs Global .....	88
P300.....	91
ROIs .....	93
ROI ERPs and ERSPs .....	96
Functional Connectivity .....	100
Limitations.....	102
<b>Conclusion.....</b>	<b>104</b>
<b>CHAPTER 3: Roving Local(MMN)-Global(P300) Dual Oddball Task in Cannabis Users and Non-Users .....</b>	<b>106</b>
<b>Introduction .....</b>	<b>106</b>
MMN in Cannabis Users .....	106
MMN Hypotheses .....	107
P300 in Cannabis Users.....	107
P300 Hypotheses.....	110
<b>Method .....</b>	<b>111</b>
Participants .....	111
Experimental Procedures.....	113
Neuropsychological Testing .....	114
Self- Report Measures.....	115
EEG Acquisition .....	117
Offline Processing.....	117
Event-Related Potentials (ERPs) .....	118
Dipole Fitting (Source Localization) and ROI Selection via Cluster Analysis .....	119
Event-Related Spectral Perturbations (ERSPs) .....	120
Phase synchrony.....	120
<b>Results .....</b>	<b>122</b>
Cannabis and Other Recreational Drug Use.....	122
Self-Report Results .....	124
Neuropsychological Results .....	126
Accuracy and Reaction Time.....	127
ERP Results .....	128
ROI Cluster Analysis Results .....	134
ROI ERPs .....	137
ERSP Results .....	142
Phase Synchrony .....	148
<b>Discussion.....</b>	<b>154</b>
Demographics, Self-Report and Neuropsychological Measures .....	154
Behavioural Measures .....	155
Channel ERPs .....	157
ROIs .....	161
ROI ERPs in Users and Non-Users.....	162
ROI Oscillatory Activity in Users and Non-Users.....	165

Theta Band Functional Connectivity in Cannabis Users and Non-Users .....	169
Limitations.....	171
<b>Conclusion.....</b>	<b>174</b>
<b>CHAPTER 4: Auditory N-back: Users vs. Non-Users .....</b>	<b>175</b>
<b>Introduction .....</b>	<b>175</b>
<b>Method .....</b>	<b>180</b>
Participants .....	180
Auditory N-back Task .....	181
EEG Acquisition .....	186
Offline Processing.....	186
Event-Related Potentials (ERPs) .....	186
Dipole Fitting (Source Localization) and ROI Selection via Cluster Analysis .....	187
ROI ERPs .....	188
Event-Related Spectral Perturbations (ERSPs) .....	189
Phase Synchrony (PLVs).....	189
<b>Results .....</b>	<b>192</b>
Cannabis and Other Recreational Drug Use.....	192
Neuropsychological Tests.....	194
Self-Report Measures.....	195
Accuracy and Reaction Time.....	196
P300 ERP Results .....	199
ROI Cluster Analysis Results .....	201
ROI ERPs .....	203
Phase Synchrony .....	206
<b>Discussion.....</b>	<b>217</b>
Unexpected Superior Working Memory Performance in Cannabis Users.....	217
Demographics, Neuropsychological Tests and Self-Report Measures .....	218
P300s Reflect Memory Load but Only Partially Reflect Performance Differences	221
Localized Brain Activity and Connectivity (ROIs, ERPs, ERSPs, PLVs).....	224
Limitations.....	237
<b>Conclusion.....</b>	<b>239</b>
<b>Chapter 5: Consolidated Local MMN Analysis.....</b>	<b>241</b>
<b>Introduction .....</b>	<b>241</b>
<b>Method .....</b>	<b>242</b>
Participants .....	242
Self-Report and Neuropsychological Measures .....	243
Experimental Procedures.....	244
<b>Results .....</b>	<b>245</b>
Neuropsychological Measures.....	248
Self-Report Measures.....	249
Local MMN ERPs.....	250
Correlations Between MMN and Neuropsychological Measures .....	257
Correlations Between MMN and Self-Report Measures .....	258
<b>Discussion.....</b>	<b>262</b>
Correlations Between MMN, Cannabis, and Other Substance Use.....	264
Limitations.....	266

Conclusion.....	268
<b>Chapter 6: General Discussion and Conclusion .....</b>	<b>270</b>
Synthesis.....	270
<b>Contributions to Cognitive and Clinical Science.....</b>	<b>274</b>
Applications: From Clinical Cognitive Science to Practice.....	275
<b>Current Limitations and Future Possibilities .....</b>	<b>275</b>
Source Localization.....	275
Localized Oscillations and Functional Connectivity .....	276
Group Equivalence and Small Sample Size .....	277
Causality and the Future of Cannabis Research .....	278
<b>References.....</b>	<b>280</b>
<b>Appendices.....</b>	<b>308</b>
<b>Appendix A: Chapter 2 ERSPs for Each ROIs.....</b>	<b>308</b>
<b>Appendix B: Chapter 3 ERSP Figures.....</b>	<b>314</b>
<b>Appendix C: Chapter 4 ROI ERPs .....</b>	<b>318</b>
<b>Appendix D: Chapter 5 Correlations.....</b>	<b>330</b>

## List of Tables

Table 2.1. Behavioural Performance Data for Roving Local-Global Task.....	62
Table 2.2. Mean Amplitude and Latencies of Global MMN Difference Waves.....	63
Table 2.3. Dipole Clusters of Independent Components Identified for Roving Local Global Task and Corresponding Brain Regions.....	67
Table 2.4. Summary of Theta and Gamma ERSP Results Comparing Targets and Standards Overlapping the MMN and P300 Time Windows.....	77
Table 3.1 Percentage of CU and NU groups reporting Current Non-Cannabis Substance Use.....	124
Table 3.2 Descriptive Statistics of Self-Report Measures for Cannabis Users and Non- Users.....	125
Table 3.3 Descriptive statistics of Neuropsychological Tests for Users and Non-Users.	126
Table 3.4. Behavioural Performance Data for Roving Local-Global Task for Cannabis Users and Non-Users.....	128
Table 3.5. MMN Amplitudes and Latency.....	130
Table 3.6. Amplitudes and Latencies of P300 Difference Waves.....	133
Table 3.7. Seeded Dipole Clusters of Independent Components Identified for Cannabis Users and Non-Users and Corresponding Brain Region.....	135
Table 3.8. Summary of Gamma ERSP Results in MMN Time Window.....	143
Table 3.9. Summary of Theta and Gamma ERSP Results in P300 Time Window.....	145
Table 4.1 Percentage of CU and NU groups reporting Current Non-Cannabis Substance Use.....	193
Table 4.2 Descriptive Statistics of Neuropsychological Measures for Cannabis Users and Non-Users.....	194
Table 4.3 Descriptive statistics of Self-Report Measures for Cannabis Users and Non- Users.....	195
Table 4.4. Behavioural Performance Data for the <i>n</i> -back Task.....	198
Table 4.5. P300 Amplitudes and Latencies at Channel PZ for the <i>n</i> -back Task.....	200
Table 4.6. Seeded Dipole Clusters of Independent Components Identified for Cannabis Users and Non-Users and Corresponding Brain Region.....	202
Table 4.7. ROI ERP Summary Comparing NU and CU on the <i>n</i> -back Task.....	206
Table 5.1 Percentage of CU and NU Groups Reporting Current Non-Cannabis Substance Use.....	247
Table 5.2 Descriptive Statistics of Neuropsychological Measures for Cannabis Users and Non-Users.....	248
Table 5.3 Descriptive Statistics of Self-Report Measures for Cannabis Users and Non- Users.....	249
Table 5.4 Comparison of Local MMN Amplitude and Latency Between Tasks in Non- Users.....	251
Table 5.5. Mean Amplitude and Latencies of Local MMN Difference Waves.....	254
Table 5.6. Correlations Between Local MMN and Neuropsychological Measures for Combined (NU and CU) Sample (n=57) Across Dual Oddball and <i>n</i> -back Tasks.....	257
Table 5.7. Correlations Between Local MMN and Self-Report Measures for Combined (NU and CU) Sample (n=57) Across Dual Oddball and <i>n</i> -back Tasks.....	259
Table D.1. Chapter 5 Spearman Rank Correlations Between MMN and	

Neuropsychological Measures for Entire Sample (n=57) Across Both Studies .....330

## List of Figures

Figure 1.1. MMN Difference Wave Derived From ERPs to Standard and Deviant Stimuli in a Simple Oddball Paradigm .....	3
Figure 1.2 Neural Generators of the Auditory MMN.....	4
Figure 1.3. P300 Elicited in a Simple Oddball Task .....	9
Figure 1.4. Context Updating and the P300.....	10
Figure 1.5. Meta Analytic fMRI Activations Common to <i>n</i> -back Tasks .....	15
Figure 1.6. Recruitment Flowchart for Chapters 3, 4, and 5. ....	24
Figure 1.7. Schematic Depicting Calculation of Average PLVs Across Trials From Individual Trial Phase Difference Between Two Recording Sites .....	37
Figure 2.1 Roving Dual Oddball Task.....	48
Figure 2.2. General Workflow for EEG Processing.....	61
Figure 2.3. Grand Average MMN ERP Difference Waves for Feature Present and Feature Absent Conditions .....	63
Figure 2.4. Grand Average P300 ERP Difference Waves for Feature Present and Feature Absent Conditions. ....	64
Figure 2.5. Grand Average MMN ERP Difference Waves Comparing MMN in Feature Present, Feature Absent, and Local MMN.....	66
Figure 2.6. Dipole Cluster Plots of Retained ROIs .....	68
Figure 2.7. Grand Average ROI ERPs for Targets and Standards.....	70
Figure 2.8. ERSP Plots for Selected ROIs Comparing Targets and Standards for Feature Present and Feature Absent Conditions. ....	76
Figure 2.9. Theta-Band PLV Results for Feature Present and Feature Absent Conditions Overlapping the MMN. ....	79
Figure 2.10. Gamma-Band PLV Results for Feature Present and Feature Absent Conditions Overlapping the MMN.....	81
Figure 2.11. Theta-Band PLV Results for Feature Present and Feature Absent Conditions Overlapping the P300. ....	83
Figure 2.12. Gamma-Band PLV Results for Feature Present and Feature Absent Conditions Overlapping the P300. ....	85
Figure 3.1. Grand Average Feature Present and Feature Absent MMN ERP Difference Waves for Cannabis Users and Non-Users .....	130
Figure 3.2. Grand Average P300 ERP Difference Waves .....	133
Figure 3.3. Dipole Cluster Plots of Retained ROIs .....	136
Figure 3.4. ROI ERPs for Feature Present and Feature Absent Conditions Comparing NU and CU .....	140
Figure 3.5. Select Feature Present and Feature Absent ERSP Plots (NU vs. CU).....	146
Figure 3.6. Theta (3-7 Hz) PLV Analysis for Feature-Present Targets.....	150
Figure 3.7. Theta (3-7 Hz) PLV Analysis for Feature-Absent Targets .....	153
Figure 4.1. Simplified Diagram of 1-Back and 2-Back Tasks .....	183
Figure 4.2. Schematic of 2-Back Frequency and Pattern Match Tasks .....	185
Figure 4.3. Grand Average ERPs to Auditory <i>n</i> -Back Tasks Comparing NU and CU....	201
Figure 4.4. Dipole Cluster Plots of Retained ROIs .....	202
Figure 4.5. Frequency Match Theta (3-7Hz) Phase Synchrony (PLV) Results .....	211

Figure 4.6. Pattern Match Theta (3-7Hz) Phase Synchrony (PLV) Results .....	216
Figure 5.1. Comparison of Local MMN ERPs in Non-Users Across Tasks.....	252
Figure 5.2. Grand Average Local MMN ERP Difference Waves (NU vs CU).....	255
Figure 5.3. Local MMN Scalp Topography.....	256
Figure A.1. Chapter 2 Feature Present ERSP Plots Target vs. Standard .....	308
Figure A.2. Chapter 2 Feature Absent ERSP Plots Target vs. Standard.....	311
Figure B.1. Chapter 3 ERSP Plots.....	314
Figure C.1. ROI ERPS Comparing NU and CU for 1-Back and 2-Back Frequency Match <i>n</i> -back Task .....	318
Figure C.2. ROI ERPs Comparing NU and CU for 1-Back and 2-Back Pattern Match <i>n</i> - back Task .....	324

## **Acknowledgements**

I could not possibly express enough gratitude to my supervisor, Lawrence Ward, for his endless support and guidance throughout this process. Lawrence's willingness and enthusiasm for discussing anything and everything has brought so much wholeness to my intellectual development. I would also like to thank my committee members, Beck Todd and Wolfgang Linden, for their thoughtful feedback and helpful suggestions for honing my ideas.

I have boundless gratitude for my colleagues, Lizzy Blundon and Nick Bedo, whose camaraderie, knowledge, and support were critical to my success. I am endlessly appreciative of Matt Smith's friendship and for his technical expertise that made our old-school/boutique/hipster electrophysiological lab function. I would also like to acknowledge Fred Bushor for his kindly support and thought provoking questions during my heaviest months of writing.

A special thanks goes out to the RAs who kept this research machine running and for providing me a frequent reminder that the future is bright! In particular, I want to acknowledge Tricia Sernande for her hard work on this project and for her charisma that made the lab a fun place to be! Also, thanks to Manesh Girn and Hyemin Cho for their assistance with some of the more toilsome grunt work. And also thanks to Eric Laycock who never failed to remind me of my goals and values.

Beyond the lab, I could not have completed this program without the support of my friends (too numerous to name!) who fill my life with endless joy and meaning. In particular, I want to acknowledge Kieran Fox, Kosta Kushlev, and Mark Werner who brought light when it was dark and rainbows when it was light.

Finally, I am so grateful for my family. To my proud parents, Peter and Corinne Rumak, who kept me afloat over the years. Most importantly, words cannot possibly encompass my love and gratitude for my amazing wife, Leslie Rumak, who uprooted her life (multiple times) to love and support me every step of the way and who has selflessly picked up all the slack in raising our beautiful son while I spent countless days, nights, and weekends locked away in my ivory tower - I could not have done this without you!

## **CHAPTER 1: Cannabis Use, Auditory Cognition, and the Brain**

Cannabis use continues to be a controversial topic within the fields of psychological and medical research that is highly politicized. Presently, in North America, there appears to be momentum building for either the decriminalization of marijuana or the legalization of sales to adults for recreational use. Indeed, in 2018 the Government of Canada passed federal legislation authorizing the legal sale of marijuana. As such, there are growing concerns that removing prohibitions on marijuana sales may increase overall usage rates, especially among minors (Friese & Grube, 2013). This is a concern to many because numerous investigations have shown that cannabis users, who do not present with mental illness, perform worse on cognitive tasks and exhibit patterns of brain activity akin to those with severe mental illness (Radhakrishnan, Wilkinson & D'Souza, 2014). However, the nature of these aberrant neural processes in cannabis users has not been fully explored. The present research will attempt to address some of these issues by employing novel cognitive tasks that are conceptually related to tasks that have revealed abnormal brain activity common to both cannabis users and individuals with psychosis.

Specifically, this research will use electroencephalography (EEG) to explore aspects of auditory change detection and auditory working memory. To this end, we aim to add to existent research in these areas by articulating the complex network dynamics associated with these phenomena in an attempt to identify brain mechanisms that are affected by cannabis use. The first section of this introductory chapter provides a brief overview of research that pertains to both early (mismatch negativity) and late (oddball target detection) auditory processing, and also auditory working memory, in context of cannabis

use. The second section provides an overview of our recruitment procedures that apply to Chapters 3, 4, and 5, as well as a general overview of our EEG analyses. Finally, the third section outlines general goals and predictions, along with an overview of each chapter.

## **Overview of Auditory Cognitive Processes in Context of Cannabis Use**

The following section is intended as a brief introduction to the cognitive processes that will be discussed in this dissertation. As such a general overview will be provided for the auditory mismatch negativity (MMN), and the auditory P300 to oddball tasks, and tasks of working memory. Relevant research regarding these topics as they pertain to cannabis use will also be reviewed.

### ***The Mismatch Negativity (MMN) and its Neural Underpinnings***

In its basic form the auditory MMN is characterized as a negatively-deflected component of the Event-Related Potential (ERP) waveform that occurs in response to a deviant (or rare) stimulus that occurs within the context of a sequence of regularly occurring standard (or common stimuli) (See Figure 1.1). Deviant stimuli can be of various forms from basic feature deviance (e.g., sound frequency, duration) to more complex or abstract (e.g., sound pattern or tonal distance). The strongest evidence from neuropharmacological investigations suggests that the MMN is largely mediated by neurons that possess synapses sensitive to the neurotransmitters glutamate and GABA with some evidence for the indirect involvement of serotonin and acetylcholine (Garrido, Kilner, Stephan, & Friston, 2009; Kenemans & Kähkönen, 2011). There is some debate in the literature as to whether the MMN is related to fronto-temporal sources (see model adjustment theory below) or emerges from activity in the auditory cortex alone (see adaptation hypothesis

below). More recent approaches have combined these theories into a predictive coding framework (see hierarchical predictive coding below).

Figure 1.1. MMN Difference Wave Derived From ERPs to Standard and Deviant Stimuli in a Simple Oddball Paradigm

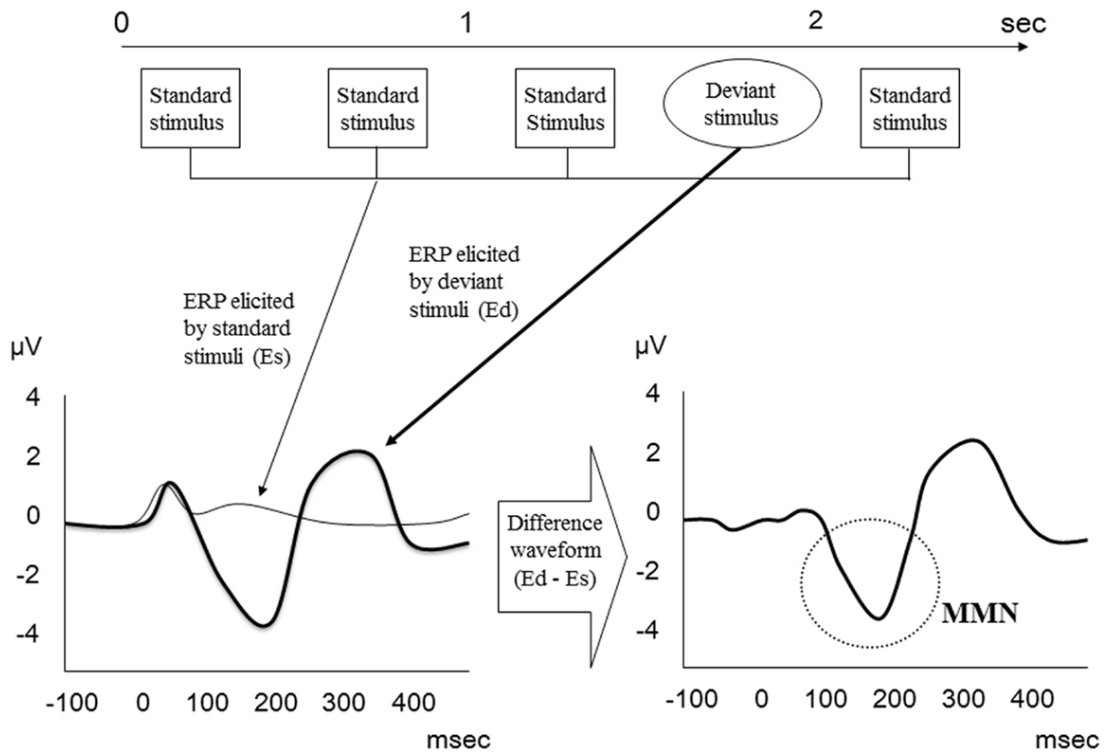


Figure 1. 1. Schematic depiction of MMN difference wave (right) calculated by subtracting ERP response to rare deviant stimuli from ERP response to common standard stimuli (left) in a simple oddball paradigm (top). Adapted from Nagai and colleagues (2013), with permission.

The model adjustment hypothesis suggests that the MMN is related to a change detection mechanism generated by a fronto-temporal network (See Figure 1. 2) where the MMN represents greater prediction error (mismatch) between the predictions that arise from top-down sources and the current sensory input (Doeller et al, 2003; Winkler, Karmos, & Näätänen, 1996). Anatomical studies in primates have verified connections between

auditory and pre-frontal areas (Barbas et al., 2005; Romanski & Goldman-Rakic, 2002). The temporal generators are likely related to sensory memory and pre-frontal generators related to a cognitive or comparator mechanism (Barbas et al., 2005). Early MMN activity (90-120ms) may relate to activity in the bilateral superior temporal gyrus and late MMN activity (140-170ms) has been sourced to the inferior temporal gyrus. Bilateral activation of the MMN temporal lobe generators has been observed for both tonal and language stimuli; however, a degree of hemispheric specificity for the frontal generators of the auditory MMN may exist. The right frontal lobe appears to be dominant for paradigms involving tone stimuli and the left frontal lobe appears to be dominant for language stimuli (Maclean, 2011).

Figure 1.2 Neural Generators of the Auditory MMN



Figure 1.2. Neural generators of the MMN derived from dipole fitting of EEG data constrained by fMRI. Figure depicts bilateral temporal (STG) and frontal (IFG) sources related to MMN generation. Figure adapted from Doeller and colleagues (2003), reprinted with permission.

In contrast, the adaptation hypothesis challenges the fronto-temporal theory of the MMN. Proponents suggest that the MMN is a feature of neuronal adaptation in the auditory cortex related to the auditory N1 component that occurs approximately 80-150ms following stimulus presentation (Jääskeläinen et al., 2004; see Näätänen, Jacobsen & Winkler, 2005 for a critique). While there is empirical evidence to support certain features of the adaptation hypothesis, a number of empirical findings demonstrate features that cannot be explained by neuronal adaptation in the auditory cortex (See Garrido, Kilner, Stephan, & Friston, 2009 for a review).

The predictive coding theory integrates features of both model adjustment and adaptation hypotheses and suggests that MMN generation relies on a reciprocal Bayesian prediction model (Garrido, Kilner, Stephan, & Friston, 2009). In short, information from temporal sources is sent to frontal sources, which in turn model incoming information from temporal sources. The MMN to deviant stimuli reflects a neural response due to prediction error. With repetitive standard stimuli prediction error decreases as the number of sequential iterations of an identical stimulus increases. As prediction error for standard stimuli decreases, however, the presentation of a deviant stimulus results in greater prediction error. Garrido and colleagues (2008) utilized a roving-frequency MMN paradigm to neutralize any effects arising from differences in stimulus properties in eliciting the MMN because the standards and deviants are physically identical in that paradigm. They identified frontal and posterior regions believed to contribute to

predictive coding, including the pre-central, insular, parietal, and inferior-temporal cortices (Garrido, Friston, & Kiebel, 2008; Garrido, Kilner, Stephan, & Friston, 2009).

Other researchers have utilized the MMN to disentangle aspects of auditory processing that are automatic and those that require conscious processing (i.e. P300; see description below). Bekinschtein and colleagues (2009) utilized a local-global dual oddball task designed to elicit both a MMN (local effect) and a P300 (global effect) and found that local expectation violations (a run of four identical tones followed by a different fifth tone, compared to a run of five identical tones) led to a typical MMN effect in the 130 ms to 300 ms range. The local MMN effect was observed during counting of global pattern deviants, attention engagement on a distractor task, and while in a mind-wandering condition, suggesting that the local effect is an automatic process. In addition to scalp EEG recordings, the authors recorded brain activity using fMRI and identified the bilateral superior temporal auditory cortices and, to a much lesser extent frontal generators, as potential sources for the local MMN. By contrast, the later occurring P300 global ERP response to rare runs of either type was present only when participants counted rare runs but not when mind wandering or when attention was directed to a distractor task. Brain network areas identified to underlie this phenomenon included the prefrontal cortex, cingulate, and temporal regions (Bekinschtein et al., 2009). This pattern of results has been replicated under varying task conditions and explained in the context of hierarchical predictive coding (Chennu et al., 2013; King, Gramfort, Schurger, Naccache, & Dehaene, 2014; Wacongne et al., 2011). In our lab, we have replicated the phenomenon but have found an asymmetry between the two types of global task, detecting a flat sequence of

tones amidst a series of sequences with a deviant at the end being more difficult and leading to a smaller P300 than the opposite (Blundon, Rumak & Ward, 2017).

A number of other experimental investigations, however, employing fMRI and high-density EEG, have moved beyond basic ERP analysis to characterize the neural sources, network dynamics and the proposed function of the brain network that generates the auditory MMN (Bekinschtein et al., 2009; Chennu et al., 2013; Garrido, Friston, & Kiebel, 2008; Maclean & Ward, 2014). In the next section we will review what is most relevant in this work for understanding the effects of cannabis use.

### ***The MMN, Psychopathology, and Cannabis Use***

Auditory change detection as indexed by the MMN has been shown to be deficient in those with serious mental illnesses such as schizophrenia (Uhlhaas, 2013), and it has been suggested that MMN deficits might be useful as an endophenotype for the disorder (Bodatsch, Klosterkötter, Müller, & Ruhrmann, 2013; Nagai et al., 2013). MMN processing deficits have also been observed in cannabis users (Greenwood et al., 2014; Rentzsch, Buntebart, Stadelmeier, Gallinat, & Jockers-Scherübl, 2011; Roser et al., 2010). Some have argued that chronic cannabis use may be a risk factor for developing psychosis (Davis, Compton, Wang, Levin, & Blanco, 2013; Radhakrishnan, Wilkinson, & D'Souza, 2014) and it has been suggested that individuals already diagnosed with some form of psychotic disorder will exhibit a worsening of symptoms following cannabis use (D'Souza et al., 2005). It has been suggested that prolonged frequent cannabis use might lead to long term glutamate dysregulation via hypofunction at NMDA receptors arising from CB1 (cannabinoid) receptor activity (Sánchez-Blázquez,

Rodríguez-Muñoz, & Garzón, 2014). At present these neurochemical findings seem far-removed from the effects of cannabis use on the MMN. It is possible that a more nuanced understanding of how brain network dynamics are affected by cannabis use would clarify how these neurochemical effects are expressed in auditory change detection tasks.

The relatively few studies that have specifically investigated the MMN in context of cannabis use have primarily utilized basic protocols involving analysis of single channel ERPs rather than network dynamics. One study of heavy cannabis users (5 times per week for at least a year) found that that users exhibited reduced MMN to pitch deviants (but not duration deviants) compared to non-users (Rentzsch et al., 2007). Another study found that long-term cannabis users (~10 years) showed reduced MMN to frequency deviants (again not to duration deviants) compared to both short-term users (~4 years) and non-users, though when both cannabis user groups were combined they did not differ from non-users (Roser et al., 2010). Using a multi-featured MMN task that included frequency, duration and intensity deviants, Greenwood and colleagues (2014) found that cannabis users exhibited reduced MMN to frequency deviants but not to duration or intensity deviants. More specific analysis revealed that long-term users (~26 years of use ranging from 10.4 to 40.3 years of use) exhibited reduced-duration MMN compared to short-term users (~ 5 years of use ranging from ~2 to 10 years of use) and non-users. They also found that MMN did not relate to psychosis proneness in cannabis users. Reductions in MMN amplitude (to frequency and duration deviant stimulus types) for long-term users, however, were associated with increased psychotic-like symptoms

during cannabis intoxication as indexed by the Cannabis Experience Questionnaire (Greenwood et al., 2014). While a causal link between cannabis use and psychosis is yet to be definitively established, the apparent similarities in early auditory processing deficits seen in those suffering psychosis and in chronic cannabis users is worthy of further exploration.

### *The P300 as an Index of Attention in Auditory Oddball Tasks*

An ERP component widely used to investigate aspects of auditory attention is the P300. Oddball tasks are most commonly used to elicit the P300, which typically occurs in response to detection of a rare target stimuli amongst commonly occurring standards (see Figure 1.3).

Figure 1.3. P300 Elicited in a Simple Oddball Task

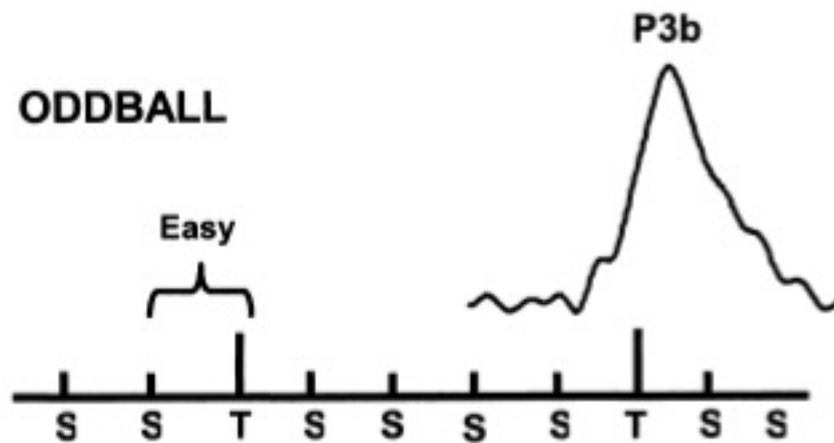


Figure 1.3. P300 response to rarely occurring target (T) stimuli detected amongst a series of commonly occurring standard (S) stimuli. This figure specifically highlights the posterior P3b component that is largest when targets are easy to discriminate from standards. Adapted from Figure 5.1 in Polich (2003), reprinted with permission.

The P300 is a positively deflected component of the ERP waveform that typically peaks anywhere from 250-500ms depending on the stimulus, task, and individual factors (Polich, 2007). Furthermore, the P300 is often subdivided into subcomponents (P3a and P3b) that show different scalp distributions and peak latencies. The later of these, the P3b, occurs approximately 300 ms after the presentation of a stimulus, shows a parietal scalp distribution, is typically larger in amplitude to targets compared to non-targets in basic oddball tasks, and is attenuated with increased task difficulty during 3-stimulus paradigms (Comerchero & Polich, 1999). The P3a occurs 60-80 ms before the P3b, shows a fronto-central distribution and is associated with stimulus-driven attentional shifting (Polich, 2007; Steiner, Barry, & Gonsalvez, 2013). Source analysis has supported that the P3a is an attentional component stemming from activity in the frontal lobe and anterior cingulate whereas the P3b relates to stimulus maintenance, evaluation, and context updating processes (See Figure 1.4) stemming from activity in the parietal lobe and posterior cingulate (Polich, 2003; Wronka, Kaiser, & Coenen, 2012).

Figure 1.4. Context Updating and the P300

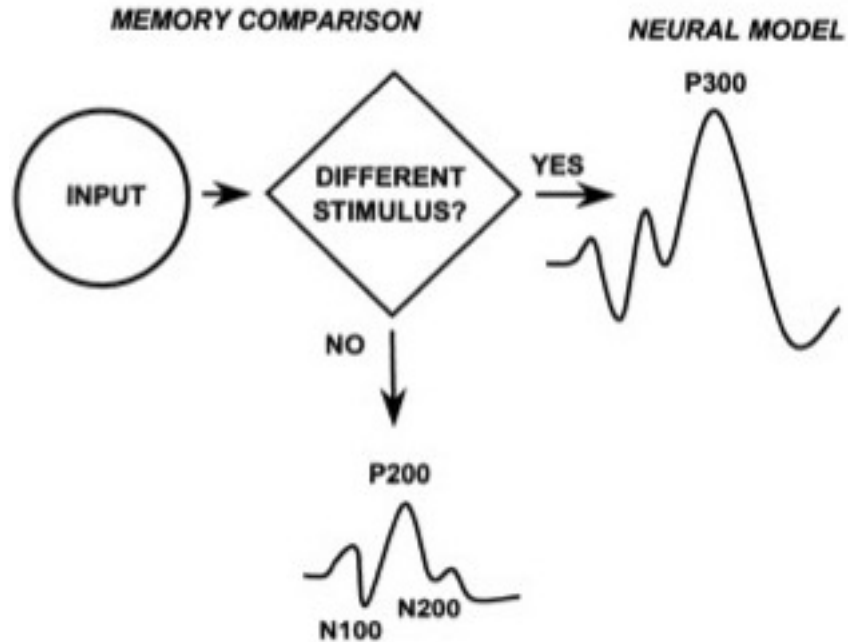


Figure 1. 4. Conceptual schematic of P300 in relation to attentional and memory processes related to context updating. Adapted from Figure 5.5 in Polich (2003), reprinted with permission.

### *The P300 and Auditory Attention in Cannabis Users*

The relatively few studies conducted on the acute effects of cannabis use on the auditory P300 appear to suggest that cannabis intoxication has disruptive effects. A double-blind crossover study investigating the acute effects of  $\Delta$ 9-THC administration in a three-stimulus auditory oddball task found that  $\Delta$ 9-THC reduced P3a and P3b amplitudes versus placebo, and that this reduction was greater in a higher dose condition (D'Souza et al., 2012). Another study investigating the acute effects of cannabis on healthy individuals while participants completed an auditory choice reaction task, where participants had to correctly respond to 1000Hz and 2000Hz tones that were randomly presented, yielded reduced P300 amplitudes when participants were administered a THC or a cannabis extract versus placebo (Roser et al. 2008).

The effect of frequent cannabis use on the P300 in oddball tasks has not been extensively investigated and the few studies have yielded mixed results. Patrick and colleagues (1995) report on an earlier study conducted by the group that utilized a simple auditory oddball design and found cannabis users (at least two uses per week) exhibited longer P300 latencies and decreased amplitudes. However, these researchers reported that the apparent differences disappeared in a follow-up study where tighter controls were enacted over patient characteristics, such as age, neurological conditions and psychiatric history (Patrick et al., 1995). Similarly, another study utilizing an auditory oddball task failed to find any P300 amplitude or latency differences between cannabis users and non-users, though the overall frequency of cannabis use was relatively low (approximate mean of 44 uses over the past 6 months) (de Sola et al., 2008).

In non-auditory domains, heavy cannabis users (approximately 9 smoked joints per week) exhibited increased P300 amplitudes versus non-users to a visual oddball in an affective oddball task (words with positive emotional valence = standards; negative words = rare targets) but no latency differences. The authors noted that negative symptoms of schizotypy were negatively associated with affective P300 amplitude and that this sample of cannabis users exhibited decreased negative symptoms compared to controls (albeit users showed increased positive symptoms and no group differences in disorganized symptoms) (Skosnik, Park, Dobbs & Gardner, 2008). Others have failed to find P300 differences between cannabis users and non-users in visual oddball tasks (Patrick et al., 1995).

Other investigations examining the auditory P300 in tasks requiring more complex cognitive processing than in basic auditory oddball tasks have been more consistent. For instance, a study investigating auditory selective attention in regular cannabis users (at least 2 years use a minimum of twice per week), where participants had to respond to infrequent target tones amongst frequent distractor tones that were similar to targets but could differ in pitch, duration, or location (left or right ear), found cannabis users had reduced P300 amplitudes but no latency difference to target stimuli versus non-users (Kempel, Lampe, Parnefjord, Hennig & Kunert, 2003). This effect was more pronounced in cannabis users who started using cannabis at an earlier age. Another study of auditory selective attention found longer P300 latency, in addition to slower reaction time and poorer performance, in heavy cannabis users (approximately 18 uses per month), compared to light users (6 uses per month) and non-users (Solowij, Michie & Fox, 1995). However, these researchers note that they failed to replicate their earlier findings showing decreased P300 amplitudes in cannabis users (Solowij, Michie & Fox, 1991), which they attributed to differences in the control groups.

### ***Auditory Working Memory***

Working memory is a process that involves the dynamic and controlled encoding, updating, and retrieval of information. Many experimental investigations spanning sensory modalities and involving diverse task specifications have been used to understand working memory. Working memory subsumes a great number of tasks believed to generalize to overall functioning (Baddeley, 2003; Ma, Husain, & Bays, 2014). The high temporal resolution of scalp electrical recordings makes them useful for

the study of the underlying processes of working memory, whose contents change dynamically and rapidly. Most investigations have focused on evoked response potentials and have identified ERP components that are sensitive to working memory load and attentional processes.

### ***Working Memory, The N-back Task, and the P300***

One particularly useful task for the study of the sub-processes involved in working memory is the *n*-back task. Specifically, the dual task nature of *n*-back tasks calls for the on-line monitoring, updating, and manipulation of items in memory (Owen, McMillan, Laird & Bullmore, 2005; Watter, Geffen & Geffen, 2001). In its basic form, a participant engaged in an *n*-back task will attend to a serial presentation of either visual or auditory stimuli. A response is required when the current stimulus matches on some predetermined feature of the stimulus that occurred *n* presentations ago where *n* is equal to an integer, most commonly 1, 2 or 3. Conditions involving larger values of *n* are typically more difficult as they require a greater number of stimuli to be dynamically maintained in memory, thus constituting a greater cognitive load. ERP investigations using *n*-back tasks have generally revealed that increasing memory load results in decreased P3b amplitude but has no effect on its latency (Evans, Selinger, & Pollak, 2011; Watter, Geffen, & Geffen, 2001).

### ***Brain Regions and Working Memory***

Identification of the underlying brain networks involved in working memory during the *n*-back task has primarily been conducted using fMRI. Owen and colleagues (2005) conducted a meta-analysis of fMRI data collected during various *n*-back tasks in healthy individuals (See Figure 1.5). They concluded that the engagement of working memory

during  $n$ -back tasks involves six fundamental brain areas constituting a fronto-parietal network made up of the bilateral and medial posterior parietal cortex including precuneus and inferior parietal lobules (BA 7/40), bilateral premotor cortex (BA 6/8), dorsal cingulate/medial premotor cortex, including supplementary motor area (BA32,6), bilateral rostral prefrontal cortex or frontal pole (BA 10), bilateral dorsolateral prefrontal cortex (BA 9, 46), and bilateral mid-ventrolateral prefrontal cortex or frontal operculum (BA 45, 47). These findings were largely confirmed by a more recent coordinate-based meta-analysis that integrated fMRI results across a variety of working memory tasks (Rottschy et al., 2012).

Figure 1.5. Meta Analytic fMRI Activations Common to  $n$ -back Tasks

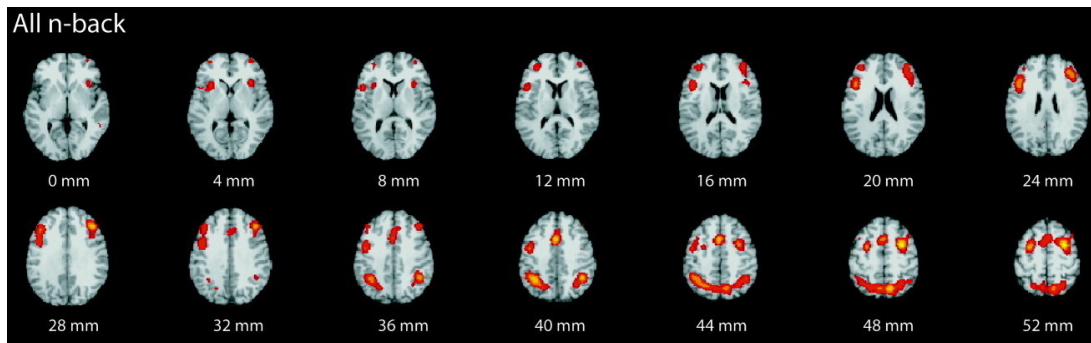


Figure 1.5. Meta analytic results of brain activations common to  $n$ -back tasks adapted from Figure 1 in Owen and colleagues (2005). Colored regions represent significant voxel wise activations ( $p < .01$ ; FDR corrected). Right side of each plot represents right side of brain. Numerical label below each plot represents Z coordinate of each slice in Talairach space. Reprinted with Permission.

### ***Oscillatory Activity, Brain Network Dynamics and Working Memory***

Several investigations have sought to understand the role that neural oscillatory activity, at various frequency bands, plays in cognitive functions such as working memory.

Accumulating evidence suggests that gamma-, theta- and alpha-band activity play a

significant role in working memory function (Roux & Uhlhaas, 2014). In this context, gamma activity (30-50Hz) is viewed as a generic working memory mechanism that occurs across all formats of items maintained in working memory. Synchronous gamma activity arises out of various cortical and subcortical structures and is believed to relate to the integration of individual neurons into larger cell assemblies. Theta activity (4-8 Hz) is believed to pertain to the temporal organization of cell assemblies and likely emanates from both the entorhinal-hippocampal system and the prefrontal cortex. Alpha activity (9-14 Hz) is believed to underlie the suppression of irrelevant information that might interfere with targets during sequential presentation of stimuli and likely arises from sensory regions and the thalamus. Studies of phase-amplitude coupling have suggested that alpha (phase)-gamma (amplitude) coupling in thalamo-cortical circuits may relate to the maintenance of sensory spatial information, and may be specifically related to the visual spatial sketchpad. Phase-amplitude coupling between theta and gamma bands in fronto-hippocampal networks may be associated with processes that maintain sequentially presented information, as it is theorized to be maintained in a phonological loop (Roux & Uhlhaas, 2014).

Whereas fMRI, because of its high spatial resolution, has been utilized to map the network underlying working memory activity, some effort has been made to use magnetic and electrophysiological source localization to better understand the temporal dynamics of working memory. An MEG study utilizing spectral analysis and beamforming to investigate focal neural oscillations revealed that gamma band activity (60-80 Hz) in the prefrontal cortex relates to working memory maintenance whereas

gamma activity in the left dorsolateral prefrontal cortex and right parietal lobe was correlated with increased working memory load. Changes to alpha band activity (10-14Hz in this case) were observed in the pre-motor/supplementary motor area (BA6) but did not change as a function of the working memory load (Roux, Wibrat, Mohr, Singer, & Uhlhaas, 2012). Luu and colleagues (2014) used temporal principle component analysis and spatial independent component analysis to decompose high-density scalp EEG signals (0.1-30 Hz) in time and space for a visual *n*-back task. They identified three partially overlapping networks. The first, a visual cortex network that included the posterior cingulate cortex, appeared to activate prior to the stimulus and was believed to be associated with anticipatory attentional processes. The second came online following stimulus presentation and involved the ventromedial prefrontal cortex, lateral prefrontal cortex and the temporal poles, and was likely associated with an executive control network. A third network involved cortices associated with the temporal-parietal junction and believed to be associated with attentional reorienting via the ventral attention network (Luu et al., 2014).

### ***Working Memory, Executive Function, and Cannabis Use***

Working memory impairments are well documented in individuals with severe mental illnesses such as schizophrenia and may constitute a fundamental process related to prolonged disability in that disorder (Barch & Ceaser, 2012). Frequent cannabis use has been associated with deficits in many domains of neurocognitive functioning (Bossong, Jager, Bhattacharyya, & Allen, 2014; Broyd, van Hell, Beale, Yücel, Solowij, 2016; D'Souza et al., 2008; Nader & Sanchez, 2018; Ramaekers, Kauert, Theunissen, Toennes,

& Moeller, 2009); however the findings of working memory impairment have been quite mixed.

For instance, a study by Thames and colleagues (2014) comparing neurocognitive function in recent cannabis users (within last 28 days) and past users (abstinent for at least 28 days) to that of non-users found that recent cannabis use was associated with worse performance in attention, working memory, processing speed and executive function. Furthermore, frequency and quantity of use showed negative correlations with cognitive performance in recent users. In abstinent cannabis users, performance deficits were only observed in the executive functioning domain. All analyses controlled for age, alcohol use and pre-morbid IQ. Interestingly, while recent users showed decrements in current neuropsychological function they actually had higher estimates of pre-morbid IQ (Thames, Arbid, & Sayegh, 2014). In another study, cannabis users were found to perform worse on verbal short term memory (story recall) and working memory (n-back) tasks, though it was found that cannabis use predicted verbal memory performance and alcohol use was the best predictor of working memory performance (Herzig, Nutt & Mohr, 2014). In a fMRI study, involving a sample of incarcerated youth, cannabis users were found to perform comparably to non-users on an n-back task; however, cannabis users exhibited greater connectivity in working memory networks, which the authors interpreted as in increased effort needed to complete the task (Cousijn, Wiers et al., 2014). However, in a 3-year longitudinal follow-up study, this same group noted similar findings in performance and working memory network connectivity and concluded that sustained cannabis use did not lead to any degradation of working memory function

(Cousijn, Vingerhoets et al., 2014). Complicating the picture further, a recent fMRI study found that medical cannabis users showed improvements in tasks of executive function and cognitive control after three months of cannabis use compared to baseline and these improvements were reflected in increased cingulate cortex activity (Gruber et al., 2017), whereas this same group had previously found executive functioning deficits in regular cannabis users (Gruber, Sagar, Dahlgren, Racine, & Lukas, 2012) and for these deficits to be more pronounced in individuals who started using before the age of 16 (Dahlgren, Sagar, Racine, Dreman & Gruber, 2016). One explanation proposed for the apparent variability in the effects of cannabis use on executive function and working memory is that a wide range of tests have been utilized (Broyd et al., 2016); however, it could also be that the effects of cannabis use are nuanced, and that too few, not too many, domains have been examined. Indeed, EEG studies examining auditory working memory are sparse, and even sparser yet, are EEG studies on auditory working memory in cannabis users.

### **General Overview of Methodology**

This next section provides a general overview of the recruitment procedures (Chapters 3,4, and 5) and provides an account of some of the ethical barriers we faced in context of political and legal factors regarding cannabis laws in Vancouver, Canada, occurring at the time of this research. This is followed by a general overview of our electrophysiological methodology, which is aimed at readers who may be less familiar with some of the technical aspects described in subsequent chapters.

### ***Recruitment of Cannabis Users and Non-Users***

This dissertation is primarily concerned with the effects of current heavy recreational cannabis use by high-functioning individuals on the neural correlates of auditory change detection and auditory working memory. Here we provide a general overview of how we operationalized current heavy cannabis use, the recruitment methods that were used to recruit our cannabis users and non-users, and discuss some of the theoretical and practical limitations faced during this process.

We classified individuals as current heavy cannabis users if they self-reported using cannabis at least 10 times in the last 30 days and classified individuals as non-users if they had not used cannabis for at least 6 months. We recognize that this definition is fundamentally arbitrary and imprecise, due to retrospective memory bias, subjective interpretation of what constitutes a session of cannabis use, and difficulty quantifying exactly how much and in what form cannabis is consumed per session. Also, we did not explicitly exclude participants with a history of using other recreational drugs (including alcohol), though we documented this use where applicable. We did not subject participants to a formal assessment of alcohol or substance use disorder, as not all recreational use is pathological, and logistical and time constraints did not allow for such procedures to be included in our research protocol.

We narrowed the focus of our research to current heavy cannabis use primarily because of the difficulty in quantifying cannabis usage patterns. For instance, someone who smokes a half gram joint every day upon awakening, the so called *wake and bake*, might

have an easy time describing their usage patterns; however, a frequent but social user, who shares a 2.5 gram blunt (hollowed out cigar filled with marijuana) with friends several times a week at varying times, might have a more difficult time describing their pattern of use.

The issue of quantifying cannabis use is further complicated by the wide range of cannabis delivery methods (e.g. joints, pipes, bongs, edibles, vaporizers etc.), forms of cannabis (weed, hash, oil, budder, shatter etc.), and literally thousands of selectively bred marijuana strains with colorful names (e.g. White Widow, Granddaddy Purple, Maui Wowie – see [www.leafy.com](http://www.leafy.com) for more examples) that are often broadly classified as sativa, indica, or hybrid, but each having varying chemical profiles of active compounds (i.e. THC and cannabidiol among other cannabinoids that are less well-understood) (Gloss, 2015). Considering all of the above, possible scenarios arise, where two individuals who report using cannabis 10 times in a 30 day period, may have in fact been exposed to widely varying dosages of cannabis. This issue will be addressed more thoroughly within the discussion sections of relevant chapters.

Some research groups have circumvented dosage issues by taking blood or urine measurements and quantifying THC metabolites (e.g. Greenwood et al., 2014), though these procedures are not without limitations (Hadland & Levy, 2016). Nonetheless, such procedures were a logistical impossibility for our lab. These issues might be also be resolved via narrowing participant selection to a specific usage pattern, delivery method, or cannabis strain, though this presents a practical difficulty for research labs, such as

ours, that do not have the resources to carry out such extensively nuanced recruitment. From an experimental perspective, it would be ideal to perform longitudinal studies while providing cannabis to participants, but ethical and legal restrictions in Canada, would prohibit such a study, not to mention its prohibitive cost.

Additionally, in terms of legal and ethical restrictions, at the time of recruitment for this study, we were required by the ethics review board at UBC to conduct screening of prospective participants via a telephone protocol rather than using our standard less onerous email recruitment procedures, out of concern for participants having their identities attached to potentially self-incriminating report of illegal activity. Anecdotally, recreational cannabis use in Vancouver appears to be qualitatively de-stigmatized, as users are, if anything, enthusiastic, about discussing their cannabis use. This may be in part due to changing attitudes amongst local law-enforcement towards pursuing criminal charges in cases of minor infractions with respect to federal cannabis drug laws (Lupick, 2015), which is evidenced by a decline in arrests in Vancouver for cannabis possession (Statistics Canada, 2018). Perhaps corroborating this, and again anecdotally, the writer, who grew up in a different Canadian province, was somewhat shocked to observe, on numerous occasions, young professionals (i.e., business people in suits), smoking cannabis in well trafficked areas, in broad daylight, in plain view of law enforcement officers – flagrant behaviour that would have certainly resulted in police intervention and/or arrest in the writer’s home province.

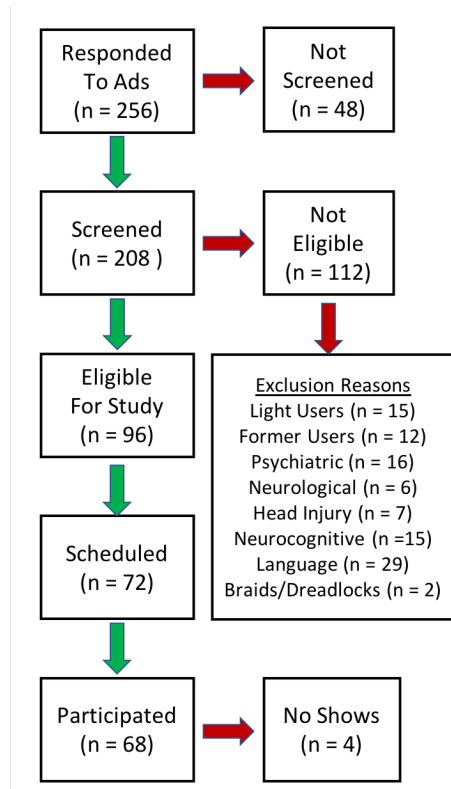
In 2014 (just prior to the onset of this research), Vancouver saw the rapid emergence of dozens of medical cannabis (existing in a legal grey zone, albeit still technically illegal) dispensaries. The writer visited many of these dispensaries handing out recruitment posters and noted a great variability amongst them. Indeed while all, on the surface, dispensed cannabis under the guise of medical necessity, it is well understood that in some cases this was a thin veneer for dispensing cannabis for recreational purposes. For instance, at one point, a legal loophole meant that out-of-province customers did not require proof of a medical condition to purchase supposed medical cannabis. More importantly, proof of medical condition was somewhat vague, in that dispensaries did not explicitly require prescriptions for cannabis, but rather a customer could demonstrate that they had a valid medical condition by presenting a prescription for a different drug prescribed for an ailment (e.g. a prescription for an SSRI or analgesic from a walk-in clinic), or could undergo a brief assessment by an on-staff naturopath or holistic health practitioner. The municipal government passed stricter laws in an attempt to regulate these businesses (e.g. restricting the distance a dispensary can be from a school) (City of Vancouver, 2015). Numerous media reports since 2014, have reported that some of these businesses were subject to periodic police raids, but due to high profitability, would re-open - often the next-day- and continue to remain open in 2018.

Also of note, while perhaps mere coincidence, the decision to place stricter ethical restrictions on our recruitment procedures was passed mere days after the former federal Minister of Health, Rona Ambrose, paid a highly-politicized visit to Vancouver, to place political pressure on local governing bodies to take a tougher legal stance toward

recreational drug use. Her stance was summarized in a public letter she addressed to the mayor of Vancouver, Gregor Robertson (Ambrose, 2015). Practically, this restriction limited the scope of the questions we were willing to ask participants on our telephone screen, which under ideal circumstances would have involved an in-depth questionnaire of cannabis use behaviours prior to being invited to participate. Instead, we had to settle for less precise *a priori* inclusion criteria, and had to resort to *post hoc* exclusion of several participants (described in methods of Chapters 3 and 4) based upon their self-report of cannabis use (ethically approved). It is likely that such ethical restrictions will become largely obsolete in Canada once recreational cannabis use becomes legal.

A detailed narrative of the recruitment procedure can be found in the Method section of Chapter 3. The same procedure was used to recruit participants for the working memory study described in Chapter 4. Participants in Chapter 5 are the same as described in Chapters 3 and 4. In total we were able to screen 208 of the 256 individuals who responded to our recruitment ads. Of these, 96 individuals met our eligibility requirements, and 72 were available to be scheduled. A total of 112 individuals were excluded because they did not meet our inclusion criteria. See Figure 1.6 for an overview of the inclusion and exclusion of participants at each stage of recruitment.

Figure 1.6. Recruitment Flowchart for Chapters 3, 4, and 5.



### ***Overview of Electrophysiological Methods***

In this dissertation, various behavioural, self-report and electrophysiological methods were employed to investigate auditory processing and working memory performance in cannabis users. Of particular note, the electrophysiological methods involved well-established channel level analyses (i.e. event-related potentials; ERPs) to interrogate cognitive processes. In addition, advanced independent component analysis (ICA) and source localization methods (i.e. dipole fitting) were utilized to identify cortical brain regions contributing to these cognitive processes. Additional techniques were used to quantify oscillatory activity (i.e. event-related spectral perturbation; ERSs) within each of these cortical regions and network analysis (i.e. phase-locking values; PLVs) was used

to identify functional connectivity within various frequency bands between cortical brain regions. A diagram of the EEG processing workflow can be viewed in the Chapter 2 Method section (see Figure 2.2).

### *Electroencephalography (EEG)*

As a large portion of the methods discussed in this dissertation relate to scalp electroencephalography (EEG) a brief, albeit shallow (literally surface level), overview of this topic is warranted. A full technical and theoretical account of the neural underpinnings of EEG is beyond the scope of this dissertation as it invariably delves deep into the realms of neuroscience, biophysics and electrical engineering. Interested readers might reference (Luck, 2005) for a more technical account of EEG.

Oscillatory electrical brain activity, the approximately 10 Hz alpha wave, in humans was first described by Hans Berger in 1924 (Haas, 2003). Over the past century recording and methods of analysis have become refined and matured into a toolset that is invaluable to both medical and cognitive sciences. In electroencephalography (EEG), a continuous waveform, or electroencephalogram, is plotted based upon high frequency sampling (usually 250 to 1000 measurements per second). In its simplest form, an electroencephalogram depicts the moment to moment fluctuations in brain-derived (in addition to artefactual electrical generators, such as eyes, muscles, heart, and surrounding electrical fields from equipment etc.) electric potential, or voltage, which is the difference between the potential measured at an electrode affixed to the scalp and a neutral reference

point (i.e., nose, ear, mastoid). In modern EEG setups, measurements are taken from electrode arrays ranging from low-density channel arrays (e.g. 8 to 16 channels) seen in medical labs used for diagnosis of sleep disorders or epilepsy, to the higher-density channel arrays (e.g. 20 to 256 channels) used in cognitive neuroscience. The analog EEG signal of each electrode channel is fed through an amplifier and subsequently digitized so that it can be stored on a computer for offline processing.

Numerous theoretical models have been put forth to account for how electrical activity at the neuronal level manifests in recognizable waveform features at the scalp level that reliably reflect neurological and cognitive processes, though the issue is still not entirely resolved and is hotly debated. Briefly, scalp level EEG activity reflects the additive sum of electrical activity derived from neuronal communication within the brain, via transmission of electrical signals along networks of billions of interconnected neurons, which transmits through the skull via processes of volume conduction (Luck, 2005). In addition to brain sources, scalp EEG also reflects various artefactual sources of electrical activity such as those that arise from eye movements, gross muscle activity, cardiac muscles, and external sources such as electrical line noise. In subsequent sections and the method sections of following chapters we describe various methods used to eliminate such artefactual activity from the data we analyzed.

The nature of neuronal communication is complex and multifaceted, though as mentioned, the summation of some of this electrical activity can be measured by scalp electrodes. Leading contemporary theories posit that EEG reflects the sum of local field

potentials, which in turn are the product of post-synaptic potentials. The latter result from depolarization of cell membranes in postsynaptic dendrites of radially-oriented pyramidal neurons situated in the neocortex, or outer layers of the brain (Luck, 2005).

### *Event Related Potentials (ERPs)*

Much of the focus of this dissertation relies upon inspection of Event Related Potentials (ERP). ERPs have been used for decades in understanding of sensory and cognitive processes. Typically, ERPs are derived from channel-level EEG recordings, though these methods can also be applied to independent components, which will be introduced in the next section. Electroencephalograms of continuous recordings of brain-derived electrical activity are useful for inferring neurological pathologies; however, the inherent noisiness of continuous EEG data makes it difficult to infer electrical response to specific sensory events or internal cognitive processes. ERP research designs make use of principles of signal averaging of continuous EEG recording over multiple repetitions of sensory stimuli or cognitive processes.

Averaging recordings over multiple trials allows temporally consistent features, or ERP components, to emerge from noisy data and can provide a temporally detailed account of electrical brain activities that are time locked to an external event, a behaviour response, or an inferred cognitive process. Averaged ERP waveforms consistently show predictable shapes, or morphologies, with positive and negative deflections of various voltage

amplitudes at certain time points depending on the type of stimulus (e.g. auditory, visual, somatosensory etc.).

Experimentally manipulating the features of external stimuli or the types of cognitive operations performed in a task (e.g. memory, categorization, discrimination, attention) can alter the shape, amplitude, and/or time-course of portions, or components, of the overall waveform. Furthermore, experimental manipulations have demonstrated that various modulations of ERP components will differentially manifest at different channel locations across the scalp, presumably reflecting cortical brain processes occurring in brain areas with varying locations and orientations in relation to the location and orientations of the recording scalp electrodes. As such, a plethora of ERP components putatively related to sensory and cognitive processes have been described in the literature.

Not only are the amplitudes and time-course, or latency, of components amenable to experimental manipulations, but also various groups of individuals (i.e., clinical populations) show consistent variations in ERP components while engaging in various experimental tasks. This makes ERP methodologies useful for understanding aberrant brain processes underlying cognitive deficits associated with various psychopathologies, neurocognitive conditions, or, more pertinent to this dissertation, alterations in brain function associated with frequent cannabis use. For instance, the specific ERP components examined in this dissertation, mismatch negativity (MMN), and auditory

P300 (described in more detail in appropriate sections), have been well documented in cognitive research and implicated in various psychopathologies (i.e. schizophrenia).

It should be noted that whereas ERPs have a definite advantage of temporal specificity (on a millisecond timescale), which is useful for delineating cognitive processes that occur rapidly, this method lacks spatial resolution compared to other imaging methods (i.e., fMRI). The following sections will describe methodologies used in this dissertation to localize scalp electrical activity to cortical generators, which somewhat overcome this disadvantage.

### *Independent Component Analysis*

Independent Component Analysis (ICA) is a blind source separation method and has broad applications (e.g. sound and video processing, telecommunication etc.) (Stone, 2002). A full technical account of ICA is beyond the scope of this dissertation, but a brief discussion is warranted as ICA was utilized in each study described in this dissertation to facilitate the identification and removal of artefactual activity from the channel data (e.g. eyeblinks, muscle activity, and channel noise) (Viola et al., 2009). Furthermore, independent components (ICs) form the basis upon which the scalp level activity was localized to brain sources (see Source Localization section below), and upon which subsequent analyses of localized oscillatory brain activity (see ERSP section below) and interregional functional connectivity analyses (see PLV section below) were performed.

Recall from the previous section that the electrical activity at any given scalp electrode is the additive sum of numerous brain processes. ICA works from the assumption that the signal measured at each scalp sensor is a linear additive mixture of numerous generators (i.e., in this case collective fields generated by the post synaptic potentials of the radially oriented pyramidal neurons in cortical brain tissue), which through volume conduction, propagates to all channels to some degree (Makeig, Jung, Bell, Ghahremani & Sejnowski, 1997). Differences observed between channels at any given time point arise from differences in the position and orientation of the sensor with respect to generators of the electrical signal. Because all scalp channels will contain some information in common with all other channels, however, they are not independent from each other, which makes raw channel recordings unsuitable for source localization and limits the interpretability of functional connectivity analysis based only on channel-level data.

A useful (though not completely equivalent) analogy is that of a band playing a concert. If one were to take a recording from multiple microphones spread out throughout the venue, each recording would contain aspects of the performance, but given their differing locations, the sound properties of each recording would vary to some degree. Some of the recorders might have a louder signal from the guitar, others the vocals or keyboard, and some will pick up noise from audience members. ICA could be used to separate the individual components (i.e. instruments or the noise) by taking advantage of the correct assumption that the generators of the various sound components (i.e. musicians, audience etc.) are independent from each other and are generating a signal that is not random (i.e. non-Gaussian) (Stone, 2002).

In a similar sense, brain sources can be considered independent and non-Gaussian (Stone, 2002). ICA takes advantage of these statistical properties via an algorithm that takes into account the time-series of electrical recordings across the entire range of sensors, and outputs statistically independent signals along with matrices of weighting coefficients that map the relative contribution of each resultant independent component to each sensor (Stone, 2002). These weighting matrices allow the sources to be recombined to recreate the original signal at each channel. An interesting property of this process is that some of the independent sources will represent activity that is artefactual; identification of these artefacts will be addressed in more detail in Methods of subsequent chapters (see Fitzgibbon et al., 2016; Viola et al., 2009). Thus, because of the additive linear nature of composite signals, omitting these artefactual ICs from the recombination process effectively cleans the channel data of noise, while retaining relevant information from brain areas. Furthermore, as many of these components will represent discrete, dipolar, brain processes, analysis of ICs allows a more nuanced account of brain activity than is possible by examining the channel data alone (Delorme, Palmer, Onton, Oostenveld, & Makeig, 2012; Makeig et al., 1997).

#### *Source Localization (Equivalent Dipole Fitting)*

EEG scalp activity allows for high temporal resolution, which is useful for understanding the time course of momentary fluctuations of brain activity related to mental processes. Conversely, EEG is limited by its lack of spatial resolution. That is, whereas it can determine *when* processes are occurring in the brain, it can't say as much about *where* they are happening. As such, numerous methods have been developed with the aim of

localizing scalp EEG to brain sources with promising results (Grech et al., 2008), though these approaches have not been without criticism (see Luck, 2005, for example). While EEG source localization is not nearly as precise as imaging techniques such as fMRI, our lab has, nonetheless, had success in localizing ICs relevant cortical sources consistent with those that have been identified by more precise functional imaging techniques (e.g. Bedo, Ribary & Ward, 2014; Maclean & Ward, 2014). Given this convergence, we can be reasonably confident in our source localization methods.

Our lab primarily uses a method of source localization method that fits ICs (see ICA section) to single equivalent dipole models of cortical source activity (Scherg, 1990). Decomposing scalp data with ICA results in ICs that have scalp distributions of electrical current, many of which resemble projections of single electrical dipoles, which are expected based upon recordings taken from the cortical tissue. It should be noted that the brain does not contain actual dipoles, but the additive coordinated activity of radially oriented pyramidal cells within certain cortical tissues (see EEG section above) can be modelled as a dipole. Unfortunately, localizing sources to deeper structures is not highly reliable with current methodologies. It is important to emphasize that our method does not analyse the dipole source activations, which indeed are not computed. Rather we analyse the activation time series of the ICs whose sources have been localized to dipoles in various brain areas based upon established brain models (Maclean & Ward, 2014). The dipole locations aid in the interpretation of the ICs but are not used in the various analyses (ERSP, PLV, etc.) of those ICs.

Localizing sources or objects via electromagnetic activity is a common practice in science, engineering (e.g. astronomical phenomena and GPS), medicine (e.g. x-rays, MRI) and cognitive neuroscience (fMRI, MEG). EEG source localization is hampered by volume conduction (see ICA section). Given a known cortical source, it is relatively straightforward to compute how the electrical activity would appear at the scalp, such solutions are well-posed in that solutions converge on a unique solution (so-called forward models). Inferring multiple cortical sources from scalp current distributions is problematic because there are virtually an infinite number of solutions (so-called ill-posed inverse problem). The dipole fitting algorithm we use (DIPFIT2 in EEGLAB; Delorme, Palmer, Onton, Oostenveld, & Makeig, 2012) mitigates the inverse problem by first calculating the forward model for scalp distributions based upon models of all cortical equivalent dipoles (modeled on 3D spatial coordinates, orientation, and magnitude) and an established head model. The head model approximates volume conduction based on known electrical properties of various tissues and then projects these into the 3-dimensional MNI (Montreal Neurological Institute) coordinate space of a standardized brain. We use a 4-shell Boundary Element Model (BEM), which models volume conduction of four tissue types (brain, cerebral spinal fluid, skull, and scalp). DIPFIT then optimally fits each IC by minimizing the residual variance between the observed scalp distribution and the projected scalp map (Scherg, 1990; Maclean & Ward, 2014). We only fit a single dipole, for each IC, as the inverse problem is well-posed for single equivalent dipoles because a gradient descent method is used to find a global minimum, whereas for multiple dipole models, many dipole configurations can give rise to observed scalp activity. Once each IC has been fitted to a dipole location, we reject ICs

that are localized outside the head or fall beyond a threshold of allowable residual variance from a single dipole model (~15%). The remaining ICs for each participant are then input into a clustering algorithm, which groups ICs based upon their spatial location (see Chapter 2 Method for more details). Clusters that meet our inclusion criteria (i.e. centroid is in theoretically relevant region of interest (ROI); cluster is densely packed around centroid; one IC per participant per cluster; and 50% of sample contributing a retained IC to the cluster) are selected for further analysis. Again, all subsequent analysis on ROIs are performed on clusters of ICs (*not* on fitted dipolar brain source activations), that have been grouped based upon their projected brain location. Thus, source localization provides a useful constraint for interpreting ICs but that is its only role (Maclean & Ward, 2014).

#### *Localized Oscillatory Activity - Event-related Spectral Perturbation (ERSP)*

Broadband EEG signals are comprised of the sum of brain oscillations at different frequencies generated by neural systems called “sources.” Once these sources have been identified using the procedures of ICA and dipole fitting, examining the various frequency components of these signals allows for a more nuanced understanding of cognitive processes. Computing event-related spectral perturbations (ERSPs) allows the quantification of the moment-to-moment fluctuations in oscillatory power in a given brain region. In context of this dissertation, ERSPs provide an additional advantage over ERP analysis, in that here they are first computed over single trials, before averaging, which captures potentially meaningful activity which may not be rigidly time-locked to a

stimulus and would otherwise be lost as noise by the summative ERP averaging procedures previously discussed.

To extract oscillatory activity from these signals, a wavelet decomposition is applied to discrete sections, or epochs, of EEG recording, time-locked to an experimentally manipulated event, which results in a time-frequency representation of the continuous EEG time-series. Such wavelet decompositions are widely applied in the fields of signal processing and have broad application in many areas of daily human life (i.e. telecommunications). ERSP of oscillatory power, expressed in decibels (dB), is the log ratio of the oscillatory power of a given frequency and time point to a standard baseline of neutral time-frequency points. The values can be used to quantify whether various cognitive processes applicable to various experimental manipulations, and/or between specified groups of individuals (i.e. cannabis users), show differing patterns of activation within localized brain regions, thus providing more detailed information pertaining to the nature of the cognitive processes and a more specific account of the effects of frequent cannabis use.

#### *Functional Connectivity - Phase Locking Value (PLV)*

Whereas ERSPs provide meaningful information for describing dynamic oscillatory activity localized to brain regions, cognitive processes are not isolated to singular brain regions, but instead reflect coordinated activity and communication between regions (Lachaux, Rodriguez, Martinerie & Varela, 1999). As such, indices of functional connectivity between highly networked brain regions are necessary to understand how these processes work and how they break down. This dissertation makes use of phase-

locking values (PLVs) to index which isolated brain regions are sharing information over discrete time periods within specific frequency bands of their oscillatory activity. The concept underlying PLV analysis is that information transfer between two brain network nodes is optimized under conditions of coordinated oscillatory activity (Fries, 2005; Varela, Lachaux, Rodriguez & Martinerie, 2001 ). Activity in both regions at a given time point may be in different phases, but across a specified series of time points, coordinated activity in this sense implies a somewhat constant relationship, or phase difference, be maintained across both regions. If a consistent pattern of phase difference persists over many trials, then these regions are said to be phase-locked and it is inferred that they are possibly sharing information and hence functionally connected (Sauseng & Klimesch, 2008). Similar to ERSPs, wavelets are used to decompose the time-series data of two brain regions into oscillatory activity; however, rather than calculating spectral power the phase information of these decomposed waveforms is used to calculate the phase locking value (PLV). The PLV indexes the degree that phase differences between brain regions remain constant across a specified time period over multiple trials. The PLV ranges from 0 to 1; where 0 represents the absence of phase-locking and 1 represents perfect phase-locking across trials. PLVs are calculated for frequency bands of interest to provide a nuanced description of functional connectivity between networked brain regions and this dissertation uses these methods to compare these functionally connected networks across experimental conditions and between groups of cannabis users and non-users. See Figure 1.7 for a general schematic of how PLVs are computed.

Figure 1.7. Schematic Depicting Calculation of Average PLVs Across Trials From Individual Trial Phase Difference Between Two Recording Sites

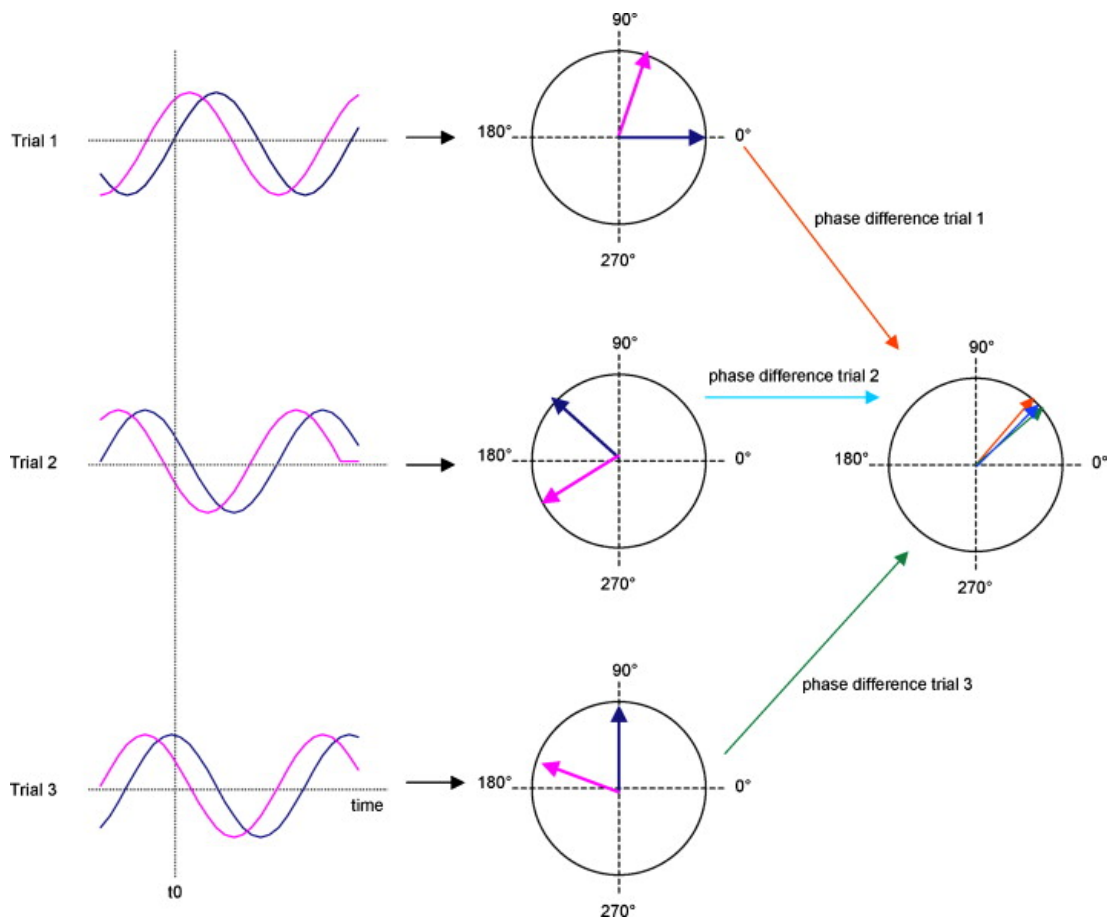


Figure 1.7. Phase synchrony as indexed by phase locking values (PLVs) represent the single trial difference of instantaneous phase angles between two recording sites averaged across all trials. The above figure demonstrates that at a particular time point the absolute instantaneous phase angles for each recording site may fluctuate from trial to trial; however, the relative difference of the phase angles between sites remains relatively constant across trials, suggesting functional connectivity between the sites. Figure adapted from Sauseng and Klimesch (2008), reprinted with permission.

## Overall Goals, Outline, and Predictions

This research adds to the literature by providing a sophisticated analysis of the underlying network dynamics associated with the MMN, oddball P300, and working memory deficits observed in chronic cannabis users. Pursuant to this goal, we utilize a roving local-MMN-global oddball P300 task along with a modified *n*-back task using identical

basic auditory stimuli. This enabled a more nuanced characterization of the frontal and posterior generators thought to underlie the MMN, oddball P300, and auditory working memory.

More specifically, Chapter 2 introduces a novel roving local-global oddball task that extends research conducted in our lab by Elizabeth Blundon that in turn is an extension of research by Bekinschtein and colleagues (2009). This task is unique in that it allows within a single task the ability to examine both MMN responses to local deviations embedded within each stimulus as well as P300 responses to global oddball pattern deviants. As it was our goal to better understand brain activity underlying this experimental task, Chapter 2 moves beyond relatively simple channel level ERP findings to describe activity in task relevant localized brain regions derived from clustered independent components that have been source localized using the dipole fitting procedure. Within these localized regions we then examined broadband ERPs and oscillatory activity using event-related spectral perturbation (ERSP). Finally, we describe communication between brain regions by looking at synchronous activity inferred from phase locking values (PLV) within particular frequency bands of interest. The findings of this study inform the choice of analysis used in Chapter 3.

Chapter 3 builds upon the methods described in Chapter 2, by using the roving dual (local global) oddball task to investigate the effects of chronic cannabis use on behavioural performance, neurocognitive functioning, MMN and P300 ERP response, as well as underlying brain activity and network activity associated with these phenomena. The

oving dual oddball task provides a wealth of information particularly pertinent to understanding the effects of frequent cannabis use as both the MMN and P300 have been shown to be impacted by chronic cannabis use. Since the underlying electrophysiological brain network activity associated with the effects of cannabis use are less well understood, our aim was to add to the literature by better articulating these processes by examining ERSPs and PLVs, as was discussed for Chapter 2. We expected to observe attenuated MMN amplitudes in cannabis users, and we expected that cannabis users would perform more poorly on the more difficult condition of this task resulting in attenuated P300 amplitudes and/or longer latencies and that these effects would be particularly reflected in underlying fronto-parietal brain network activity.

The design of Chapter 4 is identical to Chapter 3 except that a novel auditory *n*-back task is used to examine the effects of frequent cannabis use on auditory working memory. The task itself maintains similarity to the task employed in Chapter 3 in that the stimuli are identical. As with the previous chapters, we examined channel level ERP activity (i.e. P300) and provided a more detailed appraisal of the underlying brain network activity pertaining to auditory working memory. Memory deficits have been well documented in cannabis users, although as a whole auditory working memory has been less well researched compared to other modalities (i.e. visual, verbal, semantic etc.), so the study described in this chapter contributes to a better understanding of both auditory working memory and the impact of frequent cannabis use on underlying brain processes. We expected that cannabis users would perform more poorly on the working memory tasks,

and predicted that this should be reflected in attenuated P300 amplitudes and in underlying network activity.

Chapter 5 looks at combined data from Chapters 3 and 4 to compare local MMN ERP responses across a larger sample of frequent cannabis users and non-users. While the tasks in these studies examine different cognitive functions, the use of identical stimuli in both the roving local global task and the auditory *n*-back tasks allowed us to investigate MMN responses elicited by local deviations within the stimuli. MMN responses of these sorts have been posited to be largely automatic and somewhat invariant to task demands. In particular, we examined channel level MMN ERPs and looked at associations between these and self-report measures that measure subjective experiences related to aberrant sensory processing and trait schizotypy, and also associations with performance on neuropsychological tests indexing IQ, verbal and perceptual reasoning, working memory, and sustained attention. We expected to see attenuated MMN amplitudes in cannabis users, as well decreased working memory performance, and higher scores on trait schizotypy. We also expected to see increased aberrant subjective sensory experiences in cannabis users and for these to be associated with the MMN.

Finally, Chapter 6 provides a synthesis of all the studies contributing to this dissertation, discusses the contributions and application of this research to the broader field of research and practice, and concludes by addressing general limitations and future directions.

## **CHAPTER 2: A Novel Roving Auditory Local-Global MMN/P300 Task**

### **Introduction**

Various theories have been put forward to explain the nature of the auditory mismatch negativity (MMN) and a multitude of studies have been published and indeed entire conferences (Sussman & Shafer, 2014) have been dedicated to better understanding variable patterns of results that have emerged under various experimental conditions. Decades of investigations into the MMN using simple oddball MMN paradigms using frequency (pitch), duration, and sound intensity deviants has led to two major, seemingly contrasting, theoretical models: the model adjustment theory and the adaptation theory (see chapter 1 for more detailed description). More recent investigations have drawn on evidence from more complex MMN designs, such as using roving frequency stimuli, or presenting deviants in both ears (Deouell & Bentin, 1998; Haigh et al., 2017; MacLean & Ward, 2014), which suggests that hierarchical predictive coding models might best account for experimental observations that seemingly appear to differentially support the model adjustment and adaptation theories.

Directly pertinent to the current study, researchers have sought to use dual-oddball MMN/P300 tasks to disentangle aspects of auditory processing that are automatic from those that require conscious processing. Bekinschtein and colleagues (2009) utilized a dual (local-global; MMN/P300) oddball task in which series of 5-sound patterns were presented. Some patterns consisted of five identical sounds (“flat” run), whereas others consisted of four identical sounds followed by a different fifth one (“change” run).

Comparison of ERPs to the fifth tones of the two patterns generated a “local” MMN. They found that violation of the local expectation generated by the first four sounds in a pattern yielded a typical MMN effect in the 130 ms to 300 ms range. This local MMN was observed during various different task conditions, including counting of global pattern deviants, attention engagement on a distractor task, and while mind-wandering, suggesting that the local MMN is generated by an automatic process. They identified the bilateral superior temporal auditory cortices and frontal generators (though stated that this was to a lesser extent) as potential sources for the local MMN. A response to a global oddball (i.e., rare sound *pattern* generating a P300 ERP component) was present only when participants counted the global oddballs, and not when mind wandering or when attention was directed to a distractor task. Brain network areas identified to underlie this phenomenon included the prefrontal cortex, cingulate, and temporal regions (Bekinschtein et al., 2009). This pattern of results has been replicated under varying task conditions and has been explained in the context of hierarchical predictive coding (Chennu et al., 2013; King, Gramfort, Schurger, Naccache, & Dehaene, 2014; Wacongne et al., 2011). In our lab, we have replicated the phenomenon but have found an asymmetry between the two types of global task; detecting a flat run amidst a series dominated by change runs is more difficult and generates a later P300 than detecting a change run amidst a series dominated by flat runs. We also observed a behavioural asymmetry between these conditions, in that participants were more accurate and faster at detecting rare change runs amongst common flat runs compared to detecting rare flat runs amongst common change runs (Blundon, Rumak & Ward, 2017).

In unpublished data from our lab, we also observed a similar local asymmetry effect in the MMN amplitude to salient stimuli, with larger and later MMNs in response to rare target change runs compared to another condition where identical change runs appeared as common standards. This finding contrasts with Bekinschtein and colleagues' (2009) suggestion that the local MMN to change stimuli is invariant to the global context in which the stimulus appears (i.e. MMN to frequent, non-target, change runs is the same as MMN to rare, target, change runs).

The current study builds on the Bekinschtein et al. (2009) paradigm by adding a roving component where each stimulus has a different base frequency (defined by the tone frequency of the first four tones in each 5 tone stimulus) from the one that preceded it and in a sense merges the Bekinschtein et al. (2009) and the Garrido et al. (2008) paradigms (see also Haenschel, Vernon, Dwivedi, Gruzelier & Baldeweg, 2005). The idea here is that the asymmetry we identified in the Bekinschtein et al. paradigm could be due to different attentional strategies used to identify salient vs. non-salient rare targets. The change runs have a built-in salient feature that makes it pop out amongst a series of non-salient flat runs. Thus, when detecting rare target change runs, it is plausible that participants might use a more diffuse attentional strategy that relies more on salient feature detection rather than a more directed search strategy needed to detect non-salient rare target flat runs amongst a series of salient non-target change runs.

The aims of the current study are to determine whether adding a frequency roving feature to the paradigm mitigates the asymmetry seen in the MMN and P300 elicited by identical

changing stimuli but occurring in different contexts, and whether frequency roving mitigates behavioural and observed latency asymmetries between salient and non-salient global targets. The MMN/P300 results of the present study will also be used to determine how the conditions will be compared in Chapter 3, where the same experimental paradigm is utilized to investigate the effects of recreational cannabis use. Finally, as this is a relatively novel paradigm, the final aims of this study were to identify the relevant brain network nodes derived via source localization (i.e., dipole IC clusters), investigate ERP and theta and gamma oscillatory activity (ERSPs) within these nodes, and describe patterns of brain network communication between these nodes within these frequency bands (i.e., PLVs). Again, these analyses establish the foundation for interpreting the results of Chapter 3, and to some extent, to aid interpretation of Chapter 4, which uses identical stimuli to the ones used in this chapter, albeit in a different task, to probe working memory in cannabis users and non-users.

## **Method**

### ***Participants***

Data were collected initially from 23 participants. Two participants opted to discontinue the task prior to completion and thus these data were not included in analysis. Of the 21 remaining participants, data from three participants were excluded due to extreme behavioral measures ( $d' < .05$  averaged across conditions), or for excessive noise in the EEG recordings. Thus, 18 participants (13 female, age 18 to 31 years, mean age 22.3 (SD= 3.8)) were included in the analysis. The experimental protocol was approved by the

University of British Columbia Behavioural Research Ethics Board in accordance with the provisions of the World Medical Association Declaration of Helsinki. Participants gave informed consent and were offered monetary compensation (\$10/hr) for their participation. All participants but one were right-handed and no participants reported hearing or neurological difficulties.

### ***Experimental Procedures***

#### *Roving Dual Oddball Stimuli*

Auditory stimuli consisted of auditory runs that were 650ms in duration. Runs were comprised of 5x50ms tones (100 ms SOA), presented at 70 dB SPL via insert earphones (Etymotic EAR 3A) in a sound attenuated chamber using Presentation software (Neurobehavioural Systems, Berkeley, CA). There were two categories of auditory runs: flat and change runs. Flat runs consisted of five tones of the same frequency and change runs consisted of 4 identical tones of the same ('base') frequency plus a fifth tone that that was +/- 50 Hz (change runs). To facilitate the inter-trial frequency roving feature of this experimental task, base frequencies varied from 500 Hz to 800 Hz in 50Hz steps (i.e. 500, 550, 600, 650, 700, 750, and 800 Hz), resulting in seven varieties of flat runs and 14 varieties of change runs (7 change-up and 7 change-down).

#### *Procedure*

Participants were presented with two conditions (termed here feature present and feature absent) of a roving dual (local-global) oddball task where participants were asked to respond to rarely occurring oddball target runs embedded in a sequence of commonly occurring standard runs. The task was designed to investigate both (i.e. dual oddball)

global effects of auditory change detection (i.e. response to rare oddball targets; P300) and local effects (i.e. response to 5<sup>th</sup> tone in change stimuli; MMN). In the feature present (FP) condition rare targets were change runs and common standards were flat runs; whereas in the feature absent (FA) condition, targets were flat runs and standards were change runs. The feature present condition is named as such because it is analogous to visual paradigms where the goal is to detect rare salient *feature present* stimuli amongst a field of commonly occurring less salient *feature absent* stimuli (i.e. detecting a Q amongst Os: O O O O Q O O); in the present study the rare change runs contain a salient distinguishing feature whereas the flat runs do not. Similarly, the feature absent condition is analogous to detecting rare less salient *feature absent* stimuli amongst commonly occurring *feature present* stimuli (i.e. detecting an O amongst Qs: Q Q Q Q O Q Q). There were eight experimental blocks with the FP and FA conditions each being repeated four times in a pseudorandom order. Prior to starting the experiment, participants were familiarized with the stimuli and provided on-screen instructions describing the task. At the beginning of each block participants were instructed to pay attention to the initial sequence of stimuli to determine whether flat or change-runs were rare targets and to respond via button press to rare runs using their dominant hand. For each condition, the oddball sequence began with 30 standard runs after which target runs were presented randomly, 20% of the time. Each oddball sequence lasted approximately 4.5 minutes, in which participants heard approximately 18 to 30 target runs. Within each oddball sequence, stimulus presentation was pseudorandom in that a minimum of two standard runs always preceded a target run. Additionally, to facilitate the frequency-roving feature of this task, each run (whether target or standard) always differed in base frequency from

the preceding run. Successive runs were separated by an ITI that varied randomly from 1000 ms to 1650 ms (See Figure 2.1).

Figure 2.1 Roving Dual Oddball Task

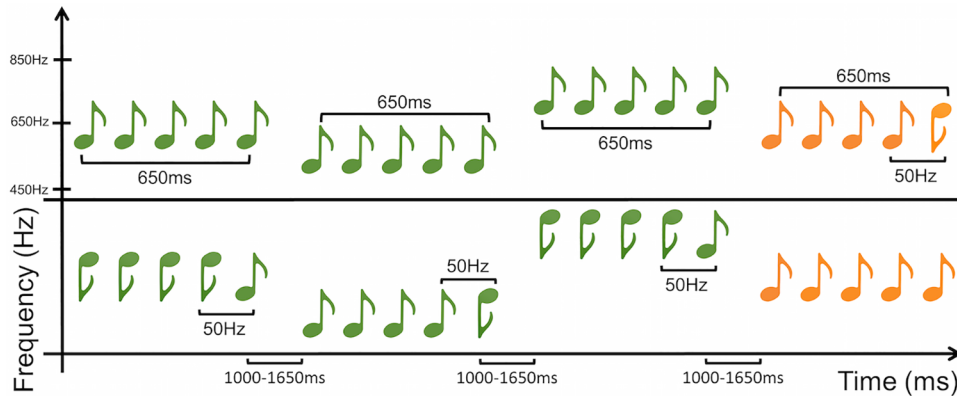


Figure 2.1 Participants completed both feature present (top) and feature absent (bottom) conditions, each involving an extended series of auditory runs. In the feature present condition, flat runs were common and change runs were rare targets. In the feature absent condition change runs were common and flat runs were rare targets. The base frequency of flat and change runs varied in pitch and change runs could change up or change down (+/- 50Hz) from the base frequency (see Methods). Common runs are depicted in green, rare runs are in orange. Figure adapted from Blundon, Rumak and Ward (2017).

### ***Behavioural Analysis***

Behavioural accuracy was determined by computed by using d-prime ( $d'$ )

discriminability index scores based upon hit rates and false alarm rates for both FP and FA conditions, for each participant separately. In cases where participants demonstrated either perfect hit rates or demonstrated no false alarms, a score of 0.5 (i.e., chosen to distinguish participants with perfect hit or false alarm rates from those who had 1 miss and/or 1 false alarm) was either subtracted from total hits, or added to total false alarms, respectively, to allow  $d'$  to be calculated; the assumption being that given an infinite

number of trials a participant would eventually miss a target, or respond to a non-target (Macmillan & Creelman, 2005).

Mean reaction times (RT) were also computed for each participant's correct response to FP and FA targets. As participants were instructed to withhold responses until the termination of each run, mean reaction times (in ms) are presented in reference to onset of the final tone.

### ***EEG Acquisition***

EEG recording parameters were identical to those specified in Blundon, Rumak and Ward (2017). Scalp EEG signals were digitized at a sampling rate of 500 Hz (National Instruments Inc Vaudreuil-Dorion QC Canada) from a 60-channel electrode cap (Electrocap Inc Eaton OH USA, International 10-10 placement) using a right mastoid reference. Prior to digitization, EEG signals were amplified and analog bandpass filtered from 0.1 Hz to 100 Hz (SA Instrumentation San Diego CA USA). Four periocular electrodes were used in a bipolar arrangement to measure vertical and horizontal eye movements. Prior to recording, impedances for each electrode site were inspected and adjusted to ensure that each was below 10 k $\Omega$  (amplifier input impedance > 2 g $\Omega$ ).

### ***Offline Processing***

Offline EEG data analysis was conducted using EEGLAB software (Delorme & Makeig, 2004). Data were first down-sampled to 250 Hz and re-referenced to average reference. Continuous EEG data unrelated to active task condition (i.e., rest periods and instructions etc.) were pruned manually, so as not to introduce extraneous noise into subsequent independent component analysis (ICA). We subjected the channel data to an infomax

based ICA algorithm (runica algorithm in EEGLAB; Bell and Sejnowski, 1995; Delorme, Palmer, Onton, Oostenveld & Makeig, 2012). This blind source separation method takes into account the information from all EEG channels to create independent components (ICs) represented as new virtual channels containing independent signals free of the volume conduction observed in scalp electrodes and relatively free of EMG contamination. Artifacts were rejected by visually inspecting and removing noisy ICA components (i.e., spectra that were not 1/f-like, or whose continuous plot were indicative of EoG, EMG, or bad channel data) (Fitzgibbon et al., 2016). A simplified overview of the EEG processing steps can be viewed in Figure 2.2.

### ***Channel Level ERP Analysis***

ERPLAB (Lopez-Calderon & Luck, 2014), an ERP analysis software that runs in EEGLAB, was used to process and visualize channel level ERP data. ERP processing was conducted as reported in Blundon, Rumak and Ward (2017). Continuous EEG data were divided into 2200 ms epochs (-200 to +2000 ms relative to onset of first tone for each run) for each participant. For analysis of local MMN response, two epoch types were created (change and flat) for all auditory runs ignoring whether a run appeared as a rare target or common standard and ignoring any correct or incorrect behavioural responses. For analysis of FP and FA MMN and P300 ERPs to global oddball targets, averaged epochs were created for rare oddball target runs that were correctly responded to and the common runs that immediately preceded each of these target runs, which resulted in four epoch types (rare change, rare flat, common change and common flat). This ensured equal numbers of common and rare-run-epochs for the latter analyses. As the base frequency of each sequentially presented stimulus randomly roved from 500-

800Hz, each epoch type constituted the average over all seven of the base frequencies. The randomization algorithm tended to distribute base frequencies uniformly across the four epoch types; we did not examine ERPs to each separate base frequency as there would have been too few epochs in each category to reliably calculate ERPs. All epochs were low-pass filtered at 30 Hz using a FIR filter, and baseline corrected (-200 to 0 ms relative to the onset of first tone in each run). Where applicable, for ease of visualization and interpretation, shortened segments of these epochs were chosen for display purposes, especially in cases where ERPs following onset of the fifth tone were of interest.

### ***Local MMN ERP Measurement***

Local MMNs were measured at fronto-central channels (Fz, FCz, and Cz) and characterized as difference waves (deviant – standard) between an ERP response to changing runs and flat runs regardless of whether the change run was rare (global oddball target) and the flat run was common (global oddball standard), or vice versa (i.e. all change runs – all flat runs). This allowed an analysis of all stimuli (at least several hundred for each participant), which enhanced overall signal to noise ratio, and allowed for statistically powerful comparisons of MMN components that are presumably invariant to task demands across the various tasks. The peak MMN amplitude and latency was defined as the largest negative deflection within an extraction window of 700ms to 850ms (100 to 250ms after onset of 5<sup>th</sup> tone in each stimulus run). A local peak selection method of 5 time points (10 ms to each side of the peak) was used to account for local fluctuations that may bias peak selection.

### ***Measurement of Feature Present and Feature Absent MMNs***

MMNs were measured at fronto-central channels (Fz, FCz, and Cz) and characterized as difference waves between an ERP response to rare global oddball target runs and immediately preceding common global standard runs. As such, separate difference waves were computed for FP (rare change runs – common flat runs) and FA (common change runs – rare flat runs) conditions. For the FA condition, a common minus rare arrangement was used to calculate the difference wave because the changing common run represents the deviant stimulus in the pairing; and, it was found that computing difference waves using rare minus common resulted in an inverse MMN morphology (i.e. positively deflected waveform) that was putatively dissimilar to MMNs typically described in the MMN literature. The extraction of peak latencies and amplitudes for both FP and FA difference waves were identical to those described for the local MMNs (see Local MMN ERP Measurement section above).

### ***P300 ERP measurement***

P300 characterization was identical to that outlined in Study 5 of Blundon, Rumak & Ward (2017). P300s were measured at channel Pz and defined as difference waves between a P300 response to the final tone of a run when that run was the rare target run compared to when that run was the standard non-target run. For example, when calculating FP P300s, we took the average ERPs to correctly-responded-to rare target change runs (across all base frequencies) and subtracted the average ERPs to all correctly-ignored common change runs (i.e. from the feature absent condition). This approach was taken to allow for a determination of the effect of the oddball targets within

the global context of the overall sequence of stimuli independent of the physical makeup of the run. Latency extraction windows were determined by examining the beginning and end of the entire P300 ERP morphology, taken from the grand average difference wave (average ERP from all participants) of each condition from the zero crossing where the potential begins to ascend from zero to the second zero crossing where the potential descends to zero. For each participant separately, the peak P300 amplitude and latency was defined as the largest positive deflection within an extraction window of 800ms to 1600ms (200 to 1000 ms after onset of 5<sup>th</sup> tone in each stimulus run). A local peak selection method of 10 time points (20 ms to each side of the peak) was used to account for local fluctuations that may bias peak selection. Measurement of P300 peak amplitude/latency was chosen rather than average amplitude across the extraction window to facilitate examination of temporal (i.e. latency) cognitive processing differences and to maintain consistency with the bulk of the literature that has examined the effects of cannabis use (pertaining to Chapters 3 and 4) on the P300 (e.g. D'Souza et al., 2012; de Sola et al, 2008; Theunissen et al., 2012).

### ***Dipole Fitting (Source Localization) and ROI Selection via Cluster Analysis***

Source localization was utilized to allow for clearer interpretation and selection of independent components (ICs) for further component ERP, ERSP and PLV analysis. The dipole localization of each IC was mapped to Talairach coordinates based upon the Montreal Neurological Institute (MNI) average brain, using the DIPFIT2 function included in the Fieldtrip plugin for EEGLAB.

Cortical regions of interest (ROI) included in ERSP and PLV analysis were derived via a two-stage process of group level  $k$ -means clustering and subsequent seeding of dipole locations using EEGLAB functions and custom MATLAB scripts. The  $k$ -means algorithm optimally minimizes intra-cluster distance while simultaneously maximizing inter-cluster distance. The resultant centroid of each cluster is the mean Euclidean distance of each IC that contributes to the cluster. Initially, 159 ICs (across all participants) with dipole fits of less than 20% residual variance (RV) were included in the clustering algorithm. The selection of the number of clusters to create using the  $k$ -means algorithm is an iterative process as there is no ideal *a priori* solution to the problem. As such, a common starting point involves making the number of clusters equal to the number of participants (18 in this case) and then iteratively increasing or decreasing the number of clusters based upon visual inspection of the tightness of the resulting clusters and considering the number of participants included in each cluster. Our criteria for including a cluster into an analysis requires that at least 50% of participants (9 in the case of this study; maximum of 1 IC per participant per cluster) be represented in each cluster. Specifying a larger number of clusters will typically result in clusters that are tightly packed around their centroid but with fewer ICs in each, while specifying fewer clusters will result in somewhat looser clusters with more ICs. Inspecting the output for the various different iterations involving variable numbers of clusters allows for a judgment to be made on the stability of various clusters and reduces the likelihood of spurious inclusion of ICs in a cluster. At each iteration, cluster centroids were identified and compared and clusters that appeared at various iterations increased confidence in the final cluster solution. For this sample, a solution of  $k=11$  clusters was deemed to be a

satisfactory compromise based upon the spatial packing of ICs around each centroid, the percent of participants included, and the clusters representing theoretically meaningful brain locations.

In stage 2 of the clustering process, the centroid locations for each cluster from stage 1 with more than 50% of participants represented were submitted into a seeding algorithm (Blundon & Ward, unpublished manuscript). This second stage of processing improves upon the single stage *k*-means clustering we have utilized in previous studies, as it mitigates bias introduced into the procedure by bypassing the necessity for manual pruning of ICs that the *k*-means algorithm places into respective clusters but appear to fall outside the cluster of densely packed ICs, and allows for the inclusion of ICs that may have been skipped over by the initial random assignment of ICs to clusters. This cluster seeding process involves selecting ICs that fall within a specified distance from a specified centroid location. For this sample, a Euclidian range of 30mm (in MNI space; Talairach locations were converted using the `tal2mni` function in Matlab) was deemed most suitable for generating tightly packed clusters that largely corresponded with the clusters generated in via *k*-means in the first stage of clustering. A total of eight of the 11 clusters from the *k*-means clustering were included (two left frontal and one spurious, albeit stable, subcortical clusters were omitted) in the seeding process resulting in six clusters (two fell below 50% participant inclusion criterion) to be included for further analysis (see Table 2.3 in Results Section).

### ***Event-Related Potentials (ERPs) for Independent Component Clusters***

Event-related potentials (ERPs) were computed by averaging epoched EEG independent component (IC) activity for each participant across trials for each of the four epoch types (feature present and feature absent targets and standards) for each IC ROI using STUDY level functions built into EEGLab, as ERPLab does not have functions to handle clusters/ICs. Cluster ERPs utilized a longer epoch (-1000 to 2000ms) than the channel level analysis above to accommodate the ERSPs and PLV analysis described in subsequent sections. Epochs were baseline corrected relative to a 200 ms pre-stimulus window and low-pass filtered at 30 Hz. ERPs from each condition were then compared using pairwise *t*-tests at each time point. Uncorrected analyses ( $\alpha = .05$ ) were used for this analysis as instances of significant differences between conditions sustained across multiple time points were primarily intended to provide a frame of reference to inform subsequent analyses of oscillatory and network connectivity.

### ***Event related spectral perturbation***

Computing Event-related spectral perturbations (ERSPs) is a method that allows the quantification of the moment-to-moment fluctuations in oscillatory power in a given brain region that provides a more nuanced examination of neural processes compared to ERPs as much of this information is often lost due to signal averaging. ERSP of oscillatory power, expressed in decibels (dB), is the log ratio of the oscillatory power of a given frequency and time point over a standard baseline of neutral time-frequency points. Wavelet coefficients were used to derive time-frequency oscillatory power for each cluster of ICs remaining after the previous pruning process. Power from 3 to 50 Hz was

computed using a sliding Hanning-windowed sliding cosine wavelet (EEGlab timenewf function; 1.5 Hz steps from 3-50 Hz) with linearly increasing cycles (1.8 cycles at 3 Hz to 30 cycles at 50 Hz) for each 3000ms epoch (-1000ms to 2000 relative to onset of first tone; 750 time points) resulting in a spectral output from 3 to 50Hz in 95 log spaced frequency bands over a compressed time range containing 471 time points (-440 to 1440 ms relative to onset of the first tone). ERSP comparisons were made for each time-frequency point for targets versus standards in each condition relative to a common baseline (dB). As error theory for this data type has not been established, a non-parametric permutation test using a surrogate distribution was used to test ERSP data for significance (400 permutations;  $\alpha = .005$ ). The surrogate distribution was generated using the ERSP data that have been scrambled and randomly distributed. Given the vast quantity of data points, and thus large potential for inflated family-wise error rate, only ERSPs containing large clusters of contiguous data significant at the group level were considered. The rationale for this is that large contiguous clusters have an extremely small probability of occurring by chance given the low probabilities of independent individual time-frequency points being significant in the group test. The minimum threshold of significant time points required decreases as frequency increases because the temporal resolution of the wavelet decomposition increases with frequency. As such, for the theta band we used a minimum threshold of 150ms (~38 time points) of continuous significance and 25ms (~6 time points) for gamma band activity (Onton, Delorme & Makeig, 2005).

### ***Phase synchrony***

Analysis of phase synchrony allows for the assessment of the relative degree of information sharing or functional connectivity between two brain regions. Theta band (3-7 Hz) phase-locking values (PLVs) between each pair of ICs localized to specific brain regions were investigated. PLVs indicate the degree of constancy of the phase differences between signals at a specific oscillatory frequency across trials with values ranging from 0 to 1 (0 = no phase locking; 1 = perfect phase locking). It is expected that a given time-series neural noise will lead to only stochastic phase locking ( $0 < \text{PLV} < 1$ ) (McDonnell & Ward, 2011). EEGLab's *newcrossf()* function was used to calculate PLVs for each participant for each of the 15 pairings of ROI clusters (i.e. a participant had to contribute ICs to each; see ICA above) at each time-frequency point within single trials, which were then averaged across epochs corresponding to correct targets and preceding standards in each condition separately, according to the following formula (Delorme & Makeig, 2004):

$$PLV_{1,2}(f,t) = \frac{1}{N} \sum_{k=1}^N \frac{W_{1,k}(f,t)W_{2,k}^*(f,t)}{|W_{1,k}(f,t)W_{2,k}(f,t)|}$$

where  $W_{i,k}(f,t)$  represents the wavelet coefficients at each frequency,  $f$ , and time point,  $t$ , for each independent component,  $i$ , and  $k = 1$  to  $N$  indexes each epoch. The resulting PLV output for each averaged epoch thus contained PLV values for each of the 471 time points (spanning -440 to 1436 of the original epoch) at each of the 95 (spanning 3 to 50 Hz) narrow frequency bands (a total of 44,745 time-frequency points). Obtained PLVs were then baseline adjusted by subtracting the mean baseline PLV value (-250 to -50 ms window preceding the onset of respective correct target or standard runs) for each narrow

frequency band, for each condition, from each data point of the 471 time points, separately for each participant. The resulting PLVs were then collapsed across the theta (3-7 Hz) and gamma (30-50 Hz) frequency bands by extracting the maximum absolute value at each time point for each respective frequency band.

Comparisons were made between target and standards separately for each condition (feature present and feature absent) within two time windows roughly corresponding to the MMN (700 to 850 ms) and P300 (850 to 1200 ms) peak latencies (see results section). Two-tailed *t*-tests ( $\alpha = 0.05$ ) were computed between targets and standards at each time point within each time window. Similarly, to characterize network connectivity versus baseline within each condition and target type, *t*-tests ( $\alpha = 0.05$ ) were used to determine if the average PLVs for each target type were significantly greater than zero. Computing baseline activations provides a means to interpret target versus standard comparisons as differences that emerge that are not accompanied by activation versus baseline are likely to be spurious. In this case, two-tailed *t*-tests ( $\alpha = 0.05$ ) were used to identify significant deviations from zero. It should be reiterated, that raw PLVs by definition cannot be less than zero; however, baseline adjusted PLVs can sometimes result in negative values. In this study negative values were not observed, so these were not represented in output figures.

To account for multiple comparisons, regions were only considered to be functionally connected if more than 50% of the time points within the time window were significantly greater for a target versus standard, or vice versa (or versus 0 for baseline connectivity).

The rationale for this chosen threshold rests on the assumption that the binomial probability of getting 50% or more significant tests within such a time window is extremely low. We used  $p = 0.05$  ( $q = 1 - p = 0.95$ ) as the probability of a success in a single binomial trial to compute the binomial probability of getting 50% or more significant time points by chance out of the total of time points in each bin, 19 of 37 for MMN and 44 of 88 for P300 window (Onton, Delorme & Makeig, 2005). This probability is  $1.4 \times 10^{-15}$  for the MMN window and  $1.6 \times 10^{-33}$  for the P300 window if all of the time points in a bin represented independent tests. This assumption is probably not precisely correct, although it is not too unreasonable because the tests were made across subjects, who were independent of each other. Since we made 15 (inter-regional) comparisons (each possible pairing of 6 different ROIs) for 2 time bins, there were  $2 \times 15 = 30$  such tests for each of 6 comparisons (2 conditions + 4 baseline comparisons). Thus, the experiment-wise error probability for each set of  $t$ -tests, assuming independence, was  $(30 \times 6 \text{ comparisons} \times 2 \text{ frequency bands} \times 1.3 \times 10^{-15}) + [30 \text{ pairs} \times 6 \text{ comparisons} \times 2 \text{ frequency bands} \times 1.6 \times 10^{-33}] \approx 4.8 \times 10^{-13}$ . Again, these tests are likely not independent so this is a liberal estimate of the experiment-wise probability of Type I error. For each MMN and P300 time bins, pairings that were significant, were plotted onto separate 6x6 matrices (representing each of the 30-connections for the 6 ROIs) for each condition. These were then fed into the BrainNet Viewer toolbox for MATLAB (Xia et al., 2013) to generate brain connectivity maps depicting the statistically significant functional connectivity between the various ROIs for each time bin.

Figure 2.2. General Workflow for EEG Processing

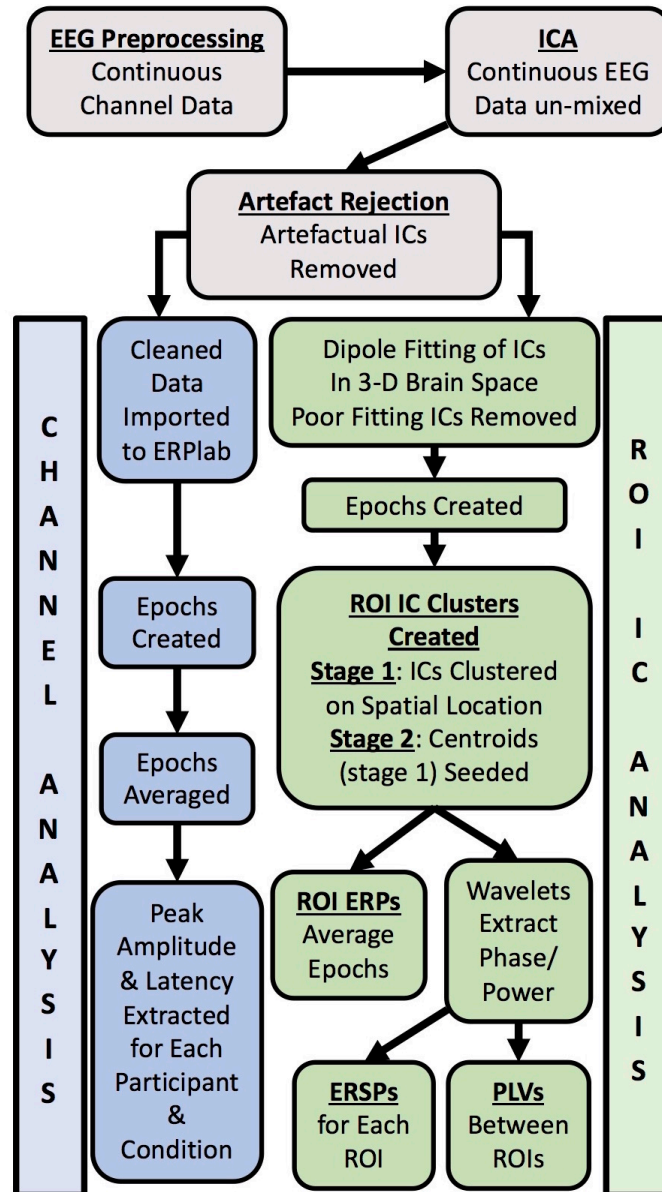


Figure 2.2. Simplified overview of EEG processing workflow. Top portion (grey) depicts preprocessing, independent component analysis (ICA) and artefact rejection processing steps preceding and common to analyses of both channel level data (blue) and independent components (ICs) localized to brain regions (green) of interest (ROI). ERP = event related potential; ERSP = event related spectral perturbation; PLV = phase locking values (i.e. phase synchrony/network functional connectivity). See respective Method subsections for more details.

## Results

### *Accuracy and Reaction Time*

Behavioural results can be found in Table 2.1. A paired sample *t*-test comparing  $d'$  scores for feature present and feature absent conditions revealed that participants were significantly ( $t(17) = 3.43, p = .003$ ) better at identifying target salient change runs in the feature present condition than they were at identifying less salient flat runs in the feature absent condition. A paired sample *t*-test ( $t(17) = -1.89, p = .075$ ) also revealed that participants had marginally faster mean RTs to feature present stimuli compared to feature absent stimuli.

Table 2.1. Behavioural Performance Data for Roving Local-Global Task

Measure	Mean (SD)		p-value (2-tailed)
	Feature Present	Feature Absent	
$d'$	4.45 (0.92)	3.93 (0.97)	.003
RT (ms)	541.58 (131.84)	562.10 (113.19)	.075

### *Channel Level ERP Analysis*

#### *Global Feature Present and Feature Absent MMN ERPs*

ERPs of difference waves at fronto-central midline sites (FZ, FCZ, CZ) to global deviants can be viewed in Figure 2.3 and values for mean amplitude and latency can be viewed in Table 2.2. Paired sample *t*-tests revealed that MMN amplitudes were larger at all three electrode sites for the feature present condition: Fz  $t(17) = -2.61, p = .018$ ; FCz  $t(17) = -3.66, p = .002$ , and; Cz  $t(17) = -4.57, p < .001$ .

Paired sample t-tests also revealed longer MMN latencies at all three electrode sites for the feature present condition: Fz  $t(17) = 4.24, p = .001$ ; FCz  $t(17) = 4.85, p < .001$ , and; Cz  $t(17) = -2.93, p = .009$ .

Figure 2.3. Grand Average MMN ERP Difference Waves for Feature Present and Feature Absent Conditions

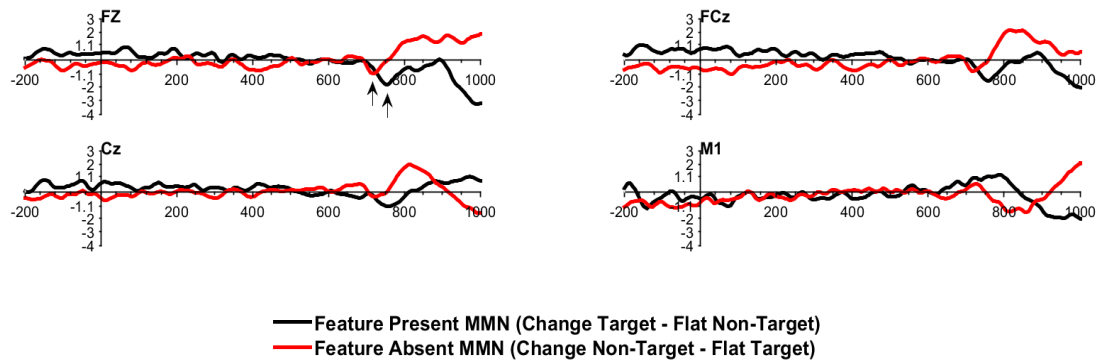


Figure 2.3. Grand average MMN ERP difference waves at channels FZ, FCZ, CZ, and M1 (left mastoid) for feature present and feature absent conditions. For display purposes only, ERPs were calibrated so that the waveform at 600ms corresponding to the onset of the 5<sup>th</sup> tone is at 0  $\mu$ V. Arrows at site FZ indicate the location of the MMN. Larger amplitude (more negative) MMNs occurring at a later latency are clearly visible at each midline site between 700 and 850ms (i.e. 100 to 250 ms post 5th stimulus onset at 600 ms) for the feature present condition. At the mastoid channel, the MMN reverses polarity, which indicates that the ERP component features highlighted at the frontal midline channels are indeed MMNs.

Table 2.2. Mean Amplitude and Latencies of Global MMN Difference Waves

Measure	Mean (SD)		<i>p</i> -value (2-tail)
	Feature Present	Feature Absent	
<b>Amplitude (<math>\mu</math>V)</b>			
Fz	-3.30 (2.47)	-1.24 (2.25)	.018
FCz	-3.17 (1.91)	-0.72 (2.09)	.002
Cz	-2.38 (1.11)	-.54 (1.57)	<.001
<b>Latency (ms)</b>			
Fz	172.22 (41.90)	126.89 (22.20)	.001
FCz	174.22 (37.73)	128.44 (18.55)	.000

Cz	170.00 (36.25)	135.33 (25.75)	.009
----	----------------	----------------	------

*P300 ERPs*

ERPs of P300 difference waves at sites at the midline parietal site (Pz) can be viewed in Figure 2.4. A paired sample t-test revealed that the P300 amplitudes at Pz were larger,  $t(17) = -2.61, p = .028$  for the feature present condition ( $M = 9.16 \mu\text{V}; SD = 3.49$ ) compared to the feature absent condition ( $M = 8.04 \mu\text{V}; SD = 3.49$ ). Mean peak latencies did not differ,  $t(17) = -0.92, p = .368$ , between the feature present ( $M = 497.56 \text{ ms}; SD = 124.23$ ) and feature absent conditions ( $M = 522.89 \text{ ms}; SD = 165.24$ ).

Figure 2.4. Grand Average P300 ERP Difference Waves for Feature Present and Feature Absent Conditions.

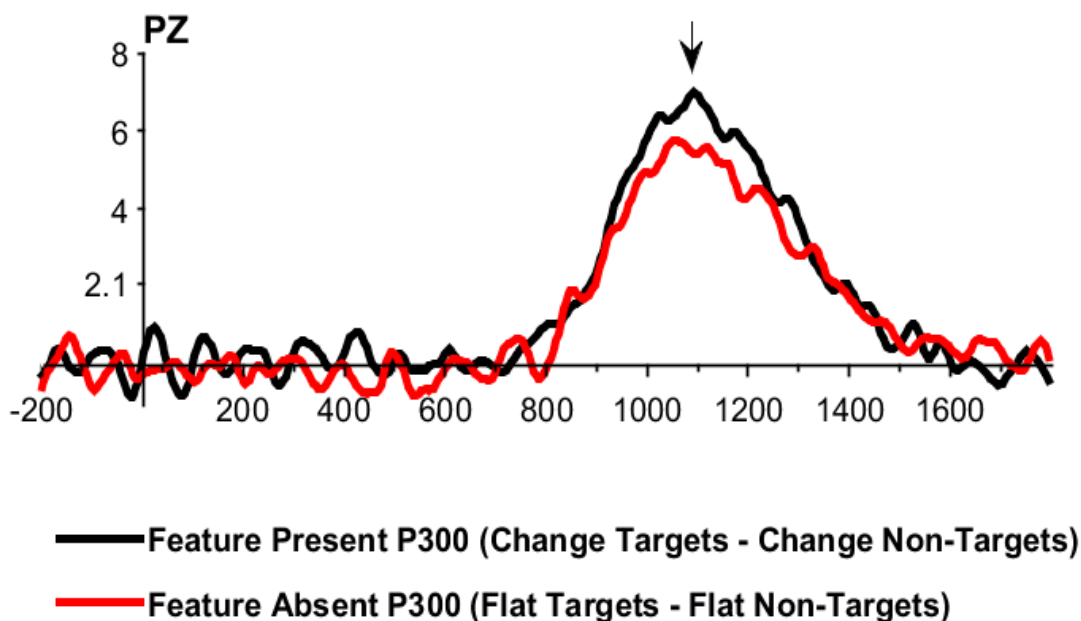


Figure 2.4. Grand average P300 ERP difference waves at channel Pz for feature present and feature absent conditions. The arrow indicates the location of the P300 peak at Pz. Both feature present and feature absent conditions can be seen to have similar latencies though a larger positive amplitude can be seen for the feature present condition.

### *Local MMN analysis*

ERPs of difference waves at sites at fronto-central midline sites to local deviants can be viewed in Figure 2.5. The local MMN amplitudes were computed at FZ ( $M = -1.39, \mu\text{V}$ ;  $SD = 1.26$ ), FCZ ( $-1.27 \mu\text{V}$ ;  $SD = 1.18$ ), and CZ ( $-1.06 \mu\text{V}$ ;  $SD = 0.85$ ). The local MMN mean latency values were measured at FZ (141.33 ms;  $SD = 30.31$ ), FCZ (134.44 ms;  $SD = 13.03$ ), and CZ (130.67 ms;  $SD = 16.58$ ) with respect to the onset of the 5<sup>th</sup> tone at 600 ms.

A fully-within 1 by 3 repeated measures Analysis of Variance (ANOVA) was conducted at each electrode site separately comparing peak amplitudes of all three conditions (global feature present, global feature absent, and local MMNs). At Fz, degrees of freedom were corrected due to a violation of sphericity ( $X^2(2) = 15.56, p < .001$ ) using a Greenhouse-Geisser correction ( $E = .617$ ). There was a significant main effect of condition,  $F(1.23, 20.96) = 7.54, p = .009, \eta_p^2 = .307$ . Pairwise comparisons revealed that feature present MMN amplitudes were larger (more negative) than both feature absent and global MMNs. Feature absent and global MMN amplitudes did not differ from one another. The exact same pattern of results was observed for MMN amplitudes at FCz,  $F(1.15, 19.48) = 13.37, p = .001, \eta_p^2 = .440$  (Greenhouse-Geisser corrected:  $X^2 = 21.90$ ;  $E = .573$ ) and Cz,  $F(1.31, 22.26) = 16.03, p < .001, \eta_p^2 = .485$  (Greenhouse-Geisser corrected:  $X^2 = 12.00$ ;  $E = .655$ ).

A similar ANOVA was carried out for peak MMN latencies across all three conditions for each electrode. At Fz, there was a main effect of condition,  $F(2.34) = 11.39, p < .001$ ,

$\eta_p^2 = .401$ . Pairwise comparisons revealed that feature present MMN latencies were later than both feature absent and global MMN peak latencies. Feature absent and local MMN latencies did not differ from one another. The same pattern of results was observed for MMN latencies at FCz,  $F(1.48, 25.21) = 20.43, p < .001, \eta_p^2 = .547$  (Greenhouse-Geisser corrected:  $X^2 = 6.86; E = .741$ ) and Cz,  $F(1.45, 24.60) = 16.03, p = .001, \eta_p^2 = .384$  (Greenhouse-Geisser corrected:  $X^2 = 7.71; E = .723$ ).

Figure 2.5. Grand Average MMN ERP Difference Waves Comparing MMN in Feature Present, Feature Absent, and Local MMN.

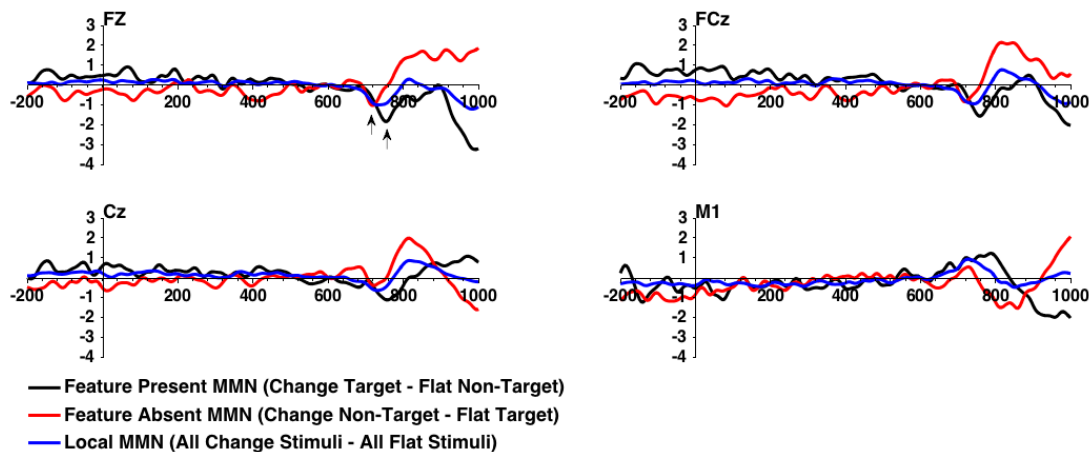


Figure 2.5. Grand average MMN ERP difference waves at channels FZ, FCZ, CZ, and M1 (left mastoid) for global MMNs (feature present and feature absent) and local MMNs (all change stimuli minus all flat stimuli). For display purposes only, ERPs were calibrated so that the waveform at 600ms corresponding to the onset of the 5<sup>th</sup> tone is at 0  $\mu$ V. Arrows at site FZ indicate the location of the MMN. Larger amplitude (more negative) MMNs occurring at a later latency are clearly visible at each midline site between 700 and 850ms (i.e. 100 to 250 ms post 5<sup>th</sup> stimulus onset) for the feature present condition compared to both the feature absent and local MMNs. Feature absent and local MMNs show similar amplitudes and latencies at each electrode site. At the mastoid channel, the MMN reverses polarity, which indicates that the ERP component features highlighted at the frontal midline channels are indeed MMNs.

### ***ROI Cluster Analysis***

Results of dipole clustering and identification of ROIs can be viewed in Table 2.3 and plots of retained clusters can be viewed in Figure 2.6. In total, six clusters pertaining to theoretically relevant brain areas met our criteria of containing over 50% of the sample participants. The locations selected were: right temporal-parietal junction (R.TPJ), L medial frontal gyrus (L.medFG), anterior cingulate cortex (ACC), posterior cingulate cortex (PCC), left cingulate (L.Cing), and the right precentral gyrus (R.preCG). These regions were included in subsequent ERP, ERSP and PLV analyses. Two clusters (left temporal-parietal junction and left pre-central gyrus) were excluded because they contained an insufficient number of participants to warrant further analysis. Contrary to expectations no auditory temporal clusters (i.e. right superior temporal lobe) were observed (at least in this study); this conspicuous omission will be addressed in the discussion section.

Table 2.3. Dipole Clusters of Independent Components Identified for Roving Local Global Task and Corresponding Brain Regions.

			<b>Centroid Talairach Coordinates</b>			
	<b>Percent Contributing</b>	<b>% VAF</b>	<b>X</b>	<b>Y</b>	<b>Z</b>	<b>BA #</b>
<b>Retained ROIs</b>						
R.TPJ	55.6%	85.86	32	-54	25	39
L.medFG	61.1%	87.28	-5	54	-15	11
ACC	66.7%	87.25	16	20	-4	47
PCC	72.2%	92.71	-1	-39	45	31
L.Cing	55.6%	87.8	-7	-1	27	24
R.preCG	55.6%	91.43	33	-7	48	6

Rejected ROIs						
L.preCG	33.3%	89.7	-36	-4	55	6
L.TPJ	33.3%	89.41	-36	-57	19	22

Figure 2.6. Dipole Cluster Plots of Retained ROIs

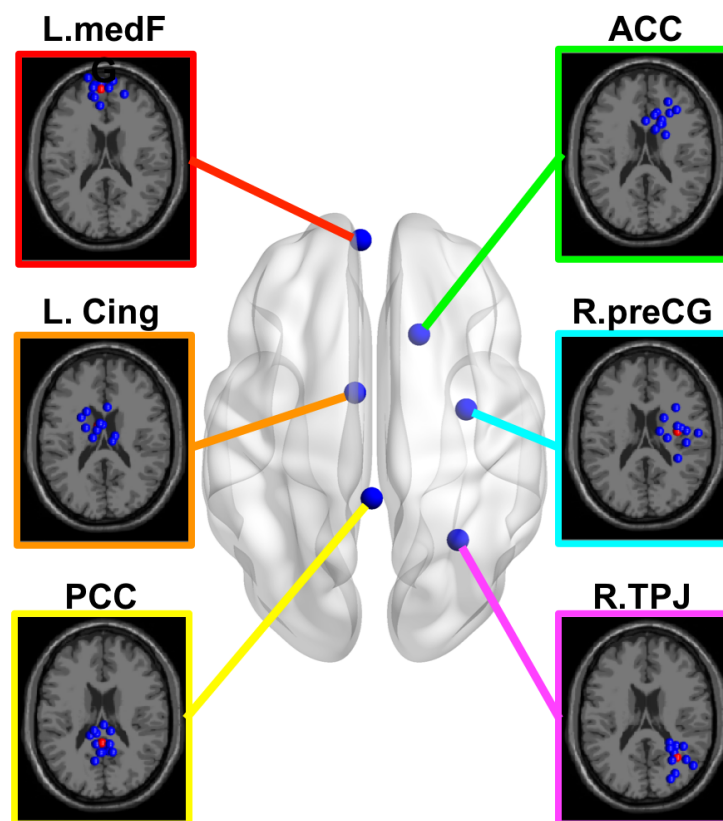


Figure 2.6. Dipole cluster plots for roving dual oddball task. Blue dots depict individual ICs and red dots depict cluster centroids. Note: Some ICs/centroids are not visible due to being hidden beneath other ICs.

### ***ROI Cluster ERPs***

ERPs were examined for each of the six selected ROIs (R.TPJ, L.medFG, ACC, PCC, L.Cing, and R.preCG). The primary goal of this ERP analysis was to provide a general overview of areas of difference between the four stimulus types (feature present and feature absent targets and standards) in order to provide an interpretive framework to

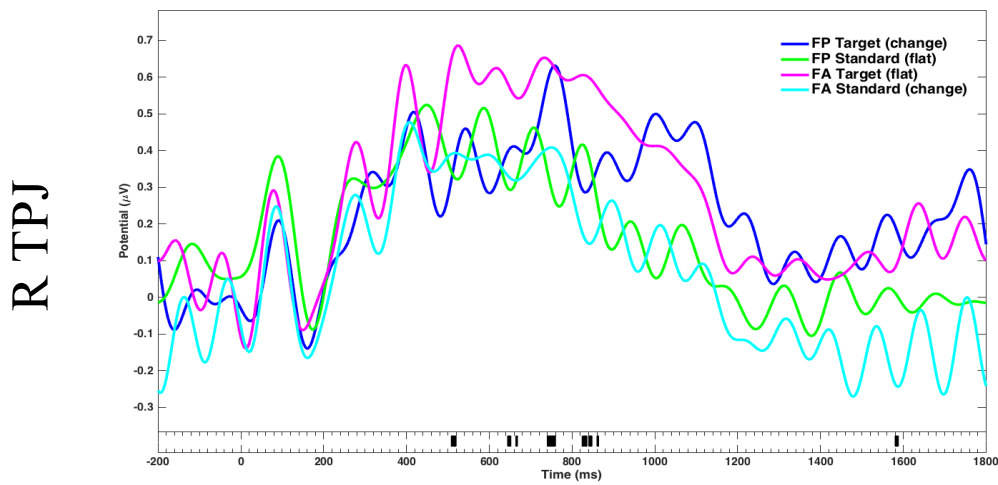
compare channel level ERP analysis discussed in the previous sections and the more nuanced examination of oscillatory activity (ERSPs) and functional network connectivity (PLVs) that will be the focus in the subsequent sections. As such, uncorrected ( $\alpha = .05$ ) within-subject one-way ANOVAs were run across ERP waveforms for each ROI separately. For ease of interpretation results are discussed in context of the time windows roughly corresponding to the channel level data for the MMN (~700 to 850 ms) and P300 (~850 to 1400 ms), respectively. ERP waveforms averaged across subjects for each condition and ROI can be viewed in Figure 2.7.

Areas that differentiate stimulus types in the MMN range include the RTPJ, L.MedFG, and to a smaller extent the L.Cing. It should be noted, that the PCC showed a region of significance that partially overlapped the MMN time range, though overall this waveform appears largely more consistent with the P300 morphology.

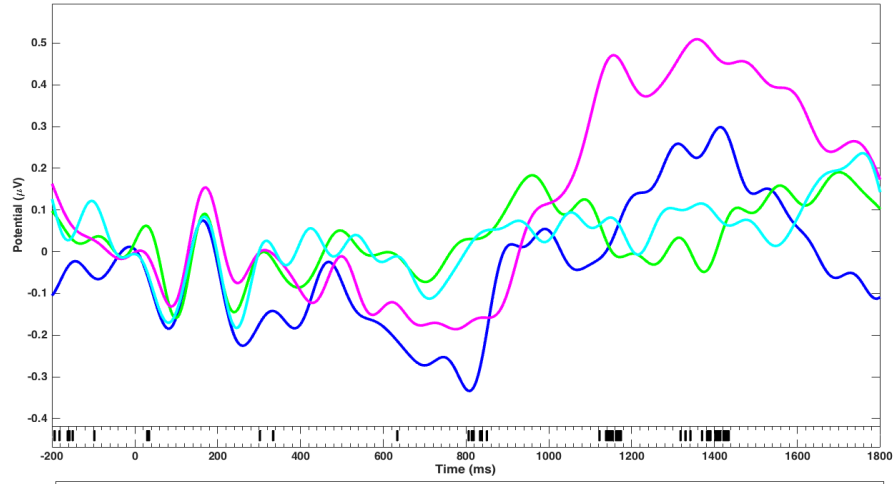
Areas that appear to overlap the P300 and show increased amplitudes to targets versus standards include the PCC, L.medFG, and the R.preCG. In particular, the PCC and R.preCG show waveforms that have similar morphologies to channel level P300 ERPS that also show a similar pattern of amplitude asymmetry in that there are larger amplitudes to feature present targets (change runs) versus feature absent targets (flat runs); however pairwise comparisons comparing feature present targets and feature absent targets revealed that the amplitude asymmetry was significant only for the R.preCG but not the PCC. Interestingly, pairwise comparisons of the frontal ROI cluster situated near the L.medFG revealed significantly larger amplitudes to feature absent

targets versus feature present targets, suggesting more frontal involvement in the behaviourally more difficult feature absent condition. Also of note, the ROI cluster corresponding to the L.Cing also appears to differentiate targets and standards with standards eliciting a positively deflected waveform and targets eliciting a negatively deflected waveform, though there appears to be little difference between change targets and flat targets, or between flat standards and change standards. Finally, the ACC ROI appears to be similarly active for each stimulus type across the entire epoch.

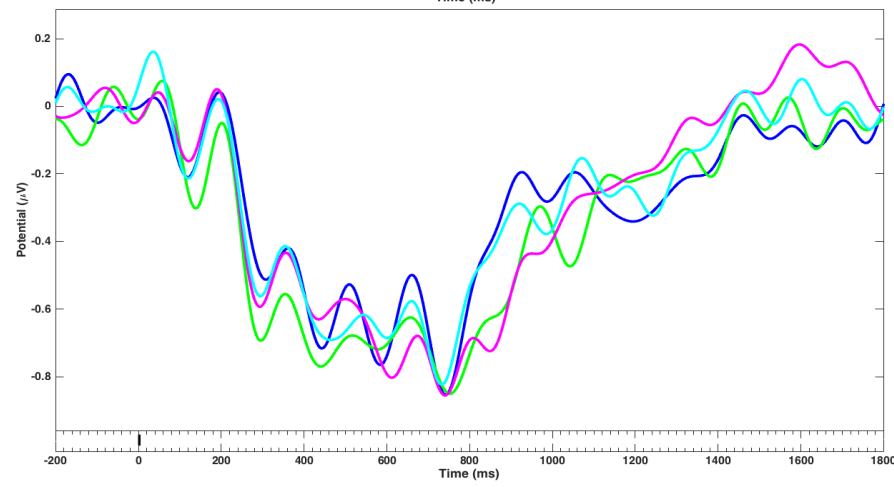
Figure 2.7. Grand Average ROI ERPs for Targets and Standards



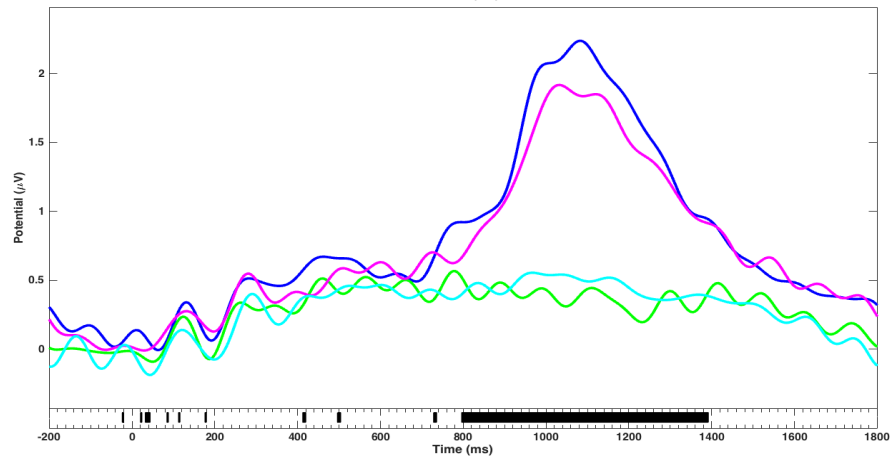
L medFG



ACC



PCC



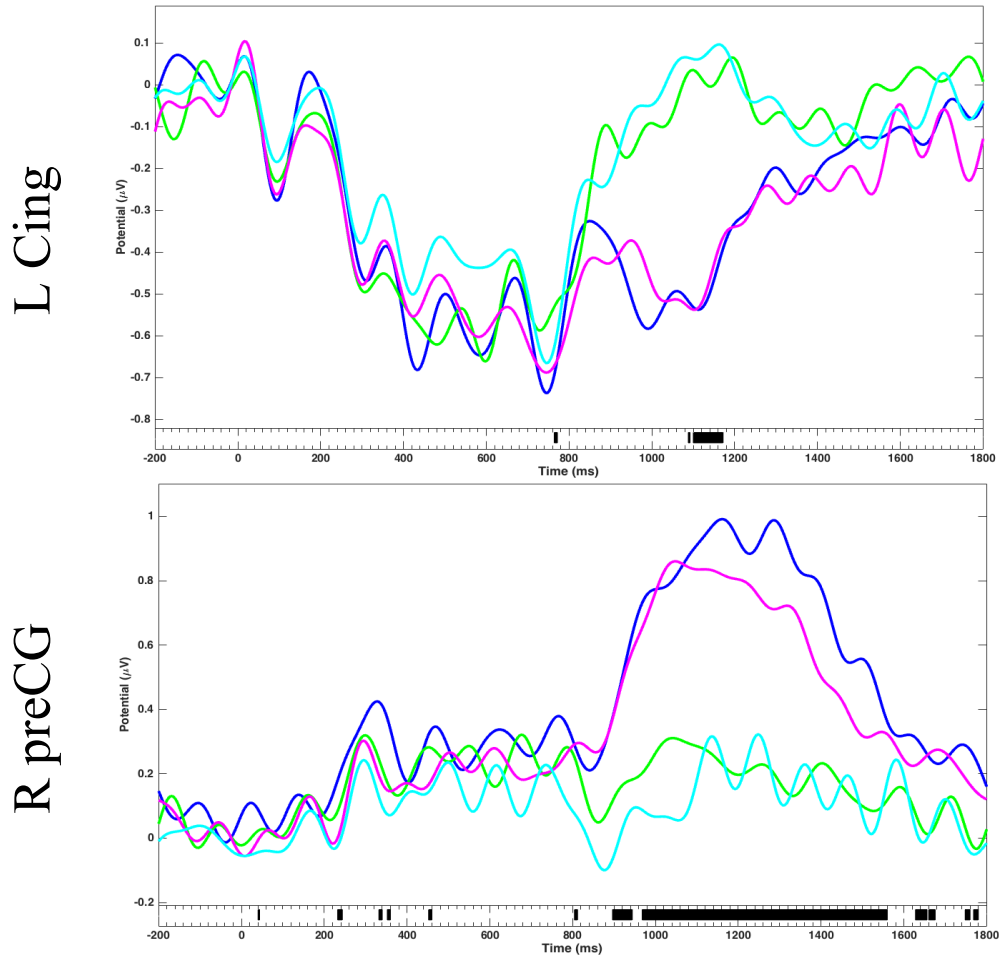


Figure 2.7. Grand average ERPs for each ROI comparing all targets and standards across both feature present (FP) and feature absent (FA) conditions. Areas of significance represent an uncorrected ( $p=.05$ ) fully-within one-way ANOVA.

### ***ERSP Results***

We focused our ERSP analysis on theta (3-7Hz) and gamma (30-50Hz) band oscillatory activity within the time windows of the MMN (~700 to 850ms) and the P300 (~850 to 1200ms) for each of the six selected ROIs (RTPJ, L.medFG, ACC, PCC, L.Cing, and R.preCG). Example ERSPs for the RTPJ, L.medFG and PCC can be viewed in Figure 2.8. Enlarged versions of the ERSP figures for all ROIs can be viewed in Appendix A.

Given the ERP asymmetries noted for MMNs and P300 between the feature present and feature absent conditions, we compared targets and standards within each condition separately using conservative non-parametric permutation based t-tests ( $\alpha = .005$ ; 400 permutations) at each 4ms time-frequency point. Since the large number of comparisons being made increased the chance of Type-I error, we only considered time windows significant if the number of significant time-frequency points exceeded a minimum threshold of significant points. The minimum threshold of significant time points required decreases as frequency increases because the temporal resolution of the wavelet decomposition increases with frequency. As such, for the theta band we used a minimum threshold of 150ms (~38 time points) of continuous significance and 25ms (~6 time points) for gamma band activity corresponding to at least a single cycle within each frequency band (Onton, Delorme & Makeig, 2005). Windows of significance for each ROIs ERSP (see Figure 2.8) were noted and then categorized as overlapping the MMN or P300 time windows, or falling outside these windows (see Table 2.4).

It should be noted that the distinction of the MMN and P300 time windows is somewhat arbitrary when considering a continuous time-series of electrophysiological data, however, we thought this approach prudent to best understand these data in context of the MMN and P300 ERP analyses discussed in previous sections. Where appropriate we highlighted windows of significance that overlapped two or more of these arbitrary time windows.

Finally, it should also be noted that the ERSP figures corresponding to each condition also include information pertaining to alpha (8-12 Hz; significance threshold = 100 ms) and beta (13-29 Hz; significance threshold = 50 ms) band activity; however, these will not be addressed in detail as they are theoretically less central to the aims of this study. Interested readers can view differences within these frequency bands in the figures included in Appendix A.

#### *Feature Present: Targets vs. Standards*

Within the MMN range, rare target change stimuli showed increased gamma and theta power in the L.MedFG, increased gamma in the PCC, and increased theta activity in the L.Cing compared to common non-target flat stimuli suggesting increased synchronization within these bands spatially localized to these regions.

In the P300 time window, increased localized evoked theta activity to targets was observed in the R.TPJ and L.Cing and increased gamma activity was observed in the L.MedFG. Increased theta activity was also observed to non-targets in the R.TPJ and L.Cing, though in both cases this tended to occur later in the P300 window (~1200ms) than was seen for targets. Increased theta to non-targets was observed in the R.PreCG and increased gamma in the PCC and the L.Cing.

#### *Feature Absent: Targets vs Standards*

Within the MMN range of the feature absent condition we observed a somewhat different pattern of results, there being no differences in theta activity between rare target flat

stimuli and common non-target change stimuli in any of the ROIs. Increased gamma to non-target change runs was observed in the R.TPJ and R.preCG.

In the P300 time window, we observed increased theta activity primarily to non-target change runs localized to the R.TPJ that spanned the entire P300 window. This differs from the feature present condition where we observed increased theta activity in the early portion of the P300 range for change targets but increased activity at later latencies for flat non-targets, which suggests that within the R.TPJ more resources are being allocated to processing the highly salient non-targets in the feature absent condition.

We also observed increased theta in both the L.Cing and R.preCG to non-targets in the feature absent compared to targets which is consistent with the pattern of increased theta to non-targets that we saw for this ROI in the feature present condition, though it should be noted that in both these regions that this increase in theta occurred approximately 50ms earlier (~1100 ms) in the feature present condition.

We observed increased gamma activity localized to the R.TPJ, L.MedFG, L.Cing, and R.preCG for feature absent standards. The increased gamma activity is consistent with increased gamma in processing non-targets in the feature present condition; however, the increased gamma in R.TPJ, L.MedFG and L.Cing to non-targets in the feature absent condition again imply more resources applied to processing the salient non-target change stimuli.

In summary, these results are indicative of an asymmetry between the feature present and feature absent conditions within both the MMN and P300 time windows, with change runs displaying greater theta and gamma activity particularly when these stimuli appear as rare targets in the feature present condition, but also when they appear as non-targets in the feature absent condition.

Figure 2.8. ERSP Plots for Selected ROIs Comparing Targets and Standards for Feature Present and Feature Absent Conditions.

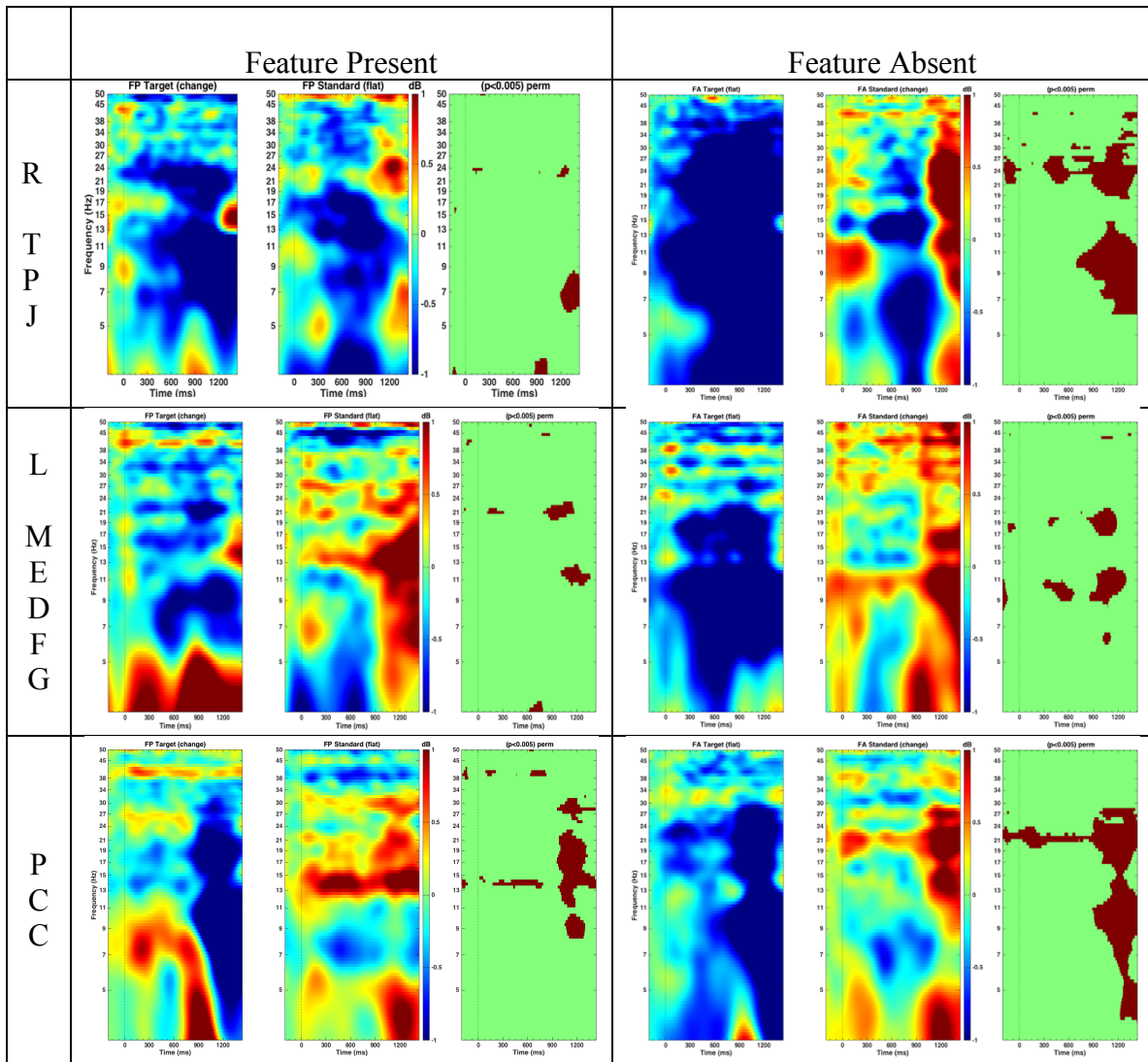


Figure 2.8. ERSP time-frequency plots for selected ROIs comparing targets and standards for feature present (left) and feature absent (right) conditions. Top-left panel displays

enlarged axis and scale labels for enhanced visibility – larger versions of figures for all ROIs can be viewed in Appendix A. Scale represents is +/- 1dB with warm colours representing increased local synchronization and cool colours representing decreased synchronization versus a common baseline (-250 to -50ms relative to onset of 1<sup>st</sup> tone). Left and middle plots of each panel represent ERSPs for targets and standards, respectively, within that condition. Right hand plot of each panel represents conservative pairwise significance (alpha = .005) derived by non-parametric *t*-tests (400 permutations). To further control type-I error due to multiple comparisons, areas of significance were only considered if they met a minimum threshold of significant time-frequency points, which varied depending on the frequency band: theta (3-7Hz) = 150ms; gamma (30-50Hz) = 25ms. R TPJ = right temporal-parietal junction; L MEDFG = left medial-frontal gyrus; PCC = posterior cingulate cortex.

Table 2.4. Summary of Theta and Gamma ERSP Results Comparing Targets and Standards Overlapping the MMN and P300 Time Windows.

ROI		Feature Present				Feature Absent			
		MMN		P300		MMN		P300	
		T > S	S > T	T > S	S > T	T > S	S > T	T > S	S > T
R TPJ	$\theta$			X	X				X
	$\gamma$						X		X
L MedFG	$\theta$	X							
	$\gamma$	X		X					X
ACC	$\theta$								
	$\gamma$								
PCC	$\theta$								X
	$\gamma$	X			X				
L Cing	$\theta$	X		X	X				X
	$\gamma$				X				X
R PreCG	$\theta$				X				X
	$\gamma$						X		X

Table 2.4. Summary of significant Theta (3-7Hz) and Gamma (30-50Hz) ERSP results comparing targets (T) and standards (S) for each condition overlapping the MMN (~700 to 850ms) and P300 (~850 -1400ms). To control type-I error due to multiple comparisons, areas of significance were only considered if they met a minimum threshold of significant time-frequency points, which varied depending on the frequency band: theta = 150ms; gamma = 25ms. R TPJ = right temporal-parietal junction; L MEDFG = left medial-frontal gyrus; PCC = posterior cingulate cortex.

### ***Phase Synchrony Results***

Phase synchrony (PLVs) was used to characterize functional connectivity within the theta (3-7 Hz) and gamma (30-50 Hz) frequency bands between ROIs within the narrow MMN time window (700 to 850 ms) and a wider time window that overlapped with the peak latency of the P300 (850 to 1200ms). Two types of functional connectivity analyses were conducted. First, functional connectivity was characterized separately for each of the four stimulus types (targets and standards for feature present and absent conditions) by determining if there was greater connectivity versus the pre-stimulus baseline. The second analysis compared functional connectivity between targets and standards within each condition (feature present and feature absent). For each analysis, a connection between ROIs was deemed significant if greater than 50% of the time points within that window showed a significant difference by a pairwise *t*-tests ( $p < .01$ ). The two analyses were conducted to allow for a conservative (perhaps, overly so) interpretive context for differences between conditions. For instance, a significant difference in phase locking between targets and standards within a condition across two brain regions might not actually be meaningful if neither the targets or standards being compared exhibit increased connectivity versus the pre-stimulus baseline within the time window being examined. On the flip side, in the absence of significant differences between targets and standards, examination of functional connectivity versus baseline allows for a qualitative appraisal (albeit, not so conservative) of different functional connectivity across conditions.

### *MMN Theta PLVs*

Within the MMN time window, targets demonstrated increased theta band functional connectivity versus baseline for both feature present and feature absent targets (see figure 2.9). For feature present targets (rare change stimuli) the R.TPJ appeared to be connected to the PCC and ACC. In particular, greater connectivity for feature present targets versus feature present standards (common flat stimuli) was seen between the RTPJ and PCC. For feature absent targets (rare flat stimuli), there was a greater number of connected nodes versus baseline compared to the feature present condition as there were significant connections between the R.TPJ, ACC, PCC, and R.preCG, though interestingly, no direct connection between the PCC and R.TPJ as was observed for the feature present condition. In the feature absent condition, no significant differences were observed between targets and standards.

Figure 2.9. Theta-Band PLV Results for Feature Present and Feature Absent Conditions Overlapping the MMN.

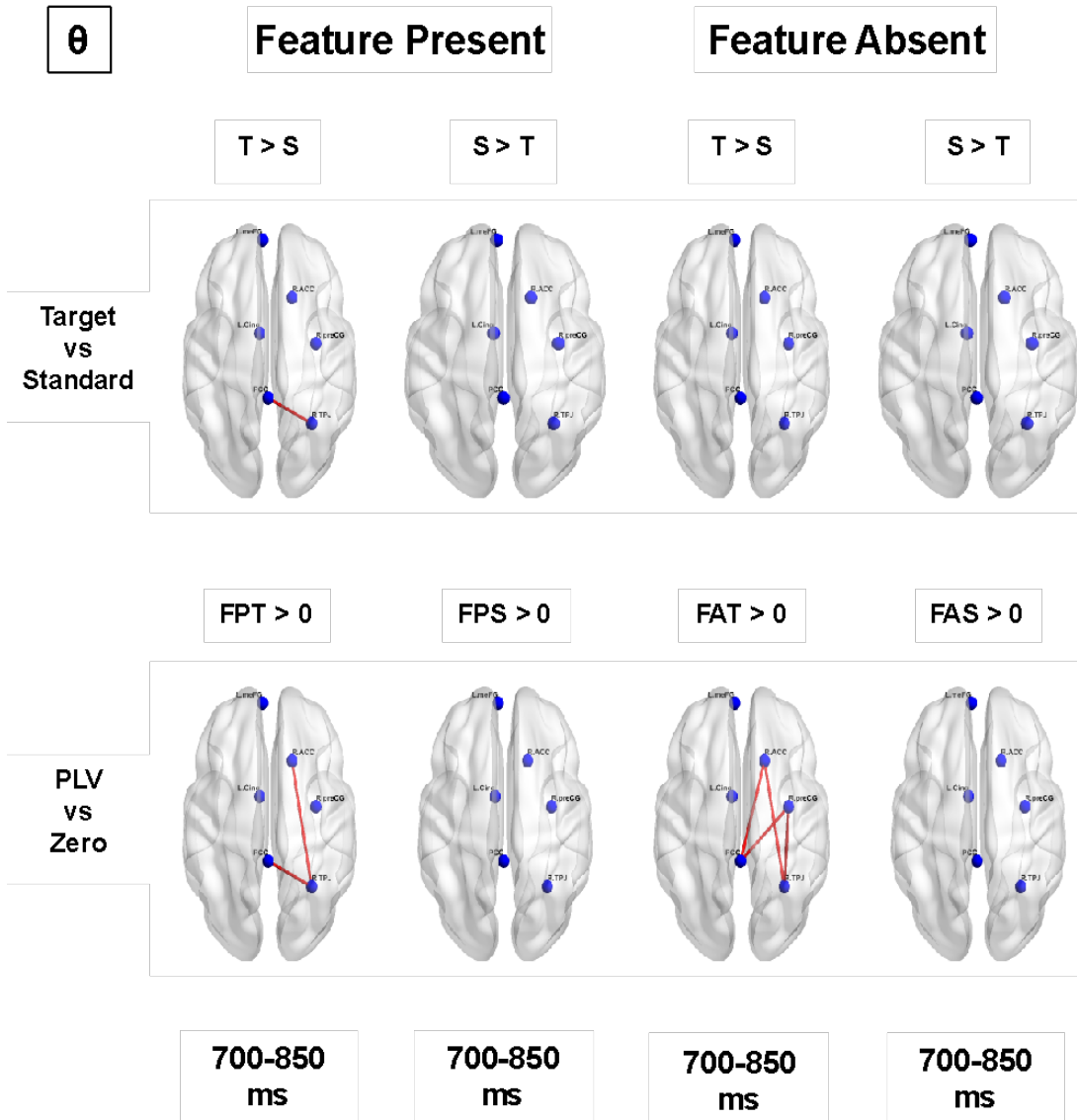


Figure 2.9. Theta-band phase synchrony characterizing functional connectivity between ROIs for feature present (left side) and feature absent (right side) conditions within the MMN time window (700 to 850ms). Top row: Compares targets (T) and standards (S) for each condition (i.e. T > S implies greater theta phase synchrony in targets versus standards for that condition). Bottom Row: Shows results of binomial tests characterizing functional connectivity for each stimulus type within the 700 to 850 ms time window relative to the pre-stimulus baseline. FPT = feature present targets (change); FPS = feature absent standards (flat); FAT = feature absent targets (flat); and FAS = feature absent standards (change). Each highlighted connection represents significant connectivity in that at least half of the data points within the time window (19 time points in this case) had to reach significance by *t*-test ( $p < 0.01$ ) in order for the connection to be deemed significant.

### *MMN Gamma PLVs*

In terms of gamma synchrony within the MMN range (see figure 2.10), only feature present targets demonstrated significant functional connectivity between the R.TPJ and the ACC, which was similar to what was seen in the theta band for these stimuli. No significant gamma synchrony differences were observed between targets and standards within the feature present and feature absent conditions.

Figure 2.10. Gamma-Band PLV Results for Feature Present and Feature Absent Conditions Overlapping the MMN.



### *P300 Theta PLVs*

Within the P300 time window (see figure 2.11), targets demonstrated different patterns of increased theta band functional connectivity versus baseline between the feature present and feature absent conditions. Specifically, for feature present targets (rare change runs), the PCC appeared to be connected to the LmedFG. However, for feature absent targets (rare flat runs), similar to what was observed in the MMN range, there appeared to be a greater number of significantly connected nodes than was seen in the feature present condition. Specifically, versus baseline, there were significant connections between the PCC, L.Cing, and ACC, and also the R.TPJ was connected to the R.preCG and the ACC; however, the PCC-L.medFG connection seen for the feature present condition was absent. No significant theta synchrony differences were observed between targets and standards in either the feature present and feature absent conditions.

Figure 2.11. Theta-Band PLV Results for Feature Present and Feature Absent Conditions Overlapping the P300.

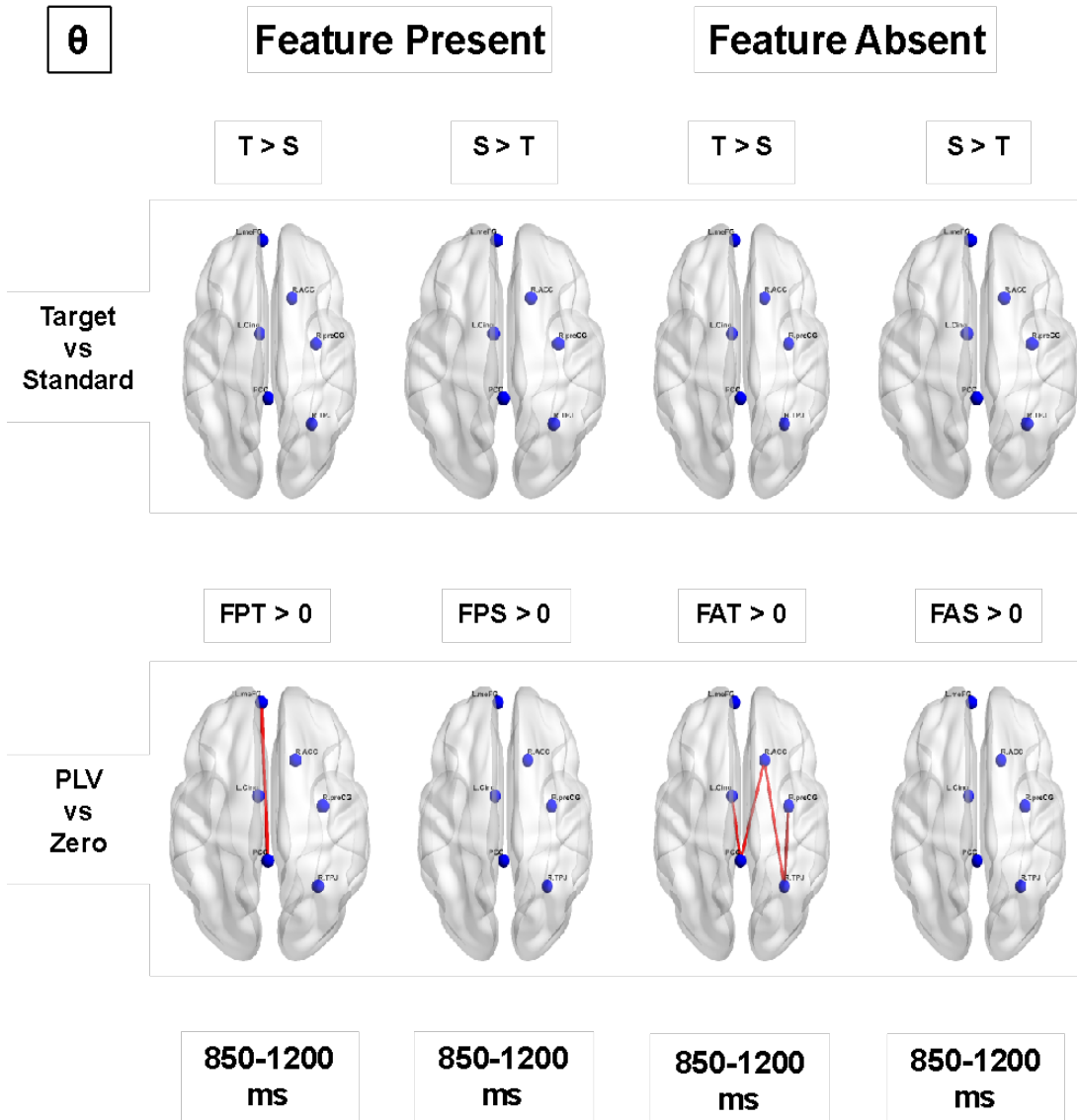


Figure 2.11. Theta-band phase synchrony characterizing functional connectivity between ROIs for feature present (left side) and feature absent (right side) conditions within the MMN time window (850 to 1200 ms). Top row: Compares targets (T) and standards (S) for each condition (i.e.  $T > S$  implies greater theta phase synchrony in targets versus standards for that condition). Bottom Row: Shows results of binomial t-tests characterizing functional connectivity for each stimulus type within the 850 to 1200 ms time window relative to the pre-stimulus baseline. FPT = feature present targets (change); FPS = feature absent standards (flat); FAT = feature absent targets (flat); and FAS = feature absent standards (change). Each highlighted connection represents significant connectivity in that at least half of the data points within the time window (19 time points in this case) had to reach significance by  $t$ -test ( $p < 0.01$ ) in order the connection to be deemed significant.

### *P300 Gamma PLVs*

In terms of gamma synchrony within the P300 range (see figure 2.12) only feature absent targets PLVs revealed significant functional connectivity between the PCC and the ACC, which was similar to what was seen in the theta band for these stimuli. Gamma synchrony between the ACC and PCC in feature absent targets was also significantly greater for targets versus standards. Feature present targets demonstrated significantly greater gamma synchrony versus feature present standards between the PCC and L.medFG, but since neither targets nor standards in this condition demonstrated significant connectivity between these areas versus baseline, this difference will not be discussed further.

Figure 2.12. Gamma-Band PLV Results for Feature Present and Feature Absent Conditions Overlapping the P300.

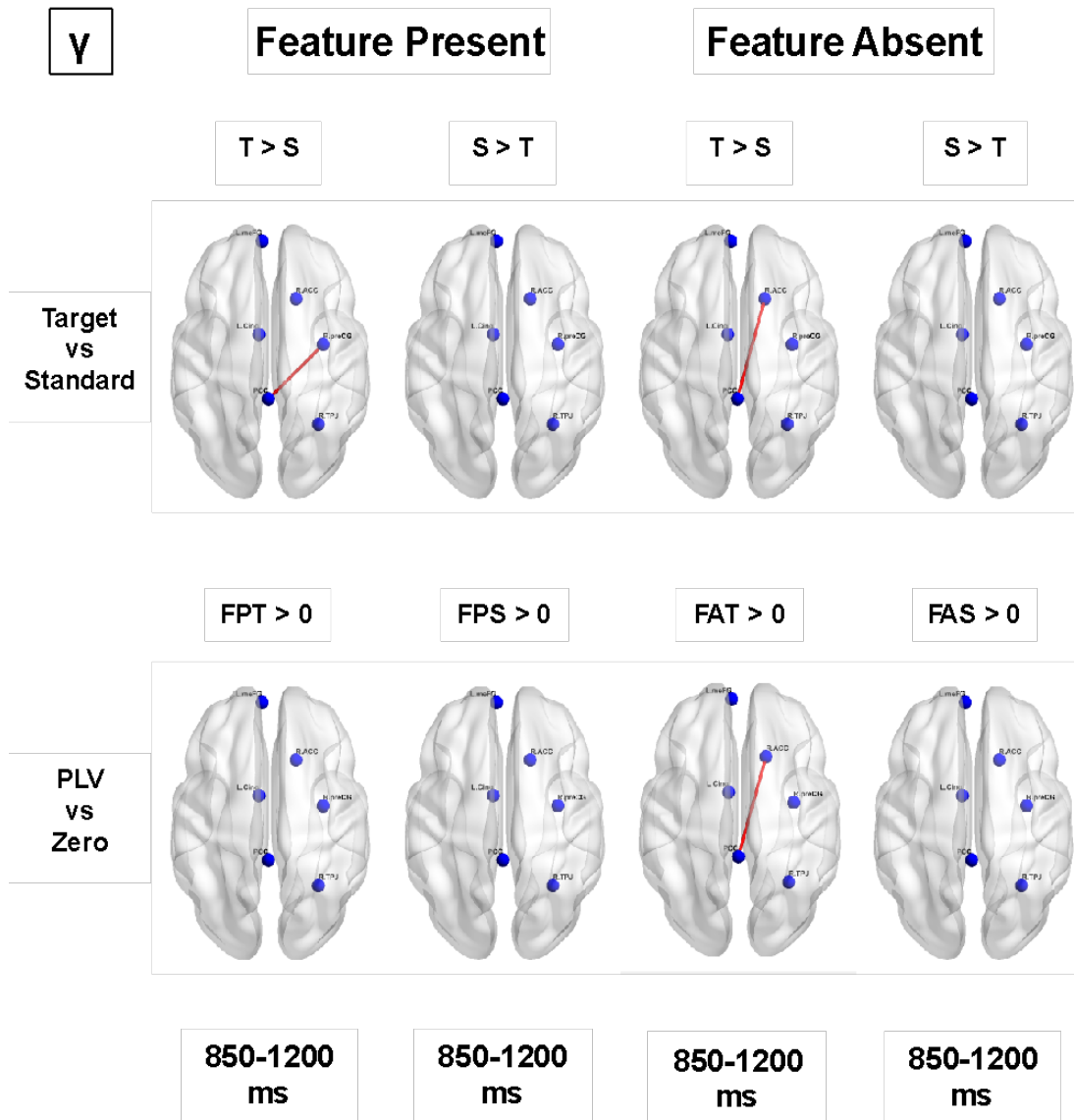


Figure 2.12. Gamma band phase synchrony characterizing functional connectivity between ROIs for feature present (left side) and feature absent (right side) conditions within the MMN time window (850 to 1200 ms). Top row: Compares targets (T) and standards (S) for each condition (i.e.  $T > S$  implies greater gamma phase synchrony in targets versus standards for that condition). Bottom Row: Shows results of binomial t-tests characterizing functional connectivity for each stimulus type within the 850 to 1200 ms time window relative to the pre-stimulus baseline. FPT = feature present targets (change); FPS = feature absent standards (flat); FAT = feature absent targets (flat); and FAS = feature absent standards (change). Each highlighted connection represents significant connectivity in that at least half of the data points within the time window (19 time points in this case) had to reach significance by *t*-test ( $p < 0.01$ ) in order the connection to be deemed significant.

## **Discussion**

This study introduced a novel auditory local-global dual oddball task that added a roving frequency component to an existing paradigm, which was an attempt to mitigate behavioural and ERP asymmetries (MMN and P300) observed between conditions where targets were salient to when they were not (Blundon, 2015, Blundon, Rumak & Ward, 2017). This study also served as a proof-of-concept to guide data analysis in subsequent chapters where this experimental paradigm was used to examine the effects of frequent cannabis use. Similarly, source localization (i.e. dipole ROIs), spectral analysis (ERSPs), and functional connectivity (PLVs) were characterized to inform analyses carried out in subsequent chapters. In the present study we found that this new paradigm only partially mitigated the asymmetries initially observed in the non-roving form of this task (Blundon, 2015, Blundon, Rumak & Ward, 2017).

### ***Behavioural Asymmetry***

Behaviourally we observed a clear performance bias favouring the feature present condition in that participants' were more accurate in correctly identifying rare salient change runs embedded in a sequence of commonly occurring flat runs compared to the feature absent condition where participants identified less salient rare flat runs embedded in a sequence of salient change runs. We did, however, observe, a partial mitigation of a reaction time asymmetry in that reaction times between the feature present and feature absent condition were only marginally significant, whereas the non-roving version of this task yields increased accuracy and faster response times in the feature present condition (Blundon, Rumak & Ward, 2017).

### ***MMN Asymmetry: Local vs Global***

We observed an asymmetry between conditions in terms of both MMN amplitude and latency. The feature present condition shows larger MMN amplitude and a longer latency than those observed in the feature absent condition. The larger MMN amplitudes in the feature present condition are understandable given that targets that are both rare and contain a salient feature would be expected to be easier to discriminate than rare target flat runs amongst a background of changing runs. If we only observed an amplitude difference between conditions, we might infer that the MMN derived from the difference waves reflects the same underlying process, albeit attenuated in the feature absent condition due to stimulus features; however, the observed latency differences may imply that different ERP subcomponents may be driving the MMN differences between conditions.

We believe that both conditions fundamentally represent an MMN process due to the observed wave morphology (i.e. fronto-central scalp distribution, and the observed polarity inversion at the mastoids); however, the feature present MMN may occur later and have a larger amplitude due to additional frontal attentional processes associated with processing of the rare salient targets. Indeed, for this reason it can be difficult to disentangle the MMN and the P300 in the same condition due to N2 components which often give rise to a P3a (though we did not observe a prominent P3a component in the feature present condition versus the feature absent condition as we did in a non-rolling version of this task: see Blundon, Rumak & Ward, 2017) (Sussman, 2007). Further to this, when we calculated the MMN response to all stimuli (change minus flat) ignoring

whether the stimuli were targets or standards, and hence ignoring potential attentional factors related to task demands, which we dubbed the local MMN, we found that these local MMNs were similar to the feature absent MMNs and significantly different from feature present MMNs in terms of both amplitude and latency. While MMNs are often thought of as an automatic pre-attentional phenomenon, given that in canonical MMN task designs they are elicited when attention is directed away from the stimuli, or even while participants are unconscious (Morlet & Fischer, 2014), in reality, the processes that comprise the regularity encoding aspect (i.e. the standard) of the MMN are to some degree impacted by attentional manipulations under some circumstances (Sussman, Chen, Sussman-Fort & Dinces, 2014). The aim of the frequency roving feature of this task was to lessen the likelihood that participants would engage in a diffuse attentional strategy as we have previously argued may be the case in the feature present condition of the non-roving version of this dual oddball task (Blundon, Rumak & Ward, 2017). Specifically, we argued that when flat standards are of an identical base frequency, as is also the case for classic MMN paradigms utilizing frequency deviants to elicit MMNs, participants can engage in a diffuse search strategy that picks out the salient feature (a pop-out feature likely relying on a P3a process; see next section). Other research has determined that roving MMN paradigms elicit an MMN response, and MMNs occur with or without attention directed to stimuli (i.e. counting deviants or reading a book and ignoring stimuli), so we expected to see a MMN response to each change run given the local violation of expectancy (Bekinschtein et al., 2009; Garrido et. al., 2009). We also expected the MMN response to be more prominent when there is also a global violation of expectancy, though in the feature present condition it may be difficult to identify

because the MMN automatically generated by the local deviant feature is possibly overlapping with the more deliberate conscious attentional processes required to categorize the rare salient stimulus as a target (i.e., P300 process). This issue would not arise in the feature absent condition because the salient change runs are common non-targets that are not being categorized, so the local MMN generated by these should be more akin to those observed in pure MMN designs. Furthermore, in the present task, since the base frequency of each stimulus changes from trial to trial, participants likely have to allocate more attentional resources (i.e. a more focal attentional strategy) to each stimulus in order to identify target features. While presumably this attentional allocation would be identical for all stimuli, it could modulate the MMN in a manner that cannot be clearly identified with the current task design. Future research, might explore this issue by including a passive version of the task where participants are asked to focus attention on an irrelevant task (i.e. watching a movie).

In summary, we continue to observe a MMN asymmetry between the feature present and feature absent conditions, possibly reflecting the contribution of different attentional processes in each condition. This asymmetry implies that it is most appropriate to analyze the feature present and feature absent conditions separately (i.e. not pooling them together) when applying this task to cannabis users (see chapter 3). Additionally, we saw that calculating the local MMN by subtracting the mean ERP response of all flat stimuli from all change stimuli (ignoring whether they are global targets or standards) suitably indexes the MMN responses to local deviants, which partially justifies our decision to examine MMNs across a larger sample of cannabis users and non-users (chapter 5) across

two studies with different task demands (chapter 3 and 4) but identical change and flat stimuli.

### ***P300***

In examining the P300 response to oddball targets at the midline parietal electrode site (Pz), we found increased amplitude in the feature present condition but no latency difference between conditions. We view this as a partial resolution of the asymmetry observed between feature present and feature absent conditions we previously reported in the non-roving version of the task where peak P300 latencies were significantly shorter in feature present condition (Blundon, Rumak & Ward, 2017). Additionally, the feature present targets of the *non-roving* version of this task elicited a distinct P3a component at frontal sites, whereas we did not observe a well-defined frontal P3a in this experiment, suggesting that successful target discrimination in this roving task is subsumed largely by the stimulus categorization processes more typically associated with the P3b component. The P3b amplitude asymmetry observed between the feature present and feature absent conditions (i.e. smaller amplitudes to feature absent targets) likely reflects increased difficulty in discriminating rare flat targets amongst changing standards than vice versa, which was evidenced by poorer behavioural performance in the feature absent condition.

Unfortunately, with the present experimental task it is not possible to definitively discern whether this partial resolution in asymmetry is driven by the addition of the inter-stimulus frequency roving feature, or by the reduced intra-stimulus frequency difference between the 5<sup>th</sup> tone of change runs and the base frequency of the preceding four tones (i.e. the 5<sup>th</sup> tone is 50Hz higher or lower in the roving task and 500Hz higher or lower in

the non-roving task). Based upon other research it is evident that all auditory P300s contain contributions from both P3a and P3b processes that can be independently modulated under specific experimental conditions (Polich, 2007). In the case of the present experiment, for the feature present condition, it is most likely that the reduced intra-stimulus frequency deviation of the 5<sup>th</sup> tone would reduce the contribution of frontal attentional orienting networks, typically manifesting in a frontal P3a component (Friedman, Cycowicz & Gaeta, 2001). However, in terms of this dual oddball task, future research might examine this issue by utilizing a non-roving paradigm that compares P300 responses to large intra-stimulus frequency changes to P300 responses to small frequency changes.

As mentioned in the previous section, we believe the addition of the inter-stimulus roving component reduces the likelihood that participants could engage in a diffuse attentional strategy in their search for targets, especially in the feature present condition. Ultimately, inter-stimulus frequency roving makes both feature present and feature absent conditions of the roving task more attentionally demanding (and hence more difficult) than their non-roving counterpart; however, it might be informative for future studies to tease apart the specific effects of the roving component by contrasting P300 responses to variations of the roving and non-roving versions of the feature present condition involving both large and small intra-stimulus frequency changes between the base frequency and the frequency of the 5<sup>th</sup> tone in change stimuli. It would be interesting to see if large intra-stimulus frequency changes in a roving paradigm would restore the frontal P3a component and whether inter-stimulus roving is directly responsible for mitigating the

posterior P300 latency asymmetry that we previously reported (Blundon, Rumak & Ward, 2017).

While the nuanced mechanistic contribution of the roving feature of this experimental task remains unresolved, the primary aim in examining the P300 responses of this present study was to inform the analyses in subsequent chapters where this paradigm is applied to cannabis users and non-users. Since both a behavioural and P300 amplitude asymmetry was observed between the feature present and feature absent conditions, it appears prudent, as is the case for the MMN, to analyze these conditions separately. This decision carries with it the disadvantage of reduced signal-to-noise ratio and increased likelihood of participants being excluded from the analysis (resulting in reduced statistical power) due to having an inadequate number of correct trials to reliably calculate the P300. However, we have demonstrated that the P300s in each condition follow a similar time course differing only in amplitude, so separate analysis of these conditions carries with it the advantage of comparing groups under relative easy and difficult task conditions, which we ultimately believe will allow for a more nuanced account of group performance.

### ***ROIs***

We identified six clusters of ROIs, based upon estimated locations of dipole models that were fit to independent components for each participant, that contained ICs from at least half of the participants. The cluster corresponding to the PCC and the R.preCG appear to correspond most closely to the P300 ERP seen in the channel level data and these nodes

are likely components of a top-down dorsal attentional network (DAN; Kim, 2014; Justen & Herbert, 2018). It should be noted that the PCC cluster is proximally located to the superior parietal lobe; however, both these regions are considered key neural generators of the P3b ERP component (Wronka, Kaiser, & Coenen, 2012).

The L.medFG, L.Cing, and R.preCG roughly correspond to locations identified by previous research conducted in our lab using simple MMN oddball paradigms, albeit with slight differences likely attributable in part to the imprecise nature of EEG source localization and in part due to the complex stimulus and task parameters of the current study. The L.medFG appears to lie proximal to the orbital gyrus source (both BA 11) identified in the previous study, which contributed to the MMN network in both active and passive oddball paradigms (MacLean & Ward, 2014).

The RTPJ (BA 39) ROI in this study appears to be active during time periods overlapping both the P300 and the MMN. This region corresponds roughly to temporal-parietal/inferior parietal lobe (IPL) locations seen in other EEG source analysis studies active over MMN and P300 time windows in active auditory oddball paradigms (Wronka, Kaiser & Coenen, 2012; Justen & Herbert, 2018). We've chosen to label this region the RTPJ as opposed to IPL because it falls somewhat more ventral and posterior to more typical IPL regions, likely reflecting overlap with posterior temporal regions. A meta-analysis of fMRI oddball studies also found this area to be active during these tasks and it is believed to be a component within the ventral attention network (VAN) reflecting stimulus-driven attentional processing (Kim, 2014).

The cluster termed the ACC appears to fall within the white matter of the ACC, which is likely due to imprecise spatial resolution of EEG source localization. The ACC cluster does not appear to differentiate targets and standards in either condition when examining the ERPs or when considering ERSs in the theta and gamma range. Furthermore, this area appears to be networked to nodes from both the dorsal attentional (i.e. PCC) and ventral attentional networks in both the MMN and P300 range, suggesting interaction with both networks. It should be noted that the centroid of the ACC cluster is also proximal to various other brain regions due to its central location and spatial orientation. For instance, this cluster is proximal to the right insula (BA13), which along with the ACC and TPJ has been characterized as part of a ventral attentional network, which is believed to act as a sort of “circuit breaker” for the dorsal attentional network (Kim, 2014). This characterization of this cluster is compelling, given it is networked with VAN and DAN nodes; however, other research has shown the insula to be more active in passive oddball paradigms (Justen and Herbert, 2014) and again the lack of differentiation within this area across stimulus types and conditions suggests this cluster is serving a more general purpose. The centroid of this cluster also falls near the pars orbitalis (BA 47) located in the medial portion of the inferior frontal gyrus, which has been shown to be active in processing of both musical and non-spatial auditory stimuli (Arnot et al, 2004; Wong et. al, 2002; Levitin, 2003). Based on the present data it is uncertain, however, if this area were actually BA 47, how specifically it would function within context of an oddball paradigm, or if it would again constitute the same circuit

breaking function within the VAN that was described for the insula (Corbetta & Shulman, 2002).

Contrary to expectation, we did not see contributions from the inferior frontal gyrus (IFG) or the superior temporal gyrus (STG), which are key network nodes typically observed in simple and roving MMN studies (Garrido, 2008; MacLean & Ward, 2014). During the iterative process of identifying ROIs, small clusters localized to the IFG and STG containing ICs from a few participants did appear; however, there were never enough participants to warrant including these clusters in subsequent analyses. In the next chapter we will see that the same task but with more participants and a slightly modified electrode array yields stable STG clusters (though IFG clusters, while present, again have too few participants to analyze), so it seems likely that in the present study these temporal and frontal sources are contributing to the MMNs observed in the channel level data, but could not be resolved in the source analyses (i.e., ROI ERPs, ERSPs and PLVs). The absence of the STG sources limits the interpretability of the functional connectivity analysis, particularly those overlapping with the MMN time window.

### ***ROI ERPs and ERSPs***

#### *MMN*

Within the MMN time window the ERPs corresponding to the R.TPJ and the L.medFG appeared to differentiate targets and standards. We tended to see a larger ERP response in the R.TPJ in the feature absent condition to non-salient flat targets suggesting that more cognitive resources are being allocated to processing these stimuli, which is consistent with this condition being more difficult. A more complex picture of the asymmetry

emerges when examining the oscillatory activity in the theta and gamma range derived from the ERSP analysis. No difference was seen in either theta or gamma activity in the R.TPJ for the feature present condition, but greater gamma activity was seen in the MMN range for non-target change standards in the feature absent condition, suggesting additional localized stimulus driven processing of salient non-targets, which unsurprisingly may imply that non-target change runs are more distracting than non-target flat runs due to the feature change within the run.

A different pattern of asymmetry was seen in the MMN range for the L.MedFG cluster. The ERPs for this frontal cluster shows larger negative responses to target stimuli in both conditions with the largest response seen to target change runs in the feature present condition, which is consistent with the asymmetry seen in MMNs at the channel level, with there being larger MMNs for the feature present condition. The ERSPs revealed larger localized theta and gamma response to feature present change targets versus standards but there was no such difference in the feature absent condition, which may lend further support for our earlier assertion that there is greater involvement of frontal areas in processing salient oddball targets consistent with an attention mediated N2 process underlying the MMN asymmetry between conditions at the channel level.

Also in the MMN range, the ERPs emerging from the PCC and the L.Cing tended not to differ; however, there was greater gamma activity in the PCC and more theta activity in the L.Cing for the feature present targets and no difference in the feature absent condition. This is further indicative of an asymmetry between the conditions, in that

greater top-down frontal processing contributes to the larger MMNs in the feature present condition observed at the channel level.

Taken together, these results suggest differential frontal-parietal and temporoparietal activity in processing change-runs in different contexts implying that top-down processes contribute to the generation of the MMN when a local deviant change run is a target versus a more bottom-up process contributing to the MMN when the local deviant change run is a non-target. These findings are consistent with other research that suggests the MMN is not invariant to attentional manipulation (Sussman, Chen, Sussman-Fort & Dinces, 2014); however, in future research it would be interesting to see if a similar pattern emerges in a passive version of the task where participants attention is directed away from the stimuli.

### *P300*

Within the time-window of the P300, we observed that the ERPs pertaining to the L.MedFG, L.Cing, PCC and the R.preCG tended to distinguish between targets and standards. The ERPs localized to the PCC in particular tended to closely correspond to P300 described for the channel level data at site Pz, which was expected given that this region is a likely a key generator of the P3b ERP component (Wronka, Kaiser, & Coenen, 2012).

As would be expected, examination of the oscillatory activity provides a more nuanced and complicated picture of the processes underlying the P300 as much of this information

tends to be eliminated during the signal averaging used to generate ERPs. In the feature present condition we saw increased theta to change targets in the R TPJ and L Cing occurring somewhat early in the P300 window (~850 to 1100ms), which is consistent with other research showing increased theta to targets (Başar-Eroglu, Başar, Demiralp & Schürmann, 1992; Mazaheri & Picton, 2005). Unexpectedly, theta was also increased to flat standards in these areas, though this tended to occur later in the P300 window (after ~1200ms); in the feature absent condition, increased theta was only seen to change standards (also late in the P300 window), which is further indicative of an asymmetry in processing targets in each condition. Taken together, these findings suggest a differential role in processing targets and standards with early theta activity related to processing salient targets and late occurring theta related to processing non-targets. The late-occurring theta to non-targets seen in this study, which is not seen in other studies, may reflect the more difficult nature of this roving oddball task as compared to simple two-stimulus auditory oddball tasks. In simple tasks it would be expected that consecutive exposure to identical stimuli would result in decreased processing as evidenced by decreased theta relative to processing rare targets (Harper, Malone & Iacono, 2017).

In the gamma range, we saw increased gamma to feature present targets in the L.MedFG occurring quite early in the P300 window (and overlapping with the MMN), but increased gamma in the L.Cing and PCC occurring late in the P300 window. Similar to the pattern that was seen for theta, increased gamma activity to standards occurring late in the P300 window was seen in most of the ROIs. These findings are suggestive of greater processing of salient (change run) standards in the feature absent condition, which

again reflects the asymmetry between these two conditions. The increased gamma to feature present (flat) standards in the PCC may seem surprising given that the ERP for this cluster closely approximates the channel level data in showing increased amplitude response for feature present targets; some researchers have observed a similar pattern of increased gamma to standards when examining channel level oscillatory activity (Marshall, Mölle & Bartsch, 1996; Fell, Hinrichs & Röschke, 1997; Mazaheri & Picton, 2005), but others have observed the opposite (Gurtubay et al., 2001; Haig, De Pascalis & Gordon, 1999). However, it is interesting that that despite increased gamma to standards in the feature absent condition in most regions, the PCC, which shows increased gamma in the feature present condition, does not show increased gamma activity to standards in the feature absent condition, suggesting a differential role of the PCC in processing salient and non-salient non-target stimuli. In a somewhat similar vein, the increased early gamma activity to change targets in the L.MedFG is also present in response to change standards (in addition to late gamma processing) in the feature absent condition, which possibly suggests that early detection of salient features within the change stimuli may enhance processing of feature present targets, but this same process may lead to more difficulty in disregarding change stimuli when they are feature absent standards.

### ***Functional Connectivity***

#### *MMN Networks*

The functional connectivity within the MMN range is likely obscured due to the absence of temporal sources, which contribute strongly to the generation of the MMN (Garrido, Kilner, Stephan & Friston, 2009); nonetheless, some meaningful patterns emerged. In the feature present condition we saw greater TPJ and PCC connectivity in the theta band to

targets possibly reflecting communication between ventral and dorsal attentional networks and perhaps suggesting that bottom-up stimulus information reflecting the local deviancy within change runs is being fed from the ventral network to the dorsal network to aid in target selection; however, it is not actually possible to tease apart the direction of information transfer between network nodes using PLV analysis. We do not see this pattern of connectivity in processing non-target change runs in the feature absent condition, which would imply that information about the local deviant is not being fed forward, despite the increased local gamma activity in the R.TPJ that was discussed in the previous section. Furthermore, we see overall greater connectivity in both ventral and dorsal attentional networks while processing feature absent flat target runs with both the PCC and R.TPJ showing connectivity with the ACC and the R.preCG, and not with each other, though again, the direction of information transfer cannot be determined. This increased connectivity is further indicative of the asymmetry seen between the two conditions and may reflect greater attentional resources necessary to extract the non-salient stimulus information of the rare flat targets embedded amongst highly salient common change runs.

### *P300 Networks*

Within the theta band we saw an overall pattern of network activity suggesting dorsal attentional activation in processing feature present targets and greater network connectivity in the feature absent condition suggestive of an interplay between the ventral and dorsal attentional networks. Interestingly, the overall pattern of theta connectivity to targets in the feature absent condition was similar to what was seen in the MMN range,

whereas in the feature present condition there appeared to be more ventral attentional activation in MMN range as opposed to the more dorsal frontal–parietal activation in the P300 range. Similarly, in the gamma range increased synchrony was seen in the dorsal attentional network and this difference was greater for feature absent targets when contrasted with feature absent standards, which may imply greater activation of the dorsal attentional system necessary for successful target selection in the feature absent condition due to more difficult task demands.

Taken together these results are largely consistent with other fMRI and EEG source localization that show a dynamic interplay between ventral and dorsal attentional systems with predominately stimulus-driven ventral attentional networks active during the MMN range of active oddball tasks and both dorsal and ventral systems being active during the P300 range (Kim, 2014; Justen & Hebert, 2018). The greater connectivity in both the dorsal and ventral systems while processing targets during the more difficult feature absent condition could imply greater involvement of the proposed “circuit breaking” function of the ventral system which facilitates the dorsal system in successfully selecting otherwise difficult to detect targets (Corbetta, Patel & Shulman, 2008).

### ***Limitations***

Several limitations within this study are worth noting. First, a single left-handed participant was included, though this did not appear to have a great effect on channel ERPs (especially considering that only midline sites were examined) or reaction time. It is possible, however, that left handedness may have led to altered patterns of lateralized brain activity and connectivity that could plausibly skew the results in an unpredictable

manner, though this is unlikely to have played a large role considering only a single participant was left handed. A second limitation is that a couple of participants did not complete the experiment because they reported frustration due to difficulty detecting target tones. Excluding these participants seemed prudent at the time, though a better approach (as was done for subsequent studies discussed in chapters 3 and 4) might have been to encourage these participants to do the best they can. While data for these participants would have almost certainly been excluded for the behavioural and P300 analysis, it may have been informative to see if these participants elicited a local MMN response. A third limitation, is that this study did not utilize as detailed a screening process as is described in subsequent chapters. As such, it is possible (given the number of individuals screened out for studies in chapter 3 and 4; see chapter 1 for details) that this study included individuals who were regular cannabis users and/or individuals meeting criteria for neurocognitive disorders (i.e. ADHD) or other psychiatric conditions. However, the screening protocol used for the present study is typical for non-clinical cognitive labs, so such issues are likely endemic (and unreported) in the published literature. Fourth, as this was meant as a proof-of-concept study, no neuropsychological testing or self-report measures were included, which limits comparability to the study discussed in chapter 3. A fifth limitation of this study, as referred to in the discussion section, is absence of a passive condition and also a condition containing change stimuli with larger pitch differences between the 5<sup>th</sup> tone and the base frequency, which might have allowed for a clearer delineation of attention effects, particularly on the MMN. Inclusion of additional conditions (particularly a passive condition) was considered during the design phase of the experiment; however, this would have drastically

increased the EEG recording time (which was already approximately an hour), which likely would have led to increased fatigue and overall poorer quality EEG recordings (i.e. increased electrode noise and increased movement artefacts etc.). It is not believed that the omission of these additional conditions critically impacts the interpretability of these findings; however, additional studies involving a passive version of this task and also a version using modified stimulus parameters may be viable targets for future research. A final limitation of this study is the apparent absence of temporal sources, which are well documented in the MMN literature. This limits the interpretability of the MMN source localization for the present study. As mentioned in the discussion, temporal sources emerged, though they were insufficient to warrant analysis. As will be seen in subsequent chapters, with slightly varied electrode arrangements and the addition of more participants, this paradigm elicits clear temporal sources, so the absence of these regions here is believed to reflect a problem limited to this particular study and not a limitation of the paradigm itself. Furthermore, since this is a multifaceted task that generates both MMN and P300 components, the elicitation of network nodes related to the dorsal and ventral attentional systems are in themselves sufficiently meaningful and theoretically relevant even with the absence of temporal sources.

## **Conclusion**

This study demonstrates the viability of the roving dual-oddball paradigm that is an extension of previous research in our lab. The addition of a frequency roving feature partially resolved the asymmetry observed in non-roving versions of this task (Blundon, Rumak & Ward, 2017); however, given the persistence of behavioral and channel level MMN and P300 asymmetry, along with apparent differential activation of dorsal and

ventral attentional networks between the feature present and feature absent conditions, it was deemed prudent to examine these conditions separately in the next chapter. Despite the limitations in deriving key temporal sources, we demonstrated attentional networks consistent with the previous literature. The characterization of localized and network synchronization within the theta and gamma bands provide a useful framework for interpreting the results of subsequent chapters that will examine the effects of heavy cannabis use on these brain processes.

## **CHAPTER 3: Roving Local(MMN)-Global(P300) Dual Oddball Task in Cannabis Users and Non-Users**

### **Introduction**

The present chapter builds upon Chapter 2 by using the same experimental task, the roving dual-oddball task, to investigate the effects of frequent cannabis use on brain processes associated with the auditory MMN and P300 ERP components.

### ***MMN in Cannabis Users***

As previously summarized (see Chapter 1), reduced MMN amplitudes in schizophrenia populations have been widely reported in the literature; however, only a handful of investigations, typically utilizing task designs with simple auditory stimuli (single tones deviating in pitch, intensity, or duration), have been conducted on cannabis users. Most commonly heavy cannabis users appear to exhibit reduced MMN to pitch deviants. For instance, one study found reduced MMN to pitch deviants (but not duration deviants) in heavy cannabis users (5 uses per week for at least a year) compared to non-users (Rentzsch et al., 2007). Another study found that long-term cannabis users (average 9.5 years of use) showed reduced MMN to pitch deviants (but not to duration deviants) compared to both short-term users (average 4.4 years of use) and non-users (Roser et al., 2010). A study using a multi-faceted MMN task (including pitch, intensity and duration deviants) again revealed decreased MMN response to pitch deviants, whereas MMN decrements to duration deviants emerged only in long-term users (average of 26.1 years

use) when comparing to short-term users (average of 5 years of use) and non-users (Greenwood et al., 2014).

### ***MMN Hypotheses***

Whereas our task specification is somewhat more complex compared to the previously mentioned studies, we expected cannabis users to similarly show reduced MMNs compared to non-users because we used pitch to delineate deviancy (i.e. change runs) in both local and global contexts. Furthermore, we expected to see similar brain regions active as were described in Chapter 1 (as the tasks are identical). In terms of oscillatory activity, as these have not been well characterized detailed *a priori* hypothesis were not possible. Previous research in our lab, utilizing an active, albeit different, MMN paradigm (Maclean & Ward, 2014) did observe greater right temporal lobe gamma ERSP and greater right inferior frontal theta ERSP to deviant stimuli in the MMN time range. Thus, we expected to see this pattern for the non-user group in the present study. We expected that this pattern might be weaker for cannabis users and may manifest as reduced gamma/theta ERSP to change runs and/or increased gamma/theta ERSP to flat runs. Although network dynamics have not been fully articulated in the literature, we suspected that any differences between users and non-users should manifest in our characterizations of network connectivity via phase synchrony and allow us to observe differences in network connectivity in cannabis users.

### ***P300 in Cannabis Users***

The relatively few studies conducted on the acute effects of cannabis use on the auditory P300 appear to suggest that acute cannabis intoxication has disruptive effects. A

double-blind crossover study investigating the acute effects of  $\Delta$ 9-THC administration in a three-stimulus auditory oddball task found that  $\Delta$ 9-THC reduced P3a and P3b amplitudes versus placebo and that this reduction was greater in a higher dose condition (D'Souza et al., 2012). Another study investigating the acute effects of cannabis on healthy individuals while participants completed an auditory choice reaction task, where participants had to correctly respond to 1000Hz and 2000Hz tones that were randomly presented, yielded reduced P300 amplitudes when participants were administered a THC or a cannabis extract versus placebo (Roser et al. 2008).

The chronic effects of frequent cannabis use on the P300 in oddball tasks has not been extensively investigated and the few studies have yielded mixed results. One study utilizing a simple auditory oddball design found cannabis users (at least two uses per week) exhibited longer P300 latencies and decreased amplitudes. However, these differences disappeared in a follow-up study where the researchers enacted tighter controls over patient characteristics, such as age, neurological conditions and psychiatric history (Patrick et al., 1995). Similarly, another study utilizing an auditory oddball task failed to find any P300 amplitude or latency differences between cannabis users and non-users, though the overall frequency of cannabis use was relatively low (approximate mean of 44 uses over the past 6 months) (de Sola et al., 2008).

In non-auditory domains, heavy cannabis users (approximately 9 smoked joints per week) exhibited increased P300 amplitudes versus non-users to a visual oddball and affective oddball tasks (words with positive emotional valence = standards; negative words = rare

targets) and no latency differences. The authors noted that negative symptoms of schizotypy were negatively associated with affective P300 amplitude and that this sample of cannabis users exhibited decreased negative symptoms compared to controls (albeit users showed increased positive symptoms and no group differences in disorganized symptoms) (Skosnik, Park, Dobbs & Gardner, 2008). Others have failed to find P300 differences between cannabis users and non-users on visual oddball tasks (Patrick et al., 1995).

Other investigations examining the auditory P300 in tasks requiring more complex cognitive processing than in basic auditory oddball tasks have been more consistent. For instance, a study investigating auditory selective attention in regular cannabis users (at least 2 years use a minimum of twice per week) where participants had to respond to infrequent target tones amongst frequent distractor tones that were similar to targets but could differ in pitch, duration, or location (left or right ear), found cannabis users had reduced P300 amplitudes but no latency difference to target stimuli versus non-users and noted that this effect was more pronounced in cannabis users who started using cannabis at an earlier age (Kempel, Lampe, Parnefjord, Hennig & Kunert, 2003). Another study of auditory selective attention found longer P300 latency, in addition to slower reaction time and poorer performance, in heavy cannabis users (approximately 18 uses per month), compared to light users (6 uses per month) and non-users who did not differ (Solowij, Michie & Fox, 1995). However, these researchers note that they failed to replicate their earlier findings showing decreased P300 amplitudes in cannabis users (Solowij, Michie & Fox, 1991), which they attributed to differences in the control groups.

### ***P300 Hypotheses***

In context of the present study, findings from the previous chapter indicated that the feature-present condition of the roving dual-oddball task was less cognitively demanding, hence easier, than the feature-absent condition, so any differences between cannabis users and non-users would become most apparent in the more difficult feature-absent condition. So, for the P300 range we anticipated reduced P300 amplitudes and increased latencies compared to non-users particularly in the more difficult feature-absent condition, which would also be reflected in poorer accuracy and slower reaction times in that condition.

While oscillatory and network dynamics of the P300 in context of cannabis use have not been fully articulated in the literature (see Introduction for review of non-users), we suspected that any differences should manifest in our characterizations of network connectivity via phase synchrony and allow us to observe differences in network connectivity in cannabis users. Given that auditory oddball tasks are believed to involve a complex interplay between dorsal and ventral attentional networks along with involvement of frontotemporal networks, we expected to observe altered theta and gamma oscillatory activity within these network nodes and disruption in long range theta connectivity, especially in the more cognitively demanding feature-absent condition. Since cannabis users appear to do worse on tasks requiring a larger degree of top-down cognitive control, we anticipated that these differences would manifest as decreased

activity within nodes constituting the frontotemporal and frontoparietal networks. Furthermore, we expected to see differences in frontotemporal and/or frontoparietal connectivity, such as delayed and more sporadic connectivity between temporal and frontal sources in cannabis users.

## **Method**

### *Participants*

We were interested in assessing differences between heavy current users (CU) and current non-users (NU). An overview of the recruitment procedure can be viewed in the Chapter 1. Prospective participants who responded to online ads or posters hung in the community went through a brief structured telephone pre-screening interview administered by a research assistant to determine eligibility. The telephone screening format, in addition to a limited question set regarding cannabis use, was utilized to assuage concerns raised by the ethics review board regarding the collection of data about potentially illicit activities (i.e. illegal drug use). All participant responses were coded and identifying information was kept in a separate password protected file.

General inclusion criteria included being age 18 to 35, English proficiency, normal or corrected vision, normal hearing. General exclusion criteria included a history of serious head injury, history of neurological conditions (e.g. epilepsy, Parkinson's disease), history of neurocognitive conditions (e.g. ADHD), learning disabilities or reading disabilities, a diagnosis of serious mental illnesses (e.g. schizophrenia, bi-polar disorder, or major depression), or current use of medications to treat any mental health issues.

Individuals were also excluded from participation if they reported having braided or dreadlocked hair, as this would interfere with application of our EEG cap. After meeting the general inclusion/exclusion criteria participants were screened to determine eligibility as either a current heavy cannabis user or current non-user. Individuals who reported using cannabis at least 10 times over the last 30 days were invited to participate as cannabis users. Individuals were invited as to participate as non-users if they had not used cannabis in the past six months and had never used cannabis more than 10 times in a 30-day period.

A total of 33 cannabis users (CU) and non-users (NU) were invited to participate in this study based upon their responses on the telephone screen. Of those individuals invited to participate 14 heavy cannabis users and 14 non-users were included in the EEG and behavioural data analysis for this study. Data for two participants were excluded from analysis because they did not complete the experiment due to technical issues with the recording equipment. Additionally, one participant's data from the non-user group was excluded because at the time of testing they reported cannabis use in the last six months and had a history of heavy cannabis use. Due to participant availability, for some participants there was an unavoidable scheduling delay between screening and participation; as such, data for two participants were excluded from the heavy cannabis user group because at the time of testing their self-reported frequency of cannabis use was well below our criteria of 10 uses in the past 30 days to be classified as a current heavy cannabis user. Additionally, one participant in the non-user group completed the EEG portion of the study but had to discontinue the study prior to completing

questionnaires or neuropsychological testing; attempts to re-schedule this participant were unsuccessful.

The NU (M = 22.07 years, SD = 3.50) and CU (M=21.14 years, SD=3.70) groups did not significantly differ in age. There were more males than females (28.6% female) in the CU group and an equal number of females and males (50% female) in the NU group, though these did not differ significantly. Groups did not differ significantly on verbal comprehension, perceptual reasoning, current psychopathological symptomology, perceptual disturbances, or trait schizotypy (see results section for more details).

### ***Experimental Procedures***

The experimental procedures were nearly identical to those described in Chapter 2 (e.g., experimental task, behavioural analysis, EEG acquisition, offline processing, identification of ERPs, ICA, ROI selection procedures, rendering of ERSPs, and phase synchrony analysis). A slight variation in ROI selection was implemented to ensure that at least 50% of participants from NU and CU groups were represented in each cluster (See Table 3.7). In addition to these procedures, participants were administered various neuropsychological tasks and questionnaires, which will be described below.

Approximately half of the participants completed the questionnaires and testing before EEG and half completed after, though this was done on an ad hoc basis, primarily to accommodate appropriate cleaning and drying of the EEG equipment as multiple participants were often run on the same day.

### *Neuropsychological Testing*

Participants underwent several neuropsychological tests in a quiet and well-lit room using standardized procedures outlined by the test manufacturers. Tests were administered by the author, a senior graduate level clinical psychology student trained in the administration and interpretation of these tests. For the purposes of the present experiment, self-report and neuropsychological tests were used primarily to assess potential confounding factors across NU and CU groups; however, these will be revisited in greater detail in Chapter 5, where we examine consolidated findings from this experiment and the experiment described in Chapter 4.

*Vocabulary (VC)*: The VC subtest of the WAIS-III (Wechsler, 1997) tests verbal comprehension and expression ability. This orally presented test asks the participant to verbally define increasingly difficult words. Answers are recorded and scored but participants do not receive individual or normative performance feedback.

*Matrix Reasoning (MR)*: The MR subtest of the WAIS-III (Wechsler, 1997) tests non-verbal reasoning and pattern recognition. The test asks participants to solve a series of incomplete sequences by indicating which stimulus from a choice of stimuli fits within a sequence of stimuli. Each consecutive puzzle becomes increasingly difficult until participants complete all the puzzles or they satisfy a discontinuation rule by responding incorrectly to a pre-determined number of items. Answers are recorded and scored but participants do not receive individual or normative performance feedback.

*Oklahoma Premorbid Intelligence Estimate – 3 (OPIE-3)*: The OPIE-3 (Schoenberg, Duff, Scott & Adams, 2003) is a regression derived formula to estimate full-scale IQ (FSIQ). The two subtest version combines WAIS-III VC and MR raw subtest scores along with demographic variables. The test was initially developed as a test of premorbid functioning in clinical samples, but has also been used as a means of quickly estimating IQ in research samples (Spinks et al., 2009).

*Letter Number Sequencing (LNS)*: The LNS subtest of the WAIS-III (Wechsler, 1997) tests working memory. Participants are orally presented with jumbled lists of letters and numbers at a rate of one letter/number per second. They are then be prompted to repeat the sequence back to the tester in an unscrambled form of numbers (lowest to highest) and then letters (alphabetically). Responses are recorded and scored but participants do not receive individual or normative performance feedback.

*Continuous Performance Test - Identical Pairs (CPT-IP)*: The CPT-IP is a computer administered test included in the MATRICS Consensus Cognitive Battery (MCCB) (Nuechterlein & Green, 2006). This test of attention and vigilance takes about 10 minutes to administer. Participants are presented with sequences of 2, 3 and 4 digit numbers and are asked to press a key when the current number is identical to the last number that appeared. Participants do not receive individual or normative performance feedback.

### ***Self- Report Measures***

*Symptom Checklist 90, Revised (SCL-90-R)* (Derogatis, 1994): The SCL-90-R is a 90–

item self-report inventory that indexes a range of current (past seven days) psychological symptom patterns that manifest, to varying degrees, in both community and clinical settings. This questionnaire takes approximately 10-15 minutes to administer and asks participants to make a distress rating from 0 (not distressed) to 4 (extremely distressed). Scores on each item contribute to nine symptom dimensions (Somatization, Obsessive Compulsive, Interpersonal Sensitivity, Depression, Anxiety, Hostility, Phobic Anxiety, Paranoid Ideation) and a total score (Global Severity Index).

*The Schizotypal Personality Questionnaire – Brief (SPQ-B)* (Raine & Benishay, 1995):

The SPQ is a 22-item self-report measure containing three subscales (disorganized, cognitive-perceptual and interpersonal) that asks participants to report the presence or absence (Yes/No) of symptom traits associated with schizotypal personality disorder that exist to varying degrees in the general population. Given that some of the experiences described in this measure may be similar to those experienced under the influence of cannabis or other recreational substances, participants were explicitly instructed to answer affirmatively to situations in which they were not under the influence of cannabis or other substances.

*Sensory Gating Inventory (SGI)* (Hetrick, Erickson & Smith, 2012): The SGI is a 36-item self-report measure where participants rate items pertaining to phenomenological aspects of sensory experience on a Likert scale (0 = Never True to 5 = Always True). Scores on these items contribute to a full-scale score and four subscales (perceptual modulation; distractibility; over-inclusion; fatigue-stress vulnerability).

### ***EEG Acquisition***

EEG recording parameters were identical to those specified in Blundon, Rumak and Ward (2017) and identical to those described in the previous chapter (see Chapter 2 Method for more details). However, due to technical difficulties that emerged between studies, the EEG recordings for the present study were collected using a different EEG amplifier than in Chapter 2. These amplifiers are virtually identical, though it should be noted that the amplifiers are calibrated using slightly different scaling values for each channel, which would impact the overall amplitude of raw recordings in a linear fashion, but should have no impact on the overall pattern of results. Furthermore, since Chapter 5 only combines results from the present chapter and the next (not Chapter 2), this equipment change has no impact on our interpretations. The present study (and also the study described in Chapter 4) also utilized an EEG cap with a slightly modified electrode arrangement compared to the one used in the previous chapter to facilitate identification of temporal sources. As such, several sensors previously located over the inion and sub-inion areas were relocated to lateral frontal and temporal-parietal locations (AF7, AF8, TP9, TP10).

### ***Offline Processing***

Offline EEG data analysis was conducted using EEGLAB software (Delorme & Makeig, 2004). Identical parameters (250 Hz down sampling, average re-reference, data pruning, ICA, and artefact rejection) to those described in the previous chapter (see Chapter 2 Method; also see figure 2.2. for a simplified overview of the EEG processing steps) were used to process the EEG data and will not be described in detail.

### ***Event-Related Potentials (ERPs)***

ERPs were processed and calculated in an identical fashion to what was described in Chapter 2, except the local MMN was not examined in this study. Feature present and feature absent MMN difference waves were calculated at frontal-central channel locations (Fz, FCz, CZ) using ERPLAB. MMN difference waves were calculated for each condition by subtracting average ERP responses to flat runs from average ERP response to change runs, such that MMN difference waves for the feature-present condition were calculated by subtracting mean ERP responses to flat standard runs from mean ERP responses to target change runs and feature-absent MMNs were calculated by subtracting flat targets from change non-targets. For each participant separately, the peak MMN amplitude and latency was defined as the largest negative deflection within an extraction window of 700ms to 850ms (100 to 250ms after onset of 5<sup>th</sup> tone in each run). A local peak selection method of 5 time points (10 ms to each side of the peak) was used to account for local fluctuations that may bias peak selection.

P300 difference waves were calculated at channel Pz for feature-present targets and feature-absent targets separately. These were defined as difference waves between the P300 response to the final tone of a target run minus the ERP response to that same type of run when it was a non-target standard in the opposing condition (e.g. feature-present P300 = feature-present change targets – feature-absent change non-targets). For each participant separately, the peak P300 amplitude and latency was defined as the largest positive deflection within an extraction window of 800ms to 1600ms (200 to 1000 ms

after onset of 5<sup>th</sup> tone in each run). A local peak selection method of 10 time points (20 ms to each side of the peak) was used to account for local fluctuations that may bias peak selection.

### ***Dipole Fitting (Source Localization) and ROI Selection via Cluster Analysis***

Source localization was utilized to allow for clearer interpretation and selection of independent components (ICs) for further ERP, ERSP and PLV analysis. The dipole localization of each IC was mapped to Talairach coordinates based upon the Montreal Neurological Institute (MNI) average brain, using the DIPFIT2 function included in the Fieldtrip plugin for EEGLAB, which was identical to Chapter 2.

The steps taken to identify cortical regions of interest (ROI) included in ERSP and PLV analysis were derived using the same two-stage process of k-means clustering and subsequent seeding of dipole locations using EEGLAB functions as was described in Chapter 2, and will not be described in detail. One notable differences in this study was that we were able to use a more conservative 15% residual variance (RV; or 85% Variance Accounted For - VAF) threshold due to a greater number viable ICs being available. Also, when selecting clusters, clusters had to include 50% of participants from each group (CU and NU). In stage 1, 411 ICs (non-artefactual with less than 15% RV) were submitted to k-means (k = 15) clustering resulting in 14 viable (1 deep brain artifactual cluster omitted) clusters. In stage 2, the centroids for each stage 1 cluster were submitted to the seeding algorithm (Euclidian distance = 35mm; 1 IC per participant per cluster) resulting in 8 theoretically relevant ROI clusters that contained 50% of participants from each group (see Table 3.7 in Results Section).

### ***Event-Related Spectral Perturbations (ERSPs)***

ERSPs measuring momentary fluctuations in oscillatory activity in theta (3-7 Hz) and gamma (30-50 Hz) were calculated in an identical fashion to what was described in Chapter 2 for each ROI included in the study. ERSPs were derived for each trial containing a correctly-responded-to target or standard for both conditions (feature-present and feature-absent) and for each participant separately. Separate pairwise analysis (see Chapter 2 Method and Results sections below for additional details regarding permutation statistics and control of Type-I error) were utilized to compare NU and CU ERSP responses at each time-frequency point for feature-present and feature-absent correctly identified targets and standards. Only differences within the theta and gamma bands were interpreted.

### ***Phase synchrony***

Phase Locking Values (PLVs) were used to assess differences in phase synchrony between cannabis users and non-users within the theta (3-7 Hz) band. PLVs between pairs of ICs localized to specific brain regions were computed in an identical manner to Chapter 2 for targets within each condition for each participant separately (see Chapter 2 Method). We conducted a more nuanced analysis of theta-band network connectivity compared to the previous study, so group comparisons (NU vs CU) were made separately for targets (feature present and feature absent) over a 500 ms (700-1200 ms) period split into 10 x 50 ms windows that encompassed both the MMN and P300. Two-tailed *t*-tests ( $\alpha = 0.05$ ) were computed between groups for each time point within each 50 ms time window. A similar approach was used within each group for each condition/target to

identify significant activations versus baseline to provide a framework for interpreting any group differences, as group differences that emerge in absence of significant within group activations are likely spurious. In this case, two-tailed  $t$ -tests ( $\alpha = 0.05$ ) were used to identify significant deviations from zero. It should be reiterated, that raw PLVs by definition cannot be less than zero; however, baseline adjusted PLVs can result in negative values. In this study, no significant negative values were observed, so these were not included in the figures.

To account for multiple comparisons, regions were only considered to be functionally connected if more than 50% of the time points within the time window (7 time points for each 50 ms window) were significantly greater for a group versus the other (or versus 0 for baseline connectivity). The rationale for this chosen threshold rests on the assumption that the binomial probability of getting 50% or more significant tests within such a time window is extremely low. We used  $p = 0.05$  ( $q = 1 - p = 0.95$ ) as the probability of a success in a single binomial trial to compute the binomial probability of getting 50% or more significant time points by chance out of the total of 7 (of ~13) time points in each bin (Onton, Delorme & Makeig, 2005). This probability is  $9.9 \times 10^{-6}$  (10 bins  $\times$   $9.9 \times 10^{-7}$ ) if all of the time points in a bin represented independent tests. This assumption is probably not precisely correct, although it is not too unreasonable because the tests were made across subjects, who were independent of each other. Since we made 28 (inter-regional) comparisons (each possible pairing of 8 different ROIs), there were 28 such tests for each of the 6 comparisons (2 group comparisons + 2 NU baseline comparisons + 2 CU baseline comparisons) being made. At most ( $p = 0.05$ , with the minimum 7 of 13

significant data points per each of the 10 x 50 ms bins), the experiment-wise error probability for each set of *t*-tests, assuming independence, was (28 pairs x 6 comparisons x 1 frequency band x  $9.9 \times 10^{-6}$ )  $\approx 1.7 \times 10^{-3}$ . Again, these tests are likely not independent so this is a liberal estimate of the experiment-wise probability of Type I error. For each of the 50 ms time bins, pairings that were significant, were plotted onto separate 8x8 matrices (representing each of the 28-connections for the 8 ROIs) for each group. These were then fed into the BrainNet Viewer toolbox for MATLAB (Xia et al., 2013) to generate brain connectivity maps depicting the statistically significant functional connectivity between the various ROIs for each time bin.

## **Results**

### ***Cannabis and Other Recreational Drug Use***

Heavy cannabis users reported an average of 36.43 (SD=36.14) instances of cannabis use over the past 30 days and an average of 9.50 (SD = 10.60) instances over the past 7 days. At the time of testing, cannabis users reported that an average of 1.64 (SD = 1.97) days had elapsed since last using cannabis. The mean age of first cannabis use amongst users was 15.29 (SD = 1.38) years. One individual in the NU group reported a single instance of cannabis use approximately 300 days prior to testing, the remaining participants denied ever using cannabis.

In addition to cannabis use, participants were asked to self-report whether they considered themselves current users of any other recreational substances (including caffeine, nicotine and alcohol). Participant responses were grouped into seven substance

categories (see Table 3.1): caffeine (e.g. coffee, tea, soda & energy drinks) nicotine, alcohol, stimulants (e.g. cocaine and amphetamine), hallucinogens (e.g. MDMA, LSD, psilocybin & designer research chemicals), opioids (e.g. morphine, heroin, OxyContin etc.), sedatives (e.g. benzodiazepines), and other (i.e. dissociative drugs such as PCP or ketamine, or inhalants etc.). A greater proportion of participants in the CU group reported current nicotine and hallucinogen use. A marginally larger proportion of CU participants reported current alcohol use. Groups did not differ in proportion of current caffeine or stimulant users. There were no current opioid or sedative users in either group and no participants in either group reported current use of other categories of recreational substances.

Unlike for cannabis use, for other substance use participants were only asked to quantify frequency of use based upon five broad categories (1 = Once or twice ever; 2 = A few times a year; 3 = A few times per month; 4 = More than once each week; 5 = Daily). Frequency comparisons were only made for alcohol and caffeine use, given that there were a substantial proportion of current alcohol and current caffeine users in each group. The self-reported frequency amongst alcohol users in the CU group ( $M = 3.31$ ;  $SD = .630$ ) did not differ significantly from the NU group ( $M = 2.75$ ;  $SD = 1.17$ ). The self-reported frequency of caffeine use also did not differ significantly between the CU ( $M = 4.38$ ;  $SD = .92$ ) and NU ( $M = 3.75$ ;  $SD = .50$ ) groups. The CU participants who reported current stimulant or hallucinogen use, indicated infrequent use of only a few times each year, thus these participants were not examined more closely to determine if substance use was confounded with any of the measures discussed in this chapter. Half the

participants in the CU group reported frequent nicotine use (most of which indicated daily use) and there is some evidence that nicotine may impact the MMN (Dunbar et al., 2007); however, overall there were too few nicotine users to warrant a detailed analysis for the present study, so this will be addressed in greater detail with a larger sample in Chapter 5.

Table 3.1 Percentage of CU and NU groups reporting Current Non-Cannabis Substance Use

	NU (n = 13)	CU (n = 14)	$\chi^2$	<i>p</i> -value
	%	%		
Caffeine	38.5	64.3	1.80	.180
Nicotine	7.7	50.0	5.79	.016
Alcohol	61.5	92.9	3.83	.050
Stimulants	0	14.3	2.01	.157
Hallucinogens	0	28.6	4.36	.037
Opioids	0	0	n/a	n/a
Sedatives	0	0	n/a	n/a
Other	0	0	n/a	n/a

Table 3.1. Percentages of participants who reported being a current user of non-cannabis recreational substances. *p*-values were determined using chi-squared analysis of proportion of participants in each group who reported being a current user of a substance within each respective class.

### ***Self-Report Results***

A summary of self-report measures for each group can be seen in Table 3.2. Independent samples *t*-tests did not reveal any significant differences between NU and CU on overall self-reported psychopathological symptoms (SCL-90) over the past week. Similarly, there were no overall significant differences between these samples in terms sensory perceptual disturbances (SGI) or schizotypal traits (SPQ-B). The CU group showed a

trend toward increased trait schizotypal disorganization though this difference did not reach statistical significance,  $t(25)=-1.983$ ,  $p=.058$ , Mean Diff = -1.286, SE = .648, 95%CI = -2.621 to .050.

Table 3.2 Descriptive Statistics of Self-Report Measures for Cannabis Users and Non-Users.

	NU (n = 13)	CU (n = 14)	<i>p</i> -value
	M (SD)	M (SD)	
<u>Symptom Checklist 90</u>			
General Symptom Index	55.08 (48.91)	70.93 (39.58)	.362
Somatic	8.62 (7.91)	8.21 (5.15)	.876
OCD	10.69 (8.65)	12.14 (5.30)	.608
Interpersonal Sensitivity	6.38 (5.55)	8.21 (6.71)	.449
Depression	9.85 (7.56)	13.93 (8.86)	.211
Anxiety	4.00 (5.48)	7.50 (5.63)	.114
Hostility	2.62 (3.89)	3.71 (3.22)	.430
Phobia	1.23 (2.42)	2.29 (2.56)	.282
Paranoia	2.92 (4.35)	3.50 (3.03)	.691
Psychotic Experience	3.23 (5.33)	4.57 (4.18)	.472
<u>Sensory Gating Inventory</u>			
Total	65.08 (30.02)	64.64 (25.20)	.968
Perceptual Modulation	21.85 (11.83)	20.43 (11.29)	.753
Distractibility	17.92 (9.39)	18.14 (7.85)	.948
Over Inclusiveness	14.38 (6.38)	15.71 (7.96)	.638
Fatigue Stress Vulnerability	10.92 (5.42)	10.36 (4.48)	.769
<u>Schizotypal Personality Questionnaire</u>			
Total	8.85 (5.57)	9.50 (4.13)	.730
Cognitive Perceptual	2.85 (2.12)	3.14 (1.88)	.703
Interpersonal	4.00 (2.86)	3.07 (2.30)	.364
Disorganized	2.00 (2.04)	3.29 (1.27)	.058 <sup>†</sup>

Table 3.2. Descriptive statistics of self-report measures for non-users (NU) and cannabis users (CU). One participant was excluded from the NU group because they did not complete this portion of the experiment.

### *Neuropsychological Results*

A summary of neuropsychological results can be seen in Table 3.3. Independent samples *t*-tests did not reveal significant differences between NU and CU on estimated IQ, verbal comprehension (vocabulary), non-verbal reasoning (matrix reasoning), working memory (letter number sequencing), attention/vigilance (continuous performance task – identical pairs).

Table 3.3 Descriptive statistics of Neuropsychological Tests for Users and Non-Users.

	NU (n = 13)	CU (n = 14)	
	M (SD)	M (SD)	<i>p</i> -value
Estimated IQ <sup>a</sup>	112.35 (4.63)	110.75 (5.38)	.419
Vocabulary <sup>b</sup>	55.38 (6.53)	53.64 (8.08)	.545
Matrix Reasoning <sup>b</sup>	22.38 (1.81)	21.86 (2.11)	.493
Letter Number Sequencing <sup>b</sup>	15.38 (3.18)	13.00 (3.26)	.066
<u>Continuous Performance</u>			
<u>Task<sup>c</sup></u>			
2-digit	4.00 (.22)	3.88 (.37)	.317
3-digit	3.47 (.48)	3.37 (.78)	.711
4-digit	2.22 (.57)	2.00 (.65)	.359

Table 3.3. Descriptive statistics of neuropsychological tests for non-users (NU) and cannabis users (CU). a) Estimated Full-Scale IQ derived by using OPIE-3 algorithm (see Method section) b) VC, MR, and LNS scores are based upon raw scores derived from

each test. c) Scores represent  $d'$  values for each condition generated automatically by the CPT-IP software included in the MATRICS battery. One participant was excluded from the NU group because they did not complete this portion of the experiment.

### ***Accuracy and Reaction Time***

Behavioural results can be found in Table 3.4. Separate 2x2 mixed measures ANOVAs with condition (feature-present and feature-absent) as a within subjects factor and user group (NU and CU) as a between subjects factor was run on accuracy ( $d'$ ) scores and reaction time (RT) for correct responses.

In terms of response accuracy, there was a significant main effect of condition  $F(1,26)=12.31, p = .002, \eta_p^2 = .32$  suggesting that participants in both groups responded more accurately in the feature-present condition when they were responding to rare salient targets (change runs) compared to the feature-absent condition, where they were responding to less salient (flat runs) targets. The between group and the condition by user group effects were not significant.

In terms of response time, there was a significant main effect of condition  $F(1,26) = 5.14, p = .032, \eta_p^2 = .17$ , which was qualified by a condition by user group interaction,  $F(1,26) = 6.28, p = .02, \eta_p^2 = .19$ . Simple effects analysis revealed that the cannabis users had slower reaction times in the feature-absent condition compared to their response times in the feature-present condition (Mdiff = -52.60 ms, SE = 15.89,  $p = .002$ , 95% CI = [-86.26 to -20.05]) whereas non-users did not show a significant reaction time difference between

conditions ( $M_{diff} = 2.68$  ms,  $SE = 15.89$ ,  $p = .867$ , 95% CI = [-29.976 to 35.34]. The between group main effect was not significant.

Table 3.4. Behavioural Performance Data for Roving Local-Global Task for Cannabis Users and Non-Users

	Feature Present		Feature Absent	
	NU M (SD)	CU M (SD)	NU M (SD)	CU M (SD)
$d'$	3.87 (1.34)	4.00 (1.29)	3.47 (1.24)	3.41 (1.43)
RT	568.77 (96.16)	540.04 (103.98)	566.08 (89.08)	593.64 (106.12)

Table 3.4. Mean accuracy ( $d'$ ) and reaction time (RT) data for non-users (NU;  $n = 14$ ) and cannabis users (CU;  $n = 14$ ) in feature present and feature absent conditions. RT was measured with respect to the onset of the 5<sup>th</sup> tone (600 ms) in auditory runs .

### ***ERP Results***

#### *MMN*

Mean amplitudes and latencies for MMN difference waves for each condition and user group can be found in Table 3.5 and MMN waveforms can be viewed in Figure 3.1.

Since MMNs were calculated using correctly identified targets and the immediately preceding non-target standards, we set a minimum threshold of 50 epochs per participant per condition to reliably calculate MMNs. As such, two participants from the NU group and one participant from the CU group were excluded from the MMN analyses because they had inadequate number of correct responses in one or both conditions. For both amplitude and latency, separate 2x3x2 mixed measures ANOVAs were run with

condition (feature-present and feature-absent) and channel (FZ, FCZ, CZ) as within subjects factors and user group (NU and CU) as a between subjects factor.

For MMN amplitude, there was a main effect of channel. Degrees of freedom for the main effect of channel were corrected due to a violation of sphericity ( $X^2(2) = 19.136, p < .002$ ) using a Greenhouse-Geisser correction ( $E = .698, F(1.40, 32.10) = 11.51, p = .001, \eta_p^2 = .334$ ), suggesting larger MMN amplitudes at anterior sites. The main effect of channel was qualified by a channel by condition interaction. Degrees of freedom for the interaction were corrected due to a violation of sphericity ( $X^2(2) = 12.480, p = .002$ ) using a Greenhouse-Geisser correction ( $E = .633, F(1.27, 29.10) = 11.51, p = .001, \eta_p^2 = .331$ ). Follow up analysis revealed that there were larger MMN amplitudes at CZ ( $M_{diff} = -1.094, SE = .347, p = .004, 95\%CI = [-1.811 \text{ to } -0.377]$ ) for the feature-present condition compared to the feature-absent condition. There were no significant between groups effects, or significant interactions (condition by user group, channel by user group and condition by channel by user group).

For MMN latency, there was a significant condition by channel interaction. Degrees of freedom for the interaction were corrected due to a violation of sphericity ( $X^2(2) = 6.142, p < .002$ ) using a Greenhouse-Geisser correction ( $E = .804, F(1.61, 36.99) = 5.04, p = .017, \eta_p^2 = .180$ ). Follow up analyses revealed longer latencies at channel FZ in the feature-present condition compared to the feature-absent condition ( $M_{diff} = 22.71, SE = 6.73, p = .003, 95\%CI = [8.77 \text{ to } 36.64]$ ). There were no other significant within subjects

effects (channel), significant between groups effects, or significant interactions (condition by user group, channel by user group, and condition by channel by user group).

Table 3.5. MMN Amplitudes and Latency

	Feature Present				Feature Absent			
	NU Mean	SD	CU Mean	SD	NU Mean	SD	CU Mean	SD
<b><i>Amplitude (uV)</i></b>								
FZ	-1.03	1.55	-0.96	0.91	-1.49	1.37	-1.61	1.26
FCZ	-1.36	1.33	-1.12	1.16	-0.94	1.21	-0.86	1.31
CZ	-1.45	1.02	-1.27	1.19	-0.32	0.65	-0.21	1.30
<b><i>Latency (ms)</i></b>								
FZ	766.7	33.7	770.5	42.3	736.3	33.6	755.4	41.6
FCZ	761.7	27.7	755.4	38.6	739.7	33.2	764.9	34.9
CZ	744.3	23.2	751.4	39.3	753.7	46.5	753.2	31.1

Table 3.5. Amplitudes and latencies of MMN Difference waves at channels FZ, FCZ, and CZ for non-users (NU; n = 12) and cannabis users (CU; n =13) in feature present and feature absent conditions. Latencies are measured from onset of the first tone (0 ms) of auditory runs.

Figure 3.1. Grand Average Feature Present and Feature Absent MMN ERP Difference Waves for Cannabis Users and Non-Users

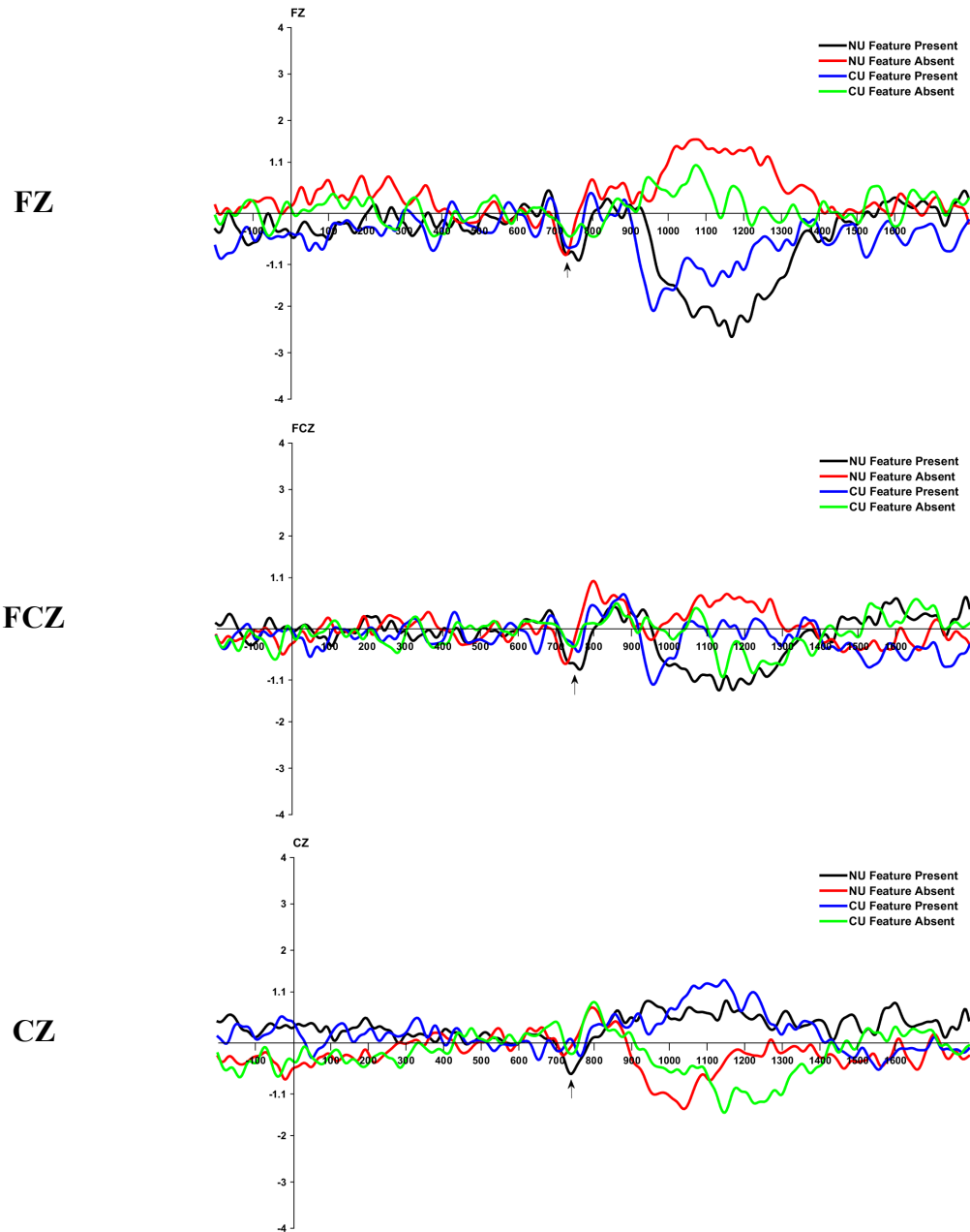


Figure 3.1. Grand average MMN ERP difference waves at channels FZ, FCZ, CZ for feature-present and feature-absent conditions for non-users (NU) and cannabis users (CU). For display purposes only, ERPs were calibrated so that the waveform at 600ms corresponding to the onset of the 5<sup>th</sup> tone is at 0  $\mu$ V. Arrows indicate the location of the MMN.

### *P300 ERP Results*

Mean Amplitudes and Latencies for P300 difference waves for each condition and user group for each condition can be found in Table 3.6 and P300 waveforms can be viewed in Figure 3.2.

Unlike MMNs, fewer epochs are required to achieve reliable P300 measurements, so initially all participants were included in the analysis. However, examination of latencies revealed that one participant from each group was identified as an outlier based upon both boxplot outlier analysis in SPSS and also by their Cook's distances, which were greater than four times the sample mean. While ANOVA methods can often be robust to violations of normalcy, in this instance, after running ANOVAs with and without these subjects, it was determined that these cases had undue influence on the overall model. As will be seen, removal of these participants resulted in findings that were largely consistent with what would be expected given our behavioural results (which remained significant even when removing these participants from that analysis).

For P300 amplitude at channel PZ, there was a significant main effect of condition  $F(1,24) = 5.53, p = .027, \eta_p^2 = .187$  suggesting larger P300 amplitude response to targets in the feature-present condition. The between groups main effect and condition by user group interaction were not significant.

For P300 latency at channel PZ, there was a significant condition by user group interaction,  $F(1,24) = 4.87, p = .037, \eta_p^2 = .169$ . Follow-up analyses revealed that the CU

group had longer latencies in the feature-absent condition compared to the feature-present condition ( $M_{diff} = -51.69\text{ms}$ ,  $SE = 25.04$ ,  $p = .05$ ,  $95\%CI = [-103.37 \text{ to } -0.01]$ ) whereas latencies for the NU group did not significantly differ between conditions ( $M_{diff} = -26.46 \text{ ms}$ ,  $SE = 25.04$ ,  $p = .301$ ,  $95\%CI = [-25.22 \text{ to } 78.14]$ ). There was also a trend toward the NU group having longer latencies in the feature-present condition compared to the CU group ( $M_{diff} = 55.69\text{ms}$ ,  $SE = 31.9$ ,  $p = .094$ ,  $95\%CI = [-10.16 \text{ to } 121.55]$ ). There were no significant main effects of condition or group.

Table 3.6. Amplitudes and Latencies of P300 Difference Waves

	Feature Present				Feature Absent			
	NU Mean	SD	CU Mean	SD	NU Mean	SD	CU Mean	SD
<b><i>Amplitude (uV)</i></b>								
PZ	5.21	2.03	4.83	2.37	4.35	1.68	4.35	2.14
<b><i>Latency (ms)</i></b>								
PZ	1092.9	85.4	1037.2	77.1	1066.5	83.3	1088.9	120.7

Table 3.6. Amplitudes and latencies of P300 Difference waves at channel PZ for non-users (NU;  $n = 13$ ) and cannabis users (CU;  $n = 13$ ) in feature present and feature absent conditions. Latencies are measured from onset of the first tone (0 ms) of auditory runs.

Figure 3.2. Grand Average P300 ERP Difference Waves

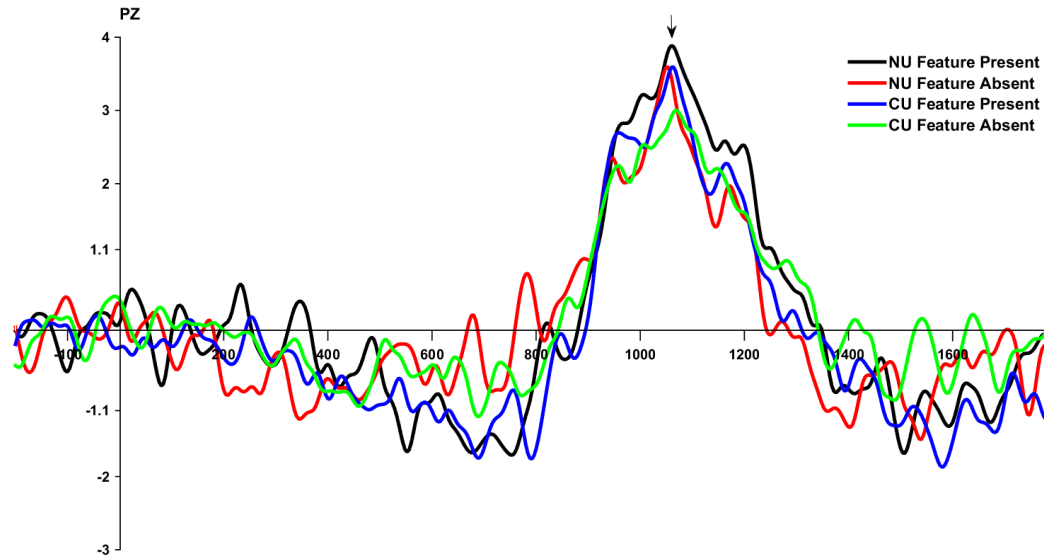


Figure 3.2. Grand average P300 ERP difference waves at channel Pz for feature-present and feature-absent conditions for non-users (NU) and cannabis users (CU). The arrow indicates the location of the P300 peak at Pz. Both feature-present and feature-absent conditions can be seen to have similar latencies, though a larger positive amplitude can be seen for the feature-present condition.

### ***ROI Cluster Analysis Results***

Results of dipole clustering and identification of ROIs can be viewed in Table 3.7 and plots of the retained clusters can be viewed in Figure 3.3. In total, eight clusters pertaining to theoretically relevant brain areas met our criteria of containing at least 50% of individuals from each group. The locations selected were: bilateral superior temporal lobes (RSTG & LSTG), bilateral temporal parietal junction (RTPJ & LTPJ), right posterior cingulate (RPCC), a more anterior region falling proximal to left cingulate (LCing), and bilateral pre/post central gyri (RPCG and LPCG). These regions were included in subsequent ERP, ERSP and PLV analyses.

The bilateral STG regions were not observed in the previous study (Chapter 2), but are expected given the auditory nature of this task. The TPJ sites are similar to those from the

previous study (albeit slightly posterior) and tend to fall within the white matter at the junction of the temporal-parietal-occipital regions; given the proximity of these regions to those from the previous study they will be referred to as TPJ. Unlike in the previous study, enough participants contributed ICs to the L TPJ to warrant further analysis. Also, similar to the previous study, a centrally localized posterior cingulate cluster emerged that is also proximal to the superior parietal lobe, though it should be noted that this cluster is slightly posterior compared to the previous study and contains more ICs that are localized to the right hemisphere. The cingulate cluster (here referred to as the LCing), is situated right anterior and dorsal to the similarly named cluster in the previous study and falls somewhat proximal to the medial frontal gyrus falling somewhere between the ACC and LCing of the previous study. Unlike the previous study, more anteriorly situated frontal lobe clusters did not emerge. Frontal clusters (bilateral IFG) and also one proximal to the medFG cluster from the previous study appeared but fell short of the threshold for inclusion.

Table 3.7. Seeded Dipole Clusters of Independent Components Identified for Cannabis Users and Non-Users and Corresponding Brain Region

ROIs	Contributing		% VAF	Talairach			BA #
	NU %	CU %		X	Y	Z	
<b>Retained</b>							
R.STG	79	79	91	53	-31	11	22,41,42
L.STG	57	64	90	-50	-33	2	22,21
R.TPJ	93	100	95	26	-61	24	39,31
L.TPJ	86	93	94	-23	-68	21	31,18,39
R.PCC	79	93	96	3	-54	43	7,31
L.Cing	57	64	93	-2	16	40	32,8
L.PCG	79	79	94	-24	-30	45	3,4
R.PCG	57	79	94	29	-26	46	3,4
<b>Rejected</b>							

R.preCG	36	50	95	46	-2	40	6,4
L.preCG	36	64	94	-44	-10	47	4,6
R.IFG	36	50	92	29	27	1	13,47,45
L.IFG	36	43	92	-45	20	19	46,9,45
L.PCC	29	43	95	-2	-76	27	7,31,18
ACC	29	43	94	-3	46	5	32,10

Figure 3.3. Dipole Cluster Plots of Retained ROIs

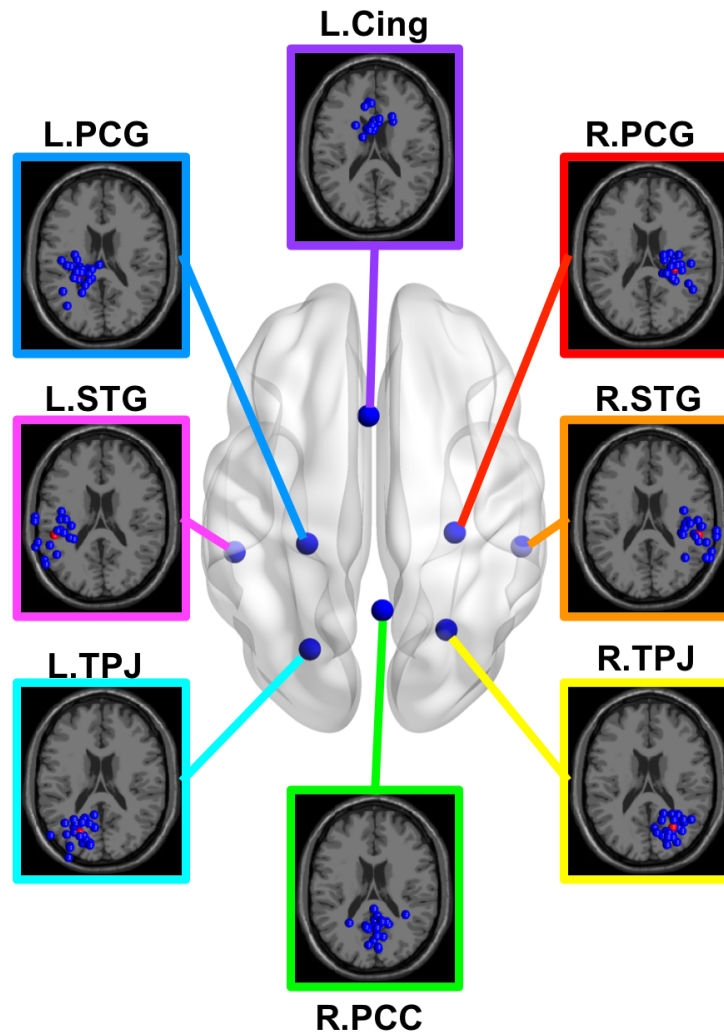


Figure 3.3. Dipole cluster plots of retained ROIs for roving dual oddball task. Blue dots depict individual ICs and red dots depict cluster centroids. Clusters represent both cannabis users and non-users. Note: Some ICs/centroids are not visible due to being hidden beneath others.

### ***ROI ERPs***

ERPs were examined for each of the eight selected ROIs (RSTG, LSTG, RTPJ, LTPJ, RPCC, LCing, RPCG & LPCG). Like the previous study, the primary goal of this analysis was to provide a general overview of areas of difference between groups for each of the four stimulus types (feature-present and feature-absent targets and standards) in order to provide an interpretive framework to compare channel level ERP analysis discussed in the previous sections and examination of oscillatory activity (ERSPs) and functional network connectivity (PLVs) that will be the focus in the subsequent sections. As such, uncorrected ( $\alpha = .05$ ) within-subject one-way ANOVAs were run across ERP waveforms for each ROI separately. For ease of interpretation results are discussed in context of the rough time windows observed in channel level data for the MMN (~700 to 850 ms) and P300 (~850 to 1200 ms) and activity that occurs later in the epoch (~1200+ ms). ERP waveforms averaged across subjects for each condition and ROI can be viewed below in Figure 3.4.

In the MMN time range (~700-850 ms), small windows of significant differences emerged in the bilateral STG, L TPJ, and R PCC. The waveforms localized to the superior temporal lobes displayed morphology consistent with the negative peaks of the channel level MMNs. In the R STG, the CU group showed a more negative amplitude (~780-844 ms) to flat feature-present standards; however, in the L STG they displayed a more negative amplitude to feature-present targets (~824-832). Also, in the L STG the CU group exhibited larger amplitudes to flat feature-absent targets (~716-724 & 820-828). This may suggest that the temporal lobes of the CU group are engaged in additional

processing of local standards (response to the 5<sup>th</sup> tone in flat runs) compared to the NU group. Additionally, the greater involvement of the left temporal lobe in response to local deviant change stimuli (at least when they are targets) may in part account for the absence of differences in MMN difference waves seen at the channel level. The CU group also showed a similar pattern of increased activity to flat feature-absent targets in the LTPJ, though this appeared to happen somewhat early in the MMN window (~680 to 708). Finally, the NU and CU groups displayed differential activity in the R PCC with the CU group again showing increased activity to flat feature-present standards (~692-708 ms & 772-824 ms) and flat feature-absent targets (~696 to 744ms).

In the P300 range (~850-1200 ms), clearer differences emerged between the groups primarily in the bilateral STG, R PCC, bilateral PCG, and L Cing. The NU group displayed larger positive amplitudes in the RSTG to both feature-present targets (~1060 to 1248) and feature-absent targets (~1116 to 1320), which began in the P300 range and appeared to extend to past 1200ms. Interestingly, the CU group only showed greater L STG amplitudes post 1200 ms to targets in both conditions and also to flat standards in the feature-absent condition.

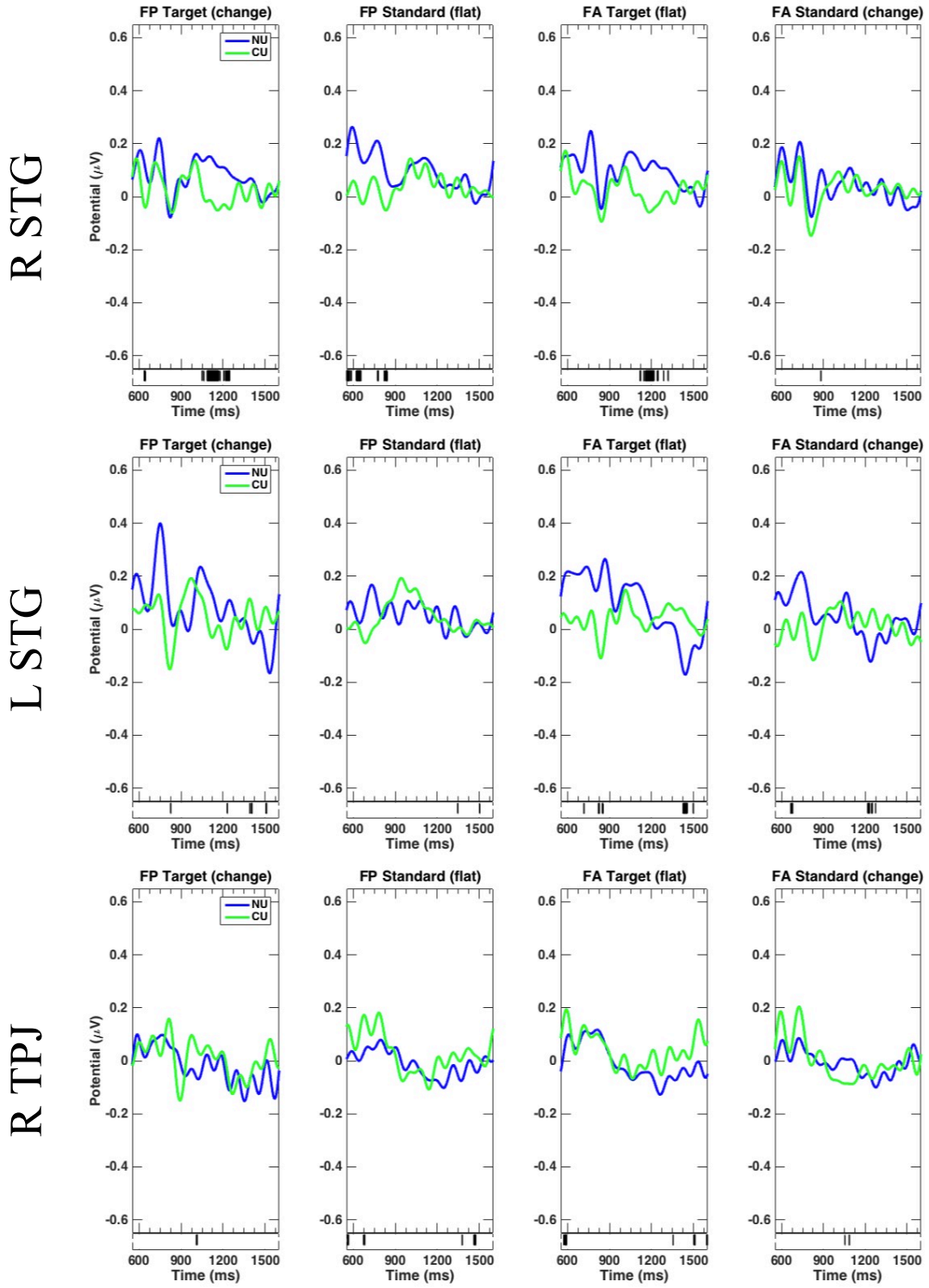
The ERP localized to the R PCC appears to show a morphology most closely resembling the P300 to targets seen at the channel level. There were no P300 differences in this apparent P300 component to targets, but the groups appeared to show differences earlier in the P300 window to non-target stimuli with NU displaying more negative amplitudes to flat feature-present standards (~880-908 ms) and CU group displaying more negative

amplitudes to feature-absent change standards (~940 to 952). The NU group tended to show larger late (after 1200 ms) positive amplitudes to feature-present standards and to both feature-absent targets and standards.

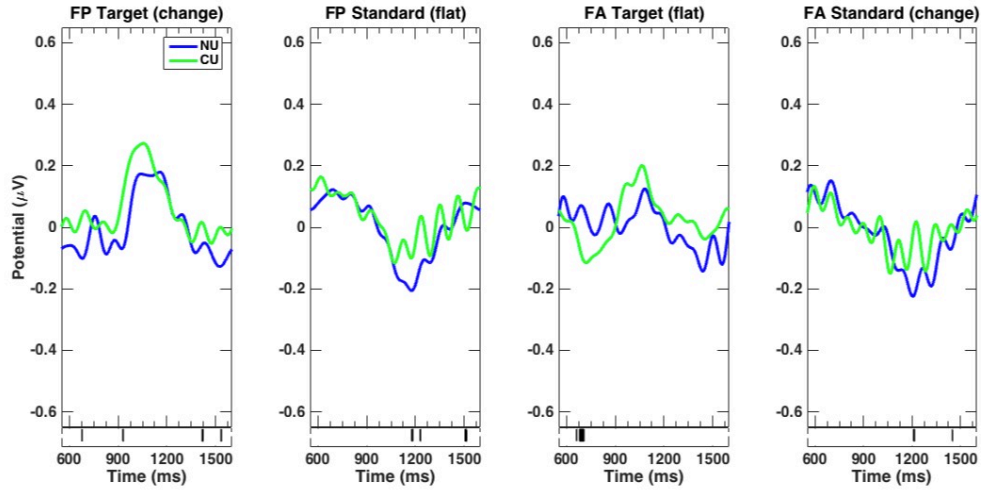
The bilateral PCG (especially the left) also appeared to show a ERP morphology similar to the channel level P300 waveforms. In the RPCG the CU group appeared to show a larger positive amplitude to feature-present targets (~1112-1136 ms), though examination of the waveforms appeared to show a similar component occurring earlier (albeit not significant) in the NU group. More apparent differences emerged between groups in response to standards with the NU group exhibiting larger amplitudes to both feature-present (~956-968 ms & 1056-1064) and feature-absent (~888-908 ms & 1020-1056 ms) standards, while the CU group displayed increased late amplitude (after 1200 ms) amplitudes to standards in both conditions. Similarly, in the LPCG, the CU group had increased late amplitudes to standards in the feature-absent condition.

The most striking differences between groups in processing both feature-present and feature-absent targets appeared in more frontally situated ERPs localized to the L Cing. The NU group displayed more negative amplitudes to both feature-present targets (~1032-1064 ms & 1156-1248) and feature-absent targets (~920-960 ms, 1104-1112 & 1176-1184). The NU group also exhibited increased late (post 1200 ms) frontal amplitudes to targets in both conditions. Taken together it appears that the frontal areas of the NU group are more active in processing targets compared to the CU group.

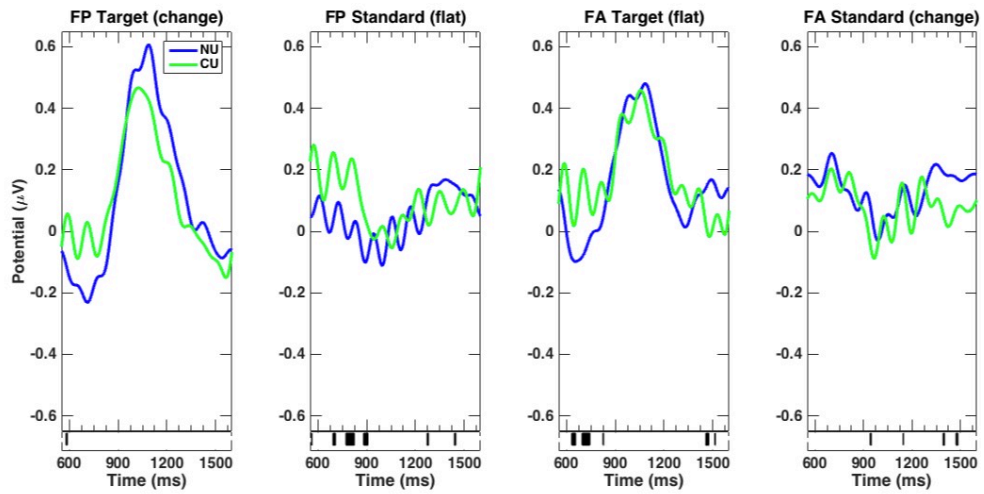
Figure 3.4. ROI ERPs for Feature Present and Feature Absent Conditions Comparing NU and CU



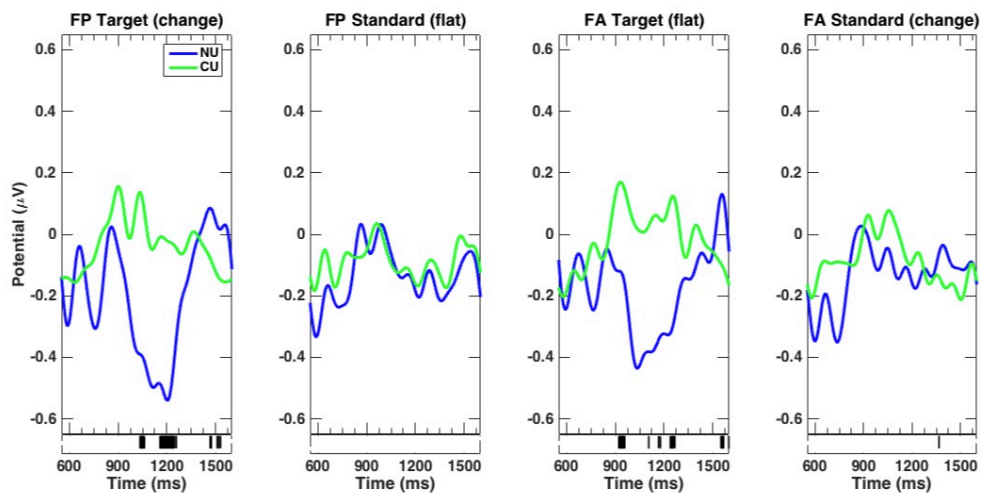
L TPJ



R PCC



L CING



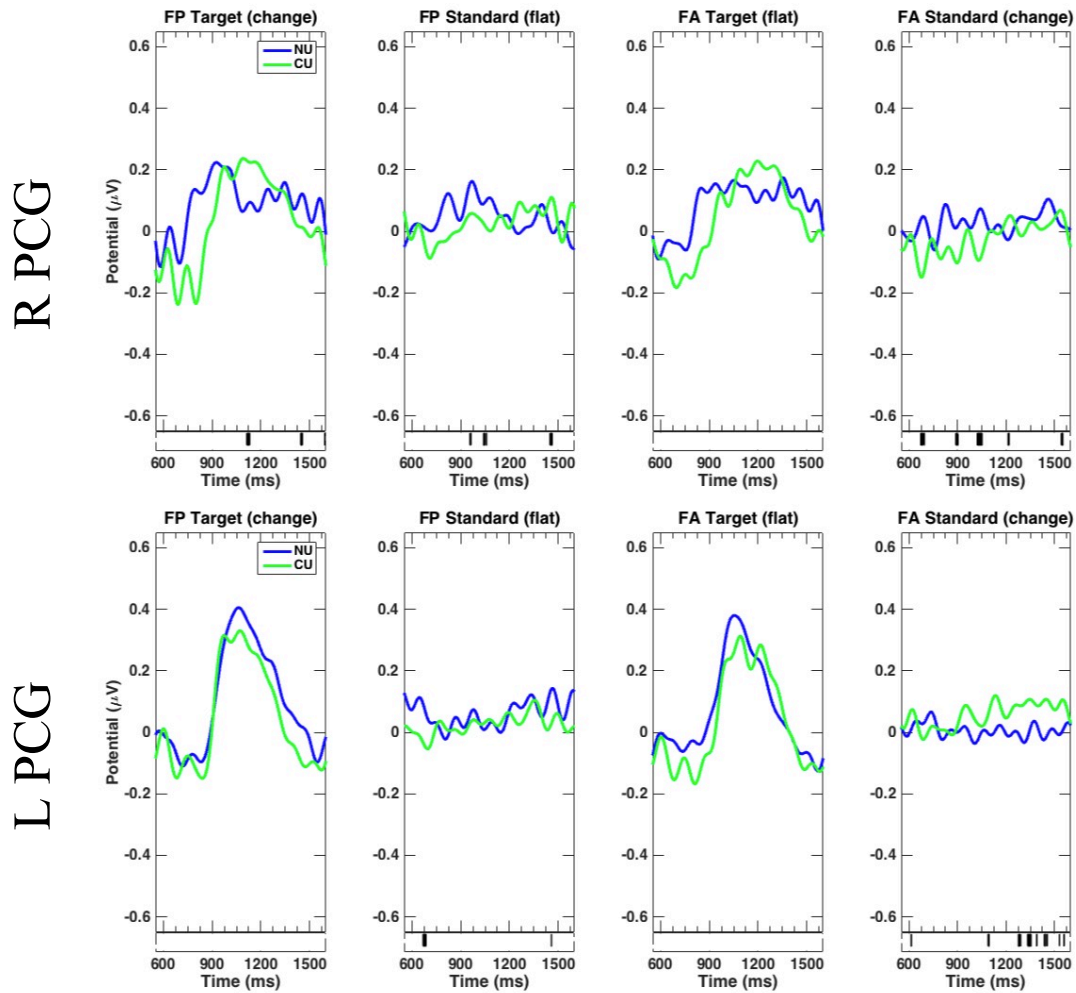


Figure 3.4 Independent component ERPs to targets and standards in feature present (FP) and feature absent (FA) conditions comparing non-users (NU; blue) to cannabis users (CU; green) for each selected brain region of interest (ROI). Dark areas below each plot represent time windows of significance ( $p < .05$ ; uncorrected). Regions of Interest (ROIs): R and L designate right and left hemisphere; STG = superior temporal gyrus; TPJ = temporal-parietal junction; PCC = posterior cingulate cortex; Cing = cingulate; PCG = post central gyrus.

### ***ERSP Results***

A summary of the ERSP results within the MMN range can be viewed in Table 3.8 and in Table 3.9 for the P300 range. Selected ERSP figures can be viewed in Figure 3.5, and the remaining ERSP plots can be viewed in Appendix B.

### *MMN Range ERSPs*

Within the MMN time window (~700-850 ms), no significant differences emerged between groups within the theta (3-7 Hz) band; however, there were several notable differences in gamma (30-50 Hz) band activity (See Table 3.8 for summary of MMN range ERSP results) particularly in the RSTG, RTPJ, LTPJ, and LCing suggesting differential processing of targets and standards between groups.

In the feature-absent condition, in response to flat targets, the CU group displayed greater gamma activity localized to the RSTG. In the RTPJ, the NU group displayed greater gamma activity to feature-present change targets and the CU group greater gamma ERSP to feature-absent flat targets. In the LTPJ, the CU group showed greater gamma ERSP to both feature-present change and feature-absent flat targets, in these instances (especially for feature-present change stimuli) the gamma activity appeared to be sustained over a long interval preceding the onset of the 5<sup>th</sup> tone in the run. The NU group also demonstrated a larger gamma response to feature-absent flat targets, though this occurred at a higher frequency band and was only significantly greater over a circumscribed period entirely within the MMN window. The NU group also showed greater gamma response to non-target change stimuli in the feature-absent condition, which slightly preceded the onset of the 5<sup>th</sup> tone for both the LTPJ and the L Cing.

Table 3.8. Summary of Gamma ERSP Results in MMN Time Window

	<b>Feature-Present</b>	<b>Feature-Absent</b>
--	------------------------	-----------------------

<b>ROI</b>	<b>Target (Change)</b>	<b>Standard (Flat)</b>	<b>Target (Flat)</b>	<b>Standard (Change)</b>
<b>R STG</b>			CU+ 772-840 <sub>γ</sub>	
<b>R TPJ</b>	NU+ 588-764 <sub>γ</sub>		CU+ 764-880 <sub>γ</sub>	
<b>L TPJ</b>			CU+ 552-916 <sub>γ</sub>	
	CU+ 416-1400 <sub>γ</sub>		NU+ 796-860 <sub>γ</sub>	NU+ 532-824 <sub>γ</sub>
<b>L Cing</b>				NU+ 540-728 <sub>γ</sub>

Table 3.8. Summary of significant Gamma ( $\gamma$ ) [30-50 Hz] ERSP results comparing non-users (NU) to cannabis users (CU) for feature-present and feature-absent targets and standards overlapping the MMN (~700 to 850ms). NU+ indicates NU > CU and CU+ indicates CU > NU for spectral power at  $p < .005$  based upon permutation statistics. To control type-I error due to multiple comparisons, areas of significance were only considered if they met a minimum threshold of significant time-frequency points, which varied depending on the frequency band: theta = 150ms; gamma = 25ms. Regions of Interest (ROIs): R and L designate right and left hemisphere; STG = superior temporal gyrus; TPJ = temporal-parietal junction; PCC = posterior cingulate cortex; Cing = cingulate. Note: There were no significant results in the Theta ( $\theta$ ) [3-7 Hz] range, or in the LSTG, R PCC or PCG ROIs, so they are not represented here.

### *P300 Range ERSPs*

In the P300 range (~850-1200 ms), the only notable theta-band ERSP difference that emerged was in the R PCC, where NU had larger theta response to feature-absent non-target stimuli late in the P300 window and extending beyond the 1200ms time point.

In terms of P300 range gamma-band activity, group differences emerged in the R STG, R TPJ, L TPJ, PCC, L Cing, L PCG and R PCG suggesting differential processing of targets and standards, which was most prominent in the feature absent condition. CU showed greater activity in the R STG to feature-absent targets early in the P300 window

(overlapping the MMN) and also late in the P300 window extending beyond 1200ms. NU showed greater gamma to feature-present non-targets in bilateral TPJ locations, within and beyond the P300 range and greater LTPJ gamma activity to targets in the feature-absent condition. In contrast, the CU group showed greater RTPJ gamma to feature-absent targets early in the P300 window and overlapping with the MMN. CU also evidenced greater LTPJ gamma response to targets in both conditions, though in the feature-present condition this preceded the onset of the 5<sup>th</sup> tone and was sustained throughout the MMN window and extended beyond the P300; whereas, their greater gamma to feature-absent targets preceded the 5<sup>th</sup> tone and overlapped with the MMN and extended into the early P300 window, but interestingly did not overlap with the time window where NU showed greater gamma. The CU group also demonstrated late (after 1200ms) greater gamma activity to feature-absent targets.

No gamma differences were observed to targets in the R PCC, though the CU group did exhibit greater gamma activity to non-targets in the feature-absent condition. The NU group showed greater gamma to feature-absent non-targets localized to the L Cing. In the LPCG, the CU group showed greater gamma activity in response to feature-present standards within the P300 window and after 1200 ms, whereas NU displayed greater R PCG gamma activity to feature absent standards early in the P300 window and late in the P300 window extending beyond 1200ms.

Table 3.9. Summary of Theta and Gamma ERSP Results in P300 Time Window

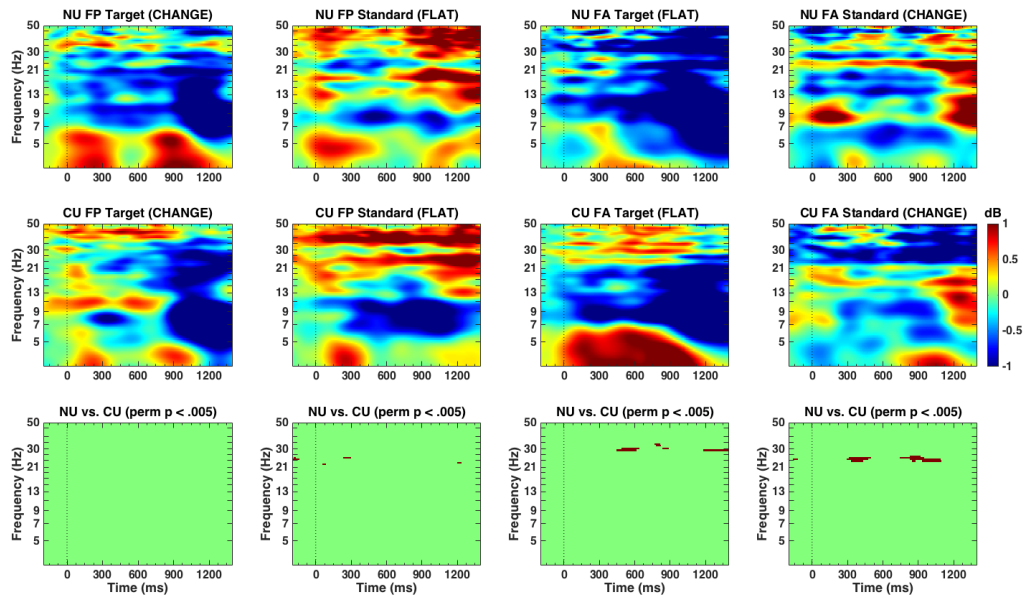
	<b>Feature-Present</b>	<b>Feature-Absent</b>
--	------------------------	-----------------------

ROI	Target (Change)	Standard (Flat)	Target (Flat)	Standard (Change)
R STG			CU+ 836-888 $\gamma$	
R TPJ		NU+ 1092-1400 $\gamma$		
L TPJ	CU+ 416-1400 $\gamma$	NU+ 1096-1240 $\gamma$	CU+ 552-916 $\gamma$ 1204-1280 $\gamma$ *  NU+ 936-972 $\gamma$	NU+ 1024-1400 $\gamma$
R PCC				CU+ 932-1000 $\gamma$ NU+ 1152-1396 $\theta$ *
L Cing				NU+ 980-1052 $\gamma$
L PCG		CU+ 932-1076 $\gamma$ 1300-1400 $\gamma$ *		
R PCG				NU+ 844-888 $\gamma$ 1196-1400 $\gamma$ *

Table 3.9 Summary of significant Theta ( $\theta$ ) [3-7 Hz] and Gamma ( $\gamma$ ) [30-50 Hz] ERSP results comparing non-users (NU) to cannabis users (CU) for feature-present and feature-absent targets and standards overlapping the P300 (~850 -1200ms). Time ranges marked with an \* fall within the P300 extraction window but later than 1200 ms and likely correspond to late processing of stimuli. NU+ indicates NU > CU and CU+ indicates CU > NU for spectral power at  $p < .005$  based upon permutation statistics. To control type-I error due to multiple comparisons, areas of significance were only considered if they met a minimum threshold of significant time-frequency points, which varied depending on the frequency band: theta = 150ms; gamma = 25ms. Regions of Interest (ROIs): R and L designate right and left hemisphere; STG = superior temporal gyrus; TPJ = temporal-parietal junction; PCC = posterior cingulate cortex; Cing = cingulate; PCG = post central gyrus. Note: There were no significant results for the L STG ROI.

Figure 3.5. Select Feature Present and Feature Absent ERSP Plots (NU vs. CU)

RSTG



RTPJ

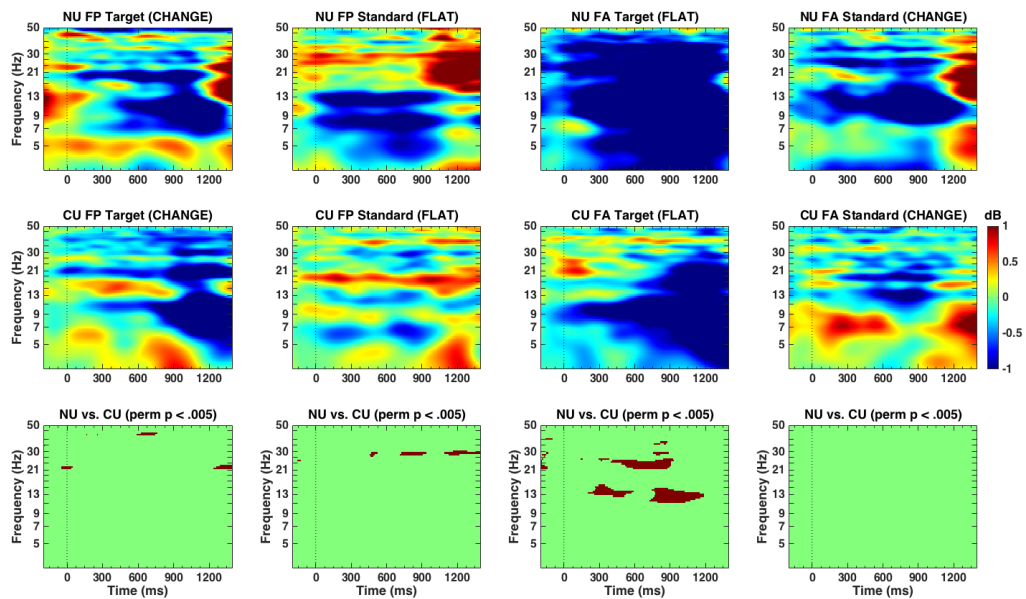


Figure 3.5. ERSP (3-50Hz) plots from (-200-1400 ms; onset of 5<sup>th</sup> tone is 600 ms) for RSTG and RTPJ comparing non-users (NU; top row of each figure) and cannabis users (CU; middle row) for targets and standards in both the feature present (FP) and feature absent (FA) conditions. Plots are scaled from -1 (blue) to +1 (red) dB. Significance plots (bottom) represent pairwise comparisons computed using EEGLab permutation statistics ( $p < .005$ ). ERSP plots for all ROIs can be found in Appendix B.

### *Phase Synchrony*

Figures depicting the theta frequency PLV analyses to feature-present and feature-absent targets can be viewed in Figures 3.6 and 3.7, respectively. Unlike, ERSPs which index localized synchronization, PLVs index longer range network communication, therefore discussion was primarily focused on the theta (~3-7 Hz) band. Furthermore, emphasis was placed on theta connectivity for feature-present and feature-absent targets. Finally, similar to the previous chapter, the PLV analyses were temporally constrained to time-ranges roughly corresponding to the time windows in which the MMN (700-850 ms) and the P300 channel level ERP components appeared; however, unlike the previous study, which aimed to provide a general description of the brain networks contributing to the MMN and P300, the present study broke these time windows down into smaller 50ms segments to facilitate a more precise examination of the temporal dynamics coinciding with the MMN and P300.

#### *Theta PLV to Feature-present Targets*

In the MMN range, in response to salient targets, no theta connectivity group differences emerged; however, examination of connectivity versus baseline (NU>0 and CU>0 in figure 3.6) revealed different patterns for each group. Both groups exhibited RSTG-PCC connectivity in the 800-850 range, though overall NU primarily demonstrated fronto-temporal connectivity (LSTG-LCing), whereas, at this early stage in processing, the CU group exhibited a pattern of fronto-parietal (RTPJ-LCing; LTPJ-RPCG) connectivity, perhaps suggesting a more stimulus driven ventral attentional processes.

In the P300 range, NU had significantly greater fronto-temporal (LSTG-LCing) theta connectivity than CU from about 900-1000 ms and also greater connectivity between frontal and sensorimotor cortices (LCing-LPCG). NU also displayed greater posterior parietal (RTPJ-PCC) connectivity from 1100-1150 and greater temporal-parietal (LSTG-RTPJ) and temporal-frontal (RSTG-LCing) from 1150-1200 ms). While not significant at the group level, NU displayed a pattern of fronto-posterior dorsal attentional connectivity (PCC-LCing) from 1100-1150, that was largely absent in CU.

CU by contrast, only displayed significantly greater fronto-parietal (LCing-LTPJ) connectivity than NU early in the P300 window from 850-900ms; however examination of the overall connectivity pattern, suggested that CU deployed a more distributed pattern of bilateral network connectivity. In particular, CU exhibited sustained bilateral fronto-parietal (LTPJ-LCING; RTPJ-LCING) connectivity throughout the P300 window along with bilateral temporal lobe (RSTG-LSTG) and left temporo-parietal (LSTG-LTPJ) connectivity.

Taken together, while both groups had similar behavioural performance in identifying salient feature present change targets, the CU group showed an overall pattern of sustained connectivity between temporo-parietal and fronto-parietal regions likely reflecting coordinated activation of the stimulus-driven ventral attentional network. NU, on the other hand, showed a lesser degree of ventral attentional activation, and greater fronto-temporal and temporo-parietal connectivity, with the appearance of dorsal attentional activity later in the time window, which may indicate more dynamic interplay

between the auditory cortices along with both stimulus-driven ventral attentional processes and top-down dorsal attentional processes.

Figure 3.6. Theta (3-7 Hz) PLV Analysis for Feature-Present Targets

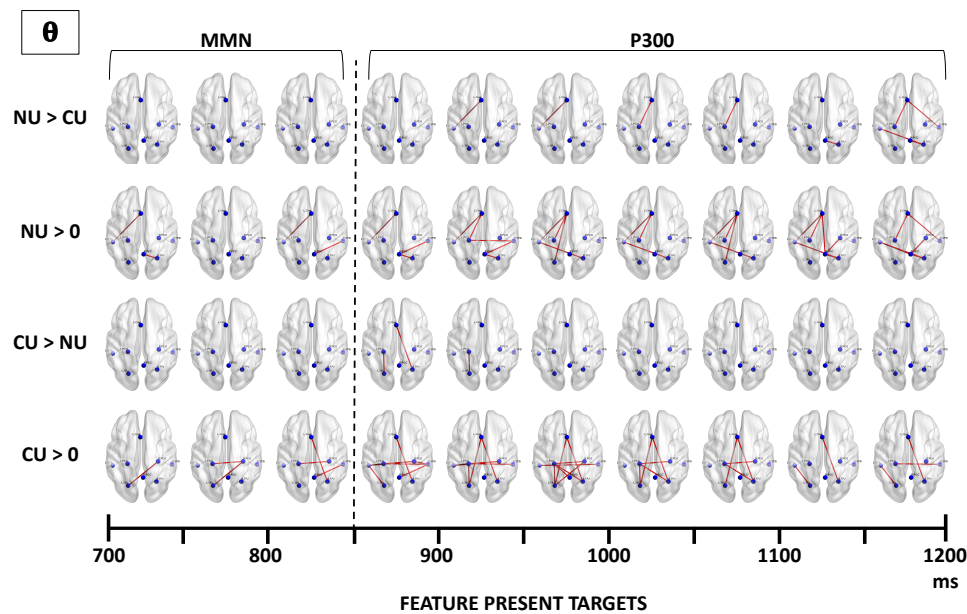


Figure 3.6. Theta (3-7 Hz) phase synchrony to feature-present targets (change runs) corresponding to MMN (700-850 ms) and P300 (850-1200 ms) for non-users (NU) and cannabis users (CU). Each image represents 50ms windows. First Row: Connections indicate nodes where NU showed greater PLV versus CU (NU>CU). Second Row: Displays connections in NU that were significantly larger than baseline (NU > 0). Third Row: Connections indicate nodes where CU showed greater PLV versus NU (CU>NU). Fourth Row: Displays connections for CU that were significantly larger than baseline (CU>0). To minimize the chance of Type I error, significant group differences (rows 1 & 3) were not considered meaningful unless the group with significantly greater PLVs also showed significantly greater PLVs versus baseline (rows 2 & 4).

#### *Theta PLVs to Feature-absent Targets*

Clearer theta connectivity differences emerged between groups in response to less-salient targets (flat runs) in the feature-absent condition. In the MMN range, examination of

overall patterns of increased synchronization versus baseline (see  $NU > 0$  and  $CU > 0$  in Figure 3.7) appeared to show fronto-temporal connectivity in both groups, though this appeared to be bilateral in NU and left lateralized in CU. NU showed a pattern of fronto-parietal connectivity in ventral attention nodes (LTPJ-LCing; not significant at group level) from 750-850 ms and significantly greater right fronto-temporal connectivity (RSTG-LCing) from 800-850 ms. In CU, unlike what was seen in the feature-present condition, did not exhibit a pattern of fronto-parietal connectivity, but instead showed significantly greater left temporo-frontal (LSTG-LCing) connectivity from 700-750 ms and significantly greater temporo-sensorimotor (RSTG-LPCG) connectivity from 750-800 ms. CU also displayed increased connectivity versus baseline between dorsal attention nodes (PCC-LCing) and left temporal-sensorimotor nodes (LSTG-LPCG) from 800-850 ms.

In the P300 range, NU exhibited a distributed pattern of connectivity between frontal, parietal, and temporal areas. Specifically, in NU, examination of the overall pattern of connectivity versus baseline revealed sustained bilateral temporal connectivity (LSTG-RSTG) from 850-1050ms, fronto-temporal (LSTG-LCing) from 900-1100 ms, fronto-parietal (LTPJ-LCing) from 900-1200 ms along with posterior cingulate-sensorimotor connectivity from 950-1000 ms (PCC-LPCG) and posterior cingulate-temporal (PCC-RSTG) connectivity from 1100-1150 ms. NU showed significantly greater connectivity than CU between bilateral posterior parietal (RTPJ-LTPJ) areas from 850-950 ms, greater fronto-temporal (LSTG-LCing) from 950-1000 ms, and greater posterior cingulate-temporal (RSTG-PCC) from 1050-1100 ms.

By contrast, CU primarily exhibited an overall pattern of posterior connectivity and a conspicuous absence of fronto-parietal and right fronto-temporal connectivity throughout most of the P300 window. In particular, CU exhibited bilateral temporal connectivity (RSTG-LSTG), which was similar to NU, but over a shorter interval from 850-900 ms. CU demonstrated sustained connectivity between left temporal and posterior cingulate (LSTG-PCC) areas, temporal-sensorimotor (LSTG-RPCG) areas from 850-1000 ms, and between posterior cingulate-sensorimotor (PCC-LPCG) areas throughout most of the P300 window from 850-1150 ms. CU also exhibited sustained parietal-sensorimotor (RTPJ-LPCG) connectivity throughout most of the window from 900-1200 ms, which was significantly greater than NU from 1100-1200 ms.

In summary, the pattern of theta connectivity suggests that when searching for less perceptually salient rare auditory targets (flat runs) amongst salient distractors (change runs), NU displayed greater right fronto-temporal connectivity in the MMN range. In the P300 range, NU exhibited an interplay between bilateral auditory cortices and left fronto-temporal areas, along with early (beginning in the MMN range) sustained fronto-parietal connectivity, likely indicating ventral attentional network activity. NU also displayed circumscribed connectivity between dorsal attentional nodes and sensorimotor areas. In contrast, CU displayed greater left fronto-temporal and right temporo-sensorimotor connectivity to flat targets in the MMN range. Within the P300 range, CU exhibited primarily posterior connectivity (most notably with the PCC) and an apparent

absence of fronto-parietal and fronto-temporal connectivity, which was in stark contrast to the pattern observed in NU. Interestingly, in the feature present condition CU had prominent fronto-parietal connectivity but a general absence of fronto-temporal connectivity. The apparent different patterns of network connectivity between groups are especially interesting when considering that the groups showed similar response accuracy in both conditions but CU had slower reaction times in identifying feature absent targets compared to their response times in the feature present condition. This will be addressed further in the discussion section.

Figure 3.7. Theta (3-7 Hz) PLV Analysis for Feature-Absent Targets

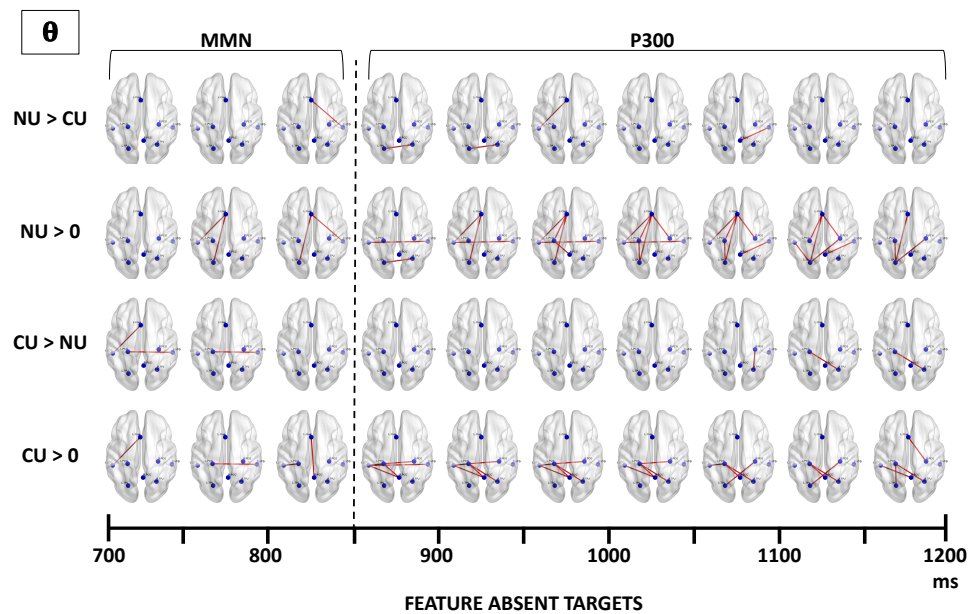


Figure 3.7. Theta (3-7 Hz) phase synchrony to feature-absent targets (flat runs) corresponding to MMN (700-850 ms) and P300 (850-1200 ms) for non-users (NU) and cannabis users (CU). Each image represents 50ms windows. First Row: Connections indicate nodes where NU showed greater PLV versus CU (NU>CU). Second Row: Displays connections in NU that were significantly larger than baseline (NU > 0). Third Row: Connections indicate nodes where CU showed greater PLV versus NU (CU>NU).

Fourth Row: Displays connections for CU that were significantly larger than baseline (CU>0). To minimize the chance of Type I error, significant group differences (rows 1 & 3) were not considered meaningful unless the group with significantly greater PLVs also showed significantly greater PLVs versus baseline (rows 2 & 4).

## **Discussion**

The present study had cannabis users (CU) and non-users (NU) complete an auditory roving dual-oddball task and compared them on behavioural performance measures (reaction time and accuracy) and several measures of electrophysiological brain activity, including channel ERPs (MMN and P300), source localized ERPs, localized oscillatory activity (theta and gamma ERSPs), and functional brain network connectivity (theta PLVs). The groups were also compared on self-report measures indexing various facets of psychopathology and also compared on various neuropsychological measures.

### ***Demographics, Self-Report and Neuropsychological Measures***

Groups were largely similar on demographic variables; however, a greater number of cannabis users reported concurrent use of nicotine and there was a marginally larger proportion of individuals in this group that reported current alcohol use. The self-reported frequency of alcohol use did not differ between groups. The effects of alcohol and nicotine will be addressed in greater detail with the larger sample in Chapter 5. There were also more CU individuals who reported hallucinogen use; however, these individuals reported relatively infrequent use, so it is not believed that this would have had a substantial impact on the various measures of brain or behaviour used in this study.

Groups did not differ significantly on self-report measures pertaining to recent experience of distressing psychological symptoms, aberrant sensory processing, or on neurocognitive measures. The NU group did, however, exhibit marginally higher scores on the letter-number sequencing test of working memory and the CU group exhibited marginally higher scores on a subscale of the SPQ indexing schizotypal traits of disorganized thinking and behaviour. Given the small sample size, these marginal differences will not be addressed further in this chapter. Instead, a more detailed examination of self-report measures involving a larger more powerful sample (combining samples from this chapter and the next) can be found in Chapter 5.

### ***Behavioural Measures***

In the present study, groups did not significantly differ in response accuracy in either the feature present or feature absent conditions. For both CU and NU, poorer response accuracy was noted in the feature-absent condition compared to the feature-present condition, which is consistent with the behavioural asymmetry observed in Chapter 2 and in similar paradigms (Blundon, Rumak & Ward, 2017). In terms of reaction time, NU did not show significant reaction time differences between the feature-present or feature-absent conditions, which is consistent with the findings reported in chapter 2; however, CU had slower reaction times in the feature-absent condition when identifying less salient rare targets (flat runs) amongst commonly occurring salient standards (change runs). This finding, coupled with the comparable accuracy between groups across conditions, may reflect a speed-accuracy trade-off in CU, that manifests under more perceptually or cognitively demanding contexts, at least in the auditory domain. Specific mechanisms

contributing to this reaction time decrement cannot be directly inferred from these behavioural data, though it seems unlikely that the roving feature of this task alone is enough to cause slower reaction times in CU, as they do not show any performance deficits in the feature-present condition. Previous research from this lab comparing non-roving and roving versions of this task revealed a similar pattern of performance asymmetry between feature-present and feature-absent conditions, but also noted that overall performance on the roving task is worse compared to non-roving versions of the task (Blundon, Rumak & Ward, 2017). As such, it would be interesting to see if cannabis users show similar speed-accuracy trade-offs in the non-roving version of this task to determine whether this apparent difficulty in selecting less salient auditory targets (feature absent flat runs) reflects a general difficulty with feature selection, or whether such difficulties emerge only within dynamic (i.e. roving) auditory contexts.

While no controlled tests of perceptual motor ability or processing speed were administered, it seems unlikely that the reaction time decrement is due to a general processing speed deficit as groups did not differ significantly in the feature-present condition, and while not significant, CU tended to show a slightly faster mean reaction times in that condition. Furthermore, exploratory analysis of the reaction time output of the computerized visual CPT task of vigilance (not a standardized variable for this task) revealed no group differences or interactions between group and attentional load. This suggests that the decrement in processing time in the feature-absent condition may not generalize to other cognitive domains, though future studies would have to include

additional auditory tasks to determine if this slowed reaction time effect is specific to this dual oddball paradigm, or reflects a general auditory cognitive processing deficit.

### ***Channel ERPs***

#### *MMN*

As this study used an identical paradigm to that described in chapter 2, we expected that the MMN asymmetry (larger MMN amplitudes and longer latencies in the feature-present condition) would also appear in the present study. These findings partially replicated in the present study as the feature-present MMNs tended to be larger and longer, though these became significant only at channel Cz for amplitude and Fz for latency. This partial replication may be due to a small but non-significant interaction effect of user group and/or a product of the relatively small sample size. In the previous study, we had 18 participants; however, in the current study only 12 non-users remained in the analysis after removing participants with too few correct trials to calculate reliable MMNs. Nonetheless, even taking account these factors, it appears that there is some asymmetry in the MMN between the feature-present and feature-absent condition.

In comparing NU and CU, it was expected that CU would display smaller MMNs in both conditions; however, no group differences were observed in MMN amplitude or latency. This finding is inconsistent with other research that demonstrated reduced MMN amplitudes in cannabis users (Rentzsch et al., 2007; Roser et al., 2010; Greenwood et al., 2014). One explanation for this discrepancy, is that the present study lacked statistical power due to small sample size. At most channels (except Fz in the feature-absent condition) users tend to show a pattern of smaller MMN amplitudes, though overall these

differences are quite small and would require a much larger dataset to achieve significance. These small differences might be compounded by the complex nature of this MMN task: its frequency roving stimuli, the complexity of the stimuli (5 consecutive tones with only 100ms separating each onset) with only a small frequency shift (50 Hz up or down) distinguishing the 5<sup>th</sup> tone in change stimuli from the preceding 4 tones, and the relatively small number of trials contributing to the MMN, all of which might be expected to elicit smaller MMNs overall. In contrast, the above-mentioned studies used classic oddball MMN paradigms with simpler stimuli (single tones), with larger gaps between stimuli (typically 500 ms), larger frequency shifts (100Hz to 1000Hz) differentiating targets and standards, and hundreds of trials. A recent review has revealed that complex MMN tasks tend to have smaller effect sizes compared to simple MMN paradigms, at least in clinical samples (Avisar, Xie, Vail, Lopez-Calderon, Wang & Javitt, 2018). Furthermore, others have failed to replicate reduced MMNs in cannabis users to pitch deviants, utilizing a simple design that included only small pitch differences between deviants and standards (Impey, El-Marj, Parks, Choueiry, Fisher, & Knott, 2015). In sum, although the expected MMN differences between NU and CU were not observed, possible limitations with the design may have impacted the results. In chapter 5, an attempt will be made to overcome some of the shortcomings of the present study by amalgamating this dataset with the one described in chapter 4, which will increase statistical power. Furthermore, power will be further increased via enhanced signal-to-noise ratio as that analysis will utilize the local MMN (described in chapter 2 – amalgamating feature-present and feature-absent conditions), which calculates MMN based on hundreds of stimuli for each participant.

### *P300*

The overall pattern of P300 results in the present study effectively replicated those reported in chapter 2, which revealed an asymmetry between feature-present and feature-absent conditions where P300 amplitudes to feature-present targets were larger than P300 amplitudes to feature-absent targets. These findings also correspond to the response accuracy findings that show overall poorer accuracy in the feature-absent condition.

Given the somewhat limited findings of P300 differences amongst cannabis users in simple auditory oddball tasks (Patrick et al., 1995; de Sola et al., 2008), but more consistent findings suggesting reduced amplitudes and longer latencies in tasks requiring greater attentional resources (Kempel, Lampe, Parnefjord, Hennig & Kunert, 2003; Solowij, Michie & Fox, 1991, 1995), we expected to see minimal differences between groups in the less demanding feature-present condition and reduced amplitudes and prolonged latencies in the more difficult feature-absent condition. These predictions were partially confirmed. P300 amplitude differences between groups were not observed for either condition; however, CU tended to show longer P300 latencies to feature-absent targets relative to their P300 latencies to feature-present targets, whereas for NU latencies did not differ between conditions. This pattern of results mirrors the pattern seen for reaction time, where CU displayed slower reaction times to feature-absent targets. The absence of amplitude differences in the feature-absent condition may reflect the similar accuracy seen for both groups in each condition. Taken together, these findings may suggest that the speed-accuracy tradeoff evidenced in the reaction time findings for the

feature-absent condition possibly arises from CU's less effective use of top-down attentional mechanisms necessary to identify difficult to discriminate targets (flat runs) amongst salient distractors (change runs). In the feature-present condition, the feature (changing 5<sup>th</sup> tone) of targets, likely results in a stimulus-driven process that mitigates any top-down attentional deficits. Given the apparent absence of MMN differences in either condition this stimulus-driven process likely reflects activity within the ventral attentional system and not early sensory processes, per se. Interestingly, in the feature-present condition there was a trend towards faster P300 latencies for CU in the feature-present condition versus NU (presumed faster as opposed to slower for NU, as NU do not show latency or RT differences across conditions), which might further suggest a stimulus-driven process that may be advantageous for detecting salient targets, but may become a disadvantage when tasked to detect less salient targets. Given that these results were not significant, this interpretation is tentative at best; however, this issue will be revisited in a subsequent section, namely when discussing functional network activity.

An additional factor that must be considered is the trend toward (albeit insignificant) higher scores in NU on the working memory (LNS) neuropsychological test. It is not anticipated that this marginally significant difference would have impacted the MMN as one study examining this issue found that larger MMN amplitudes were associated with general functioning but not associated with scores on neurocognitive measures (including LNS) in individuals whose scores fell within the normal range (Light, Swerlow & Braff, 2007).

### ***ROIs***

Eight ROI clusters were selected for inclusion in ERP, ERSP and PLV analysis. Two key brain areas underlying the MMN include the bilateral STG and bilateral IFG (Garrido, 2008; MacLean & Ward, 2014). Unlike the previous study described in chapter 2, clear bilateral STG sources were resolved. However, while somewhat stable IFG sources emerged in the cluster analysis, there were an insufficient number of participants contributing ICs to these clusters. While this state of affairs represents an improvement over the previous study, interpretation of the cortical sources underlying the MMN are likely incomplete.

The TPJ sites identified in the present study appear similar to the R TPJ site identified in the previous study (albeit slightly posterior). Again, it is possible that these clusters constitute sources of the inferior parietal lobe (IPL) as has been documented in other EEG source localization studies investigating the MMN and P300 time windows during active auditory oddball paradigms (Wronka, Kaiser & Coenen, 2012; Justen & Herbert, 2018); however, as was the case in the previous study, the centroid of these ICs tended to fall within the white matter at the junction of the temporal-parietal-occipital regions. Consistent with the TPJ characterization, an fMRI meta-analysis found this area to be active during oddball tasks and it has been proposed that it contributes to stimulus-driven attentional processing within the ventral attention network (VAN) (Kim, 2014).

The cingulate cluster (here referred to as the LCing), has a centroid located slightly dorsal and anterior with respect to the LCing cluster (falling between the ACC and LCing)

identified in the previous study. The centroid of this cluster is proximal to a number of brain areas, most notably the posterior section of the medFG (BA 8). The ERP of this cluster is largely similar to the LCing of the previous study but the PLV analysis of the present study shows that this area is highly networked with temporal areas and also various nodes of the dorsal attention network (DAN) and VAN. Due to the poor spatial resolution of EEG source localization, the precise location of this particular source cannot be specified with certainty; however, it is apparent that the ICs contributing to this cluster constitute a central interface or potential control hub connecting various other brain networks (Corbetta & Shulman, 2002; Kim, 2014).

The clusters corresponding to the PCC and the bilateral PCG are similar to those identified in the previous study, though they fall slightly posterior to those in the previous study. In particular, the ERPs localized to these areas appear to resemble the P300 ERP seen at the channel level (particularly the PCC and LPCG) data and these nodes are likely components of a top-down dorsal attentional network (Kim, 2014; Justen & Herbert, 2018). It should be noted that the PCC cluster is proximally located to the superior parietal lobe; however, both these regions are considered key neural generators of the P3b ERP component (Wronka, Kaiser, & Coenen, 2012).

### ***ROI ERPs in Users and Non-Users***

#### *ROI ERPs in MMN Time Window*

Only small group differences emerged in the MMN range (700-850 ms) in the IC clusters localized to the bilateral superior temporal lobes, left temporal-parietal area, and posterior cingulate. The relative absence of large differences across brain regions is largely

consistent with the non-significant group differences observed in the MMN channel level difference waves. Breaking from the difference wave (deviant – standard) that was conducted at the channel level, here individual stimuli were compared separately to determine whether there might be differential processing of targets and standards for CU and NU in each condition.

Of all the ROIs identified in this study, the bilateral superior temporal lobe (RSTG & LSTG) clusters are the only ones that have been identified as putative generators of the MMN (Bekinschtein et al., 2009; Garrido, Kilner, Klaas & Friston, 2009). Only minor differences between groups were observed in the RSTG (feature-present condition) and LSTG (feature-absent condition), which may point to subtly increased processing of flat runs (local standards) amongst CU regardless of whether those stimuli are targets or non-targets. However, in the feature-present condition, CU exhibited a larger negative LSTG amplitude to change stimuli (local deviants), which may, in a sense, compensate for the increased response seen in the RSTG to flat standards in that condition, which could plausibly cancel out any additive effects seen in the difference waves at the channel level.

Other observed differences within the 700-850 ms range occurred in regions not typically associated with the MMN (LTPJ and PCC) and likely relate to other early cognitive processes temporally overlapping with the MMN. A passive version of this task would have to be employed to determine whether this activity pertains to stimulus driven perceptual or attentional processing or more top-down attention or control processes. Finally, CU and NU appear to differ in their early PCC ERP responses to flat runs,

whether targets or non-targets. Interestingly, NU tends to exhibit a clear morphological difference in early PCC response between targets and non-targets whereas this distinction is less clear for CU, especially in the feature-absent condition. Given that this waveform appears most responsive to targets and non-targets rather than being responsive specifically to change and flat runs, the apparent group differences here might reflect the cognitive processes associated with the difficulties that CU had in efficiently selecting less salient targets in the more difficult feature absent condition.

#### *ROI ERPs in P300 Time Window*

Contrary to the MMN analysis, the P300 has been shown to reflect activity in a more distributed network of brain sources (Bachiller et al, 2015; Justen & Herbert, 2018; Polich, 2007). Thus, all of the identified ROIs are potentially relevant to the P300. In particular, the waveforms localized to the PCC, LPCG showed morphologies that clearly resembled the channel level P300 waveforms. To a lesser extent, ERPs localized to the LTPJ and RPCG also exhibited P300-like qualities. Interestingly, these areas did not show prominent differences between groups in processing targets in either condition and only minor differences emerged in processing non-targets within the P300 window (prior to 1200 ms). Considered together with the absence of P300 amplitude differences to targets at the channel level, and similar accuracy performance across conditions, the pattern of these results suggests that the CU group overall has intact ability to accurately detect and categorize rarely occurring stimuli.

The most prominent differences in processing targets emerged in the LCing cluster which differed between groups in both conditions, though most prominently to targets in the feature-present condition. This finding is supportive of less effective top-down attentional/control processes in the CU group that could plausibly impact reaction time in the more difficult feature-absent condition, where greater top-down attentional control would be required, but have little impact in the feature-present condition where timely identification of targets might rely on more stimulus-driven attention. Also of note, RSTG response to targets within the P300 range appeared to differ between CU and NU with NU showing larger amplitudes in each condition. This area is believed to play a role in conjunction with frontal and parietal sources for generating both the posterior P3b and frontal P3a (Bachiller et al, 2015), so in this context, along with the differences in the frontal LCing cluster, the differences noted here may reflect the observed differences in frontal-temporal connectivity that will be discussed further in subsequent sections.

### ***ROI Oscillatory Activity in Users and Non-Users***

Contrary to the ERP analysis, which only represents evoked broadband activity (phase locked to stimulus onset due to signal averaging), ERSP analysis afforded a more nuanced examination of induced (non-phase locked) neural activity within narrow frequency bands, information that is typically lost to signal averaging. In the present study, we compared NU and CU theta and gamma activity in each of the ROIs, within the time windows that overlapped the MMN (700-850 ms) and the P300 (850-1200 ms). The majority of the differences observed occurred in the gamma band, which likely reflect increased local processing shown to support a diverse array of cognitive process, including memory, attention, perceptual binding, and object representation (Herrmann,

Fründ & Lenz, 2010), and have been linked to hemodynamic response within brain regions (Koch, Werner, Steinbrink, Fries & Obrig, 2009; Niessing et al, 2005).

#### *Oscillations in the MMN and P300 Time Windows*

In the MMN time window (~700-850 ms), we anticipated that in ICs localized to temporal sources, CU would exhibit less gamma ERSP to change runs (local deviants) and greater gamma to flat runs (local standards); however, this was only partially confirmed as CU only exhibited greater gamma in the R STG to flat runs in the feature-absent condition. This might reflect subtle context dependent differences in CU in encoding the regularity of the repetitive auditory stimuli in sensory memory (Sussman, 2017). Although the MMN has often been conceptualized as a pre-attentive automatic process for detecting stimulus feature differences between a deviant oddball stimulus and a sensory memory representation of previously occurring standard stimuli, an accumulating body of work has suggested that MMN is actually related to two distinct but intertwined processes: deviance detection and standard formation, with deviance detection being highly dependent on standard formation (Sussman, 2007, 2017). Whereas deviance detection might be seen as a largely automated process, the formation of a standard representation in sensory memory, on the other hand, is highly context-dependent and influenced both by bottom-up stimulus properties and by top-down task demands, suggesting that this process is not entirely pre-attentive for basic auditory features (Sussman, Chen, Sussman-Fort & Dinces, 2014). In the feature-absent condition, the flat runs represent local standards (in terms of MMN generation) and global targets in terms of the P300, so the increased gamma activity seen in CU could reflect attentional modulation of how CU is representing local standards (flat runs) in

sensory memory influenced by the fact that these flat runs are also global targets, which may be consistent with other research demonstrating increased gamma power to target-related attentional processes (Debener, Herrmann, Kranczioch, Gembris & Engel, 2003) rather than stimulus-driven processes. This conceptualization may also explain why increased gamma is not observed to flat non-targets in the feature-present condition as it is possible that CU is having greater difficulty encoding the repeating standards when they are more difficult to detect in the global context (i.e. feature absent target flat runs).

The ICs localized to the bilateral TPJ and L Cing show group differences in gamma activity within the time window of the MMN, but since these are not known generators of the MMN they likely reflect early stimulus-driven and top-down attentional processes (Behrmann, Geng & Shomstein, 2004). NU and CU groups appear to show differential processing to targets and standards in each condition in both the right and left TPJ. NU displayed greater RTPJ gamma to feature present targets over a relatively short time period, whereas CU displayed greater LTPJ gamma over a prolonged period, possibly reflecting slightly variant feature-driven attentional processing streams between groups that nonetheless result in equal behavioural outcomes (i.e accuracy and RTs). To feature-absent flat targets both CU (more prolonged in CU) and NU show greater gamma ERSP in the LTPJ in overlapping time periods, however at different bands within the gamma range (higher in NU), which may imply differential processing (Herrmann, Fründ & Lenz, 2010). Furthermore, CU also shows greater gamma ERSP in the RTPJ to feature-absent targets, again suggesting greater stimulus based attentional processing for CU. Interesting, NU also shows increased RTPJ gamma ERSP to feature-absent change non-

targets along with increased gamma ERSP in the frontally situated LCing, which may reflect top-down control processes inhibiting processing of these salient non-targets, though this is, at best, speculative.

In the P300 window (~850-1200ms), the pattern of oscillatory activity was again reflective of bias towards stimulus-driven processing for CU and greater top-down attentional control for NU, which became especially apparent in the feature-absent condition. In the feature-absent condition, we saw greater LTPJ gamma ERSP in CU to change targets, whereas NU had greater gamma ERSP to non-targets in bilateral TPJ. In the feature-absent condition both groups showed greater LTPJ activity to flat targets with CU having periods of greater gamma early (overlapping MMN) and late in the P300 window and NU showing greater gamma in between. Also similar to the MMN window, CU showed increased RSTG gamma early and late in the window, which again likely reflects additional stimulus-based processing of feature-absent stimuli in this group. Finally, the NU group showed greater ERSP to change non-targets in the LTPJ (similar to the feature-present condition) along with greater gamma ERSP in the LCing and RPCG, which again may possibly reflect the recruitment of top-down attentional processes to inhibit responses to these salient non-targets. Interestingly, the only theta-band difference observed was greater PCC theta ERSP in NU to change non-targets in the feature-absent condition. However, increased attention-related theta power is typically observed in frontal areas in response to targets in cognitively demanding tasks (Ishii et al, 2009; Mazaheri & Picton, 2005), so the reason for increased theta here is not immediately clear. The difference noted here happened to occur very low in the theta range (~3Hz), so this

might reflect overlapping delta band (0.5-3.5Hz) activity, which in posterior areas has been associated with attentional inhibition of sensory afferents that might interfere with task performance and would be consistent with the overall picture of NU utilizing greater top-down attentional processes to inhibit response to salient non-targets (Harmony, 2013).

### ***Theta Band Functional Connectivity in Cannabis Users and Non-Users***

The overall picture of more stimulus-driven attentional processing in cannabis users versus more top-down attentional processing in non-users was largely supported by the PLV analysis within the theta band. Theta band connectivity reflects large-scale communication and integration of cognitive processes across diffuse network nodes (von Stein & Sarnthein, 2000).

In the MMN range, there was some evidence for a pattern of left fronto-temporal connectivity for NU that was absent in CU, whereas both groups showed similar patterns of right posterior cingulate-temporal connectivity. In processing flat target runs in the feature-absent condition, CU displayed increased left fronto-temporal connectivity whereas NU showed increased right fronto-temporal connectivity. Fronto-temporal theta synchronization, has been related to the MMN (Choi et al., 2013; Hsiao, Wu, Ho & Lin, 2009); however, the absence of inferior frontal ROIs in the present study limits the interpretability of these findings (Garrido, 2008; MacLean & Ward, 2014).

In the P300 range of the feature present condition, both groups demonstrated activations of frontal-parietal attention networks (similar to what was seen in chapter 2), though in

CU a pattern of bilateral frontal-parietal connections emerged that appeared to onset earlier along with left-right temporal connectivity. In contrast, NU exhibited primarily left fronto-parietal connectivity along with temporo-parietal and also fronto-temporal connectivity that was significantly greater than and seemingly absent in CU. The enhanced fronto-temporal activity in NU may reflect greater integration of top-down processes with sensory memory information and the seemingly dominant fronto-parietal connections in CU may represent a largely stimulus-driven attentional processes. These apparent differences, however, did not appear to impact behavioural performance in the feature present condition as both groups performed comparably well, which is consistent with others who have noted increased fronto-parietal functional connectivity in cannabis users in the absence of enhanced behavioural performance (Harding et al., 2012).

In contrast, in the more difficult feature-absent condition, NU exhibited similar left fronto-parietal connectivity, though prolonged, and a similar pattern of fronto-temporal connectivity, along with sustained bilateral temporal connectivity. Whereas for CU, the fronto-parietal connectivity seen in the feature-present condition was largely absent and theta connectivity was largely between posterior nodes linking parietal, cingulate, temporal and sensorimotor areas. While CU had comparable accuracy in this condition, they showed slower reaction times and longer P300 latencies. This pattern of connectivity suggests that under more difficult target detection conditions, the NU group outperforms the CU group due to enhanced top-down attentional processes, likely due to intact fronto-temporal connections. Others have noted altered activity within the frontal and temporal regions (Sneider et al., 2008) and in fronto-temporal connectivity in cannabis users

(Houck, Bryan, Feldstein Ewing, 2013). Furthermore, theta band fronto-temporal functional connectivity has been associated with network coordination between processes pertaining to attentional orienting and memory that facilitate categorization and context updating while detecting rare targets in oddball tasks (Harper, Malone, Iacono, 2017). Since PLV analysis can only show that that two areas are likely sharing information; the direction of information transfer cannot be inferred, so it is not clear whether sensory information is being fed to the frontal areas, or whether frontal areas are controlling the flow of sensory information, or some combination of the two. Future research utilizing causal connectivity methodologies (e.g. transfer entropy or dynamic causal modelling) might be able to resolve this issue.

### ***Limitations***

This study improved upon the study described in Chapter 2 in several notable ways (e.g. stricter recruitment criteria that excluded individuals with history of psychiatric/neurocognitive conditions and medication use; inclusion of detailed demographics, self-report measures of psychological symptoms, and neurocognitive tests; and, participants were encouraged to complete EEG experiment even if performing poorly); however, there are several notable limitations. Despite the improved screening protocol several participants were recruited who did not meet our criteria for being a heavy cannabis user or a non-user and these participants had to be excluded after testing, so improvements on the screening protocol could be made (also see Chapter 1: Recruitment of Cannabis Users for discussion of roadblocks).

The collection of cannabis use data was adequate, albeit a more comprehensive or standardized measure would have been useful here. Furthermore, a more rigorous collection of data on alcohol and other substance use (especially nicotine use; Dunbar et al., 2007) would have been beneficial. While the focus of this research was on recreational cannabis use and not Cannabis Use Disorder, per say, a structured clinical interview would have been beneficial for indexing the severity and functional impact of cannabis use. A clinical interview would have also provided a more sufficient screen of psychiatric history, than mere self-report. Unfortunately, inclusion of such measures would have greatly extended this already lengthy protocol and exceeded the material resources of this lab.

Another limitation with the present study is the inherent difficulty disentangling the acute and chronic effects of cannabis. While the acute subjective effects of cannabis usually wear off in several hours,  $\Delta 9$ -THC is known to have a long half-life and is detectable in blood plasma for over a day (and likely longer in lipid rich brain tissue) after abstinence, which may persist longer in heavy cannabis users and may in part account for sustained neurocognitive effects (Grotenhermen, 2003; Karschner et. al, 2009). To this point, we found that amongst cannabis users the self-reported time since last usage showed a trend negative association ( $r_s = -.51$ ,  $p = .088$ ) with response time in the feature present condition and a significant negative association ( $r_s = -.73$ ,  $p = .007$ ) in the feature absent condition. The association between time since last use and P300 latency was not significant for the feature present condition ( $r_s = -.38$ ,  $p = .227$ ) and showed a trend negative association ( $r_s = -.53$ ,  $p = .078$ ) in the feature absent condition. There were no

significant associations between time since last use and P300 amplitude, nor were there significant associations with MMN amplitude or latency. Taken together these findings suggest that the apparent decrement in response time and P300 latency observed in cannabis users in the feature absent condition may be related to lasting acute effects and not chronic effects of cannabis. However, given the small sample size, the imprecise nature of the self-reported estimates of time of last usage, and the absence of more objective measures of plasma  $\Delta 9$ -THC levels (i.e. blood testing), these findings should be interpreted with caution until they can be verified in a larger sample with tighter controls and implementing more rigorous and objective measures.

There are several limitations with the various self-report measures and neuropsychological tests employed, which will be addressed in detail in Chapter 5. A more comprehensive protocol was initially considered, but again not chosen for logistical reasons. The sample sizes were relatively small, which likely limited statistical power for the self-report, neuropsychological tests and EEG measures. In chapter 5, an attempt is made to address this issue by amalgamating sample test scores from this study and the study described in chapter 4. Furthermore, a local MMN will be calculated across the larger sample, though unfortunately the P300 and ROI analyses (ERPs, ERSs, and PLVs) cannot be practically combined across the samples due to different task parameters. In the present study, while interpretable and interesting results emerged in the ROI analyses, employing clustering techniques to identify ROIs limits the number of participants that are included (see Chapter 6 General Limitations for more details). While this study improved on the previously study by successfully identifying bilateral superior

temporal lobe clusters, the absence of inferior frontal clusters limits the interpretability of the MMN PLV results. Furthermore, an equivalent cluster to the MedFG cluster in the previous chapter, which appeared to strongly network with the PCC (implying DAN activity), did not emerge in the present study and limits comparisons to the previous study and the overall interpretation about the relative interplay between the DAN and VAN. Finally, as discussed for the previous study (see Chapter 2: Limitations), this study does not include a passive condition, which would help delineate the effects of directed attention on the MMN ERP asymmetry and would help clarify the origins of the apparent brain activity (see ERSPs, ROI ERPs and PLV analyses) overlapping the MMN time window, but occurring in brain areas not generally attributable to the MMN.

## **Conclusion**

This study replicated many of the main findings described in Chapter 2, thus reaffirming the asymmetry in the roving version of this dual-oddball task (Blundon, Rumak & Ward, 2017). More importantly, this study demonstrated the expected slowed reaction time and prolonged P300 ERP latency in heavy cannabis users in the more demanding feature-absent condition, whereas, unexpectedly, MMNs did not differ between users and non-users in either condition. Source-localized ERPs, gamma-band oscillatory activity, and theta-band PLV functional connectivity, all suggest that cannabis users' performance may suffer somewhat because of a stimulus-driven attentional strategy that does not impair performance under easy auditory task conditions, but slows reaction time and cognitive processing under difficult task conditions. This slowed performance coincided with decreased fronto-parietal network functional connectivity, which in turn may arise from decreased fronto-temporal connectivity.

## CHAPTER 4: Auditory *N*-back: Users vs. Non-Users

### Introduction

Reports of memory deficits in cannabis users are prevalent in the literature (see chapter 1 for an overview) though evidence of impaired working memory performance in cannabis users has been somewhat equivocal (Bhattacharyya & Schoeler, 2013; Nader & Sanchez, 2018). The study of working memory is of particular interest in the context of cannabis use because of its possible role as an underlying factor in various forms of cognitive impairment and the pathogenesis of severe psychopathology (e.g., psychosis). In this study we sought to build upon the research discussed in Chapters 2 and 3 by having cannabis users (CU) and non-users (NU) perform memory operations on the same stimuli while they attended to basic auditory stimulus features (pitch or pattern) under easy and difficult memory load conditions. Because other auditory deficits have been reported in the literature (i.e. MMN), we sought to investigate whether this would extend to basic auditory working memory deficits in cannabis users. Furthermore, a secondary aim of this study was to extend the understanding of electrophysiological correlates and brain network dynamics of auditory working memory, given that basic auditory working memory is relatively understudied (compared to visual modalities or semantic verbal memory).

Although numerous experimental paradigms exist for examining various facets of working memory, the auditory stimuli used in our roving local-global dual oddball task lend themselves well to be arranged into an auditory *n*-back task. Two variants of *n*-back task were used in this study, each with a low memory load and high memory load

condition. The first variant, the frequency match task, had participants recall whether the base frequency (first four tones) of flat and change runs matched the base frequency of the previous run (1-back; low memory load) or the run that occurred prior to last (2-back; high memory load). The second variant, the pattern match task, was identical in structure to the frequency match task, except that participants were asked to recall the overall pattern of the run (change vs. flat) rather than base frequency.

In terms of neuropsychological measures, given findings from previous research (discussed in Chapter 1) we expected that CU might show some impairment in working memory performance on the letter-number sequencing task, but given our small sample we did not expect to see differences in estimated IQ. Furthermore, differences in IQ were expected to be especially unlikely since our samples were mostly drawn from a highly educated and high achieving population at a competitive university, in which individuals would be expected to show less variation in IQ.

In terms of psychological self-report measures, we did not expect to see large differences between in self-reported psychopathological symptoms because we excluded participants who reported a history of severe mental illness. We expected higher trait schizotypy scores in CU given previous findings reported in the literature (Fridberg, Vollmer, O'Donnell & Skosnik, 2011), though this prediction was tentative given the small sample size. Similarly, in light of reports of aberrant sensory gating in cannabis users we expected some evidence of increased self-reported aberrant sensory processing even in the absence of overt psychopathological symptoms (Broyd et al., 2016; Micoulaud-

Franchi et al., 2015), though again these predictions were tentative in light of the small sample size. In Chapter 5, we address the issue of small sample size by combining participants from the present study with the sample discussed in Chapter 3, but chose to include these measures in the present study to provide interpretive context specific to working memory in cannabis users.

In terms of behavioural performance on the  $n$ -back task, it was expected that performance would decrease under increasing memory load for each task. Under the assumption that heavy cannabis use negatively impacts working memory, we expected CU to show poorer performance on both the frequency and pattern match tasks, especially under high memory load. Furthermore, since auditory sensory processing is believed to be impacted by heavy cannabis use, we expected that the behavioural deficits would be most apparent for cannabis users when trying to recall the base frequencies in the frequency match condition.

Even though there are relatively few electrophysiological investigations using auditory  $n$ -back tasks, we were able to make some predictions based upon general principles gleaned from other behavioural and ERP studies investigating working memory. Congruent with other ERP investigations involving  $n$ -back tasks, we focused primarily on P3b amplitudes over the midline parietal location (i.e., channel Pz). In line with other research findings, we expected to see reduced P3b amplitudes under increased memory load for both experimental tasks (McEvoy, Pellouchoud, Smith & Gevins, 2001; Scharinger, Soutschek, Schubert & Gerjets, 2017). Although it would be advantageous to combine

analysis across both pattern and frequency match conditions, we suspected that this might not be possible, because of the different attentional focus required for each task. For example, when attending to base frequency, the focus is on the first four tones of each auditory run, whereas for the pattern match condition, the focus is on the final tone. We reasoned that these task differences would likely result in a modulation of the ERP waveform at different latencies for each task, which may obfuscate any findings should they be combined. As such, we chose to analyze each task separately. While we expected a typical P3b ERP component in the pattern match condition to occur after the onset of the final stimulus, we expected that the directed attention to the base frequency of the first four tones of auditory runs in the frequency match condition would necessitate an analysis of the ERP waveform prior to the onset of the 5th tone. Overall, we expected that if indeed cannabis users demonstrated poorer working memory performance, then this should result in reduced P3b amplitudes in both conditions, especially under increased memory load.

In terms of source localization, the loci of neural generators in *n*-back tasks using EEG has not been well characterized. A meta-analysis of fMRI findings by Owen and colleagues (2005) suggested the involvement of six key areas associated with working memory, including a fronto-parietal network, various prefrontal areas, and motor/sensorimotor areas (see overview in Chapter 1). Given that previous research in our lab (see Bedo et al., 2014, for example) utilizing source localization methodologies similar to the ones used for the present study was able to localize activity to some of these regions, we expected to localize clusters of independent components (ICs) to some

of the regions reported in the fMRI literature. However, given that the above-mentioned review largely consisted of visual stimuli across various types of working memory tasks, we also expected to localize ICs to the superior temporal gyrus (auditory cortex). Furthermore, given that the present experiment utilized identical stimuli to the MMN task described in Chapter 2 and 3, we expected at least some overlap between the studies.

In terms of oscillatory activity, we predicted that ERSs should reveal patterns of increased theta (primarily frontal), reduced alpha, and increased gamma with under high memory load (Lisman & Jensen, 2013; Roux & Uhlhaas, 2014). We expected that CU would exhibit the same overall pattern as NU, but to a lesser extent. We also expected CU to show less gamma compared to non-users in temporal and frontal regions related to auditory memory and executive control.

Specific a priori predictions regarding theta phase synchronization between localized brain sources were more difficult to make as it has not, as of yet, been well characterized in auditory working memory, though we anticipated patterns of long range communication via theta-band phase synchrony between temporal and frontal sources to become disrupted under increased memory load and for this disruption to be more prevalent in CU.

## Method

### *Participants*

We were interested in assessing differences between heavy current cannabis users (CU) and current non-users (NU). Recruitment procedures and inclusion and exclusion criteria were identical to those described in Chapter 3. Individuals who reported using cannabis at least 10 times over the last 30 days were invited to participate as cannabis users.

Individuals were invited to participate as non-users if they had not used cannabis in the past six months and had never used cannabis 10 times in a 30 day period.

A total of 35 self-identified CU and NU were invited to participate in this study based upon their responses on the telephone screen. Data for two participants (one CU and one NU) were excluded from analysis because they opted to discontinue the experimental task prior to completion. Two self-reported NU were excluded because they reported recent cannabis use at the time of testing. Two self-reported CU were excluded because they did not classify as heavy users (less than 10 reported instances of cannabis use in last 30 days) at the time of testing. Finally, two participants (one CU and one NU) were excluded due to difficulty grasping the task despite additional coaching, which resulted in excessively low behavioral performance (i.e.  $< 0.3 d'$  scores) on the low memory load (i.e. 1-back) conditions of the  $n$ -back task. As such, of those individuals invited to participate, 27 participants (NU = 15 and CU = 12) were included in the EEG, behavioural, and self-report data analysis for this study.

The NU ( $M = 23.47$ ,  $SD = 3.52$ ) and CU ( $M=22.17$ ,  $SD = 2.59$ ) groups did not significantly differ in age. There were more males than females in the CU (41.7% female) group and more females than males in the NU (60% female) group, though these did not differ significantly. Groups were mostly right-handed (NU = 93.3%; CU = 83.3%) and not differ significantly. Groups were comparable on verbal comprehension, perceptual reasoning, and overall current psychopathological symptomology, though some differences were observed in self-reported use of other recreational substances (see results section for more details).

### ***Auditory N-back Task***

Two variants (frequency match and pattern match) of an auditory  $n$ -back task, each with two memory load conditions (1-back and 2-back) were used to test working memory and executive functioning. See Figure 4.1 for a simplified schematic of 1-back and 2-back tasks. Participants were introduced to the experimental stimuli and presented with on-screen instructions describing the experimental task. Participants were asked to focus on a fixation cross to minimize eye movements while they listened to a continuous sequence of flat and change auditory runs that were identical to those described for the roving local-global dual oddball tasks described in Chapters 2 and 3. Participants were instructed to respond via button press anytime a current auditory-run matched a run on features (described in next section) that preceded the current run by one (1-back) or two (2-back) trials. Participants were asked to respond as quickly as possible, but to withhold responses until after the final tone of each stimulus. Each experimental block contained 50 stimuli and the task was designed such that each trial had a 50% probability of being a

matching target. Each block lasted approximately two to three minutes and participants were given a 30 second rest period between blocks to minimize fatigue. Each participant completed 16 blocks containing both 1-back (3 frequency match and 3 pattern match) and 2-back (5 frequency match and 5 pattern match) conditions. The distribution and proportion of experimental blocks was optimized based upon behavioral pilot data to ensure enough correct trials to allow adequate signal averaging for the ERP analysis. Blocks were pseudo-randomized, such that the six 1-back tasks always preceded the ten 2-back tasks to allow participants to be familiar with the task parameters by the time they engaged in the more difficult 2-back conditions. Otherwise, the sequence of tasks was ordered randomly by use of a randomization sheet that was prepared in advance by the experimenter. Given the complexity of the task, performance for the first 1-back condition of each type was monitored by the experimenter to ensure that participants fully understood the task instructions. Approximately 10 participants required some form of additional instruction as it was clear that they were responding incorrectly. In these instances, these tasks were repeated and the initial blocks were not included in the analysis. Repeats were permitted at most one time, for each condition (i.e. frequency and pattern match) and only for the 1-back condition.

### *Stimuli*

The auditory stimuli used for the  $n$ -back tasks were identical to the 5-tone (5 x 50ms; 100ms SOA) flat and change runs of varying pitch used for the roving local-global oddball task described in Chapters 2 and 3. Stimuli were presented simultaneously to both ears using identical equipment as described in previous chapters (70 dB SPL, presented through insert earphones in a sound attenuated room). A uniform randomized

inter-stimulus interval ranging from 2150 to 2800ms was used for each task and condition.

Figure 4.1. Simplified Diagram of 1-Back and 2-Back Tasks

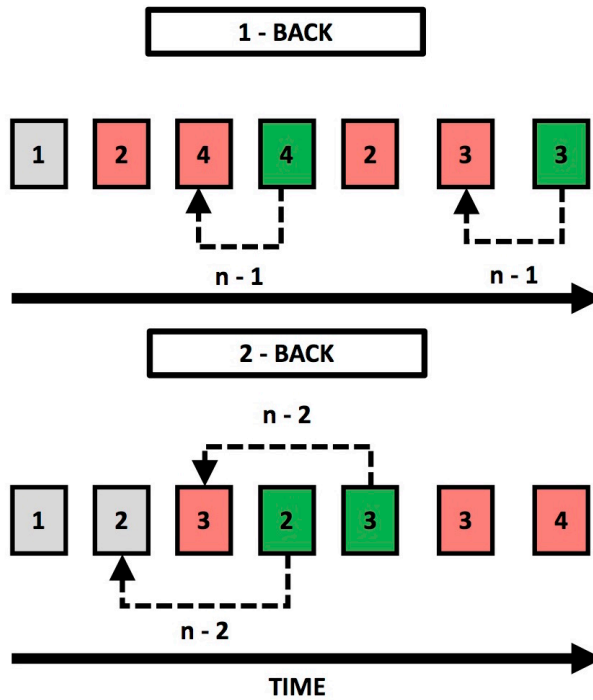


Figure 4.1. Simplified outline of 1-back (top) and 2-back (bottom) tasks. The boxes represent sequentially presented stimuli of different types (numbers). After each stimulus presentation a participant judges whether the stimulus just heard matches the stimulus that occurred one or two instances ago. In the 1-back condition green boxes represent targets that match the previous stimuli ( $n-1$ ). In the 2-back condition, green boxes match the stimuli that occurred two instances ago ( $n-2$ ). Red boxes in both conditions are non-targets because they do not match. Grey boxes in 1-back and 2-back cannot be targets because there is no  $n-1$  or  $n-2$ , respectively.

*Frequency Match Condition*

In this task, participants were asked to attend to the base frequency of each auditory run (i.e. the first four tones) and to ignore the overall pattern (i.e. whether the run was change

or flat). In the 1-back condition, participants responded whenever the base frequency (first four tones) of the current ( $n$ ) run were identical to the first four tones of the previous ( $n-1$ ) run they heard. In the more difficult memory load condition (i.e. 2-back condition), participants were asked to respond whenever the base frequency of the current run was identical to the run they heard two instances ( $n-2$ ) ago. Again, participants were explicitly instructed to ignore whether the runs were changing or flat and to attend only to the base frequency. The task was programmed such that matching runs were never identical in pattern. For instance, if a matching target in the 2-back frequency match condition was a flat run with a base frequency of 550Hz, the matching  $n-2$  stimulus would have been either a change-up or change-down run with a base frequency of 550Hz. Similarly, if the matching target was a change-up run with a base frequency of 700Hz, the  $n-2$  run would have either been a flat run or a change-down run with a base frequency of 700Hz (See Figure 4.2 for a depiction of this task).

#### *Pattern Match Condition*

In this task, participants were asked to attend to the overall pattern of each run (changing or flat) and to ignore the base frequency of each run. Participants were explicitly instructed to treat change-up and change-down runs as identical in that a change-up run would match a change-down run, because they are both changing. In the 1-back condition, participants responded as quickly as possible whenever the pattern (changing or flat) of the current ( $n$ ) run was identical to the pattern of the  $n-1$  run. In the 2-back condition, participants were asked to respond whenever the pattern of the current run was identical to the pattern of the  $n-2$  run. Again, participants were explicitly instructed to

ignore the base frequency of each run and to attend only to whether each run was changing or flat. Similar to the frequency match condition, the task was programmed such that matching runs were never identical and always had different base frequencies. For instance, if a matching target in the 2-back condition was a flat run with a base frequency of 600Hz, the  $n-2$  run would have been a flat run with a different base frequency. Similarly, if the matching target was a change-up run with a base frequency of 700Hz, the matching  $n-2$  run would have either been a change-up or change-down run with a different base frequency. (See Figure 4.2 for a schematic depiction of this task).

Figure 4.2. Schematic of 2-Back Frequency and Pattern Match Tasks

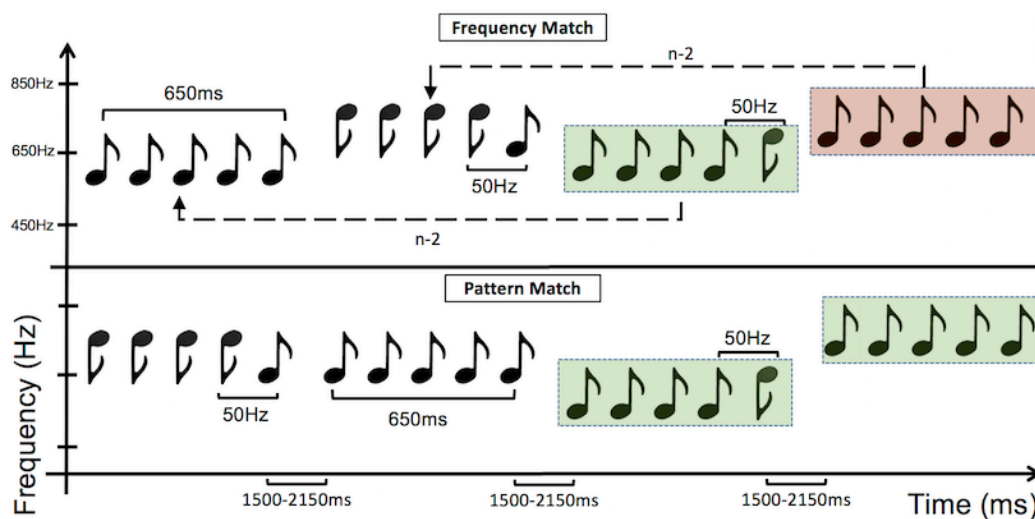


Figure 4.2. Diagram of the 2-back condition for both frequency (top) and pattern match tasks. Dotted lines point to the auditory run that occurred two instances ( $n-2$ ) ago (i.e. 2-back). Match trials are highlighted in green and mismatch trials are highlighted in red. In the frequency match condition a match occurs if the first four tones (base frequency) of the current run match the base frequency of the  $n-2$  run, ignoring the overall pattern. In the pattern match condition, a match occurs if the overall pattern (flat or changing) matches the overall pattern of the  $n-2$  run, ignoring the base frequency. Note: change-up and change-down runs are considered matching.

### ***EEG Acquisition***

EEG recording procedures were identical to those described in Chapter 3 (also see Chapter 2 Method section for additional details).

### ***Offline Processing***

Offline EEG data analysis was conducted using EEGLAB software (Delorme & Makeig, 2004). Parameters (down sampling, pruning, ICA, and artefact rejection were identical to those described in Chapters 2 and 3 (see figure 2.2. for a simplified overview of the EEG processing steps).

### ***Event-Related Potentials (ERPs)***

Event related potentials were computed in a similar fashion to what has been previously described in Chapters 2 and 3 using automated procedures included in the ERPlab toolbox. As an index of working memory, we extracted P300 local peak amplitudes and latencies at channel Pz based upon averaged epochs for each participant for correctly responded to matching targets for each task and memory load condition. Epochs extended from 200ms prior to the onset of the first tone in each target run until 1800ms after the onset of the first tone. After averaging, all epochs were filtered using a 30Hz FIR low pass filter. Similar to the P300s discussed in Chapters 2 and 3, the extraction window for the P300 was based upon visual inspection of the morphology of the overall grand average ERP waveform and the topographic scalp maps for each condition. We chose an extraction window of 250ms to 500ms (relative to onset of first tone) for the frequency match condition and 850 to 1100ms (250 to 500ms after onset of 5<sup>th</sup> tone) for determining local peak P300 amplitude and latency. A local peak selection method of 10 time points

(20 ms to each side of the peak) was used to account for local fluctuations that may bias peak selection. As described previously, the measurement of P300 peak amplitude/latency was chosen rather than average amplitude across the extraction window to facilitate examination of temporal (i.e. latency) cognitive processing differences and to maintain consistency with the bulk of the literature that has examined the effects of cannabis use on the P300 (e.g. D'Souza et al., 2012; de Sola et al, 2008; Theunissen et al., 2012).

### ***Dipole Fitting (Source Localization) and ROI Selection via Cluster Analysis***

Source localization was utilized to allow for clearer interpretation and selection of independent components (ICs) for further ERP and PLV analysis. The dipole localization of each IC was mapped onto Talairach coordinates based upon the Montreal Neurological Institute (MNI) average brain, using the DIPFIT2 function included in the Fieldtrip plugin for EEGLAB, which was identical to Chapters 2 and 3.

The steps taken to identify cortical regions of interest (ROI) included in ERSP and PLV analysis were derived using the same two-stage process of k-means clustering and subsequent seeding of dipole locations using EEGLAB functions as was described in Chapter 2, and will not be described in detail. Similar to Chapter 3, we used a 15% residual variance (RV; 85% Variance Accounted For - VAF) threshold and clusters selected for further analysis had to include 50% of participants from each group (CU and NU). In stage 1, a total of 677 ICs (non-artefactual with less than 15% RV) were

submitted to  $k$ -means ( $k = 15$ ) clustering resulting in 13 viable (two clusters were omitted: one loosely packed posterior visual cortex and one subcortical cluster) clusters. In stage 2, the centroids of each stage 1 cluster were submitted to the seeding algorithm (Euclidian distance = 35mm; 1 IC per participant per cluster) resulting in 11 theoretically relevant ROI clusters that contained 50% of participants from each group (see Table 4.6 in Results Section).

### ***ROI ERPs***

ERPs were examined for each of the 11 selected ROIs. The primary goal of this analysis was to provide a general overview of areas of difference between groups for each task (frequency match and pattern match) at each memory load (1-back and 2-back) in order to provide an interpretive framework to bridge the channel level ERP analysis with the more nuanced theta band functional network connectivity (PLVs) that will be the focus in subsequent sections. As such, uncorrected ( $\alpha = .05$ ) pairwise comparisons were run across ERP waveforms for each ROI separately. Given the likelihood of type-I error, we ignored significant results that consisted of only one or two time points and generally considered meaningful only time regions that spanned a minimum of ~20ms (5 significant time points). In a few cases, time regions were considered meaningful if there were a number of individual significant time points distributed within a short time frame; however, in these instances at least half of the time points in that range had to be significant and there had to be at least 5 of them (i.e., over a 40ms window there had to be at least 20 ms or 5 time points that were significantly different). For the frequency match condition, only significant differences in the 0-600 ms window were considered as they were most likely to correspond to working memory processes temporally

overlapping with the channel level P300 (250-500 ms; see channel level ERP analysis in this chapter). Similarly, for the pattern match condition, only the 600-1200 ms time window was considered, which overlaps with the corresponding P300 window (850-1100 ms). While differences that occur within the entire 600ms have been documented in Table 4.7, detailed descriptions have been restricted to time windows directly overlapping the P300 extraction windows (250-500 and 850-1100ms) for each task.

### ***Event-Related Spectral Perturbations (ERSPs)***

ERSPs were initially carried out in the theta, alpha and gamma frequency bands in a similar manner as described in previous chapters. However, examination of the results revealed methodological limitations in applying this method to this particular paradigm due to the *n*-back task having an active baseline that distorts the results. Since the ERSP computes spectral power (in dB) as a ratio of change versus baseline, the observed baseline differences will distort the output. See Discussion for more details.

### ***Phase Synchrony (PLVs)***

Phase Locking Values (PLVs) were used to assess differences in phase synchrony between cannabis users and non-users within the theta (3-7 Hz) band. PLVs between pairs of ICs localized to specific brain regions were computed in an identical manner to Chapter 2 and 3. Average PLVs were computed for each participant and condition at each time point within epochs for each of the 55 pairings of ROI clusters (i.e. a participant had to contribute ICs to each) for correct matching targets in each task and memory load

condition (see Chapter 2 Method section for more details regarding time-frequency decomposition).

Group comparisons (NU vs CU) were made separately for each task and memory load within a 600 ms (4 x 150 ms) time window that encompassed the P300 for that task. Specifically, for the frequency match task, analyses were run on the 0-600 ms range and for the pattern match condition analyses were run on the 600-1200 ms range. Two-tailed  $t$ -tests ( $\alpha = 0.05$ ) were computed between groups for each time point within each 150 ms time window. A similar approach was used within each group for each task/memory load to identify significant activations versus baseline to provide a framework for interpreting any group differences, as group differences that emerge in absence of significant within group activation are likely spurious. In this case, two-tailed  $t$ -tests ( $\alpha = 0.05$ ) were used to identify significant deviations from zero. It should be reiterated, that raw PLVs by definition cannot be less than zero; however, baseline adjusted PLVs can result in negative values. Unlike the previous study, significant negative values were observed, so these were included in the figures.

To account for multiple comparisons, regions were only considered to be functionally connected if more than 50% of the time points within the time window (19 time points for each 150ms window) were significantly greater for a group versus the other (or versus 0 for baseline connectivity). The rationale for this chosen threshold rests on the assumption that the binomial probability of getting 50% or more significant tests within such a time window is extremely low. We used  $p = 0.05$  ( $q = 1 - p = 0.95$ ) as the

probability of a success in a single binomial trial to compute the binomial probability of getting 50% or more significant time points by chance out of the total of 19 (37) time points in each bin (Onton, Delorme & Makeig, 2005). This probability is  $5.4 \times 10^{-15}$  ( $4 \text{ bins} \times 1.3 \times 10^{-15}$ ) if all of the time points in a bin represented independent tests. This assumption is probably not precisely correct, although it is not too unreasonable because the tests were made across subjects, who were independent of each other. Since we made 55 (inter-regional) comparisons (each possible pairing of 11 different ROIs), there were 55 such tests for each of the 12 comparisons (4 group comparisons + 4 NU baseline comparisons + 4 CU baseline comparisons) being made. At most ( $p = 0.05$ , with the minimum 19 of 37 significant data points per each of the four 150 ms bins), the experiment-wise error probability for each set of  $t$ -tests, assuming independence, was ( $55 \text{ pairs} \times 12 \text{ comparisons} \times 1 \text{ frequency band} \times 5.4 \times 10^{-15}$ ) =  $3.5 \times 10^{-12}$ . Again, these tests are likely not independent so this is a liberal estimate of the experiment-wise probability of Type I error. For each of the 150 ms time bins, pairings that were significant, were plotted onto separate 11x11 matrices (representing each of the 55-connections for the 11 ROIs) for each group. These were then fed into the BrainNet Viewer toolbox for MATLAB (Xia et al., 2013) to generate brain connectivity maps depicting the statistically significant functional connectivity between the various ROIs for each time bin.

## Results

### *Cannabis and Other Recreational Drug Use*

CU reported an average of 47.17 (SD = 48.31) instances of cannabis use over the past 30 days and an average of 10.92 (SD = 11.02) instances of cannabis use over the past 7 days. At the time of testing, cannabis users reported that an average of 0.85 (SD = 0.72) days had elapsed since last using cannabis. The mean age of first cannabis use amongst users was 16.75 (SD = 2.05) years.

Amongst NU, 66.7% reported that they had never used cannabis. Amongst the 5 current NU with a history of cannabis use, an estimated average of 522.0 (SD = 179.9) days had elapsed since they last used cannabis. The mean age of first cannabis use amongst the NU with a history of cannabis use was 18.60 (SD = 4.83) years.

In addition to cannabis use, participants were asked to self-report whether they considered themselves current users of any other recreational substances (including caffeine, nicotine and alcohol) (See Table 4.1). Participant responses were grouped into seven substance categories: caffeine (e.g. coffee, tea, soda & energy drinks) nicotine, alcohol, stimulants (e.g. cocaine and amphetamine), hallucinogens (e.g. MDMA, LSD, psilocybin & designer research chemicals), opioids (e.g. morphine, heroin, OxyContin etc.), sedatives (e.g. benzodiazepines), and other (e.g. dissociative drugs such as PCP or ketamine, or inhalants etc.). A greater proportion of participants in the CU group reported current nicotine use, however this difference was only marginally significant. There was also a significantly larger proportion of current hallucinogen users amongst the CU

group. Groups did not differ for proportions of current caffeine, alcohol, or stimulant use. There were no current opioid or sedative users in either group and no participants in either group reported current use of other categories of recreational substances.

Unlike for cannabis use, participants were only asked to quantify frequency of use of other substances based upon five broad categories (1 = Once or twice ever; 2 = A few times a year; 3 = A few times per month; 4 = More than once each week; 5 = Daily). Frequency comparisons were only made for alcohol and caffeine use, given that there was a substantial proportion of current alcohol and current caffeine users in each group. The self-reported frequency of use amongst alcohol users in the CU group (M = 3.10; SD = 0.74) did not differ significantly from the NU group (M = 2.60; SD = 0.70). The self-reported frequency of caffeine use also did not differ significantly between the CU (M = 4.33; SD = 0.82) and NU (M = 4.00; SD = .082) groups. The CU participants who reported current stimulant or hallucinogen use, indicated infrequent use of only a few times each year, thus these participants were not examined more closely to determine if substance use was confounded with any of the measures discussed in this chapter. Those who reported current nicotine use, reported using daily or several times a week; however, since relatively few individuals overall reported current nicotine use, the impact of nicotine use was not examined further for this study.

Table 4.1 Percentage of CU and NU groups reporting Current Non-Cannabis Substance Use

NU (n = 15)		CU (n = 12)		$X^2$	<i>p</i> -value
	%		%		

Caffeine	46.7	50.0	0.03	.863
Nicotine	6.7	33.3	3.14	.076
Alcohol	66.7	83.3	0.96	.326
Stimulants	0	8.3	1.30	.255
Hallucinogens	0	33.3	5.87	.015
Opioids	0	0	n/a	n/a
Sedatives	0	0	n/a	n/a
Other	0	0	n/a	n/a

Table 4.1. Percentages of participants who reported being a current user of non-cannabis recreational substances. *p*-values were determined using chi-squared analysis of proportion of participants in each group who reported being a current user of a substance within each respective class.

### ***Neuropsychological Tests***

Independent T-tests were used to compare NU and CU for each of the neuropsychological measures. A summary of neuropsychological results can be viewed in Table 4.2. Overall, groups did not differ significantly in estimated IQ, verbal, perceptual reasoning, working memory, or sustained attention.

Table 4.2 Descriptive Statistics of Neuropsychological Measures for Cannabis Users and Non-Users.

	NU (n = 15)	CU (n = 12)	<i>p</i> -value
	M (SD)	M (SD)	
Estimated IQ <sup>a</sup>	109.96 (6.29)	111.41 (7.01)	.575
Vocabulary <sup>b</sup>	54.00 (6.54)	32.36 (3.96)	.249
Matrix Reasoning <sup>b</sup>	20.00 (3.78)	20.33 (3.42)	.814
Letter Number Sequencing <sup>b</sup>	14.73 (3.11)	14.50 (2.07)	.825
HART	25.93 (3.49)	26.58 (4.01)	.657

### **Continuous Performance**

<u>Task<sup>c</sup></u>				
2-digit	3.85 (0.52)	3.99 (0.46)		.469
3-digit	3.14 (0.72)	3.22 (0.61)		.743
4-digit	1.91 (0.74)	2.12 (1.10)		.551

Table 4.2. Descriptive statistics of neuropsychological tests for non-users (NU) and cannabis users (CU). Groups were compared with independent samples *t*-tests. a) Estimated Full-Scale IQ derived by using WAIS-III MR and VC scores combined with demographics (age and education level) according to a regression algorithm (OPIE-3). b) VC, MR, and LNS scores are based upon raw scores derived from each test. c) Scores represent *d*-prime values for each condition generated automatically by the CPT-IP software included in the MATRICS battery.

### ***Self-Report Measures***

Independent *t*-tests were used to compare NU and CU for each of the self-report measures. A summary of self-report results can be viewed in Table 4.3. CU showed marginally higher scores on paranoia subscale of the SCL-90 but not on total scores or any of the other subscales of psychopathological symptoms. CU also showed marginally higher total scores on aberrant sensory processing on the SGI, along with marginally higher scores on the perceptual modulation subscale and significantly higher scores on the over-inclusiveness subscale. Groups did not differ significantly in terms of schizotypal personality traits.

Table 4.3 Descriptive statistics of Self-Report Measures for Cannabis Users and Non-Users.

	<u>NU (n = 15)</u>	<u>CU (n = 12)</u>	<u><i>p</i>-value</u>
	<u>M (SD)</u>	<u>M (SD)</u>	
<u>Symptom Checklist 90</u>			
General Symptom Index	53.67 (42.69)	61.92 (33.03)	.587

Somatic	5.73 (4.08)	6.83 (4.76)	.524
OCD	10.33 (7.23)	11.17 (4.82)	.735
Interpersonal Sensitivity	6.40 (5.89)	6.92 (5.60)	.819
Depression	11.60 (9.97)	11.42 (8.57)	.960
Anxiety	4.20 (4.68)	6.50 (5.78)	.263
Hostility	3.20 (3.86)	2.25 (1.55)	.431
Phobia	1.47 (2.59)	1.75 (2.86)	.790
Paranoia	2.13 (2.20)	4.25 (3.60)	.071 <sup>†</sup>
Psychotic Experience	3.33 (4.19)	3.92 (4.12)	.720
<u>Sensory Gating Inventory</u>			
Total	51.93 (23.49)	71.25 (30.14)	.073 <sup>†</sup>
Perceptual Modulation	14.60 (11.62)	24.42 (14.67)	.063 <sup>†</sup>
Distractibility	16.93 (7.55)	18.00 (7.78)	.722
Over Inclusiveness	11.73 (5.38)	17.67 (7.04)	.020*
Fatigue Stress Vulnerability	8.67 (4.30)	11.17 (4.86)	.169
<u>Schizotypal Personality Questionnaire</u>			
Total	8.13 (4.93)	9.25 (5.38)	.579
Cognitive Perceptual	2.33 (2.23)	3.17 (2.17)	.337
Interpersonal	3.67 (2.09)	3.08 (3.12)	.567
Disorganized	2.13 (2.13)	3.00 (1.60)	.254

Table 4.3. Descriptive statistics of self-report measures for non-users (NU) and cannabis users (CU); Independent samples t-tests were used to compare groups; \* denotes significance ( $p < .05$ ); † represents trend significance ( $p < .1$ ).

### ***Accuracy and Reaction Time***

Behavioural results can be found in Table 4.4. Separate 2x2 mixed-measures ANOVAs with memory load (1-back and 2-back) as a within subjects factor and user group (NU and CU) as a between subjects factor were computed for accuracy ( $d'$ ) and reaction time (RT) to correct targets. Analyses were run separately for the frequency match and pattern match tasks given differences in task demands for each condition that would result in bias towards faster responses in the frequency match task. In both tasks, participants were

instructed to withhold responses until termination of the final tone of an auditory run; however, when matching on frequency, participants would have presumably identified correct matching targets prior to the onset of the final tone of each target run, whereas when matching on pattern, information about whether the stimulus is a change run or a flat run is not available until hearing the final tone. This bias is most prevalent for reaction time data; and, while it would be possible to run the analyses for accuracy across both experimental tasks, we opted not to, in order to maintain coherency across comparisons and subsequent ERP analyses.

For frequency match response accuracy, there was a significant main effect of memory load ( $F(1,25) = 144.27, p < .001, \eta_p^2 = .852$ ) suggesting that participants in both groups responded more accurately in the 1-back condition compared to the 2-back condition. There was also a main effect of group ( $F(1,25) = 7.95, p = .009, \eta_p^2 = .241$ ) suggesting that CU outperformed NU in both load conditions. The memory load by user group interaction was not significant.

For pattern match response accuracy, there was again a significant main effect of memory load ( $F(1,25) = 144.27, p = .001, \eta_p^2 = .342$ ) suggesting that participants in both groups responded more accurately in the 1-back condition compared to the 2-back condition. There was also a main effect of group ( $F(1,25) = 10.24, p = .004, \eta_p^2 = .291$ ) again suggesting that CU outperformed NU in both pattern match memory load conditions. The memory load by user group interaction was not significant.

For frequency match response time, there was a significant main effect of memory load ( $F(1,25)=12.86, p = .001, \eta_p^2 = .340$ ) suggesting that participants in both groups responded more quickly to targets in the 1-back condition compared to the 2-back condition. There was no significant main effect of group or memory load by user group interaction.

For pattern match response time, there was only a marginal main effect of group ( $F(1,25)=3.44, p = .075, \eta_p^2 = .121$ ) suggesting that CU had a trend toward faster response times in both memory load conditions. There was no significant main effect of memory load and no significant interaction between memory load and user group.

Table 4.4. Behavioural Performance Data for the *n*-back Task

	Mean (SD)			
	1-BACK		2-BACK	
Frequency Match	NU	CU	NU	CU
<i>d'</i>	2.17 (0.61)	2.98 (0.93)	0.94 (0.29)	1.42 (0.74)
RT (ms)	463 (145)	483 (72)	575 (111)	528 (108)
Pattern Match				
<i>d'</i>	1.54 (1.02)	2.73 (1.05)	1.11 (0.68)	2.15 (1.13)
RT (ms)	709 (128)	650 (114)	759 (108)	659 (135)

Table 4.4. Accuracy (*d'*) and reaction time (RT) for non-users (NU) and cannabis users (CU) in both the frequency and pattern match tasks under low (1-back) and high (2-back) memory load. RT is measured relative to the onset of the 5<sup>th</sup> tone at 600 ms.

### ***P300 ERP Results***

Mean P300 amplitudes and latencies for each task, memory load, and user group can be found in Table 4.5, and figures depicting the P300 ERP waveforms at channel Pz can be viewed in Figure 4.3. P300 peak amplitude and latency were analyzed for frequency and pattern match tasks separately, using mixed-measures ANOVAs, each with memory load (1-back and 2-back) as a within subjects factor and user group (NU and CU) as a between subjects factor.

For P300 amplitude in the frequency match task (250-500 ms extraction window) at channel PZ, there was a main effect of memory load ( $F(1,25) = 5.36, p = .029, \eta_p^2 = .176, M_{\text{diff}} = .497, SE = .215, 95\% \text{ CI} = [.055 \text{ to } .938]$ ) indicating decreased amplitude with increasing memory load. There was also a main effect of user group ( $F(1,25) = 7.82, p = .010, \eta_p^2 = .238, M_{\text{diff}} = .759, SE = .272, 95\% \text{ CI} = [.200 \text{ to } 1.319]$ ) indicating larger P300 amplitude response for CU in both memory load conditions. The group by memory load interaction was not significant ( $F(1,25) = 0.532, p = .473, \eta_p^2 = .021$ ).

For P300 amplitude in the pattern match task (850-1100 ms extraction window) at channel PZ, there was a significant main effect of memory load ( $F(1,25) = 15.090, p = .001, \eta_p^2 = .376, M_{\text{diff}} = .560, SE = .144, 95\% \text{ CI} = [.263 \text{ to } .857]$ ) indicating decreased amplitude with increasing memory load. There was no significant main effect of user group ( $F(1,25) = 0.28, p = .601, \eta_p^2 = .011$ ) and the user group by memory load interaction, ( $F(1,25) = 2.68, p = .114, \eta_p^2 = .097$ ), also was not significant.

For P300 latency at channel PZ in the frequency match task, there were no significant main effects of load ( $F(1,25) = 1.42, p = .241, \eta_p^2 = .055$ ), user group ( $F(1,25) = 0.28, p = .601, \eta_p^2 = .011$ ), or load by user group interaction ( $F(1,25) = 0.11, p = .740, \eta_p^2 = .004$ ).

For P300 latency at channel PZ in the pattern match task, there was a marginal user group by memory load interaction ( $F(1,25) = 3.45, p = .075, \eta_p^2 = .121$ ). Follow-up analyses indicated a trend towards CU having longer latencies than NU, ( $M_{diff} = 44.47$  ms,  $SE = 24.15, p = .077, 95\% CI = [-30.89$  to  $76.49]$ ), in the higher memory load condition and a trend towards reduced latencies in NU, ( $M_{diff} = 46.93$  ms,  $SE = 24.14, p = .063, 95\% CI = [-2.79$  to  $96.65]$ ), with increased memory load.

Table 4.5. P300 Amplitudes and Latencies at Channel PZ for the *n*-back Task

	M (SD)			
	1-BACK		2-BACK	
	NU	CU	NU	CU
<b>Frequency Match</b>				
Amplitude (uV)	1.8 (0.6)	2.4 (1.3)	1.2 (0.8)	2.1 (0.9)
Latency (ms)	349.1 (75.5)	377.3 (105.1)	332.0 (62.0)	347.0 (87.5)
<b>Pattern Match</b>				
Amplitude (uV)	1.5 (0.9)	1.9 (1.1)	1.2 (0.6)	1.1 (0.7)
Latency (ms)	998.1 (74.7)	975.3 (56.6)	951.2 (69.0)	971.0 (65.2)

Figure 4.3. Grand Average ERPs to Auditory  $n$ -Back Tasks Comparing NU and CU

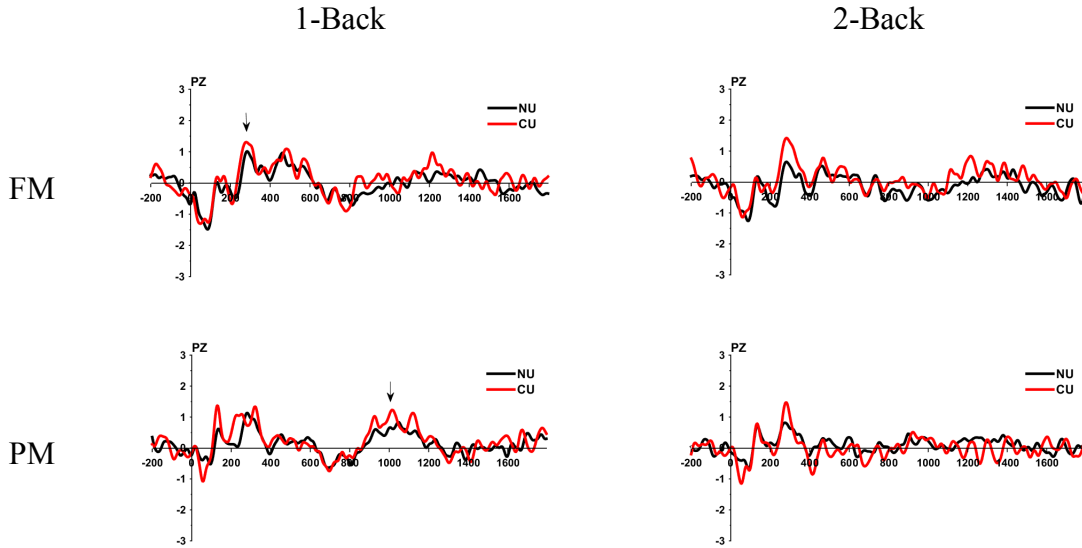


Figure 4.3. Grand average P300 ERP waves at channel Pz for cannabis users (CU;  $n = 12$ ) and non-users (NU;  $n = 15$ ) in the frequency match (FM) and pattern match (PM) tasks at both memory load (1-back and 2-back) conditions. The arrows indicates the approximate location of the P300 peak at Pz within the 250-500 ms (FM) and 850-1100 ms (PM) extraction windows respectively for each condition.

### ***ROI Cluster Analysis Results***

Results of the dipole clustering and ROI identification can be viewed in Table 4.6 and cluster plots for each retained ROI can be viewed in Figure 4.4. In total, 11 clusters pertaining to theoretically relevant brain areas met our criteria of containing over 50% of the sample participants from each group. The locations selected were: bilateral superior temporal lobes (RSTG & LSTG), bilateral temporo-parietal junction (RTPJ & LTPJ), left superior parietal lobe (LSPL), posterior cingulate cortex (PCC), anterior cingulate cortex (ACC), right prefrontal cortex (RPFC), left superior frontal gyrus (LSFG; also situated proximal to frontal eye field), and bilateral frontal pre-central areas (RPCG & LPCG). Two theoretically relevant clusters, one localized to the right medial frontal gyrus

(RmedFG) and the other localized to the left inferior frontal gyrus (LIFG) were excluded from further analysis because an insufficient number of individuals from the NU group contributed to these clusters.

Table 4.6. Seeded Dipole Clusters of Independent Components Identified for Cannabis Users and Non-Users and Corresponding Brain Region

ROIs	Contributing		% VAF	Talairach			BA #
	NU %	CU %		X	Y	Z	
<b>Retained</b>							
R.STG	<b>73.33%</b>	<b>58.33%</b>	90.57	54	-32	-1	22
L.STG	<b>53.33%</b>	<b>50.00%</b>	90.03	-57	-40	4	22
R.TPJ	<b>86.67%</b>	<b>100%</b>	96.36	26	-67	23	31
L.TPJ	<b>73.33%</b>	<b>91.67%</b>	91.29	-28	-64	19	31,18
R.PFC	<b>93.33%</b>	<b>75.00%</b>	90.07	9	38	-13	10,11
L.PCC	<b>80.00%</b>	<b>91.67%</b>	93.25	-3	-49	21	30,23
L.SPL	<b>80.00%</b>	<b>75.00%</b>	95.00	-3	-37	49	5,7
L.ACC	<b>73.33%</b>	<b>50.00%</b>	93.80	-3	21	14	24
L.SFG	<b>86.67%</b>	<b>83.33%</b>	93.23	-3	5	51	6
R.PCG	<b>93.33%</b>	<b>91.67%</b>	94.37	36	-10	43	6,4
L.PCG	<b>66.67%</b>	<b>91.67%</b>	93.90	-37	-15	45	4, 3, 6
<b>Rejected</b>							
L.IFG	<b>26.67%</b>	<b>58.33%</b>	90.97	-46	22	7	45
R.mFG	<b>33.33%</b>	<b>58.33%</b>	89.48	5	50	24	9

Figure 4.4. Dipole Cluster Plots of Retained ROIs

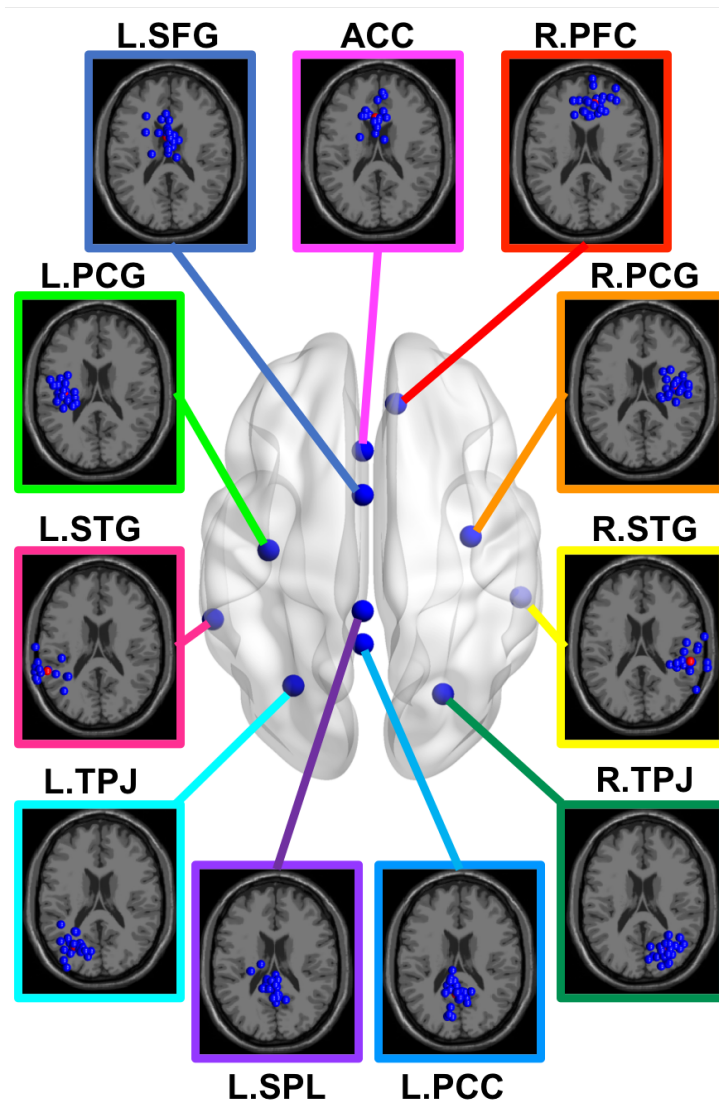


Figure 4.4. Dipole cluster plots of retained ROIs for the N-back task. Blue dots depict individual ICs and red dots depict cluster centroids. Clusters represent both cannabis users and non-users. Note: Some ICs/centroids are not visible due to being hidden beneath others.

### ***ROI ERPs***

ERPs were examined for the ICs contributing to each of the 11 selected ROIs. The primary goal of this analysis was to provide a general overview of areas of difference between groups for each task (frequency match and pattern match) at each memory load (1-back and 2-back) in order to provide an interpretive framework bridging channel and

theta-band network connectivity. As such, uncorrected ( $\alpha = .05$ ) pairwise comparisons were run across ERP waveforms for each ROI separately (See Method section for more details).

The 0 to 600 ms window was examined for the frequency match task and the 600 to 1200 ms window was examined for the pattern match task. While differences that occur within the entire 600 ms have been documented in Table 4.7, detailed descriptions have been restricted to significant differences that directly overlapped the P300 extraction windows (250-500 and 850-1100ms) for each task. It should be noted that, unlike the components of channel ERPs, the meanings of positive and negative amplitudes of ROI-based neural source IC ERPs are not well established and thus it is unknown as to whether these specifically map onto the P300 waveform morphologies seen at the channel level (See Table 4.7). ERP waveforms can be viewed in Appendix D.

#### *Frequency Match ROI ERPs*

In the 1-back condition of the frequency match task, group differences overlapping the P300 (250-500 ms) were observed in the RSTG, LSTG, RPFC, PCC, SPL and LSFG and differences were observed in the LTPJ and SPL in the 2-back condition.

More specifically in the 1-back condition, NU only displayed larger positive SPL amplitudes (390-420 ms); whereas, CU showed larger positive RSTG amplitudes (~300-400 ms), larger negative LSTG (~240-270 ms), larger positive RPFC (~300-350 ms), larger positive PCC (~300-400 ms) and larger positive LSFG (300-350 ms).

In the 2-back condition, CU showed larger positive LTPJ (~240-260 & 300-400 ms) and larger positive SPL (170-290) amplitude. Also of note, in the 1-back condition there appears to be some evidence of group differences in LSTG with the CU showing a larger negativity in the P300 range and the NU showing a positivity just after the P300 window (~500-600 ms), this is emphasized as it will be further addressed in the discussion section where we speculate about possible group differences in encoding strategies.

#### *Pattern Match ROI ERPs*

In the 1-back condition of the pattern match task, group differences overlapping the P300 (850-1100 ms) were observed in the RTPJ and LSFG and in the 2-back condition group differences were observed in the RSTG, RTPJ, LSFG, RPCG and LPCG. More specifically in the 1-back condition, CU displayed larger positive RTPJ (~1080-1100 ms) amplitudes and exhibited larger positive LSFG amplitude (~900 to 950 ms), which overlapped the P300 window. Also of note, group differences emerge late in the window in the LSTG of the 1-back (~1160-1200 ms; NU positive & CU negative), which is similar to what was observed in the 1-back condition of the frequency match condition, though the polarity is reversed, which again, will be later be discussed in context of encoding strategies.

In the 2-back condition, CU displayed larger positive amplitudes in the RSTG (~1000-1050 ms), LSFG( ~860-940), RPCG (~840-870 ms), and LPCG (~1000-1025 ms). CU also displayed a larger negative RTPJ (~865-910 ms) amplitude.

Table 4.7. ROI ERP Summary Comparing NU and CU on the *n*-back Task

ROI	FREQUENCY MATCH (0-600 ms)						PATTERN MATCH (600 -1400ms)					
	1-BACK			2-BACK			1-BACK			2-BACK		
	0-250	250-500	500-600	0-250	250-500	500-600	600-850	850-1100	1100-1400	600-850	850-1100	1100-1400
RSTG		CU+ (P3)									CU+ (P3)	
LSTG		CU- (P3)	NU-						NU+/CU-			
RTPJ				CU+				CU+ (P3)	CU+	CU-	CU- (P3)	CU-
LTPJ					CU+ (P3)	CU+	NU+					
RPFC		CU+ (P3)					CU+		CU+			
PCC		CU+ (P3)										
SPL	NU+	NU+ (P3)		CU+	CU+ (P3)							
ACC	NU+								CU+,NU-			
LSFG	CU+	CU+ (P3)		CU+			CU+	CU+ (P3)			CU+ (P3)	
RPCG			NU+/CU-				CU-				CU+ (P3)	
LPCG							NU+		NU+		CU+ (P3)	CU+

Table 4.7. Summary of ROI IC ERP results comparing non-users (NU) and cannabis users (CU) on the frequency match and pattern match *n*-back tasks under low (1-back) and high (2-back) memory loads. Significant group differences ( $p < .05$ ) have been denoted with the group (NU or CU) and a +/- to denote positive or negative deflection. Significant differences overlapping the P300 have been specified (P3) and differences overlapping the P300 where CU showed a significantly larger positive deflection have been highlighted in green.

### Phase Synchrony

Theta-band (3-7 Hz) functional connectivity, indexed via phase synchrony (PLVs), was examined for each memory load and group in the 0 to 600 ms window for the frequency match task and in the 600 to 1200 ms window for the pattern match task. In addition to between group comparisons for each task and load condition, comparisons were made within each group and condition versus baseline to provide an overall account of the pattern of functional connectivity between network nodes (ROIs) and to provide context for interpreting any group differences that emerged. The results for the frequency match condition can be viewed in Figure 4.5 and those depicting pattern match condition can be viewed in Figure 4. 6.

### *Frequency Match Theta PLVs (0-600 ms)*

The PLV results for the frequency match task can be viewed in figure 4.5. In both memory load conditions examination of functional connectivity versus baseline revealed different patterns of connectivity for each group.

In the 1-back condition, the NU group displayed a pattern of distributed connectivity. Early on, NU exhibited left temporal-frontal connectivity (LSTG-ACC; 0-150 ms) and sustained left temporal-posterior connectivity (LSTG-PCC; 0-300 ms). Right temporal connectivity emerged slightly later which appeared to network with the left precentral region along with right temporo-parietal, anterior cingulate and prefrontal regions (LPCG-RSTG, LPCG-ACC, LPCG-RTPJ, RPFC-LSFG; 150-300 ms). The connectivity between the precentral and temporal-parietal regions was sustained (LPCG-RTPJ; 300-450 ms), followed by right temporal-parietal connectivity and a reemergence of frontal connectivity (RSTG-RTPJ & RPFC-LSFG; 450-600 ms).

By contrast, in the 1-back condition, CU displayed a less distributed pattern of connectivity versus baseline, but interestingly, also displayed a pattern of decreased connectivity versus baseline that was absent in the NU group. Early in the window, CU exhibited left temporo-parietal-parietal (LTPJ-SPL; 0-150 ms) along with early, sustained connectivity between the anterior cingulate and frontal regions (ACC-SFG; 0-300ms). Slightly later posterior cingulate-frontal connectivity (PCC-PFC; 150-300 ms) emerged followed by right temporal-frontal connectivity (RSTG-LSFG; 300-450 ms).

CU also revealed decreased synchronization (unlike NU) versus baseline in a network consisting of the anterior cingulate, right temporal and superior parietal regions (ACC-RSTG-SPL; 150-300 ms) followed by decreased connectivity between left temporal and left precentral areas (LSTG-LPCG; 300-450). Finally, sustained decreased connectivity between the superior parietal and anterior cingulate (SPL-ACC; 300-600 ms) was later joined by decreased connectivity between left precentral and anterior cingulate regions (ACC-LPCG; 400-600ms).

The only group differences (NU vs. CU) that appeared in the 1-back condition were that NU showed greater early right temporal lobe and anterior cingulate connectivity (RSTG-ACC; 150-300 ms) and greater anterior cingulate and left precentral connectivity (ACC-LPCG; 450-600 ms) during a later time window. However, these differences appeared to be driven by decreased connectivity versus baseline in the CU group rather than increased connectivity in NU.

To sum up the 1-back frequency match findings, NU exhibited a pattern of widespread network connectivity between frontal, temporal, posterior cingulate, and parietal areas. Notably, NU displayed numerous connections with the left superior temporal lobe and left precentral area that were largely absent in CU. By contrast, CU, who performed better on this task, displayed less connectivity overall and showed a pattern of right temporal-frontal and also posterior cingulate-frontal connectivity that was absent in NU. Most notably, however, CU exhibited apparent widespread desynchronization versus

baseline, which was completely absent in NU. The implications of these findings will be addressed further in the discussion section.

In the 2-back condition, NU displayed a somewhat less distributed pattern of network connectivity compared to the 1-back condition with less connectivity involving left temporal areas and greater connectivity involving right temporal areas. More specifically, early in the window, NU showed connectivity between right frontal and temporal, right temporo-parietal and anterior cingulate, and left premotor and frontal areas (PFC-RSTG, RTPJ-ACC, LPCG-LSFG; 0-150 ms). This was followed by sustained connectivity between right temporo-parietal and superior parietal areas (RSTG-RTPJ; 150-600 ms) and late left temporo-parietal and temporal lobe (LSTG-LTPJ; 450-600 ms) connectivity. NU also exhibited decreased connectivity between the posterior cingulate and right precentral areas (PCC-RPCG; 450-600 ms) late in the window.

In the 2-back condition, CU also displayed a somewhat different pattern of connectivity under higher memory load compared to the 1-back condition, with less abundant posterior cingulate-frontal and less anterior cingulate-frontal connectivity, in addition to a lesser degree of desynchronization versus baseline. Furthermore, CU and NU had more connections in common for this condition. More specifically, early in the window, CU showed connectivity between right temporal, prefrontal and anterior cingulate regions (RPFC-RSTG, RSTG-ACC, ACC-RPFC; 0-150ms). Notably, the connection between the temporal and prefrontal regions was similar to what was seen in the NU group during the same time period. CU later displayed connectivity between the right temporo-parietal and

anterior cingulate areas in addition to connectivity between left temporo-parietal and right premotor areas (RTPJ-ACC, LTPJ-RPCG; 300-450 ms). The RTPJ-ACC connectivity was also observed in the NU group, albeit earlier. CU also showed decreased connectivity versus baseline between left temporal lobe, posterior cingulate, and right temporo-parietal regions (LSTG-PCC-RTPJ; 0-150 ms), though while CU displayed more desynchronization than NU, overall CU had a lesser degree of desynchronization than was observed in the 1-back condition, .

In terms of 2-back group differences, NU had greater connectivity between left temporal and superior parietal lobes early in the window (LSTG-SPL; 0-150 ms) though this appeared to be driven by decreased activity versus baseline in the CU group. CU also showed greater connectivity between the posterior cingulate and right premotor areas occurring late in the time window (PCC-RPCG; 450-600ms), which was driven by decreased activity versus baseline in the NU group.

To sum up the 2-back frequency match findings, NU displayed an overall reduction in connectivity versus the 1-back condition and greater right temporal connectivity. CU, on the other hand, showed a similar degree of connectivity compared to the 1-back condition albeit with slightly more involvement of temporal-frontal connections and reduced involvement of posterior cingulate-frontal connections. Also, CU continued to exhibit more desynchronization than NU, but less so than was observed in the 1-back condition.

Figure 4.5. Frequency Match Theta (3-7Hz) Phase Synchrony (PLV) Results

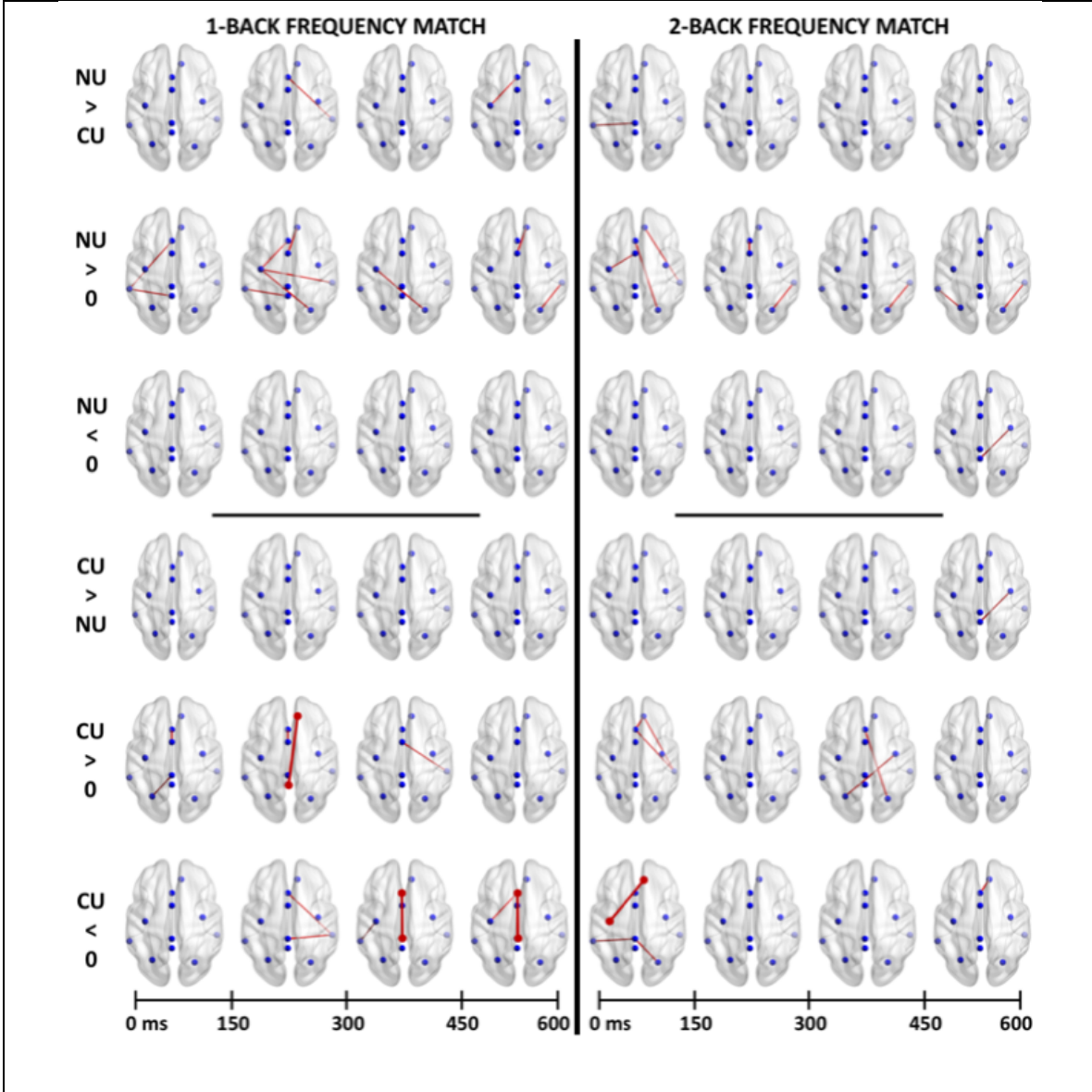


Figure 4.5. Theta (3-7 Hz) band phase synchrony for frequency match 1-back (left) and 2-back (right) conditions for non-users (NU; top) and cannabis users (CU; bottom) from 0 to 600 ms. Each image represents a 150 ms time window and red lines indicate significant ( $p < .05$ ) connectivity between regions. Rows marked NU > CU & CU > NU represent group differences where NU showed significantly greater connectivity than CU, and vice versa. Rows marked NU/CU > 0 indicate greater connectivity versus baseline (-250 to 0 ms to onset of first tone). Rows labeled NU/CU < 0 indicate decreased connectivity versus baseline. Note: Bolded connecting lines were added to clarify connections between overlapping nodes.

*Pattern Match Theta PLVs (600-1200 ms)*

The PLV results for the pattern match task can be viewed in figure 4.6. In both memory load conditions, examination of functional connectivity versus baseline again revealed largely different patterns of connectivity for each group.

In the 1-back condition, NU displayed a pattern of distributed connectivity involving frontal parietal, premotor areas and temporal (bilateral but left more prominent) areas. Early in the window, NU exhibited left temporal-frontal and left temporal-parietal connectivity (LSTG-LSFG, LSTG-SPL; 600-750 ms). Later they exhibited right temporal and left premotor connectivity (RSTG-LPCG; 750-900 ms). This was followed by a densely connected network characterized by a reemergence of left temporal-frontal connectivity, in addition to left frontal-parietal connectivity, right temporoparietal and anterior cingulate connectivity (LSTG-LSFG, LTPJ-LSFG, RTPJ-ACC; 900-1050 ms), in addition to connectivity between the superior parietal and left premotor areas (SPL-LPCG; 900-1200 ms) that was sustained to the end of the time-window. Late in the window, connectivity emerged between bilateral premotor areas and between left temporoparietal and temporal areas (LPCG-RPCG, LSTG-LTPJ; 1050-1200 ms). NU also showed a pattern of decreased connectivity versus baseline between right temporal and left temporo-parietal areas (RSTG-LTPJ; 600-750 ms) early in the window. This was followed by decreased right temporoparietal and right premotor connectivity (RTPJ-RPCG; 750-900 ms) and decreased bilateral temporal (LSTG-RSTG; 900-1050 ms) connectivity occurring later.

Similar to the 1-back condition of the frequency match task, CU displayed a less distributed pattern of network activity. Connectivity was primarily observed between right frontal-temporal, left temporo-parietal, and superior parietal and left premotor areas. More specifically, CU showed no significant connectivity versus baseline in the early half (600-900 ms) of the time window. However, later on they displayed connectivity between left temporoparietal and superior parietal areas (LTPJ-SPL; 900-1050) and sustained right temporal-frontal (RSTG-RPFC; 900-1200 ms) and superior parietal and left premotor connectivity (SPL-LPCG; 1050-1200 ms). CU showed decreased activity versus baseline early in the window between left temporal and posterior cingulate areas (LSTG-PCC; 750-900 ms) and sustained decreased connectivity between left temporoparietal and right premotor areas (LTPJ-RPCG; 750-1050 ms).

Notable group differences emerged in the 1-back condition such that NU displayed greater early connectivity between left frontal-temporal and left temporal and posterior cingulate areas (LSTG-LSFG, LSTG-PCC; 600-750 ms). This was followed by greater right temporal and left premotor connectivity (RSTG-LPCG; 750-900 ms) and then by greater connectivity between right temporoparietal and anterior cingulate areas (RTPJ-ACC; 900-1050 ms). All of these observed group differences appeared to be driven by increased NU connectivity versus baseline. Interestingly the LSTG-PCC connection decreased versus baseline in the CU group, albeit slightly later. Other group differences emerged showing greater NU connectivity (PCC-PFC, PCC-PCG) and CU connectivity (PFC-LPCG), but these were not interpreted because they did not correspond to any

increased or decreased connectivity versus baseline for either group and likely represent spurious connectivity.

To sum up the 1-back pattern match findings, despite showing poorer performance on this task, NU displayed a widespread pattern of frontotemporal (predominately left), frontoparietal, posterior cingulate-temporal (left), and right temporal with left premotor connectivity, which was often significantly greater than CU. By contrast, CU displayed a less widespread pattern of connectivity (similar to the frequency match condition), which was predominately characterized by right frontotemporal connectivity. Unlike the frequency match condition, both groups showed patterns (albeit different ones) of desynchronization.

In the 2-back condition, NU showed less overall network connectivity (and a conspicuous lack of temporal lobe connectivity) compared to the 1-back condition and again an overall different connectivity pattern compared to CU. More specifically, somewhat late in the window, NU displayed connectivity between bilateral premotor areas and connectivity between left temporoparietal and right premotor areas (LPCG-RPCG, LTPJ-RPCG; 900-1050 ms). NU also showed decreased connectivity versus baseline between left premotor and anterior cingulate areas (LPCG-ACC; 600-750 ms), followed by decreased connectivity between superior parietal and frontal areas (SPL-SFG; 750-900 ms), and later showed decreased connectivity between frontal and anterior cingulate areas (PFC-ACC; 900-1050 ms).

In the 2-back condition, CU displayed a somewhat similar number of connections compared to the 1-back condition but an overall different pattern of connectivity, characterized by connectivity with left temporal areas (versus right temporal areas in 1-back) and more connectivity between temporal, parietal, and frontal areas. More specifically, CU displayed early connectivity between right temporoparietal and left premotor areas (RTPJ-LPCG; 750-900 ms). This was followed by connectivity between left temporal and anterior cingulate areas and between left temporoparietal and prefrontal areas (LSTG-ACC, LTPJ-PFC; 900-1050 ms). Later, CU showed connectivity between left temporal and right premotor areas concurrent with connectivity between superior parietal and anterior cingulate areas (LSTG-RPCG, SPL-ACC; 1050-1200 ms). CU only displayed decreased connectivity versus baseline between bilateral temporoparietal areas (LTPJ-RTPJ; 1050-1200 ms) late in the window.

In terms of 2-back group differences, CU displayed greater connectivity between prefrontal and anterior cingulate areas (PFC-ACC; 900-1050 ms) later in the window, which was driven by decreased connectivity versus baseline in the NU group. CU also showed early RTPJ-PFC but this was not interpreted because it did not correspond to increased or decreased connectivity versus baseline in either group.

To sum up the 2-back pattern match findings, NU, who performed worse on this task, displayed a notable decrease in the overall number of network connections compared to the 1-back condition and demonstrated a clear absence of connectivity with frontal and temporal areas, as was seen in other conditions. CU, on the other hand, showed a similar

number of connections compared to the 1-back task, but exhibited a different pattern of connectivity. Unlike the 1-back condition (and also unlike the frequency match task), CU exhibited a pattern of connectivity between left superior temporal and frontal areas, in addition to connectivity between left temporo-parietal and frontal areas.

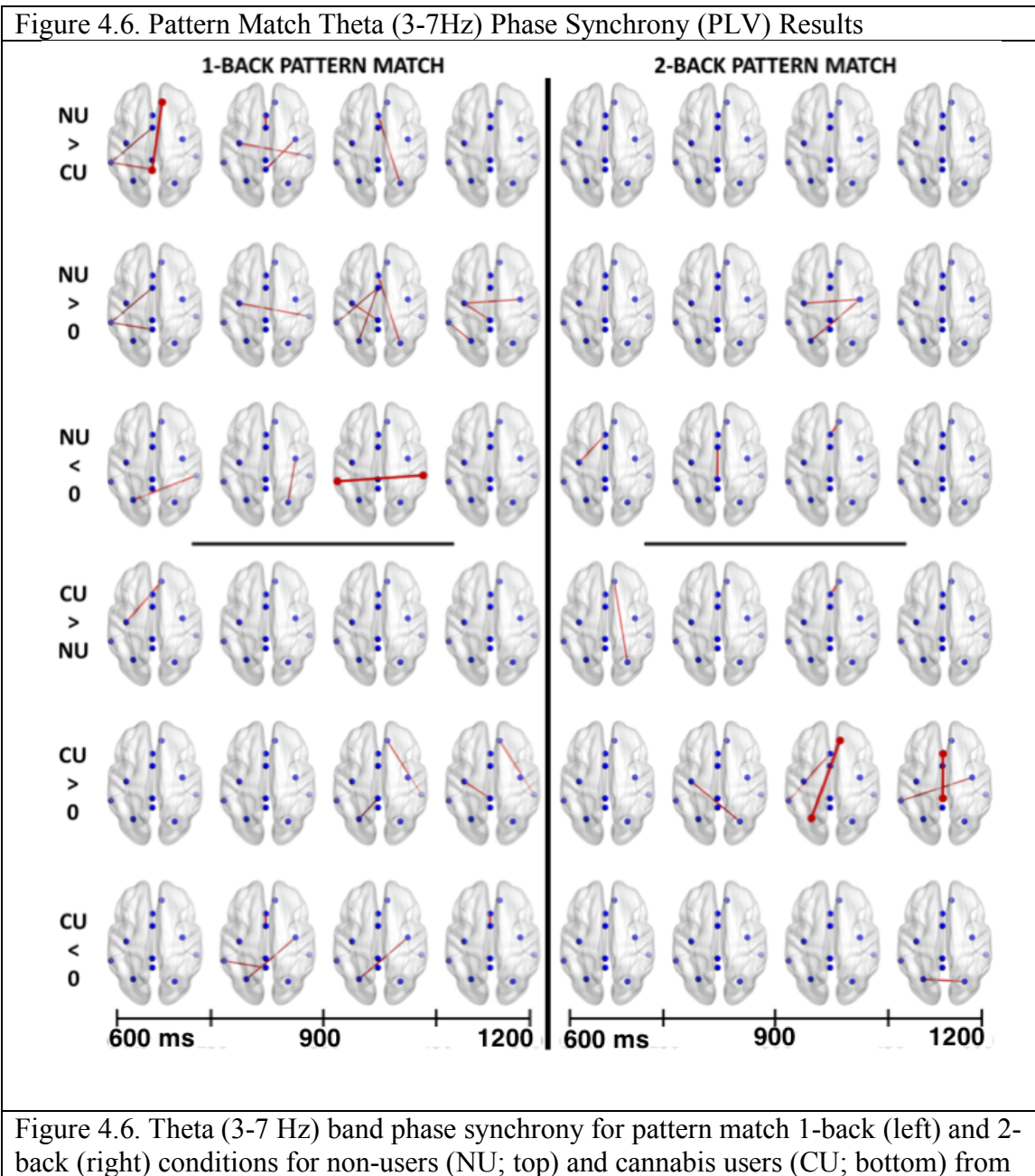


Figure 4.6. Theta (3-7 Hz) band phase synchrony for pattern match 1-back (left) and 2-back (right) conditions for non-users (NU; top) and cannabis users (CU; bottom) from

600 to 1200 ms. Each image represents a 150 ms time window and red lines indicate significant ( $p < .05$ ) connectivity between regions. Rows marked NU > CU & CU > NU represent group differences where NU showed significantly greater connectivity than CU, and vice versa. Rows marked NU/CU > 0 indicate greater connectivity versus baseline (-250 to 0 ms to onset of first tone). Rows labeled NU/CU < 0 indicate decreased connectivity versus baseline. Note: Bolded connecting lines were added to clarify connections between overlapping nodes.

## **Discussion**

### ***Unexpected Superior Working Memory Performance in Cannabis Users***

The present study compared a group of heavy cannabis users to non-users in a novel auditory working memory *n*-back task, which in different conditions had participants attend to different features (base frequency or pattern) of identical complex auditory stimulus runs under high and low memory conditions. In light of previous findings suggesting impaired working memory performance in cannabis users, we expected our sample of cannabis users to exhibit impaired performance in both conditions, especially under increased memory load. However, contrary to our expectation, this sample of cannabis users demonstrated better performance when asked to perform working memory operations while encoding the base frequency of the auditory runs and while encoding the overall pattern of the runs. Furthermore, while all participants tended to exhibit the expected worsened memory performance under increased memory load (suggesting that this *n*-back task is successfully tapping into working memory load) the cannabis users displayed better memory performance under low (1-back) and high (2-back) memory load for both the frequency and pattern match versions of the task.

### ***Demographics, Neuropsychological Tests and Self-Report Measures***

The sample characteristics do not supply any obvious clues as to why the cannabis users might outperform non-users as groups were similar in age and gender distribution, and screening procedures were conducted to exclude participants with histories of neurological, neurocognitive, or psychiatric diagnoses. Furthermore, groups also did not generally differ in overall self-reported psychological symptoms over the previous week or in the total scores of trait schizotypy. CU did show marginally increased paranoia symptoms consistent with other research (Fridberg, Vollmer, O'Donnell & Skosnik, 2011), which while perhaps concerning, would not be expected to relate to better working memory performance. Additionally, performance on neuropsychological tests did not differ between groups. Estimated IQs for participants tended to fall within the average to high average range for both groups and performance on the continuous performance task related to sustained attention and vigilance did not differ between groups. This latter task, however, is visual and cannot rule out any modality-specific attention effects.

Surprisingly, performance on the verbal working memory letter-number sequencing task did not differ significantly between groups, though it is possible that this study did not have adequate power to detect differences if they were present. Also, it is also possible that this particular working memory test does not tap into exactly the same cognitive domains as the *n*-back task. Some researchers have suggested that *n*-back performance is inconsistently correlated with traditional neuropsychological measures of working memory (Kane, Conway, Miura & Colflesh, 2007). Indeed, exploratory analyses examining Spearman rank correlations between performance on the LNS task and performance on the various *n*-back conditions for the entire sample revealed only a

significant positive Spearman rank correlation with accuracy on the 1-back frequency match condition ( $r = .39, p = .044$ ). Interestingly, however, when looking at users and non-users separately, NU did not show significant positive correlations with most of the tasks and surprisingly had a small non-significant negative correlation with 2-back frequency match accuracy. By contrast, CU performance on the LNS positively correlated ( $p < .05$ ) with performance for each  $n$ -back task (correlations ranging from .61 to .69). This observation may point to some fundamental differences in the working memory of cannabis users; however, given that this sample is very small, a larger study across a more diverse sample including an extensive battery of working memory tests across multiple sensory modalities would be required to fully explore this issue.

Neither self-reported cannabis use frequency (past week/past month) or time since last use were significantly associated with any of the behavioural or EEG measures. Another point to consider is that CU had a greater number of individuals who reported stimulant use; however, the overall number of stimulant users was low and those individuals reported very infrequent use, so unless these individuals happened to use stimulants the day of testing it would be unlikely that this would have had a drastic effect on behavioural performance in the present experiment. The CU group also had more current hallucinogen users, though again these individuals tended to use hallucinogens infrequently, and there is nothing in the literature to suggest that hallucinogen use improves working memory performance.

More CU participants reported that they were current smokers. There is some evidence that acute nicotine use may boost working memory performance, but it is believed that these effects reflect an amelioration of acute working memory deficits following prolonged abstinence rather than cognitive enhancement (Sutherland, Ross, Shakleya, Huestis & Stein, 2011). We did not collect nicotine abstinence data, though none of the participants suspended testing to consume nicotine, so if anything, participants who were smokers would more likely be suffering acute nicotine withdrawal, which if prolonged, would be expected to impair working memory performance rather than improve it.

CU had marginally larger scores on the sensory gating inventory and in particular had marginally greater scores on the perceptual modulation and significantly greater scores on the over-inclusiveness subscales of this measure. Higher scores on the SGI have been reported in the literature in individuals with schizophrenia and ADHD and these have been correlated with deficient early auditory P50 gating (Micoulaud-Franchi et al., 2015). Typically these are taken to reflect aberrant sensory processes akin to attenuated psychotic symptoms; so a standard interpretive approach would expect these to more likely correspond to impaired cognitive functioning. However, in this study, while speculative, it is possible that this measure may reflect altered (vs. aberrant) sensory processing in cannabis users, which could plausibly afford an advantage on this particular task. For instance, the over-inclusiveness scale includes items such as: “I seem to hear the smallest details of sound” and “Everything grips my attention even though I am not particularly interested in any of it.” In a real-world setting such experiences might be distracting; however, in a controlled and focused experiment it is possible that such

alterations in perceptual processing might lead to enhanced performance when the goal of the task is to attend to specific stimulus features. However, exploratory analyses did not support this idea as in CU there were strong significant negative correlations between SGI total scores and accuracy in both the frequency match ( $r = -.76$  and  $-.81$ ,  $p < .01$ ) and 1-back pattern match ( $r = -.66$ ,  $p < .05$ ) and 2-back pattern match performance ( $r = -.57$ ,  $p = .05$ ). Examination of the SGI subscales, appeared to suggest that these associations were primarily related to the aberrant perceptual modulation and fatigue stress vulnerability subscales. In sum, these findings point to interesting avenues of future research, but do not explain better behavioural performance in cannabis users, as greater alteration in sensory experience appears to be associated with worse auditory working memory performance.

### ***P300s Reflect Memory Load but Only Partially Reflect Performance Differences***

The channel-level P300 ERP results were consistent with our expectations in that we observed decreased P300 amplitudes with increased memory load in both tasks. These findings were also consistent with the decreased accuracy that was observed for the more difficult high memory load conditions. Furthermore, these results are generally consistent with other research that utilized working memory tasks, particularly  $n$ -back tasks, across a variety sensory modalities and task parameters (McEvoy, Pellouchoud, Smith & Gevins, 2001; Scharinger, Soutschek, Schubert & Gerjets, 2017).

In the frequency match task, we chose to focus on the P300 that appears in the 250-500 ms window during the initial four tones of the auditory runs. Our reasoning was that this

period is where most of the cognitive processing would be happening pertaining to working memory (i.e., encoding, template matching with stored items in memory, and target categorization) and would be most sensitive to memory load. Furthermore, the grand average ERP displayed a clear P300 waveform morphology, whereas this was not the case in the 850-1100 ms window (i.e. 250-500 ms after onset of 5<sup>th</sup> tone). Finally, P300s, including those related to working memory and oddball tasks (i.e. P3b), are typically maximal over all the midline parietal channels (Scharinger, Soutschek, Schubert & Gerjets, 2017). Examination of the channel scalp maps revealed that our chosen time window reflected this scalp distribution, whereas the 850-1100 ms window showed a somewhat frontal scalp distribution. The choice of P300 window (850-1100ms) for the pattern match condition was considerably more straight forward as the 5<sup>th</sup> tone was the feature that determined whether the run was change or flat, and hence whether it was to be encoded as a target or non-target.

The group comparison of ERP results was inconsistent with our expectations because we expected non-users to outperform cannabis users and for this to be reflected in larger P300 amplitudes for NU in both conditions. Our results are also inconsistent with other research findings that have demonstrated either reduced P300 amplitudes in cannabis users (Ilan, Smith, Gevins, 2004), or have shown no group differences (Cousijn, Vingerhoets et al., 2014). Our initial expectations were partially confirmed in that in the frequency match condition, the group performing more accurately (CU in this case) did indeed show larger P300 amplitudes, perhaps reflecting superior encoding and retention of auditory pitch features compared to non-users . However, the ERP findings in the

pattern match condition were contrary to expectation in that improved performance in CU was not matched by larger P300 amplitudes in that group, perhaps suggesting that other processes may be at play.

In contrast to the frequency match P300, the later pattern match P300 would be expected to overlap processes related to the behavioural response, so it is possible that this may have obscured any purely cognitive P300 response. Another possibility, while speculative, is that the slightly increased P300 latency (somewhat similar to what was observed in the more difficult feature absent condition in Chapter 3) may reflect recruitment of other cognitive processes that in turn attenuate the P300. Exploratory analysis extending the P300 extraction window to that used in the previous oddball studies (800-1600 ms), did appear to show increased P300 amplitudes in the 1-back condition; however, this created an unacceptable degree of variability in the latency of the selected peaks. Furthermore, the waveform morphology and scalp maps of this later window were inconsistent with typical P300s and may reflect other working memory processes (e.g. memory updating or maintenance). Future research might examine other early sensory and late ERP components, to see if those might better map on to performance in this condition, or examine responses to non-targets. Furthermore, future studies might also examine the maintenance period of the *n*-back task (Lefebvre & Jolicœur, 2016), which is not directly related to the P300.

In sum, the channel level P300 ERP results suggested that our *n*-back task is indeed engaging participants in a manner similar to other *n*-back tasks that have been reported in

the literature. Somewhat consistent with the overall better performance of the CU group, these results highlight some of the limitations of using standard ERP analyses in describing complex mental processes, especially in studies (such as this one) that use more complex stimuli. For example, had the frequency match  $n$ -back stimuli used single tone stimuli rather than 5-tone runs, a standard ERP analysis would be fully appropriate. However, even in this scenario the analysis of channel level data is of questionable utility in actually understanding the complex interplay of underlying processes that give rise to cognitive phenomena such as working memory. As cognitive neuroscience moves toward understanding more complex phenomena, more sophisticated methodology is necessary, such as the methods used in the measurement of activity localized to particular brain regions, to which we turn to next.

### ***Localized Brain Activity and Connectivity (ROIs, ERPs, ERSPs, PLVs)***

#### *ROIs Consistent with Working Memory*

The results of the cluster analysis revealed a number of frontal, parietal, pre-motor and cingulate areas of theoretical relevance to working memory and are largely consistent with meta-analyses of fMRI studies examining regional brain activations common to  $n$ -back tasks (Owen, McMillan, Laird & Bullmore, 2005; Rottschy et al., 2012). We also identified bilateral superior temporal regions that were expected given the auditory nature of this task, as has been documented in other auditory working memory and pitch discrimination tasks (Häkkinen, Ovaska & Rinne, 2015). The identified bilateral STG, bilateral TPJ, posterior cingulate, and bilateral premotor areas are situated near regions identified in the previous chapters, which would be expected given that the  $n$ -back task

used identical stimuli to the roving dual-oddball task. While different cognitive operations are being performed in this task, there is well-documented overlap between networks of attention and working memory (Huang, Seidman, Rossi & Ahveninen, 2013). Also, the identified superior frontal region is somewhat proximal to the left cingulate source identified in the previous chapter and also is near the frontal eye field and may include aspects of the supplementary motor area, all of which have been implicated in working memory (Cañas, Juncadella, Lau, Gabarrós & Hernández, 2018; du Boisgueheneuc et al., 2006). It should also be noted that two additional frontal clusters emerged, but unfortunately an insufficient number of non-users contributed to these, so they were excluded from the analyses. Similar to the previous studies, one of these frontal clusters localized to the inferior frontal gyrus, which, in concert with the superior temporal lobes, has been shown to play a role in maintaining encoded sound representations in auditory working memory (Kumar et al., 2016). Given the theoretical relevance of this area, its absence may constitute an interpretive “missing link,” especially in the context of the PLV functional connectivity analyses. Furthermore, while it may be tempting to speculate about the seemingly conspicuous absence of inferior temporal clusters in non-users across both studies, the most parsimonious explanation for this is that the independent components (ICs) that contained information from these regions were contaminated with noise and subsequently pruned from the data set, which unluckily, happened to occur more commonly in the non-users. Finally, although it is encouraging that the ROIs identified in this study generally correspond to known working-memory-related regions reported in the literature, because of inherent limitations in the spatial specificity of EEG source localization the precise location of these sources

cannot be known with absolute certainty using these methods, and are at most a best (albeit informed) guess.

#### *ERP Waveforms Localized to Brain Regions*

Although the relative positive and negative deflections of source-localized component ERP waveforms have not been well characterized, informative patterns amongst these waveforms were observed in the present study. However, it should be emphasized that inferring cognitive processes from localized brain activity is inherently problematic (i.e. reverse inference; Poldrack, 2006), so at best, any such attributions in the following sections should be considered as speculative hypotheses for future research.

The ROI ERPs in the frequency match 1-back condition showed a pattern of increased activity in several regions possibly pertaining to non-verbal auditory memory processes (RSTG), executive control (PFC), and an area known to be a generator of the P3b (PCC) related to stimulus categorization (Wronka, Kaiser & Coenen, 2012). In addition, there was also increased activity in the superior frontal cortex (SFG) also implicated in lesion studies of working memory (du Boisgueheneuc et al., 2006). These ROI ERPs are largely consistent with increased amplitudes seen for CU in the P3b channel ERPs in this condition.

A different pattern emerged in the 2-back condition, where the CU showed activation in the LTPJ and SPL, perhaps suggesting that in order to maintain accurate performance they required recruitment of different brain areas to accomplish this more difficult task.

The SPL in particular is another known generator of the P300 (Wronka, Kaiser &

Coenen, 2012), that may contribute to the manipulation of items in working memory (Koenigs, Barbey, Postle & Grafman, 2009). It is particularly interesting that under higher memory load the SPL activity appeared to distinguish CU from NU, whereas this region showed increased response in NU under low memory load.

In the pattern match condition a different picture emerged, suggesting that different brain regions are responsible for performance and possible P300 amplitude generation in this task. In common with the 1-back task, CU showed increased superior frontal activation in addition to right parietal temporal activation. The RTPJ is involved in attention networks related to P300 generation, but the apparent lack of difference in other prominent P300 generating regions, such as the PCC and SPL, might suggest that other processes are at play, and hint at why CU had better behavioural performance in the absence of greater P300 amplitudes. Interestingly, later in the window, there appeared to be a differences in LSTG activity, and as will be discussed later, NU tended to show overall more left temporal connectivity (versus right in CU), which may imply a verbal encoding strategy in NU, though this is purely speculative, as the present study did not manipulate encoding strategies. Future research might test this by contrasting different encoding strategies.

Under high memory load, in the pattern match 2-back condition, a different arrangement of activations emerged versus the low memory load condition. CU had increased right temporal, left superior frontal (similar to 1-back condition), and bilateral precentral activity. Since these areas are unlikely to be generators of the P3b, these differences may relate to other processes that come online during high memory load demand, perhaps

reflecting increased cognitive resources necessary to maintain multiple items in working memory. These activations may also hint at why no P3b differences are observed at the channel level, despite improved performance, though additional research is necessary to better understand what processes these areas support.

### *The Case of the Missing ERSPs*

The intended goal of the ERSP analysis was to provide a more nuanced picture of the underlying oscillatory activity that is typically lost to signal averaging. In line with numerous other studies, we expected to see increased frontal theta, increased gamma, and decreased alpha under increased memory load (Cooper, Wong, McKewen, Michie & Karayanidis, 2017; Hsieh & Ranganath, 2014; Roux & Uhlhaas, 2014). We also expected these differences to be less pronounced in cannabis users; however, this hypothesis was based on the assumption of worse memory performance in cannabis users, which was not the case. Nonetheless, in examining the results, it was anticipated that the pattern of oscillatory would accordingly reflect increasing memory load; however, this was not found. For instance, CU displayed decreasing frontal theta-band activity in the ACC with increased memory load in the pattern match condition and non-users showed greater ACC theta-band activity than CU in the 2-back frequency match condition, and a pattern of decreasing LSGF theta with increasing memory load. It would be tempting to interpret these as nuanced differences contributing to performance in this task; however, exploratory analysis examining the average baseline (-250 to 0 ms) log power spectral density power, which is used to compute the ERSPs, revealed systematic differences between groups that distorted the overall findings. For example, in the ACC, there was a

significant load by group interaction suggesting that in both conditions CU showed the expected increased theta power during baseline with increasing memory load, whereas NU did not change across the condition, likely suggesting improved memory maintenance for CU, which is consistent with their better performance. However, this increased baseline theta power for one group but not the other would distort the ERSP results for the P300 range, and likely reflects the unexpected decrease in ACC theta observed for the CU group. In a similar but more complicated manner, for LSFG baseline theta-band activity there was a group by condition by load interaction, where NU showed the expected increase with memory load, whereas CU did not change across conditions, but had greater theta power than NU in all four conditions. Again such a pattern of baseline differences suggests improved memory maintenance for CU, but this was not the primary focus of this research. Furthermore, analysis of the baseline power values may be suitable for this exploratory analysis, but can be quite variable, which is normally compensated for with ERSPs in calculating spectral power change versus baseline.

Many studies of working memory use variations of delayed match to sample or Sternberg tasks (Kaiser, Ripper, Birbaumer & Lutzenberger, 2003; Obleser, Wöstmann, Hellbernd, Wilsch & Maess, 2012; van Dijk, Nieuwenhuis & Jensen, 2010; Tuladhar et al., 2007), which contain a discreet passive baseline before encoding each stimulus, which presumably would not involve an active memory maintenance process and thus would not suffer the same problems of the current study. One alternative approach considered was to compare each memory condition to its respective low-memory-load (i.e. 1-back) baseline (e.g. both 1-back and 2-back frequency match vs the 1-back frequency match

baseline). However, this process is not straightforward in EEGlab and would require a considerable reprocessing of the data. Furthermore, it is not likely to resolve the issue as the baseline in the 1-back condition still involves an active memory process. To this point, a recent paper by Scharinger, Soutschek, Schubert & Gerjets (2017) examined percent change of oscillatory power activity in an *n*-back task averaged over large periods of time covering early (0-1000 ms) and late (1000-2000 ms) activity after the target stimulus. They observed similar reductions in theta (along with unexpected decreased gamma and increased alpha) power over the early time period, but also observed the expected changes over the late (presumably related to maintenance activity) period. The authors of that study largely disregarded the seemingly contradictory findings in the early period. In that study, the researchers compared all memory load conditions with a 1-back condition, so there is reason to believe that such an approach would not resolve the issue faced in the present study, since the P300 falls well within 1000ms. Other researchers have circumvented this issue by using a passive recording period as baseline, though in this case oscillatory activity was examined over the whole working memory block (~30 s), which would not be useful for understanding the dynamic brain processes associated with the P300 in working memory (Brookes et al., 2011). Future iterations of the present task would be best served by including a no-memory-load 0-back condition (Palomäki, Kivikangas, Alafuzoff, Hakala & Krause, 2012; Watter, Geffen & Geffen, 2001). This was considered in the initial design process, but unfortunately was not included for practical reasons as the current EEG portion of the experiment ran well over an hour and would have required one of the tasks to be omitted.

### *Theta Band Network Connectivity Reveals Different Patterns of Connectivity*

The results of the theta-band PLV functional brain network connectivity provided support for the notion that both NU and CU recruited nodes within frontal-temporal-parietal networks to perform both working memory tasks. This is largely consistent with what was expected based upon other research showing similar patterns of connectivity reflecting a dynamic interplay between sensory, attention and executive control processes (Kaiser, 2015). However, group comparisons differed from expectation primarily due to the fact that cannabis users unexpectedly outperformed non-users, which in turn necessitates a shift in focus in interpreting the PLV results from a perspective of what has gone wrong in the dynamic brain activity of cannabis users to a post-hoc analysis of trying to understand how it is that the brain connectivity of these particular cannabis users led to better performance in both tasks, yet only larger P3b amplitudes in the frequency match condition. As was discussed in previous sections, inferring cognitive processes from patterns of brain activity (i.e. reverse inference) is inherently problematic, so these speculative explanations should be interpreted with caution and are primarily intended to generate hypotheses, which might be tested in future studies.

In the frequency match condition, under low memory load, it was quite apparent that NU was recruiting a more distributed network of brain connectivity. If one were to view the 1-back connectivity in Figure 4.5, and had to guess which group had better performance on this task without knowing that one of the groups was a sample of cannabis users, it would be tempting to infer that the group with greater theta connectivity was performing better. However, if one were told there were no behavioural differences and had to guess

which belonged to cannabis users, previous research might lead one to conclude that the figures showing greater connectivity belonged to the cannabis users and that this indicated inefficient processing reflecting greater cognitive effort required to perform the same task (Bossong, Jager, Bhattacharyya & Allen, 2014). However, knowing that NU performed more poorly than CU requires a different interpretation.

One apparent difference is that the non-users show greater connectivity of the left superior temporal area with the anterior and posterior cingulate areas followed by a highly connected left premotor area with anterior cingulate, right superior temporal, and right temporal-parietal areas along with connectivity between the prefrontal and superior frontal areas. A highly speculative explanation (and a somewhat weak one due to reverse inference) is that this pattern of connectivity is consistent with a verbal encoding strategy and/or retrieval of information from a phonological memory loop (Grimault et al., 2014; Rogalsky, Pitz, Hillis & Hickok, 2008; van Dijk, Nieuwenhuis & Jensen, 2010). Under higher memory load the NU shows a lesser degree of left superior temporal connectivity and the emergence of right fronto-temporal and temporo-parietal connectivity, possibly reflecting a breakdown of the verbal encoding strategy, due to the higher demand on working memory resources.

In contrast, the CU group displayed a much simpler pattern of connectivity between posterior temporo-parietal and superior parietal, posterior cingulate and prefrontal, and right fronto-temporal areas, which might imply (though again speculative) they are utilizing an auditory-sensory encoding strategy rather than a more deliberate verbal

encoding strategy (Pasternak & Greenlee, 2005). The connectivity between the posterior cingulate and prefrontal cortex may reflect dorsal attentional processes. This might further support the idea that in this working memory task cannabis users are making rapid categorizations based on sensory features and may explain why they are showing larger P300 responses at the channel level. In the 2-back condition, CU did not show a major reduction in overall connectivity, as did NU, which may again suggest that they are utilizing a similar sensory-based memory strategy to the 1-back condition. Further supporting this, CU displayed more connections between right temporal and prefrontal/anterior cingulate areas along with prefrontal and anterior cingulate connectivity along with connectivity of the temporo-parietal areas with anterior cingulate and right premotor areas, which may relate to stimulus-driven attentional processing in the VAN (Kim, 2014; Justen & Hebert, 2018). Future research might test these ideas through manipulation of verbal and sensory encoding strategies.

Another, and more difficult to interpret difference in the pattern of functional connectivity between groups, is the greater number of connections suggesting desynchronization versus baseline in CU and the apparent absence of these in NU. It is important to note that PLVs by definition cannot be negative, but the relative phase synchrony between regions during a time window might be significantly less than that in the baseline period. The observed decreases in functional connectivity are a product of subtracting the mean baseline PLV value within each narrow frequency band for each subject and condition. This step is necessary, as unadjusted PLVs result in an overabundance of connectivity in the theta band (as would be expected in a functioning

brain engaged in an active task) that renders the group differences less interpretable. One interpretation of the apparent desynchronization is that this reflects an active inhibition of areas that may interfere with pitch processing. The CU groups appears to show some degree of left temporal deactivation in both memory load conditions, which is consistent with another study that found a relationship between increased alpha activity (related to active inhibition) and decreased left temporal lobe activity while participants were engaged in a pitch memory task (van Dijk, Nieuwenhuis & Jensen, 2010). Unfortunately, this cannot be confirmed in the present study since the ERSPs were not interpretable. In the 1-back condition, CU also appeared to show desynchronization versus baseline, between right temporal and anterior cingulate and temporal-parietal regions while the dorsal network were active, and shortly following this, CU appeared to show decreased dorsal activity while right temporal lobe connections were active, which might reflect a dynamic activation and deactivation of networks responsible for processes necessary for retrieval, matching and updating of auditory working memory. However, a potential problem with interpreting these apparent deactivations as active inhibition is that they could possibly be artefacts of strong connections during memory maintenance (i.e. during the baseline); this issue will be addressed further in context of limitations. Future studies using this paradigm might also investigate alpha connectivity to see if there is an interplay between alpha and theta bands reflecting dynamic inhibition processes.

In the pattern match condition, NU again displayed a much more distributed pattern of connectivity, but this time involving bilateral fronto-temporal and temporo-parietal along with right temporal-premotor connectivity that was greater than that of CU. Again, this

may be consistent with an inefficient verbal encoding strategy in addition to right-lateralized processing related to auditory pattern encoding (Grimault et al., 2014; Rogalsky, Pitz, Hillis & Hickok, 2008; van Dijk, Nieuwenhuis & Jensen, 2010), though these speculations will have to be tested with more rigorously controlled experiments. In the 2-back condition there again appeared to be a decline in overall connectivity consistent with a decline in performance.

In contrast, CU only appears to show fronto-temporal and limited connectivity between left parietal and superior parietal areas. This may again suggest a more sensory based processing, but the overall low level of connectivity does not provide many clues as to why CU is performing better than NU, though the apparent absence of dorsal and ventral attention network activity is consistent with the absence of P300 group differences in this condition. Possible explanations for the apparent lack of connectivity in this task might be that the CU group is recruiting brain regions that were excluded from the analysis (i.e. inferior frontal gyrus and medial frontal gyrus) because there were too few NU to warrant further analysis. Another possibility is that significant activations are being washed out by stronger activations during the maintenance/baseline period. Interestingly, in the 2-back condition the CU group appeared to show greater left fronto-temporal and left parietal-frontal connectivity which is a seemingly altogether different pattern of connectivity. An explanation for this altered pattern of connectivity would require additional experimentation, though one possibility (for future research) is that under high memory load the CU group compensated by utilizing a verbal encoding strategy. This is an interesting (albeit speculative) prospect because it would imply that the apparent CU

reliance on a sensory encoding strategy in other conditions is both efficient and flexible and not a consequence of being unable to recruit top-down resources necessary to utilize a higher level verbal encoding strategy. Future research could examine this by introducing task manipulations that contrasted conditions that emphasized verbal encoding strategies versus those where verbal encoding is inhibited.

Based on the above findings it is clear that the cannabis users show different patterns of connectivity, which we speculate might mean that cannabis users engaged in a flexible sensory encoding strategy that is advantageous when memorizing pitch; however, it is not immediately clear as to how the cannabis users outperformed non-users on the pattern match task. Other research has supported the idea that cannabis users might have altered functional connectivity and may employ different cognitive strategies to perform comparably to non-users (Bossong, Jager, Bhattacharyya & Allen, 2014); however, this is often interpreted as a compensatory strategy that requires greater cognitive effort, which does not appear to be the case in this study. The ROI ERPs hinted at increased frontal and bilateral premotor activity but this hardly explains these data. We also speculated that cannabis users may have adopted verbal encoding strategy under high memory load in the pattern match condition, but if this were contributing to their performance then why would non-users not show comparable performance? Future research might look at the maintenance period connectivity and other frequency bands to see if there is some pattern of dynamic activity at play that could explain these results. Furthermore, if these heavy cannabis users are employing a sensory encoding strategy, or even if this happens not to be the case, how is it they are performing better on a working memory task that involves

encoding of subtle auditory features in light of the body of literature that suggests early sensory processing deficits (i.e P50 gating and MMN) (Broyd et al., 2016; Greenwood et al., 2014; O'Donnell & Mackie, 2014; Rentzsch, Buntebart, Stadelmeier, Gallinat & Jockers-Scherübl, 2011). Given that significant differences were not found in mismatch negativity in a similar sample (see Chapter 3) or in a combined sample that included these participants (see chapter 5) it is possible that apparent deficits in early sensory processes are not generalizable to all heavy cannabis users but reflect more nuanced deficits in particular subsets of heavy cannabis users. Or it could imply that not all sensory memory processes are negatively affected by cannabis use, and that perhaps some are enhanced at least under particular circumstances, though much larger more controlled studies would be necessary to probe such questions.

### ***Limitations***

This study was run concurrently with the study described in Chapter 3, with identical recruitment procedures (albeit with different participants in each study) and a nearly identical design and with only significant difference being the experimental task. As such, the majority of the limitations mentioned for that study also apply to this one, so these won't be repeated here (see Chapter 3 limitations). It is worth repeating, however, that this study had a relatively small sample size, so there is a chance that the improved performance in CU working memory could be the result of random sampling error; replication of these results using a larger sample is necessary to rule out this possibility. While the groups did not show any significant differences on the limited number of self-report or neuropsychological tests administered, it is possible that the tests did not capture some other third variable that accounts for these results. Due to time constraints only a

single neuropsychological test (LNS) of working memory was administered. Future research might administer a more comprehensive memory battery (i.e., WMS-IV) to determine if there are any other facets of working memory, or another memory domain that may account for these results.

This study was uniquely limited by some aspects of the task design. The absence of a 0-back condition rendered the ERSPs uninterpretable due to the active nature of the baseline. Unfortunately, including a 0-back task would have led to the exclusion of one of the conditions, due to time constraints. It is plausible that the active baseline may have also impacted the PLVs, though it would not have affected them to the same degree as the calculation of the ERSP. The ERSP baseline adjustment is not equivalent to the baseline adjustment that was performed on the PLVs, as the PLV adjustment is computed after the trials are averaged, whereas the ERSP baseline would be calculated on each single trial. Furthermore, localized oscillatory activity and long-range connectivity within a particular frequency band are not necessarily related as functional dissociations have been reported (Doesburg, Green, McDonald & Ward, 2009). Even if there were an impact of the active baseline on the PLV analysis, this would have likely masked some connections (more likely in the CU group) though the overall pattern of results would likely still hold. The active baseline would not have impacted the channel or ROI ERP results (again because of how they are computed) in the same manner, so given that the PLVs were largely consistent with the ERPs and behavioural data (unlike the ERSPs that showed the opposite pattern), it seems unlikely that PLVs would have been drastically impacted. Unfortunately, the absence of a neutral baseline also makes it difficult to

examine the functional connectivity within the baseline of the 1-back and 2-back conditions, so the results described here cannot speak to maintenance period activity that might be contributing to the behavioural findings, and limits the interpretation of the apparent deactivations primarily observed in CU. Inclusion of a 0-back condition in future studies and examining other frequency bands would allow for stronger conclusions about whether there is dynamic synchronization and desynchronization at work, or if CU is merely better at maintaining auditory information in working memory.

## **Conclusion**

In summary, this study unexpectedly found that cannabis users outperformed non-users in a working memory task that had participants attend to basic features such as the pitch or pattern of auditory stimuli. These differences were not attributable to overall cognitive capacity as groups were similar in this regard. In addition, cannabis users showed larger channel P300 amplitudes when memorizing pitch, which were consistent with their behavioural performance. Furthermore, the ERPs localized to relevant brain regions and the overall pattern of functional brain connectivity in the theta band showed that cannabis users had different patterns of brain activity. We speculated that cannabis users may have engaged in a sensory encoding strategy whereas non-users engaged in a verbal encoding strategy, which is presumably less efficient, though further research is necessary to confirm this. This study also found that cannabis users outperformed non-users when memorizing the pattern of auditory runs, but in this case performance was not reflected in P300 differences between the groups, even though the ERPs displayed the expected attenuation under increased memory load. The analysis of underlying brain processes did not unequivocally explain why cannabis users might be outperforming non-users. Under

low memory load the localized ERPs and functional theta connectivity showed similar differences in brain connectivity between cannabis users and non-users as was seen in the frequency match task. However, under high memory load the cannabis users appeared to show a switch in network connectivity that was more similar to what was seen in non-users in other conditions. We speculated that this might reflect a switch to a verbal encoding strategy, suggesting that cannabis users may strategically employ sensory encoding in a deliberate and flexible manner, though this again would require additional experimental verification. Clearly more research needs to be conducted to reconcile reports of apparent aberrations in early sensory processing in heavy cannabis users and the apparent superior auditory working memory observed in the present study.

## **Chapter 5: Consolidated Local MMN Analysis**

### **Introduction**

In this chapter we combined data from the previous two chapters to allow for an examination of any local MMN (see Chapter 2) differences between cannabis users and non-users. We specifically examined the local MMN, based upon the difference between ERPs to the final tones of change runs and of flat runs, collapsing across tasks, because we hypothesized that these ERP responses to local deviations within stimuli ought to be invariant to task demands (cf. Bekinschtein, et al., 2009). To this point, in Chapter 2, we examined the local MMN and found that it closely corresponded to the MMNs derived in the feature absent condition, which had smaller amplitudes and shorter latencies compared to the feature present MMN, and which likely reflected automatic brain processes indexing intra-stimulus prediction error (i.e., the 5<sup>th</sup> tone in change runs violates the prediction that the 5<sup>th</sup> tone will have an identical pitch to the preceding four tones).

In Chapter 3, no significant differences in MMN amplitude or latency were observed between cannabis users (CU) and non-users (NU), in either the feature present or feature absent conditions. This finding was consistent with other who found no differences in cannabis users (Impey, El-Marj, Parks, Choueiry, Fisher, & Knott, 2015), but inconsistent with previous research that found reduced MMNs to frequency deviants (Greenwood et al., 2014; Rentzsch et al., 2007; Rentzsch, Buntebart, Stadelmeier, Gallinat, & Jockers-Scherübl, 2011; Roser et al., 2010). A major limitation with the study in Chapter 3 was small sample size. Furthermore, since the task was not a simple MMN task, it is possible

that the MMN elicited was smaller and constituted a weaker effect, which would be consistent with other research that has found smaller MMN effect sizes in tasks that use complex stimuli, at least in clinical samples (Avissar et al., 2018). As will be discussed, the assumption that there would be no significant difference in local MMNs across two very different tasks (albeit with identical stimuli) held true, so this study allowed us to draw stronger conclusions about the effects of heavy cannabis use on the MMN to complex auditory stimuli, as amalgamating data across all participants described in Chapters 3 and 4 constituted a larger, more powerful sample. Combining data across both samples also allowed a more powerful comparison of group differences on the various neuropsychological tests and self-report measures introduced in Chapters 3 and 4, and allowed us to examine whether individual differences in the MMN were related to these scores.

## **Method**

### ***Participants***

We were interested in assessing differences between heavy current users (CU) and current non-users (NU). As participants included in the present study represented a combination of those already described in Chapters 3 and 4, recruitment procedures and inclusion and exclusion criteria were identical to those described in Chapter 3. Data were included for heavy cannabis users and non-users (as described in Methods of Chapter 3 and 4) who completed the experimental tasks and did not exhibit any previously described recording abnormalities. Since we examined local MMN responses that are

independent of task demands and behavioural performance, no participants were excluded because of poor behavioural performance.

Of the 68 participants recruited to participate in both studies, 10 participants were excluded from the analysis. Five cannabis users were excluded because at the time of testing they reported fewer than 10 instances of cannabis use over the past 30 days; one of these individuals also reported a history of a learning disability, which was not reported during the screening process. Two non-users were excluded because they reported cannabis use over the past six months. Finally, two individuals withdrew from the study and one individual was excluded because of technical problems with the EEG recording and they did not complete any questionnaires due to time constraints. A total of 58 participants (NU = 31 and CU = 27) were included in the self-report and neuropsychological data analysis for this study. As one individual in the CU group opted out of the EEG recording but completed all other measures, so a total of 57 participants (NU = 31 and CU = 26) were included in the EEG analysis.

### ***Self-Report and Neuropsychological Measures***

Because we combined datasets of Chapters 3 and 4, the specific measures will not be described here in detail (see Chapter 3 Method section). Briefly, participants were administered the WAIS-III Vocabulary (VC), WAIS-III Matrix Reasoning (MR), WAIS-III Letter Number Sequencing (LNS), Continuous Performance Task – Identical Pairs (CPT-IP). As described in Chapter 3, the VC and MR scores were combined with

demographic variables to form an estimate of full scale IQ (OPIE-3; Schoenberg, Duff, Scott & Adams, 2003). Self-Report measures included the Symptoms Checklist-90 (SCL-90; General Symptom Index, Somatic, OCD, Interpersonal Sensitivity, Depression, Anxiety, Hostility, Phobia, Paranoia, and Psychotic Experiences), Schizotypal Personality Questionnaire – Brief Version (SPQ-B; Total, Cognitive Perceptual, Interpersonal, and Disorganized), and the Sensory Gating Inventory (SGI; Total, Perceptual Modulation, Distractibility, Over, Inclusiveness, and Fatigue Stress Vulnerability).

### ***Experimental Procedures***

#### *EEG Acquisition*

The methods for recording EEG were identical to those used in Chapters 3 and 4 (see Chapter 3 Method section).

#### *Experimental Tasks*

The experimental tasks are described in Chapters 3 and 4, so will not be described in detail here. These were the auditory roving dual-oddball task (Chapter 3) and the *n*-back task (Chapter 4). The tasks were different, but the change and flat runs used as stimuli for each were identical. The local MMN is believed to be generated by the final tone in the auditory change runs, so task performance and task demands should be irrelevant (Bekinschtein, et al., 2009; also see Chapter 2). Behavioural data are irrelevant to this study because the MMNs were calculated over all auditory runs ignoring whether a stimulus is a target or non-target and whether it was responded to or not.

### *Event-Related Potentials (ERPs)*

Local MMNs were calculated in manner identical to that described in Chapter 2. Local MMNs were measured at fronto-central channels (Fz, FCz, and Cz) and characterized as difference waves (deviant – standard) between an ERP response to all changing runs and that to all flat runs regardless of response (i.e. change – flat) across all 58 participants.

This amounted to roughly 500 to 600 change runs and 500 to 600 flat runs per participant. The peak MMN amplitude and latency were defined as the largest negative deflection, and its latency, within an extraction window of 700ms to 850ms (100 to 250ms after onset of the 5<sup>th</sup> tone in each stimulus run). A local peak selection method of 5 time points (10 ms to each side of the peak) was used to account for local fluctuations that may bias peak selection.

### **Results**

Table 5.1 displays the demographics and substance use characteristics of the combined sample. The combined NU (M = 22.74, SD = 3.53) and CU (M = 22.07, SD = 3.80) groups did not significantly differ in age. There were more males than females in the CU (33.3% female) group and more females than males in the NU (54.8% female) group, though these did not differ significantly. Groups were mostly right-handed (NU = 93.5%; CU = 85.2%) and not differ significantly on this factor. NU (M = 15.10 SD = 2.02) and CU (M = 14.41 SD = 1.99) did not differ significantly in terms of years of education. Also, mean years of parental education did not differ significantly for NU (M = 15.32, SD = 2.42) or CU (M = 15.92, SD = 2.41) between groups.

Heavy cannabis users reported an average of 41.37 (SD=40.58) instances of cannabis use over the past 30 days and an average of 9.37 (SD = 9.72) instances over the past 7 days. At the time of testing, cannabis users reported that an average of 1.08 (SD = 0.77) days had elapsed since last using cannabis. The mean age of first cannabis use amongst users was 15.85 (SD = 1.89) years.

Amongst the non-users, 80.6% reported that they had never used cannabis. Amongst the six current non-users with a history of cannabis use, an estimated average of 492.0 (SD =205.6) days had elapsed since they last used cannabis. The mean age of first cannabis use amongst the non-users with a history of cannabis use was 17.50 (SD = 4.14) years.

In addition to cannabis use, participants were asked to self-report whether they considered themselves current users of any other recreational substances (including caffeine, nicotine and alcohol). Participant responses were grouped into seven substance categories: caffeine (e.g. coffee, tea, soda & energy drinks) nicotine, alcohol, stimulants (e.g. cocaine and amphetamine), hallucinogens (e.g. MDMA, LSD, psilocybin & designer research chemicals), opioids (e.g. morphine, heroin, OxyContin etc.), sedatives (e.g. benzodiazepines), and other (i.e. dissociative drugs such as PCP or ketamine, or inhalants etc.). A greater proportion of participants in the CU group reported current nicotine and hallucinogen use. There was a marginally greater proportion of current alcohol and stimulant users amongst CU participants. There were no current opioid or sedative users in either group and no participants in either group reported current use of other categories of recreational substances.

Unlike for cannabis use, participants were only asked to quantify frequency of use of other substances based upon five broad categories (1 = Once or twice ever; 2 = A few times a year; 3 = A few times per month; 4 = More than once each week; 5 = Daily). Frequency comparisons were only made for alcohol and caffeine use, given that there was a substantial proportion of current alcohol and current caffeine users in each group. The self-reported frequency amongst current alcohol users in the CU group ( $M = 3.30$ ;  $SD = 0.64$ ) was significantly larger than the NU group ( $M = 2.70$ ;  $SD = 0.87$ ),  $t(41) = -2.64$ ,  $p = .012$ ,  $M_{diff} = -0.61$ ,  $SE = 0.23$ ,  $95\% CI = [-1.07 \text{ to } -0.14]$ ). The self-reported frequency of caffeine use did not differ significantly between the CU ( $M = 4.25$ ;  $SD = 0.86$ ) and NU ( $M = 3.83$ ;  $SD = 0.72$ ) groups. The CU participants who reported current stimulant or hallucinogen use indicated infrequent use of only a few times each year or less, thus these participants were not examined more closely to determine if substance use was confounded with any of the measures discussed in this chapter. Most of those who reported current nicotine use, reported using daily or several times a week, though too few participants in the NU group reported current nicotine use to make meaningful group comparisons. Because a large proportion of the CU group reported frequent nicotine use, however, and there is evidence that nicotine may impact the MMN, the effect of nicotine use will be examined further in subsequent sections (Dunbar et al., 2007).

Table 5.1 Percentage of CU and NU Groups Reporting Current Non-Cannabis Substance Use

NU (n = 31)		CU (n = 27)		$\chi^2$	$p$ -value
%		%			

Caffeine	38.7	59.3	2.441	.118
Nicotine	6.5	40.7	9.757	.002
Alcohol	64.5	85.2	3.215	.073
Stimulants	0	11.1	3.632	.057
Hallucinogens	3.2	29.6	7.674	.006
Opioids	0	0	n/a	n/a
Sedatives	0	0	n/a	n/a
Other	0	0	n/a	n/a

Table 5.1. Percentages of participants who reported being a current user of non-cannabis recreational substances. *p*-values were determined using chi-squared analysis of proportion of participants in each group who reported being a current user of a substance within each respective class.

### *Neuropsychological Measures*

Table 5.2 displays the descriptive statistics of neuropsychological measures for cannabis users and non-users. Independent sample t-tests revealed no significant differences between NU and CU in estimated IQ, vocabulary, matrix reasoning, or the CPT-IP.

Table 5.2 Descriptive Statistics of Neuropsychological Measures for Cannabis Users and Non-Users

	NU (n = 31)	CU (n = 27)	
	M (SD)	M (SD)	<i>p</i> -value
Estimated IQ <sup>a</sup>	110.65 (5.70)	110.40 (6.63)	.875
Vocabulary <sup>b</sup>	53.90 (7.12)	54.15 (7.95)	.902
Matrix Reasoning <sup>b</sup>	21.06 (3.08)	21.04 (2.86)	.972
Letter Number Sequencing <sup>b</sup>	14.65 (3.25)	13.59 (2.81)	.195
<u>Continuous Performance Task<sup>c</sup></u>			
2-digit	3.92 (0.40)	3.91 (0.42)	.894

3-digit	3.18 (0.73)	3.32 (0.63)	.443
4-digit	1.96 (0.71)	2.02 (0.87)	.767

Table 5.2. Descriptive statistics of neuropsychological tests for non-users (NU) and cannabis users (CU). a) Estimated Full-Scale IQ derived by using OPIE-3 algorithm (see Method section) b) VC, MR, and LNS scores are based upon raw scores derived from each test. c) Scores represent  $d'$  values for each condition generated automatically by the CPT-IP software included in the MATRICS battery. All comparisons were made using independent samples  $t$ -tests ( $df=56$ ).

### ***Self-Report Measures***

Table 5.3 displays the descriptive statistics of the self-report measures for NU and CU.

Independent sample  $t$ -tests revealed that cannabis users had marginally higher scores on the SCL-90 anxiety subscale, but did not differ on the SCL-90 general symptom index, or on the somatic, OCD, interpersonal sensitivity, depression, hostility, phobia, paranoia, or psychotic experience subscales. CU showed a weak trend towards higher scores on the SGI over-inclusiveness subscale, but did not differ on SGI total score, or on the perceptual modulation, distractibility, and fatigue-stress vulnerability subscales. CU had significantly higher scores on the SPQ-B disorganized subscale, but did not differ significantly on SPQ-B total score, or on the cognitive perceptual, or interpersonal subscales.

Table 5.3 Descriptive Statistics of Self-Report Measures for Cannabis Users and Non-Users.

	NU (n = 31)	CU (n = 27)	$p$ -value
	M (SD)	M (SD)	
<u>Symptom Checklist 90</u>			
General Symptom Index	56.45 (44.13)	66.56 (37.14)	.354
Somatic	6.90 (5.95)	8.11 (6.15)	.451
OCD	11.39 (8.30)	11.41 (5.06)	.991

Interpersonal Sensitivity	6.48 (5.36)	7.33 (6.18)	.577
Depression	11.13 (8.71)	12.48 (8.68)	.557
Anxiety	4.45 (4.95)	7.11 (5.83)	.066 <sup>†</sup>
Hostility	2.81 (3.65)	2.85 (2.69)	.958
Phobia	1.35 (2.35)	2.00 (2.62)	.326
Paranoia	2.65 (3.23)	3.85 (3.16)	.157
Psychotic Experience	3.81 (5.47)	4.44 (4.19)	.624
<u>Sensory Gating Inventory</u>			
Total	60.23 (26.69)	65.59 (25.89)	.442
Perceptual Modulation	19.06 (12.15)	21.74 (12.54)	.413
Distractibility	18.06 (8.37)	17.07 (7.05)	.631
Over Inclusiveness	13.42 (5.99)	16.30 (7.58)	.112
Fatigue Stress Vulnerability	9.68 (4.74)	10.48 (4.48)	.511
<u>Schizotypal Personality Questionnaire</u>			
Total	8.19 (5.10)	9.19 (4.56)	.441
Cognitive Perceptual	2.58 (2.06)	3.22 (1.97)	.232
Interpersonal	3.68 (2.43)	2.89 (2.56)	.234
Disorganized	1.94 (2.02)	3.07 (1.39)	.014*

Table 5.3. Descriptive statistics of self-report measures for non-users (NU) and cannabis users (CU). All comparisons were made using independent samples *t*-tests (*df* = 56). SPQ-Disorganized violated the assumption of equality of variance using Levene's test, so *df* was adjusted to 53.3.

### ***Local MMN ERPs***

#### *Local MMN in Non-Users: Dual Oddball vs N-back*

To determine whether MMNs were comparable across the two tasks we first examined MMN amplitudes and latencies for non-users. Separate mixed-measures ANOVAs were run for amplitude and latency with channel (FZ, FCZ & CZ) as a within-subjects factor and task (dual-oddball and *n*-back) as a between subjects factor. Mean amplitudes and latencies for local MMN difference waves for each task for non-users can be found in Table 5.4 and figures showing MMN waveforms can be viewed in Figure 5.1.

For MMN amplitude, there was a main effect of channel. Degrees of freedom for the main effect of channel were corrected due to a violation of sphericity ( $\chi^2(2) = 26.25, p < .001$ ) using a Greenhouse-Geisser correction ( $E = .622, F(1.24, 36.06) = 5.42, p = .019, \eta_p^2 = .158$ ), suggesting larger MMN amplitudes at channel CZ. The main effect of channel was qualified by a channel by task interaction, which became marginal after correcting for the violation of sphericity, ( $F(1.24, 36.06) = 3.65, p = .056, \eta_p^2 = .112$ ). Follow-up analyses revealed significantly larger (more negative) MMN amplitudes at CZ ( $M_{diff} = .292, SE = .115, p = .017, 95\% CI = [0.57 \text{ to } 0.528]$ ) for the *n*-back task compared to the dual-oddball task. There were no significant main effects of task. For MMN latency, there were no main effects of task, channel or channel by task interactions. However, it should be noted that there was a violation of the assumption of equality of covariance, so these results should be interpreted with caution. Given that MMN amplitudes were significantly larger at CZ, but not for FZ or FCZ, we decided to limit subsequent analyses of local MMN response comparing cannabis users to non-users to channels FZ and FCZ. The observed task differences for MMN amplitude at CZ will be addressed in the discussion section.

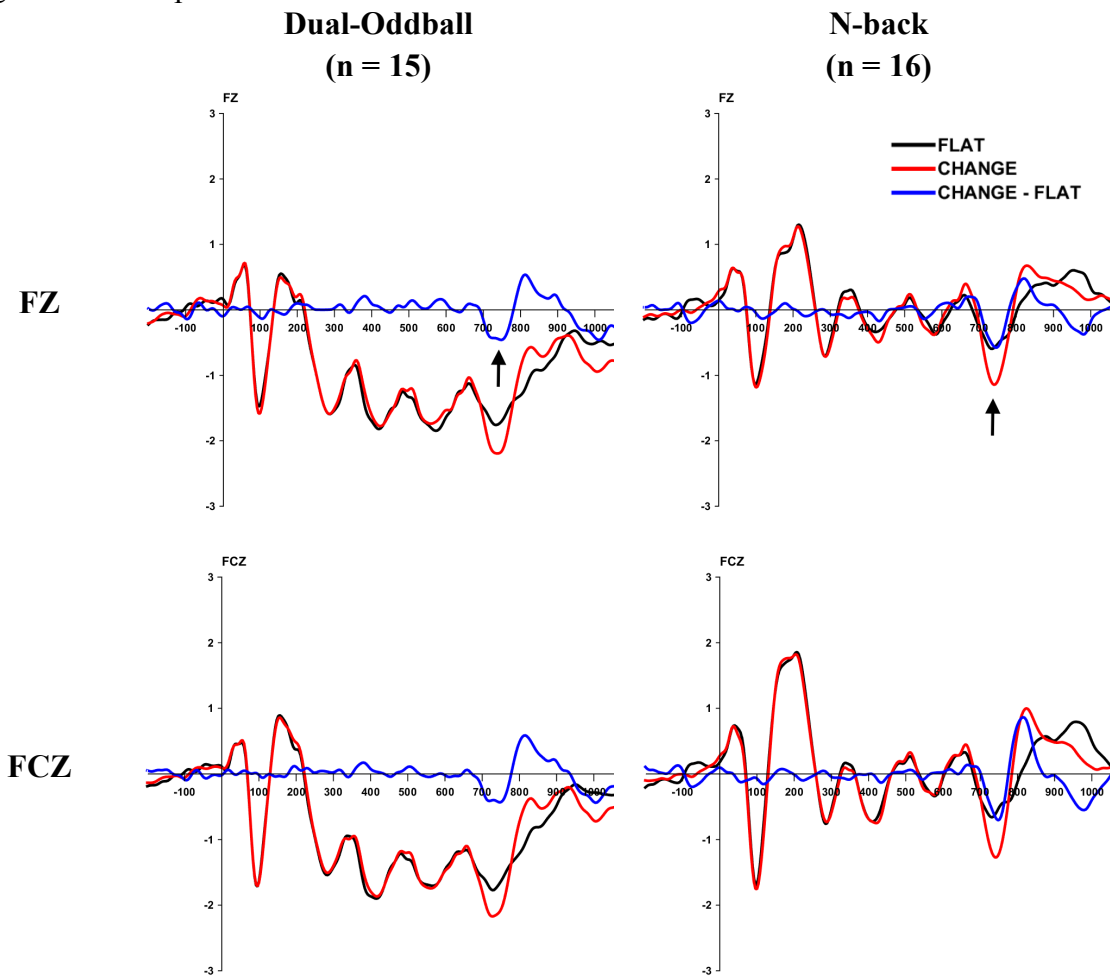
Table 5.4 Comparison of Local MMN Amplitude and Latency Between Tasks in Non-Users.

	Dual Oddball (n=15)	N-back (n=16)	<i>p</i> -value
	M (SD)	M (SD)	
<u>Amplitude (μV)</u>			
FZ	-0.71 (0.44)	-0.73 (0.28)	.883
FCZ	-0.68 (0.43)	-0.87 (0.28)	.150

CZ	-0.47 (0.37)	-0.76 (0.27)	.017*
<u>Latency (ms)</u>			
FZ	742.93 (35.60)	747.00 (30.45)	.734
FCZ	741.07 (25.81)	740.00 (16.91)	.892
CZ	746.93 (33.52)	740.00 (16.07)	.464

Table 5.4. Descriptive statistics of mean amplitudes and latency of MMN difference waves for the dual oddball and *n*-back tasks for non-users. The *p*-values represent the post-hoc pairwise comparisons of ANOVAs that were conducted separately for amplitude and latency. MMN latencies are reported in reference to onset of the first tone, the 150 ms extraction window was from 700 to 850 ms (5<sup>th</sup> tone onset = 600 ms). Note that the assumption of equality of covariance was violated for the latency analysis (but not for amplitude), so the latency results should be interpreted with caution.

Figure 5.1. Comparison of Local MMN ERPs in Non-Users Across Tasks.



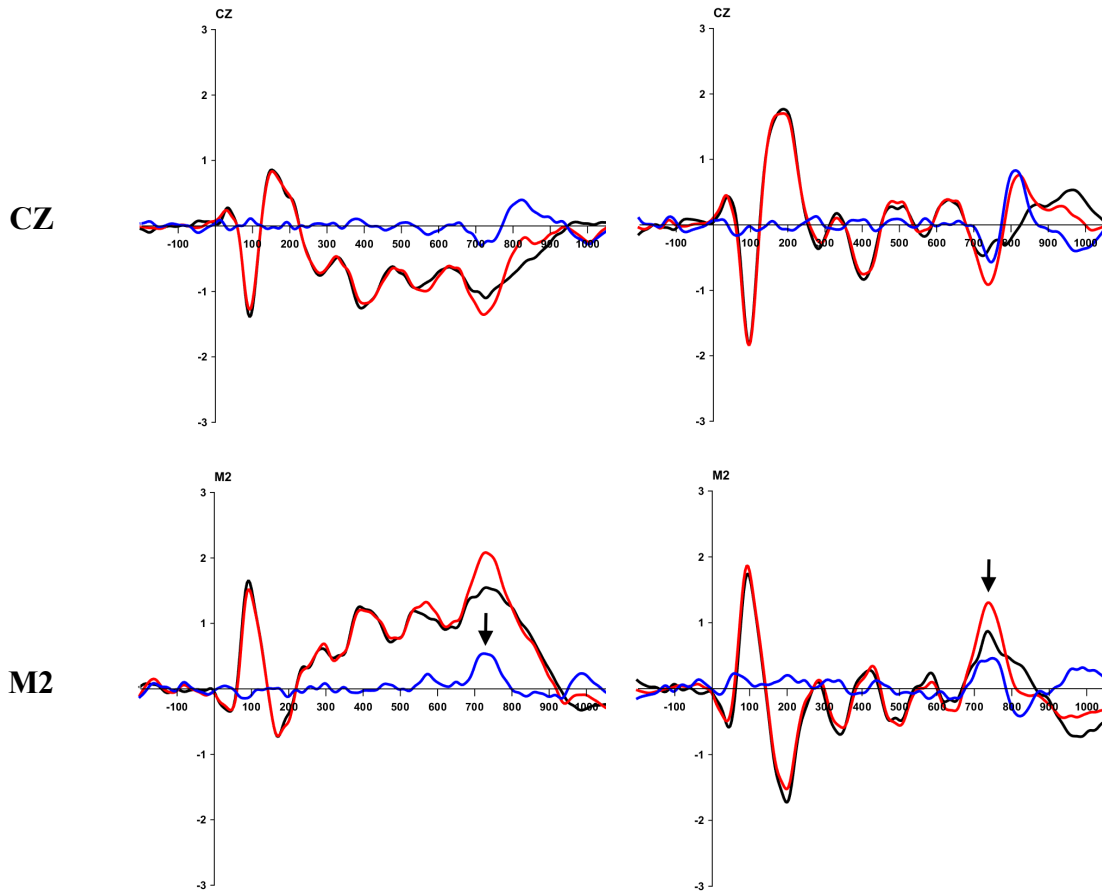


Figure 5.1. Grand average local MMN ERP waves to flat and change stimuli and corresponding difference waves (change-flat) at channels FZ, FCZ, CZ and right mastoid (M2) for non-users (NU) for the dual-oddball and n-back tasks. ERPs were baseline corrected from -200ms to 0ms. Arrows depict the location of the MMN. MMN amplitude was significantly larger in the n-back task at CZ. Clear stimulus processing differences are observable between tasks from 0 to 600ms as evidenced in the dual-oddball task by the initial smaller positive amplitudes to stimulus onset followed by a large negative polarity shift; however, calculation of the difference waves appeared to largely mitigate these task differences. At M2, the MMN reverses polarity, which indicates that the ERP components highlighted at the frontal midline channels are indeed MMNs.

#### *Local MMN: Cannabis Users vs. Non-Users*

Separate mixed-measures ANOVAs were run for amplitude and latency with channel (FZ, FCZ) as a within-subjects factor and user group (NU and CU) as a between-subjects factor to determine whether local MMNs, combined across tasks, differed between the NU and CU groups. For amplitude, the main effects of channel,  $F(1,53) = 1.37, p = .247,$

$\eta_p^2 = .025$ ), and user group,  $F(1,53) = 0.20, p = .654, \eta_p^2 = .004$ ), and the channel by user-group interaction,  $F(1,53) = 0.13, p = .716, \eta_p^2 = .003$ ), were not significant. For latency, the main effects of channel,  $F(1,53) = 0.28, p = .601, \eta_p^2 = .005$ ), and user group,  $F(1,53) = 0.02, p = .476, \eta_p^2 = .010$ ), and the channel by user-group interaction,  $F(1,53) = 0.49, p = .489, \eta_p^2 = .009$ ), were also not significant. Mean amplitudes and latencies for local MMN difference waves for each group can be found in Table 5.5 and figures showing MMN waveforms can be viewed in Figure 5.2.

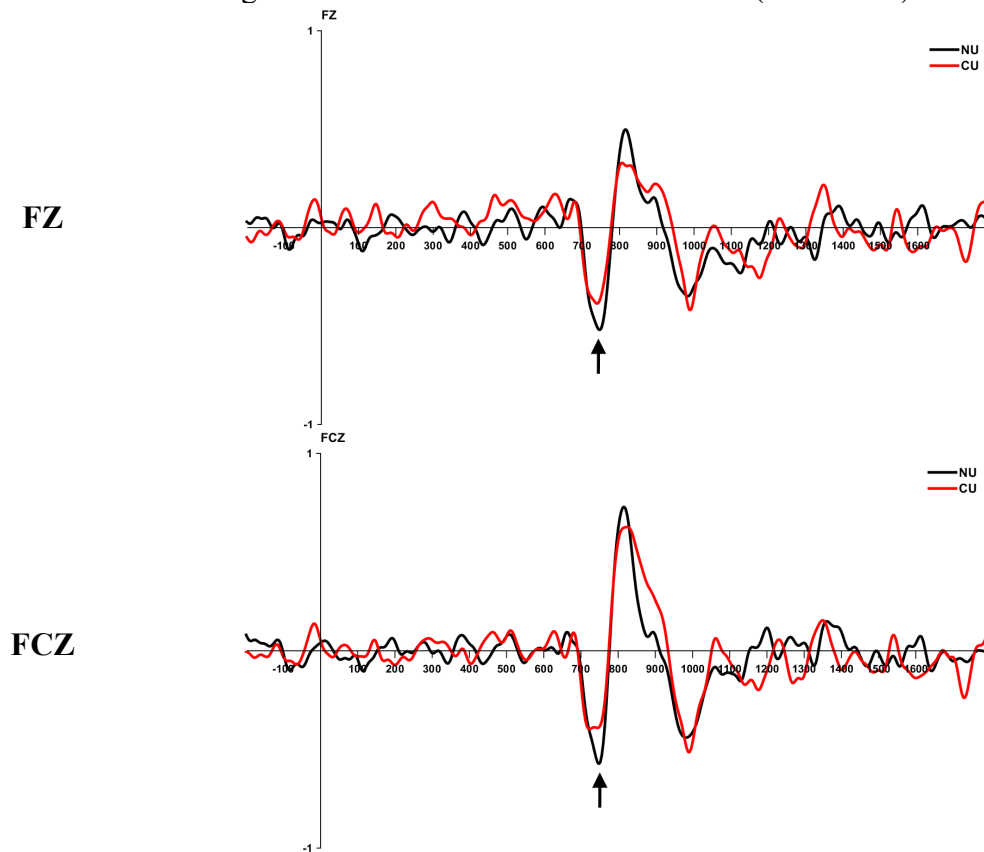
Given the absence of significant group differences using significance testing, we calculated Bayesian likelihood ratios (see equations 3 and 8 in Glover & Dixon, 2004) to investigate whether there is any evidence in support of the null hypothesis model of there being no MMN differences between the groups. For MMN amplitude there was a 6.82 likelihood ratio in favour of the null hypothesis (0.15 for the alternative hypothesis) and for MMN latency the likelihood ratio was 7.55 in favour of the null hypothesis (0.13 in favour of the alternative hypothesis). This will be addressed further in the discussion section.

Table 5.5. Mean Amplitude and Latencies of Local MMN Difference Waves

<b>Measure</b>	<b>NU (n=31) Mean (SD)</b>	<b>CU (n=26) Mean (SD)</b>	<b><i>p</i>-value (2-tail)</b>
Amplitude ( $\mu$ V)			
Fz	-0.72 (.36)	-0.69 (.45)	.743
FCz	-0.78 (.37)	-0.72 (.52)	.589
Latency (ms)			
Fz	745.03 (32.55)	741.69 (29.27)	.688

Table 5.5. Descriptive statistics of mean amplitudes and latency of MMN difference waves for non-users (NU) and cannabis users (CU) at channels Fz and FCz. MMN latencies are reported in reference to onset of the first tone, the 150 ms extraction window was from 700 to 850 ms (5<sup>th</sup> tone onset = 600 ms). The *p*-values represent the post-hoc pairwise comparisons of ANOVAs that were conducted separately for amplitude and latency.

Figure 5.2. Grand Average Local MMN ERP Difference Waves (NU vs CU)



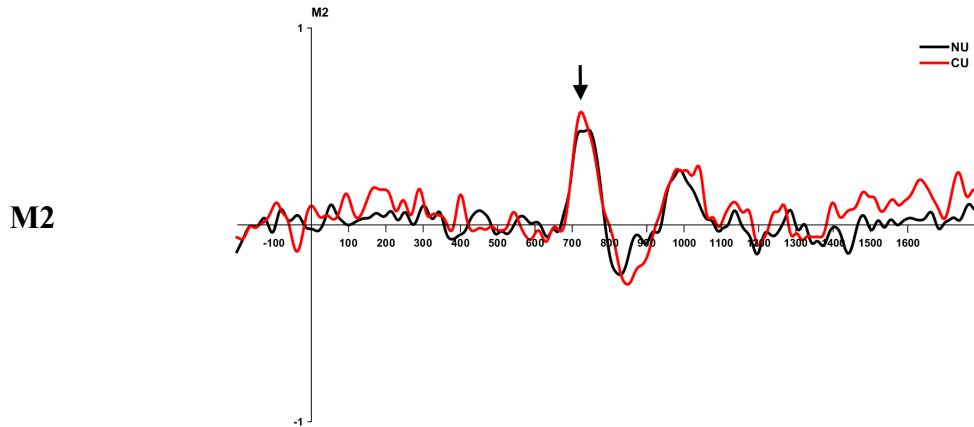


Figure 5.2. Grand average local MMN ERP difference waves at channels FZ, FCZ, and right mastoid (M2) for non-users (NU) and cannabis users (CU) combined across dual-oddball and n-back tasks. ERPs were baseline corrected from -200ms to 0ms. Arrows depict the location of the MMN. No significant differences are observed between user groups in terms of MMN amplitude or latency. At M2, the MMN reverses polarity, which suggests that the ERP components highlighted at the frontal midline channels are indeed MMNs.

Figure 5.3. Local MMN Scalp Topography

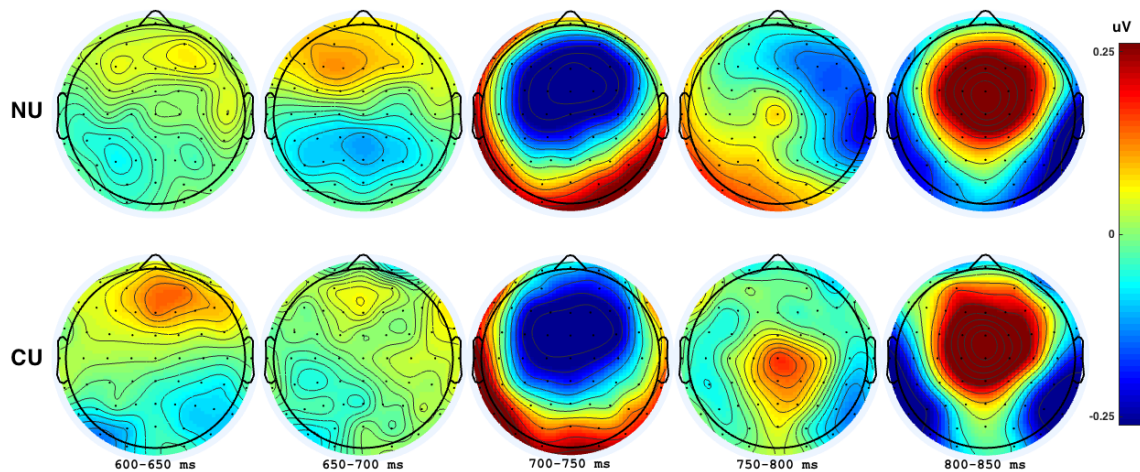


Figure 5.3. Topographic maps of grand average local MMN ERP difference waves for non-users (NU) and cannabis users (CU) combined across dual-oddball and n-back tasks. Each scalp map sequence represents voltage averaged across 50ms intervals commencing at the onset of the 5<sup>th</sup> tone (600ms) and terminating at the end of the MMN extraction window (700 to 850ms). Maps were baseline corrected from -200ms to 0ms. Figure depicts the expected fronto-central scalp distribution of negative voltage deflection from 700-750ms and positive deflection from 800 to 850 corresponding to MMN and subsequent P3a components observed in ERP difference waves at the frontal midline channels.

### ***Correlations Between MMN and Neuropsychological Measures***

Spearman rank correlations were used to explore whether any monotonic relationships exist between the MMN and cognitive performance measures. Spearman's rank correlations were chosen over Pearson correlations to mitigate the effects of outliers and deviations from normality that were observed for some of the measurements taken from this relatively small sample. For ease of interpretation, correlations with MMN amplitude and latency were conducted at channel FZ (See Table 5.5). No significant correlations were observed between local MMN amplitude or latency and any of the neuropsychological measures (Table 5.6), with the exception of a trend towards larger MMN amplitudes (more negative) in individuals who had higher estimated IQ scores.

Table 5.6. Correlations Between Local MMN and Neuropsychological Measures for Combined (NU and CU) Sample (n=57) Across Dual Oddball and *n*-back Tasks

<b>Variables</b>	<b>MMN Amplitude (<math>\mu</math>V)<sup>a</sup></b>	<b>MMN Latency (ms)<sup>a</sup></b>
Estimated IQ <sup>b</sup>	-.23 <sup>†</sup>	-.09
Vocabulary <sup>c</sup>	-.20	.12
Matrix Reasoning <sup>c</sup>	-.12	-.17
Letter Number Sequencing <sup>c</sup>	.03	.08
<u>CPT-2</u> <sup>d</sup>	-.05	-.08
CPT-3 <sup>d</sup>	-.20	-.01
CPT-4 <sup>d</sup>	-.21	-.12

Table 5.6. Spearman rank correlations ( $r_s$ ) between neuropsychological measures and MMN amplitudes and latencies. a) Mismatch negativity amplitude and latencies at channel Fz; b) Estimated Full-Scale IQ derived by using WAIS-III MR and VC scores combined with demographics (age and education level) according to a regression algorithm (OPIE-3); c) VC, MR, and LNS scores are

---

based upon raw scores derived from each test; d) Scores represent d-prime values for 2-digit (2d), 3-digit (3d) and 4-digit (4d) each condition generated automatically by the Continuous Performance Task – Identical Pairs software included in the MATRICS battery. \* < .05; \*\* < .01; \*\*\*<.001 and † represents trend significance < .10.

### ***Correlations Between MMN and Self-Report Measures***

Spearman rank correlations were used to explore whether any monotonic relationships exist between the MMN and self-report measures. For ease of interpretation, correlations with MMN amplitude and latency were conducted at channel FZ. Results of the correlation analysis (see Table 5.7) revealed that individuals who reported fewer psychopathological symptoms (SCL-90 - General Symptom Index) over the past week tended to have larger (more negative) MMN amplitudes and shorter latencies. The scores on the subscales of the SCL-90 tended to not be normally distributed; however, a correlational analysis of select SCL-90 subscales theoretically relevant to the MMN and psychosis (paranoia, psychotic experiences, depression, and anxiety) was conducted. Individuals reporting more paranoia symptoms tended to have shorter MMN latencies. Increased self-report of psychotic experiences was associated with significantly reduced MMN amplitude and a trend toward shorter latencies. Those reporting more depressive symptoms tended to have smaller MMNs, and increased symptoms of anxiety were associated with both smaller MMN amplitudes and shorter latencies. Higher total scores on the SPQ, measuring schizotypal personality traits, tended to be associated with significantly reduced MMN (more positive) amplitudes and a trend towards shorter MMN latencies. Examination of the cognitive perceptual SPQ subscale showed the same overall correlation pattern with MMN amplitude and latency. With the exception of a

trend association between increased interpersonal symptoms of schizotypy and reduced MMN amplitude, there were no other observed associations between the SPQ subscales (i.e. disorganized) and the MMN variables, suggesting that the observed relationship between higher schizotypal scores and smaller MMN amplitudes is most closely associated with the cognitive-perceptual facets of schizotypal traits. SGI scores were not associated with MMN amplitude or latency.

Table 5.7. Correlations Between Local MMN and Self-Report Measures for Combined (NU and CU) Sample (n=57) Across Dual Oddball and *n*-back Tasks

	<b><u>MMN Amplitude (<math>\mu</math>V) <sup>a</sup></u></b>	<b><u>MMN Latency (ms) <sup>a</sup></u></b>
<b><u>Symptom Checklist 90<sup>b</sup></u></b>		
General Symptom Index	.339**	-.347**
Paranoia	.186	-.307*
Psychotic Experiences	.369**	-.257 <sup>†</sup>
Depression	.307*	-.218
Anxiety	.272*	-.335*
<b><u>Sensory Gating Inventory</u></b>		
Total	.109	-.220
Perceptual Modulation	.133	-.201
Distractibility	-.018	-.171
Over Inclusiveness	.208	-.153
Fatigue Stress Vulnerability	.212	-.198
<b><u>Schizotypal Personality Questionnaire</u></b>		
Total	.314*	-.180 <sup>†</sup>
Cognitive Perceptual	.334*	-.243 <sup>†</sup>
Interpersonal	.224 <sup>†</sup>	-.013
Disorganized	.169	-.195

Table 5.x. Spearman rank correlations ( $r_s$ ) between self-report measures and MMN amplitudes and latencies. a) Mismatch negativity amplitude and latencies at channel Fz; b) Only overall related to overall psychopathological symptomology and select subscales theoretically relevant to pathological symptoms pertinent to MMN and psychosis were included here; however, complete correlation tables can be viewed in Appendix D \* < .05; \*\* < .01; \*\*\*<.001 and <sup>†</sup> represents trend significance < .10.

### *Relationship Between MMN and Demographic Variables*

Exploratory analyses were conducted to determine whether any relationships exist between the MMN and other demographic variables and other substance use. As in the previous section, we performed these exploratory analyses at channel FZ for ease of interpretation.

In terms of demographic variables, point-biserial correlations revealed no significant association between sex and MMN amplitude ( $r = -.10, p = .460$ ) or latency ( $r = .01, p = .951$ ). Spearman rank correlations revealed no significant association between education level and MMN amplitude ( $r = .09, p = .522$ ) or latency ( $r = .03, p = .844$ ). Similarly, age was not significantly associated with amplitude ( $r = -.05, p = .711$ ) or latency ( $r = -.108, p = .422$ ).

### *Relationship Between MMN and Cannabis Usage Variables Amongst Cannabis Users*

Amongst current heavy cannabis users, the number of self-reported instances of cannabis use over the past 30 days was significantly associated with shorter MMN latencies at FZ ( $r = -.48, p = .013$ ), but there was no significant association with MMN amplitude ( $r = .23, p = .264$ ). Time since last use did was not significantly associated with MMN amplitude ( $r = -.002, p = .991$ ) or latency ( $r = .03, p = .906$ ). Age of first cannabis use was not significantly associated with either amplitude ( $r = -.06, p = .785$ ) or latency ( $r = .17, p = .419$ ).

### *Relationship Between MMN and Other Substance Use Amongst All Participants*

In terms of substance use variables, point-biserial correlations revealed a significant correlation between caffeine use (split into current caffeine users and non-caffeine users) and MMN amplitude ( $r = .37, p = .004$ ) but not latency ( $r = -.13, p = .349$ ), suggesting that those who identified as caffeine users had smaller MMN amplitudes at FZ.

Amongst caffeine users ( $n = 28$ ), self-reported frequency of use was not associated with either MMN amplitude or latency; however, as detailed caffeine usage information was not collected (unlike cannabis use), caffeine frequency amongst current users fell into three broad categories (few times each month, more than once per week, and daily), so this analysis is insufficient to ascertain any potential dose response relationships between caffeine usage and the MMN.

Current nicotine use was not significantly associated with MMN amplitude ( $r = .13, p = .342$ ) or latency ( $r = -.07, p = .588$ ), though there were a disproportionately small number of nicotine users ( $n = 13$ ) versus non-users ( $n = 44$ ).

Similarly, current alcohol use was not associated with either MMN amplitude or latency; however, this should be interpreted with caution as there was a disproportionately large number of current alcohol users ( $n = 42$ ) versus non-users ( $n = 15$ ). Amongst alcohol users ( $n = 42$ ), frequent use was associated with MMN amplitude ( $r = .34, p = .030$ ), but not latency, suggesting that those who reported more frequent alcohol use had smaller (more positive) MMNs.

## **Discussion**

In this study we combined two participant samples performing different tasks, but with identical stimuli, to examine a local MMN, which is supposed to be invariant to task demands, in cannabis users and non-users. Consistent with our findings in Chapter 3, and other literature (Impey, El-Marj, Parks, Choueiry, Fisher & Knott, 2015), we failed to find attenuated MMNs to pitch deviants that have been reported by others using simple MMN paradigms (Greenwood et al., 2014; Rentzsch et al., 2007; Rentzsch, Buntebart, Stadelmeier, Gallinat, & Jockers-Scherübl, 2011; Roser et al., 2010). Whereas it is not tenable to accept the null hypothesis (of no difference between groups) when using inferential significance tests, the effect sizes of the observed differences between groups was exceptionally small, such that significant differences would likely only emerge if the magnitude of these differences remained consistent over hundreds of participants, which would likely imply that such differences were not meaningful in any tangible way.

Furthermore, the computed Bayesian likelihood ratios, which can provide support for the model representing the null hypothesis (Glover & Dixon, 2004), suggested a substantially greater likelihood of there being no effect of cannabis use on the local MMN in this sample. That being said, it is possible that the absence of a MMN effect in the present study is due to the specific nature of the stimuli used. Future research might administer a variant of these MMN tasks along with a simple MMN task to rule out any task/stimuli specific effects.

Our groups also did not significantly differ in estimated IQ (or the individual verbal and perceptual reasoning subtests), working memory, or sustained attention. Overall, CU

reported significantly higher trait schizotypal disorganized behaviour symptoms, which is consistent with other research, though CU did not differ from NU on total schizotypy scores or on the other subscales as has been reported in the literature (Davis, Compton, Wang, Levin, & Blanco, 2013; Fridberg, Vollmer, O'Donnell, & Skosnik, 2011). Consistent with the literature, across the whole sample, higher total schizotypy and cognitive perceptual subscale scores were associated with reduced MMN amplitudes, but the disorganized symptoms were not associated with the MMN (Baldeweg, Adams & Gruzelier, 1999; Broyd et al., 2016). This suggests that while CU may show some schizotypal-like disorganized traits (e.g. unusual/odd mannerisms and difficulties with communication/idiosyncratic speech), these may not be related to early auditory processing abnormalities.

With the exception of marginally higher anxiety scores, CU did not appear to exhibit significantly greater psychopathological symptoms, though when looking at the entire combined sample, higher scores on measures of psychopathology conceptually related to psychosis were associated with reduced MMN amplitude, which is consistent the broader MMN research that shows reduced MMNs in individuals with psychosis (Todd et al., 2014). In terms of aberrant sensory experiences (SGI), CU showed only marginally larger scores on over-inclusiveness, which weakens any conclusions that can be drawn on the difference observed in Chapter 4 (CU > NU in Chapter 4, but groups did not differ in Chapter 3). Furthermore, CU did not differ on any other dimensions of subjective experiences that are phenomenologically related to sensory gating deficits. Higher scores on the SGI have been associated with ADHD, schizophrenia, and EEG measures of early

auditory sensory gating deficits (i.e., P50) (Micoulaud-Franchi et al., 2015). We could not find any studies that have administered the SGI to cannabis users, though the absence of a relationship is surprising given that cannabis users have been shown to have higher scores on perceptual aberration (correlated with the SGI) and diminished P50 gating (Fridberg, Vollmer, O'Donnell & Skosnik, 2011). No studies were found that examined the relationship between the SGI and MMN. It is noteworthy, however, that the SGI scores did not correlate with the MMN in this sample because others have found associations between diminished MMNs and P50 sensory gating (Gjini, Arfken & Boutros, 2010). Taken together, this pattern of results suggests that the previously observed auditory processing deficits (putatively related to psychosis) in cannabis users may not generalize to all heavy cannabis users. Clearly, more research, utilizing larger samples, is required to resolve these apparent discrepancies in these conceptually related measures and to better understand the nuanced effects of cannabis on early auditory processes.

### ***Correlations Between MMN, Cannabis, and Other Substance Use***

Amongst cannabis users, higher frequency cannabis use over the previous month was associated with shorter MMN latencies. Shorter MMN latencies have been observed in some schizophrenia samples (Kärgel, Sartory, Kariofillis, Wiltfang & Müller, 2014), though the opposite has also been observed (Kathmann, Wagner, Rendtorff, & Engel, 1995). Interestingly, we also found shorter latencies in those who scored higher in overall psychopathological symptoms, paranoia, and anxiety. One study involving a clinical sample found that those exhibiting more positive psychosis symptoms tended to have shorter MMN latencies, which lengthened with clinical improvement. The authors

suggested that shorter latencies might reflect rapid but error-prone early auditory processing (Grzella, et al, 2001). In our sample, cannabis users did not differ from non-users in MMN latency; a possible dose-dependent MMN latency response is an interesting prospect for future research as it would be interesting to determine if MMN latency changes as a function of cannabis-use frequency. However, since anxiety was also associated with shortened latency and cannabis users showed a trend toward greater anxiety, it is not possible in the present study to determine whether cannabis-use frequency, anxiety, a combination of both, or some other factor led to shorter MMN latencies. Future research will have to implement tighter controls on these factors.

Interestingly, while frequent cannabis use did not appear to impact MMN amplitude, alcohol frequency and caffeine use appeared to be associated with attenuated MMN amplitudes. Attenuated MMN amplitudes have been reported in studies of acute and chronic alcohol use (Chitty, Kaur, Lagopoulos, Hickie & Hermens, 2011; Hirvonen, Jääskeläinen, Näätänen & Sillanaukee, 2000; Jääskeläinen et al., 1995). However, the limited number of studies directly comparing the acute effects of caffeine have not found an impact on the MMN (Hirvonen, Jääskeläinen, Näätänen & Sillanaukee, 2000; Rosburg, Marinou, Haueisen, Smesny & Sauer, 2004). The effect of chronic caffeine use on the MMN has not been well established. Nevertheless, the alcohol and caffeine findings of the present study are limited as we did not collect sufficiently detailed information regarding usage of these substance. Furthermore, we did not have enough participants to conduct a rigorous analysis of these substances while simultaneously

controlling for cannabis use. Future studies might enact more rigorous controls of both alcohol and caffeine use.

### ***Limitations***

There were notable limitations to this investigation of the local MMN. First of all, although this study constituted a larger sample and the Bayesian likelihood ratios supported the null hypothesis, the study may still be underpowered if the local MMN constitutes only a weak effect. This issue might be resolved by future studies comparing the local MMN in both passive and active tasks to more standard MMN designs using comparable stimuli within the same participants. Next, it was argued that the local MMN was comparable across the dual-oddball and *n*-back tasks even though larger MMNs at Cz were observed in the *n*-back task. Eliminating channel Cz itself is not a problem because MMN is most commonly measured at Fz or FCz. The difference at Cz is also likely not an issue, because it likely reflects overlap with the attentional N2b component, which is related to target detection (Sussman, 2007). The *n*-back task had more targets than the oddball task, so it is not surprising that a larger N2b component would be observed. Separation of the MMN and N2b components in active attention conditions is typically not possible, but in studies where attend conditions (eliciting a N2b component) were compared to passive conditions (no N2b elicited), there were no differences in MMN amplitude at frontal channels, suggesting that this attentional component has minimal impact on the MMN (Sussman, 2007). This supports our decision to omit the Cz channel from our between-group analyses while retaining Fz and FCz, as the MMN did not differ between tasks at these two sites. Future studies might verify this by comparing active and passive versions of these tasks, and/or by comparing MMN amplitudes

between oddball and *n*-back tasks when both tasks have been presented to each participant within a single recording session.

There are also some limitations related to the self-report measures and neuropsychological testing; these are also applicable to Chapters 3 and 4. The collection of cannabis use information was adequate for the purpose of this study, though use of a validated measure would have been superior. However, more detailed information regarding other substance use (especially nicotine, alcohol, and caffeine) would have been useful. Furthermore, findings regarding caffeine could easily be conflated with other factors (e.g. fatigue and/or hours of sleep etc.), so future studies would benefit by collecting information on these. The range of neuropsychological tests chosen was primarily intended to ascertain whether the groups were roughly equivalent in key domains; however, ultimately the range of tests was relatively narrow, which limits interpretability of the results. Furthermore, the OPIE-3 has been shown to perform adequately well in predicting FSIQ within the normal range, though it may underestimate scores in the upper tails of the distribution and overestimate scores in the lower end (Spinks et al., 2009). Although none of the sample had FSIQ scores that fell below the *average* range (WAIS-III FSIQ *average* range = 90-109), approximately 41% of participants had FSIQ scores in the *superior* range (FSIQ = 120-130). Scores for some of these participants might have been underestimated, but the overall pattern of results should not have been impacted because an identical number of individuals in each group (n = 12 for each group) had scores in this range. Furthermore, the OPIE-3 was developed in a U.S. sample, so it is possible that scores may have been distorted since only a small

number of participants grew up in the United States. A similar FSIQ estimation algorithm has been developed for Canadian samples (EPAC; Lange, Schoenberg, Woodward & Brickell, 2005). To this point, raw scores were reported for the VC, MR, and LNS (and also the self-report SCL-90) subtests, as a large portion of the sample grew up outside North America. The SCL-90 was chosen primarily as a means to provide a brief index of recent psychopathological symptoms, which it accomplished. However, the SCL-90 has been shown to have a unidimensional factor structure, so psychometrically, the GSI total score may be valid but the various subscales might have less validity (Rytilä-Manninen et al. 2016). Future studies more closely examining observed relationships between specific categories of psychopathological symptoms and the MMN would be improved by using more established tests. In summary, while a more comprehensive testing battery would have been preferable, it is believed that the tests chosen adequately accomplish their intended purpose of establishing group equivalence on key domains.

## **Conclusion**

In this larger sample, we again failed to find any differences in MMN between cannabis users and non-users and found only minor differences on the various self-report measures that have been examined throughout this dissertation. It is possible that proposed MMN attenuations reported by some research groups are not generalizable to all heavy cannabis users and that early auditory processing deficits are mediated by other factors.

Alternatively, it is also possible that the local MMN results in effects that are too weak to be detected except with a very large sample of participants. Both of these possibilities are worthy of future research, although in the latter case there would be some concern about the practical significance of any differences detected.

This study also found that psychopathological symptoms conceptually related to psychosis were related to attenuated MMNs, which is consistent with the literature and further validates our use of the local MMN. We also observed interesting dose-related effects suggesting shortened MMN latency in cannabis users, though it was perhaps more interesting that both caffeine use and frequency of alcohol use appeared to relate to reduced MMN amplitude, whereas cannabis use did not. Clearly future research will have to use more rigorous controls to disentangle the effects of various commonly used substances on early auditory processes.

## Chapter 6: General Discussion and Conclusion

### Synthesis

The overall goal of this dissertation was to examine various aspects of auditory processing that might be impacted by heavy cannabis use. To this end we developed a roving dual oddball task that simultaneously tested aspects of auditory memory/change detection (MMN) and more attention-driven auditory processing/stimulus categorization (P300), and also an auditory *n*-back task, using identical stimuli, to examine auditory working memory involving different features (pitch and pattern) under low and high memory load.

Chapter 2 set the groundwork for subsequent chapters by introducing the roving oddball task. The goal here was to attempt to eliminate an asymmetry identified by Blundon (2015) in a non-roving version of this task that was first described by (Bekinschtein, et al., 2009). This revealed an asymmetry in early auditory ERPs (MMN) and later attention-driven ERPs (P300). Using source localization we were able to localize a set of our ICs to specific brain regions and identified ventral and dorsal attention network nodes consistent with other oddball imaging studies. Network analysis revealed that the asymmetry was driven by different patterns of connectivity. A dorsal network was primarily active when participants attended to rare salient targets amongst non-salient common runs (feature present condition) and there was an interplay between dorsal and ventral networks when identifying rare non-salient targets amongst salient common runs (feature absent condition).

Chapter 3 used the same design as Chapter 2 to compare a group of heavy users of cannabis with a group of non-users. We largely replicated findings from Chapter 2. We did not find cannabis users to have significant attenuations in the MMN amplitude, which was in line with (Impey, El-Marj, Parks, Choueiry, Fisher & Knott, 2015) but opposed to others who have noted such differences (Greenwood et al., 2014; Rentzsch et al., 2007; Rentzsch, Buntebart, Stadelmeier, Gallinat & Jockers-Scherübl, 2011; Roser et al., 2010). As predicted, however, we found that cannabis users performed as well as non-users in the easier feature-present condition but were slower to identify targets in the more difficult feature-absent condition, which was also reflected in the latency of the P3b. Analysis of localized and network brain activity suggested that cannabis users employed a largely ventral attention-network-based, stimulus-driven strategy, whereas non-users tended to utilize more top-down attention to accomplish the tasks. This strategy appeared to be effective for CU when targets were salient; however, when targets were not salient, CU showed almost no frontal connectivity, which may have arisen from a breakdown in fronto-temporal connectivity. This is particularly significant, because a coherent picture emerged at multiple levels of analysis (behavioural, channel, local and networks). Relatively few studies show this sort of consistency and many studies rely on making inferences of brain activity in the absence of overt behavioural differences.

In Chapter 4, we introduced a novel auditory *n*-back task to examine auditory working memory for different features (pitch and pattern) under low and high memory load. We predicted that cannabis users would perform more poorly than non-users, due to impaired executive functions localized to frontal lobes and impaired sensory processing within

fronto-temporal networks. Many working memory studies that have measured brain functioning in cannabis users have found small behavioural deficits or no difference between groups (Cousijn, Wiers et al., 2014; Cousijn, Vingerhoets et al., 2014). In many of these studies, cannabis users appeared to recruit more cognitive resources, even in the absence of behavioural differences, which was interpreted as increased mental effort due to aberrant sensory and executive processes. However, we were surprised to find that cannabis users outperformed non-users despite the groups being very similar on self-report and neuropsychological measures. When memorizing pitch, CU had P3b amplitudes that were consistent with superior performance; however when memorizing pattern the P3b amplitudes were not reflective of this superior performance, even though overall P3b amplitudes demonstrated the expected attenuation under increased memory load. To further examine this, we identified brain regions largely consistent with the broad literature of working memory. Analysis of the theta band functional brain connectivity (PLVs) showed different patterns of connectivity between groups, which we speculated may imply that groups were engaged in different encoding strategies. Non-users appeared to show a much more distributed pattern of connectivity that involved the left temporal lobe and other network nodes, which we speculated may be consistent with increased mental effort and a less efficient semantic encoding strategy. CU on the other hand, showed a much less distributed pattern of right temporal activity along with frontal and parietal areas that may have implied they were relying on sensory memory. Interestingly, when memorizing patterns under high memory load, CU showed a bilateral pattern of connectivity that may have suggested that they switched to a verbal encoding strategy. This was particularly interesting because, under some task conditions (i.e.

Chapter 3, detecting non-salient rare oddballs amongst salient distractors) it appears that cannabis users suffer a breakdown in a stimulus-driven strategy related to fronto-temporal connectivity. When they are fully engaged by the demands of a difficult working memory task, however, they are fully capable of engaging auditory sensory systems to encode, maintain, and retrieve these same auditory stimuli in working memory. Furthermore, under high memory load they are able to flexibly shift to a more deliberate top-down verbal encoding strategy. This suggests that so long as they are engaged by the demands of what they are doing, their cognitive performance is not impacted, and under some circumstances this may work to their benefit. However, these interpretations can be, at best, considered hypotheses for future research because such speculations, based solely on patterns of brain activity, are fraught with fallacious reverse inference (Poldrack, 2006).

Chapter 5 described an amalgamation of data from Chapter 3 and 4. Here we combined data from two different auditory tasks to examine the impact of cannabis use on the local MMN using a larger participant sample for increased power. Again we failed to find evidence for attenuated MMN amplitude amongst heavy cannabis users and found no significant differences in cognitive functioning. Furthermore, we found only minimal differences in psychopathological symptoms (anxiety) and trait schizotypy (disorganization). Taken together these findings suggested that amongst some samples of heavy cannabis users (perhaps higher functioning ones; not directly measured but inferred from the observed higher than average intelligence and high educational attainment in these samples) basic auditory processing and cognitive functioning are

minimally impacted when compared to an otherwise similar sample of non-users. Although MMN amplitudes were not impacted by cannabis use, we did find some evidence that suggested that alcohol and caffeine might have an effect on MMN amplitude, though these findings rest on limited data and require additional verification.

### **Contributions to Cognitive and Clinical Science**

The scope of this research contributes meaningfully to the science of basic auditory sensory processing, auditory attention, and auditory working memory. The MMN and P300 have been heavily studied for decades, but this research adds to this literature by introducing a novel task that allows MMN and P300 to be tested simultaneously, and as demonstrated in Chapter 5, allows different cognitive tasks using these auditory stimuli to be meaningfully combined when more powerful samples are required. There is no reason why this can't be repeated for other cognitive variations of these tasks. This is especially advantageous in cases such as clinical cognitive neuroscience where it may be desirable to achieve adequate power while simultaneously being able to test predictions across various cognitive domains. Furthermore, auditory working memory is relatively under researched. Chapter 4 introduced a novel auditory *n*-back task and provided a detailed account at multiple levels of analysis including behaviour, traditional well-established channel ERPs (P3b), and by providing a detailed account of the underlying brain network involved in these processes using a sophisticated functional connectivity analysis (theta-band PLVs). Most importantly, this research contributes to better understanding the impact of cannabis on basic auditory processes and cognitive function, which provides a bridge between traditional cognitive neuroscience and clinical cognitive neuroscience as

many of the advanced methods used in this research have not yet been applied to the field.

### ***Applications: From Clinical Cognitive Science to Practice***

Anecdotally, many heavy cannabis users report the subjective experience of *brain fog*, a sort of mild cognitive impairment, not unlike those who struggle with chronic fatigue, that is difficult to detect, but has negative ramifications in their daily lives. If this is the case, the present set of findings implies that this may be especially true if they are in a setting that requires them to ignore salient distractors, while simultaneously having to pick out subtle targets. However, it seems that if they are engaged fully in a task and/or when there are minimal distractors, they can perform comparably to, or even better than, non-users. If this is the case, and if it generalizes beyond the auditory domain, then this may hint at possible strategies that cannabis users might use to optimize their environment so that they may perform maximally in day-to-day tasks. On the surface, these ideas appear comparable to compensatory strategies, that are often given to help individuals manage mild ADHD symptoms, or people who otherwise report mild cognitive impairments that do not appear when tested neuropsychologically. Studies such as these, might be beneficial in understanding these subtle processes - akin to a microscope - that are otherwise invisible to direct observation.

### **Current Limitations and Future Possibilities**

#### ***Source Localization***

The use of EEG source localization in the present set of studies revealed a number of theoretically relevant brain regions in each study, which is encouraging with respect to

the utility of source localization methods. However, ultimately, it should be noted that source localization of scalp activity is presently limited to cortical sources, since critical subcortical structures (e.g. the thalamus) are invisible to our analyses. Furthermore, the number of ICs identified by ICA is somewhat arbitrary, and can result in too few, or too many (in cases where single functional areas are split off into two or more areas within a single subject) regions being identified. Furthermore, as was seen in chapter 2 (i.e. absent STG sources), sometimes key regions are not identified, likely due to these ICs being contaminated by noise. Also, we chose to analyze areas that were common to both groups, which doesn't take into account the possibility that groups were recruiting different brain areas, and cannot speak to individual differences in brain activations. Finally, dipole fitting is limited by the use of standard head models, which assumes uniformity across participants when in reality brain structure is quite variable. Future research, might use multiple methods of source localization to validate results within data sets, constrain identified sources by using combined EEG/fMRI, and use structural MRI to build individualized head models for each participant.

### ***Localized Oscillations and Functional Connectivity***

Oscillatory activity, whether localized or distributed across brain networks, is limited by the sources identified, and connectivity can only be analyzed when a participant contributes ICs to each node of the pair being examined. Additionally, as stated in the previous section, important subcortical structures could not be identified, so the reported networks are fundamentally incomplete. Furthermore, bivariate functional connectivity between two brain regions does not necessary mean that those brain regions have a direct

structural connection. As such, spurious connectivity due to mediating brain areas that have not been identified cannot be completely ruled out. Also, synchronization between brain regions does not describe the direction of information flow. Particular to our analyses, we adopted a somewhat conservative approach to control for spurious connectivity, so it is likely that we have inadvertently eliminated connectivity that was present. Finally, this series of studies focused primarily on theta band connectivity, whereas activity in different frequency bands (e.g. gamma, alpha, and beta) have been suggested to play unique roles in attention and working memory and interact with each other in dynamic ways. Nonetheless, it is apparent that our examination of both localized and synchronous network activity provided rich information about underlying brain processes that could not have been inferred from channel data alone. Future studies might use combined fMRI/EEG studies to corroborate network activity, use causal network models such as transfer entropy or dynamic causal modelling to identify the direction of information flow, and our methodology for describing PLVs might be strengthened with multivariate analyses that can examine simultaneous interactions between three or more regions.

### ***Group Equivalence and Small Sample Size***

We made efforts to recruit participants that were, for the most part, equal on relevant factors that may have contributed to any group differences; however, while we believe these efforts to be adequate, they were far from comprehensive. Furthermore, even if a more comprehensive testing battery was used, the relatively small sample sizes described in this study would likely not be powerful enough to conduct the appropriate multivariate

analyses necessary to make any definitive conclusions. The small sample sizes are a limitation of these studies, but also reflective of a fundamental limitation in conducting complex cognitive neuroscience research, at least in small labs such as ours. For instance, in these studies, each participant constituted about 4 hours of data collection, most of which (with the exception of assistance with EEG capping) was carried out by this writer. Furthermore, the time spent collecting data was eclipsed by the thousands of hours spent processing (and often re-processing; the PLVs for chapter 4 took five days on a 16-core computer, only for it to crash four days in!) the data and analyzing the results, almost all of which was too nuanced to delegate to undergraduate assistants. We believe that small dedicated brain research labs, such as ours, are a species on the verge of extinction – to be replaced by massively funded big brain research conglomerates with interdisciplinary teams of cognitive scientists, clinicians, technicians, engineers, physicists and statisticians. But how else will it ever be possible to truly understand the human brain, which is, as far as we know, the most complicated thing in the universe?

### ***Causality and the Future of Cannabis Research***

The primary limitation of using a cross-sectional design is the inability to make causal inferences about the effects of cannabis on the brain. As previously reviewed, a limited number of causal studies have been conducted that have examined the acute effects of cannabis; however, the illegality of cannabis has been a barrier to conducting well-controlled longitudinal studies of the effects of chronic cannabis use on brain function. Such studies will also be necessary in order to disentangle the chronic effects of cannabis use from acute effects that may persist hours or days (i.e. see chapter 3 Limits section)

that may remit after longer periods of abstinence. Many interested parties (including cannabis users, health care professionals, politicians, and the cannabis industry, to name a few) are eager for a comprehensive understanding of the negative (and potentially positive) consequences of cannabis use. We anticipate that in the coming years, in Canada at least (with the legalization of recreational sales), will be a relative *golden age* for cannabis research.

## References

- Ambrose, R. (2015, April). Correspondence to Mayor Gregor Robertson. Ministry of Health, Ottawa, Canada. Retrieved from <https://s3.amazonaws.com/s3.documentcloud.org/documents/2064407/letter-from-rona-ambrose-to-city-of-vancouver.pdf>
- Arnott, S. R., Binns, M. A., Grady, C. L., & Alain, C. (2004). Assessing the auditory dual-pathway model in humans. *NeuroImage*, *22*, 401–8. <http://doi.org/10.1016/j.neuroimage.2004.01.014>
- Avissar, M., Xie, S., Vail, B., Lopez-Calderon, J., Wang, Y., & Javitt, D. C. (2018). Meta-analysis of mismatch negativity to simple versus complex deviants in schizophrenia. *Schizophrenia Research*, *191*, 25–34. <http://doi.org/10.1016/j.schres.2017.07.009>
- Bachiller, A., Romero, S., Molina, V., Alonso, J. F., Mañanas, M. A., Poza, J., & Hornero, R. (2015). Auditory P3a and P3b neural generators in schizophrenia: An adaptive sLORETA P300 localization approach. *Schizophrenia Research*, *169*, 318–325. <http://doi.org/10.1016/j.schres.2015.09.028>
- Baddeley, A. (2003). Working memory: looking back and looking forward. *Nature Reviews. Neuroscience*, *4*, 829–39. <http://doi.org/10.1038/nrn1201>
- Baldeweg, T., Adams, S., Gruzelier, J. (1999). 16. Electrophysiology. *Schizophrenia Research*, *36*, 251–261. [http://doi.org/10.1016/S0920-9964\(99\)90037-3](http://doi.org/10.1016/S0920-9964(99)90037-3)
- Barbas, H., Medalla, M., Alade, O., Suski, J., Zikopoulos, B., & Lera, P. (2005). Relationship of prefrontal connections to inhibitory systems in superior temporal areas in the rhesus monkey. *Cerebral Cortex*: *15*, 1356–70.

<http://doi.org/10.1093/cercor/bhi018>

Barch, D. M., & Ceaser, A. (2012). Cognition in schizophrenia: core psychological and neural mechanisms. *Trends in Cognitive Sciences*, *16*, 27–34.

<http://doi.org/10.1016/j.tics.2011.11.015>

Başar-Eroglu, C., Başar, E., Demiralp, T., & Schürmann, M. (1992). P300-response: possible psychophysiological correlates in delta and theta frequency channels. A review. *International Journal of Psychophysiology*, *13*, 161–79. Retrieved from <http://www.ncbi.nlm.nih.gov/pubmed/1399755>

Bedo, N., Ribary, U., & Ward, L. M. (2014). Fast dynamics of cortical functional and effective connectivity during word reading. *PloS One*, *9*, e88940.

<http://doi.org/10.1371/journal.pone.0088940>

Behrmann, M., Geng, J. J., & Shomstein, S. (2004). Parietal cortex and attention. *Current Opinion in Neurobiology*, *14*, 212–7. <http://doi.org/10.1016/j.conb.2004.03.012>

Bekinschtein, T. a, Dehaene, S., Rohaut, B., Tadel, F., Cohen, L., & Naccache, L. (2009). Neural signature of the conscious processing of auditory regularities. *Proceedings of the National Academy of Sciences of the United States of America*, *106*, 1672–7.

<http://doi.org/10.1073/pnas.0809667106>

Bell, A. J., & Sejnowski, T. J. (1995). An information-maximization approach to blind separation and blind deconvolution. *Neural Computation*, *7*, 1129–59. Retrieved from <http://www.ncbi.nlm.nih.gov/pubmed/7584893>

Bhattacharyya, S., & Schoeler, T. (2013). The effect of cannabis use on memory function: an update. *Substance Abuse and Rehabilitation*, *11*.

<http://doi.org/10.2147/SAR.S25869>

- Blundon, E. G. (2015). Search through time is like search through space : behavioural and electrophysiological evidence. Retrieved from <https://open.library.ubc.ca/collections/24/items/1.0166495>
- Blundon, E. G., Rumak, S. P., & Ward, L. M. (2017). Sequential search asymmetry: Behavioral and psychophysiological evidence from a dual oddball task. *PLoS ONE*, *12*(3). <http://doi.org/10.1371/journal.pone.0173237>
- Blundon, E., & Ward, L. M. (2014). Absence makes the ear work harder: An auditory analog of visual search asymmetry.
- Bodatsch, M., Klosterkötter, J., Müller, R., & Ruhrmann, S. (2013). Basic disturbances of information processing in psychosis prediction. *Frontiers in Psychiatry*, *4*, 93. <http://doi.org/10.3389/fpsy.2013.00093>
- Bossong, M. G., Jager, G., Bhattacharyya, S., & Allen, P. (2014). Acute and Non-acute Effects of Cannabis on Human Memory Function: A Critical Review of Neuroimaging Studies. *Current Pharmaceutical Design*, *20*, 2114–25. Retrieved from <http://www.ncbi.nlm.nih.gov/pubmed/23829369>
- Brookes, M. J., Wood, J. R., Stevenson, C. M., Zumer, J. M., White, T. P., Liddle, P. F., & Morris, P. G. (2011). Changes in brain network activity during working memory tasks: A magnetoencephalography study. *NeuroImage*, *55*, 1804–1815. <http://doi.org/10.1016/J.NEUROIMAGE.2010.10.074>
- Broyd, S. J., Michie, P. T., Bruggemann, J., van Hell, H. H., Greenwood, L.-M., Croft, R. J., ... Solowij, N. (2016). Schizotypy and auditory mismatch negativity in a non-clinical sample of young adults. *Psychiatry Research. Neuroimaging*, *254*, 83–91. <http://doi.org/10.1016/j.psychresns.2016.06.011>

- Broyd, S. J., van Hell, H. H., Beale, C., Yücel, M., & Solowij, N. (2016). Acute and Chronic Effects of Cannabinoids on Human Cognition—A Systematic Review. *Biological Psychiatry*, *79*, 557–567. <http://doi.org/10.1016/j.biopsych.2015.12.002>
- Bylaw to Amend License Bylaw No. 4450 Regarding Retail Dealer - Medical Marijuana -Related Bylaw. (2015). City of Vancouver.
- Chennu, S., Noreika, V., Gueorguiev, D., Blenkmann, A., Kochen, S., Ibáñez, A., ... Bekinschtein, T. A. (2013). Expectation and attention in hierarchical auditory prediction. *The Journal of Neuroscience*: *33*, 11194–205. <http://doi.org/10.1523/JNEUROSCI.0114-13.2013>
- Chitty, K. M., Kaur, M., Lagopoulos, J., Hickie, I. B., & Hermens, D. F. (2011). Alcohol use and mismatch negativity in young patients with psychotic disorder. *Neuroreport*, *22*, 918–22. <http://doi.org/10.1097/WNR.0b013e32834cdc3f>
- Choi, J. W., Lee, J. K., Ko, D., Lee, G.-T., Jung, K.-Y., & Kim, K. H. (2013). Fronto-temporal interactions in the theta-band during auditory deviant processing. *Neuroscience Letters*, *548*, 120–5. <http://doi.org/10.1016/j.neulet.2013.05.079>
- Comerchero, M. D., & Polich, J. (1999). P3a and P3b from typical auditory and visual stimuli. *Clinical Neurophysiology*: *110*, 24–30. Retrieved from <http://www.ncbi.nlm.nih.gov/pubmed/10348317>
- Cooper, P. S., Wong, A. S. W., McKewen, M., Michie, P. T., & Karayanidis, F. (2017). Frontoparietal theta oscillations during proactive control are associated with goal-updating and reduced behavioral variability. *Biological Psychology*, *129*, 253–264. <http://doi.org/10.1016/j.biopsycho.2017.09.008>
- Corbetta, M., Patel, G., & Shulman, G. L. (2008). The Reorienting System of the Human

Brain: From Environment to Theory of Mind. *Neuron*, 58, 306–324.

<http://doi.org/10.1016/j.neuron.2008.04.017>

Corbetta, M., & Shulman, G. L. (2002). Control of goal-directed and stimulus-driven attention in the brain. *Nature Reviews Neuroscience*, 3, 201–215.

<http://doi.org/10.1038/nrn755>

Cousijn, J., Vingerhoets, W. A. M., Koenders, L., de Haan, L., van den Brink, W., Wiers, R. W., & Goudriaan, A. E. (2014). Relationship between working-memory network function and substance use: a 3-year longitudinal fMRI study in heavy cannabis users and controls. *Addiction Biology*, 19, 282–93. <http://doi.org/10.1111/adb.12111>

Cousijn, J., Wiers, R. W., Ridderinkhof, K. R., van den Brink, W., Veltman, D. J., & Goudriaan, A. E. (2014). Effect of baseline cannabis use and working-memory network function on changes in cannabis use in heavy cannabis users: a prospective fMRI study. *Human Brain Mapping*, 35, 2470–82.

<http://doi.org/10.1002/hbm.22342>

Derogatis, L.R. (1994) Symptom Checklist-90-R: Administration, Scoring & Procedure Manual for the Revised Version of the SCL-90. National Computer Systems, Minneapolis.

D'Souza, D. C., Abi-Saab, W. M., Madonick, S., Forselius-Bielen, K., Doersch, A., Braley, G., ... Krystal, J. H. (2005). Delta-9-tetrahydrocannabinol effects in schizophrenia: implications for cognition, psychosis, and addiction. *Biological Psychiatry*, 57(6), 594–608. <http://doi.org/10.1016/j.biopsych.2004.12.006>

D'Souza, D. C., Fridberg, D. J., Skosnik, P. D., Williams, A., Roach, B., Singh, N., ... Mathalon, D. (2012). Dose-related modulation of event-related potentials to novel

- and target stimuli by intravenous  $\Delta^9$ -THC in humans. *Neuropsychopharmacology*, 37, 1632–46. <http://doi.org/10.1038/npp.2012.8>
- D'Souza, D. C., Ranganathan, M., Braley, G., Gueorguieva, R., Zimolo, Z., Cooper, T., ... Krystal, J. (2008). Blunted psychotomimetic and amnestic effects of delta-9-tetrahydrocannabinol in frequent users of cannabis. *Neuropsychopharmacology*, 33, 2505–16. <http://doi.org/10.1038/sj.npp.130164>
- Dahlgren, M. K., Sagar, K. A., Racine, M. T., Dreman, M. W., & Gruber, S. A. (2016). Marijuana Use Predicts Cognitive Performance on Tasks of Executive Function. *Journal of Studies on Alcohol and Drugs*, 77, 298–308. Retrieved from <http://www.ncbi.nlm.nih.gov/pubmed/26997188>
- Davis, G. P., Compton, M. T., Wang, S., Levin, F. R., & Blanco, C. (2013). Association between cannabis use, psychosis, and schizotypal personality disorder: Findings from the National Epidemiologic Survey on Alcohol and Related Conditions. *Schizophrenia Research*, 151, 197–202. <http://doi.org/10.1016/j.schres.2013.10.018>
- de Sola, S., Tarancón, T., Peña-Casanova, J., Espadaler, J. M., Langohr, K., Poudevida, S., ... de la Torre, R. (2008). Auditory event-related potentials (P3) and cognitive performance in recreational ecstasy polydrug users: evidence from a 12-month longitudinal study. *Psychopharmacology*, 200, 425–37. <http://doi.org/10.1007/s00213-008-1217-5>
- Debener, S., Herrmann, C. S., Kranczioch, C., Gembris, D., & Engel, A. K. (2003). Top-down attentional processing enhances auditory evoked gamma band activity. *Neuroreport*, 14, 683–6. <http://doi.org/10.1097/01.wnr.0000064987.96259.5c>
- Delorme, A., & Makeig, S. (2004). EEGLAB: an open source toolbox for analysis of

- single-trial EEG dynamics including independent component analysis. *Journal of Neuroscience Methods*, 134, 9–21. <http://doi.org/10.1016/j.jneumeth.2003.10.009>
- Delorme, A., Palmer, J., Onton, J., Oostenveld, R., & Makeig, S. (2012). Independent EEG sources are dipolar. *PloS One*, 7, e30135. <http://doi.org/10.1371/journal.pone.0030135>
- Deouell, L. Y., Bentin, S., & Giard, M. H. (1998). Mismatch negativity in dichotic listening: evidence for interhemispheric differences and multiple generators. *Psychophysiology*, 35, 355–65. Retrieved from <http://www.ncbi.nlm.nih.gov/pubmed/9643050>
- Doeller, C. F., Opitz, B., Mecklinger, A., Krick, C., Reith, W., & Schröger, E. (2003). Prefrontal cortex involvement in preattentive auditory deviance detection: neuroimaging and electrophysiological evidence. *NeuroImage*, 20, 1270–82. [http://doi.org/10.1016/S1053-8119\(03\)00389-6](http://doi.org/10.1016/S1053-8119(03)00389-6)
- Doesburg, S. M., Green, J. J., McDonald, J. J., & Ward, L. M. (2009). From local inhibition to long-range integration: a functional dissociation of alpha-band synchronization across cortical scales in visuospatial attention. *Brain Research*, 1303, 97–110. <http://doi.org/10.1016/j.brainres.2009.09.069>
- du Boisgueheneuc, F., Levy, R., Volle, E., Seassau, M., Duffau, H., Kinkingnehun, S., ... Dubois, B. (2006). Functions of the left superior frontal gyrus in humans: a lesion study. *Brain*, 129, 3315–28. <http://doi.org/10.1093/brain/awl244>
- Dunbar, G., Boeijinga, P. H., Demazières, A., Cisterni, C., Kuchibhatla, R., Wesnes, K., & Luthringer, R. (2007). Effects of TC-1734 (AZD3480), a selective neuronal nicotinic receptor agonist, on cognitive performance and the EEG of young healthy

male volunteers. *Psychopharmacology*, 191, 919–29. <http://doi.org/10.1007/s00213-006-0675-x>

- Evans, J. L., Selinger, C., & Pollak, S. D. (2011). P300 as a measure of processing capacity in auditory and visual domains in specific language impairment. *Brain Research*, 1389, 93–102. <http://doi.org/10.1016/j.brainres.2011.02.010>
- Fell, J., Hinrichs, H., & Röschke, J. (1997). Time course of human 40 Hz EEG activity accompanying P3 responses in an auditory oddball paradigm. *Neuroscience Letters*, 235, 121–4. Retrieved from <http://www.ncbi.nlm.nih.gov/pubmed/9406884>
- Fitzgibbon, S. P., DeLosAngeles, D., Lewis, T. W., Powers, D. M. W., Grummett, T. S., Whitham, E. M., ... Pope, K. J. (2016). Automatic determination of EMG-contaminated components and validation of independent component analysis using EEG during pharmacologic paralysis. *Clinical Neurophysiology : Official Journal of the International Federation of Clinical Neurophysiology*, 127, 1781–93. <http://doi.org/10.1016/j.clinph.2015.12.009>
- Fridberg, D. J., Vollmer, J. M., O'Donnell, B. F., & Skosnik, P. D. (2011). Cannabis users differ from non-users on measures of personality and schizotypy. *Psychiatry Research*, 186, 46–52. <http://doi.org/10.1016/j.psychres.2010.07.035>
- Friedman, D., Cycowicz, Y. M., & Gaeta, H. (2001). The novelty P3: an event-related brain potential (ERP) sign of the brain's evaluation of novelty. *Neuroscience and Biobehavioral Reviews*, 25, 355–73. Retrieved from <http://www.ncbi.nlm.nih.gov/pubmed/11445140>
- Fries, P. (2005). A mechanism for cognitive dynamics: neuronal communication through neuronal coherence. *Trends in Cognitive Sciences*, 9, 474–80.

<http://doi.org/10.1016/j.tics.2005.08.011>

Friese, B., & Grube, J. W. (2013). Legalization of medical marijuana and marijuana use among youths. *Drugs (Abingdon, England)*, *20*, 33–39.

<http://doi.org/10.3109/09687637.2012.713408>

Garrido, M., Friston, K., & Kiebel, S. (2008). The functional anatomy of the MMN: a DCM study of the roving paradigm. *Neuroimage*, *42*, 936–944.

<http://doi.org/10.1016/j.neuroimage.2008.05.018>.

Garrido, M. I., Kilner, J. M., Kiebel, S. J., Stephan, K. E., Baldeweg, T., & Friston, K. J. (2009). Repetition suppression and plasticity in the human brain. *NeuroImage*, *48*, 269–79. <http://doi.org/10.1016/j.neuroimage.2009.06.034>

Garrido, M. I., Kilner, J. M., Stephan, K. E., & Friston, K. J. (2009). The mismatch negativity: a review of underlying mechanisms. *Clinical Neurophysiology*, *120*, 453–63. <http://doi.org/10.1016/j.clinph.2008.11.029>

Gjini, K., Arfken, C., & Boutros, N. N. (2010). Relationships between sensory “gating out” and sensory “gating in” of auditory evoked potentials in schizophrenia: a pilot study. *Schizophrenia Research*, *121*, 139–45.

<http://doi.org/10.1016/j.schres.2010.04.020>

Gloss, D. (2015). An Overview of Products and Bias in Research. *Neurotherapeutics*, *12*, 731–734. <http://doi.org/10.1007/s13311-015-0370-x>

Glover, S., & Dixon, P. (2004). Likelihood ratios: a simple and flexible statistic for empirical psychologists. *Psychonomic Bulletin & Review*, *11*, 791–806.

<http://doi.org/10.3758/BF03196706>

Grech, R., Cassar, T., Muscat, J., Camilleri, K. P., Fabri, S. G., Zervakis, M., ...

Vanrumste, B. (2008). Review on solving the inverse problem in EEG source analysis. *Journal of Neuroengineering and Rehabilitation*, 5, 25.

<http://doi.org/10.1186/1743-0003-5-25>

Greenwood, L.-M., Broyd, S. J., Croft, R., Todd, J., Michie, P. T., Johnstone, S., ...

Solowij, N. (2014). Chronic effects of cannabis use on the auditory mismatch negativity. *Biological Psychiatry*, 75, 449–58.

<http://doi.org/10.1016/j.biopsych.2013.05.035>

Grimault, S., Nolden, S., Lefebvre, C., Vachon, F., Hyde, K., Peretz, I., ... Jolicoeur, P.

(2014). Brain activity is related to individual differences in the number of items stored in auditory short-term memory for pitch: Evidence from magnetoencephalography. *NeuroImage*, 94, 96–106.

<http://doi.org/10.1016/j.neuroimage.2014.03.020>

Grotenhermen, F. (2003). Pharmacokinetics and pharmacodynamics of cannabinoids.

*Clinical Pharmacokinetics*, 42, 327–60. <http://doi.org/10.2165/00003088-200342040-00003>

Gruber, S. A., Sagar, K. A., Dahlgren, M. K., Gonenc, A., Smith, R. T., Lambros, A. M.,

... Lukas, S. E. (2017). The Grass Might Be Greener: Medical Marijuana Patients Exhibit Altered Brain Activity and Improved Executive Function after 3 Months of Treatment. *Frontiers in Pharmacology*, 8, 983.

<http://doi.org/10.3389/fphar.2017.00983>

Gruber, S. A., Sagar, K. A., Dahlgren, M. K., Racine, M., & Lukas, S. E. (2012). Age of

onset of marijuana use and executive function. *Psychology of Addictive Behaviors*: 26, 496–506. <http://doi.org/10.1037/a0026269>

- Grzella, I., Müller, B. W., Oades, R. D., Bender, S., Schall, U., Zerbin, D., ... Sartory, G. (2001). Novelty-elicited mismatch negativity in patients with schizophrenia on admission and discharge. *Journal of Psychiatry & Neuroscience, 26*, 235–46. Retrieved from <http://www.ncbi.nlm.nih.gov/pubmed/11394193>
- Gurtubay, I. G., Alegre, M., Labarga, A., Malanda, A., Iriarte, J., & Artieda, J. (2001). Gamma band activity in an auditory oddball paradigm studied with the wavelet transform. *Clinical Neurophysiology, 112*, 1219–28. Retrieved from <http://www.ncbi.nlm.nih.gov/pubmed/11516733>
- Haas, L. F. (2003). Hans Berger (1873-1941), Richard Caton (1842-1926), and electroencephalography. *Journal of Neurology, Neurosurgery & Psychiatry, 74*, 9–9. <http://doi.org/10.1136/jnnp.74.1.9>
- Hadland, S. E., & Levy, S. (2016). Objective Testing: Urine and Other Drug Tests. *Child and Adolescent Psychiatric Clinics of North America, 25*, 549–65. <http://doi.org/10.1016/j.chc.2016.02.005>
- Haenschel, C., Vernon, D. J., Dwivedi, P., Gruzelier, J. H., & Baldeweg, T. (2005). Event-related brain potential correlates of human auditory sensory memory-trace formation. *The Journal of Neuroscience, 25*, 10494–501. <http://doi.org/10.1523/JNEUROSCI.1227-05.2005>
- Haig, A. R., De Pascalis, V., & Gordon, E. (1999). Peak gamma latency correlated with reaction time in a conventional oddball paradigm. *Clinical Neurophysiology, 110*, 158–65. Retrieved from <http://www.ncbi.nlm.nih.gov/pubmed/10348335>
- Haigh, S. M., Matteis, M. De, Coffman, B. A., Murphy, T. K., Butera, C. D., Ward, K. L., ... Salisbury, D. F. (2017). Mismatch negativity to pitch pattern deviants in

schizophrenia. *The European Journal of Neuroscience*, 46, 2229–2239.

<http://doi.org/10.1111/ejn.13660>

Häkkinen, S., Ovaska, N., & Rinne, T. (2015). Processing of pitch and location in human auditory cortex during visual and auditory tasks. *Frontiers in Psychology*, 6.

<http://doi.org/10.3389/fpsyg.2015.01678>

Harding, I. H., Solowij, N., Harrison, B. J., Takagi, M., Lorenzetti, V., Lubman, D. I., ...

Yücel, M. (2012). Functional connectivity in brain networks underlying cognitive control in chronic cannabis users. *Neuropsychopharmacology*, 37, 1923–1933.

<http://doi.org/10.1038/npp.2012.39>

Harmony, T. (2013). The functional significance of delta oscillations in cognitive processing. *Frontiers in Integrative Neuroscience*, 7, 83.

<http://doi.org/10.3389/fnint.2013.00083>

Harper, J., Malone, S. M., & Iacono, W. G. (2017). Theta- and delta-band EEG network dynamics during a novelty oddball task. *Psychophysiology*, 54, 1590–1605.

<http://doi.org/10.1111/psyp.12906>

Herrmann, C. S., Fründ, I., & Lenz, D. (2010). Human gamma-band activity: A review on cognitive and behavioral correlates and network models. *Neuroscience & Biobehavioral Reviews*, 34, 981–992.

<http://doi.org/10.1016/j.neubiorev.2009.09.001>

Herzig, D. A., Nutt, D. J., & Mohr, C. (2014). Alcohol and Relatively Pure Cannabis Use, but Not Schizotypy, are Associated with Cognitive Attenuations. *Frontiers in Psychiatry*, 5, 133.

<http://doi.org/10.3389/fpsyg.2014.00133>

Hetrick, W. P., Erickson, M. A., & Smith, D. A. (2012). Phenomenological dimensions

of sensory gating. *Schizophrenia Bulletin*, 38, 178–191.

<http://doi.org/10.1093/schbul/sbq054>

Hirvonen, J., Jääskeläinen, I. P., Näätänen, R., & Sillanauke, P. (2000). Adenosine A1/A2a receptors mediate suppression of mismatch negativity by ethanol in humans.

*Neuroscience Letters*, 278, 57–60. [http://doi.org/10.1016/S0304-3940\(99\)00897-6](http://doi.org/10.1016/S0304-3940(99)00897-6)

Houck, J. M., Bryan, A. D., & Feldstein Ewing, S. W. (2013). Functional connectivity and cannabis use in high-risk adolescents. *The American Journal of Drug and Alcohol Abuse*, 39, 414–23. <http://doi.org/10.3109/00952990.2013.837914>

*Alcohol Abuse*, 39, 414–23. <http://doi.org/10.3109/00952990.2013.837914>

Hsiao, F.J., Wu, Z.A., Ho, L.-T., & Lin, Y.-Y. (2009). Theta oscillation during auditory change detection: An MEG study. *Biological Psychology*, 81, 58–66.

<http://doi.org/10.1016/j.biopsycho.2009.01.007>

Hsieh, L.T., & Ranganath, C. (2014). Frontal midline theta oscillations during working memory maintenance and episodic encoding and retrieval. *NeuroImage*, 85, 721–729. <http://doi.org/10.1016/j.neuroimage.2013.08.003>

<http://doi.org/10.1016/j.neuroimage.2013.08.003>

Huang, S., Seidman, L. J., Rossi, S., & Ahveninen, J. (2013). Distinct cortical networks activated by auditory attention and working memory load. *NeuroImage*, 83, 1098–108. <http://doi.org/10.1016/j.neuroimage.2013.07.074>

<http://doi.org/10.1016/j.neuroimage.2013.07.074>

Ilan, A. B., Smith, M. E., & Gevins, A. (2004). Effects of marijuana on neurophysiological signals of working and episodic memory. *Psychopharmacology*, 176, 214–22. <http://doi.org/10.1007/s00213-004-1868-9>

<http://doi.org/10.1007/s00213-004-1868-9>

Impey, D., El-Marj, N., Parks, A., Choueiry, J., Fisher, D., & Knott, V. J. (2015).

Mismatch negativity in tobacco-naïve cannabis users and its alteration with acute nicotine administration. *Pharmacology, Biochemistry, and Behavior*, 136, 73–81.

<http://doi.org/10.1016/j.pbb.2015.07.002>

Ishii, R., Canuet, L., Herdman, A., Gunji, A., Iwase, M., Takahashi, H., ... Takeda, M. (2009). Cortical oscillatory power changes during auditory oddball task revealed by spatially filtered magnetoencephalography. *Clinical Neurophysiology*, *120*, 497–504. <http://doi.org/10.1016/j.clinph.2008.11.023>

Jääskeläinen, I. P., Ahveninen, J., Bonmassar, G., Dale, A. M., Ilmoniemi, R. J., Levänen, S., ... Belliveau, J. W. (2004). Human posterior auditory cortex gates novel sounds to consciousness. *Proceedings of the National Academy of Sciences of the United States of America*, *101*, 6809–14. <http://doi.org/10.1073/pnas.0303760101>

Jaaskelainen, I. P., Lehtokoski, A., Alho, K., Kujala, T., Pekkonen, E., Sinclair, J. D., ... Sillanauke, P. (1995). Low Dose of Ethanol Suppresses Mismatch Negativity of Auditory Event-Related Potentials. *Alcoholism: Clinical and Experimental Research*, *19*, 607–610. <http://doi.org/10.1111/j.1530-0277.1995.tb01555.x>

Justen, C., & Herbert, C. (2018). The spatio-temporal dynamics of deviance and target detection in the passive and active auditory oddball paradigm: a sLORETA study. *BMC Neuroscience*, *19*, 25. <http://doi.org/10.1186/s12868-018-0422-3>

Kaiser, J. (2015). Dynamics of auditory working memory. *Frontiers in Psychology*, *6*, 613. <http://doi.org/10.3389/fpsyg.2015.00613>

Kaiser, J., Ripper, B., Birbaumer, N., & Lutzenberger, W. (2003). Dynamics of gamma-band activity in human magnetoencephalogram during auditory pattern working memory. *NeuroImage*, *20*, 816–27. [http://doi.org/10.1016/S1053-8119\(03\)00350-1](http://doi.org/10.1016/S1053-8119(03)00350-1)

Kane, M. J., Conway, A. R. A., Miura, T. K., & Colflesh, G. J. H. (2007). Working

memory, attention control, and the N-back task: a question of construct validity. *Journal of Experimental Psychology. Learning, Memory, and Cognition*, *33*, 615–22. <http://doi.org/10.1037/0278-7393.33.3.615>

Kärgel, C., Sartory, G., Kariofillis, D., Wiltfang, J., & Müller, B. W. (2014). Mismatch negativity latency and cognitive function in schizophrenia. *PloS One*, *9*, e84536. <http://doi.org/10.1371/journal.pone.0084536>

Karschner, E. L., Schwilke, E. W., Lowe, R. H., Darwin, W. D., Herning, R. I., Cadet, J. L., & Huestis, M. A. (2009). Implications of plasma Delta9-tetrahydrocannabinol, 11-hydroxy-THC, and 11-nor-9-carboxy-THC concentrations in chronic cannabis smokers. *Journal of Analytical Toxicology*, *33*, 469–77.

Kathmann, N., Wagner, M., Rendtorff, N., & Engel, R. R. (1995). Delayed peak latency of the mismatch negativity in schizophrenics and alcoholics. *Biological Psychiatry*, *37*, 754–7. [http://doi.org/10.1016/0006-3223\(94\)00309-Q](http://doi.org/10.1016/0006-3223(94)00309-Q)

Kempel, P., Lampe, K., Parnefjord, R., Hennig, J., & Kunert, H. J. (2003). Auditory-evoked potentials and selective attention: different ways of information processing in cannabis users and controls. *Neuropsychobiology*, *48*, 95–101. <http://doi.org/10.1159/000072884>

Kenemans, J. L., & Kähkönen, S. (2011). How human electrophysiology informs psychopharmacology: from bottom-up driven processing to top-down control. *Neuropsychopharmacology*, *36*, 26–51. <http://doi.org/10.1038/npp.2010.157>

Kim, H. (2014). Involvement of the dorsal and ventral attention networks in oddball stimulus processing: a meta-analysis. *Human Brain Mapping*, *35*, 2265–84. <http://doi.org/10.1002/hbm.22326>

- King, J.R., Gramfort, A., Schurger, A., Naccache, L., & Dehaene, S. (2014). Two distinct dynamic modes subtend the detection of unexpected sounds. *PloS One*, *9*, e85791. <http://doi.org/10.1371/journal.pone.0085791>
- Koch, S. P., Werner, P., Steinbrink, J., Fries, P., & Obrig, H. (2009). Stimulus-induced and state-dependent sustained gamma activity is tightly coupled to the hemodynamic response in humans. *The Journal of Neuroscience*, *29*, 13962–70. <http://doi.org/10.1523/JNEUROSCI.1402-09.2009>
- Koenigs, M., Barbey, A. K., Postle, B. R., & Grafman, J. (2009). Superior parietal cortex is critical for the manipulation of information in working memory. *The Journal of Neuroscience*, *29*, 14980–6. <http://doi.org/10.1523/JNEUROSCI.3706-09.2009>
- Lachaux, J. P., Rodriguez, E., Martinerie, J., & Varela, F. J. (1999). Measuring phase synchrony in brain signals. *Human Brain Mapping*, *8*, 194–208. Retrieved from <http://www.ncbi.nlm.nih.gov/pubmed/10619414>
- Lange, R. T., Schoenberg, M. R., Woodward, T. S., & Brickell, T. A. (2005). Development of the WAIS-III estimate of premorbid ability for Canadians (EPAC). *Archives of Clinical Neuropsychology*, *20*, 1009–1024. <http://doi.org/10.1016/j.acn.2005.06.004>
- Lefebvre, C., & Jolicœur, P. (2016). Memory for pure tone sequences without contour. *Brain Research*, *1640*, 222–231. <http://doi.org/http://dx.doi.org/10.1016/j.brainres.2016.02.025>
- Levitin, D. J., & Menon, V. (2003). Musical structure is processed in “language” areas of the brain: a possible role for Brodmann Area 47 in temporal coherence. *NeuroImage*, *20*, 2142–52. Retrieved from

<http://www.ncbi.nlm.nih.gov/pubmed/14683718>

- Light, G. A., Swerdlow, N. R., & Braff, D. L. (2007). Preattentive sensory processing as indexed by the MMN and P3a brain responses is associated with cognitive and psychosocial functioning in healthy adults. *Journal of Cognitive Neuroscience, 19*, 1624–32. <http://doi.org/10.1162/jocn.2007.19.10.1624>
- Lisman, J. E., & Jensen, O. (2013). The  $\theta$ - $\gamma$  neural code. *Neuron, 77*, 1002–16. <http://doi.org/10.1016/j.neuron.2013.03.007>
- Lopez-Calderon, J., & Luck, S. J. (2014). ERPLAB: an open-source toolbox for the analysis of event-related potentials. *Frontiers in Human Neuroscience, 8*, 213. <http://doi.org/10.3389/fnhum.2014.00213>
- Luck, S. J. (2005). *An Introduction to the Event-related Potential Technique*. MIT Press.
- Lupick, T. (2015, Oct 1). 2015 stats for marijuana offences show police tactics changed before Vancouver's dispensary boom. *The Georgia Straight*. Retrieved from <https://www.straight.com/news/546991/2015-stats-marijuana-offences-show-police-tactics-changed-vancouvers-dispensary-boom>
- Luu, P., Caggiano, D. M., Geyer, A., Lewis, J., Cohn, J., & Tucker, D. M. (2014). Time-course of cortical networks involved in working memory. *Frontiers in Human Neuroscience, 8*, 4. <http://doi.org/10.3389/fnhum.2014.00004>
- Ma, W. J., Husain, M., & Bays, P. M. (2014). Changing concepts of working memory. *Nature Neuroscience, 17*, 347–56. <http://doi.org/10.1038/nn.3655>
- Maclean, S. E. (2011). *Temporo-frontal Phase Synchronization Supports Hierarchical Network for Mismatch Negativity*. University of British Columbia. Retrieved from <http://hdl.handle.net/2429/33788>

- Maclean, S. E., & Ward, L. M. (2014). Temporo-frontal phase synchronization supports hierarchical network for mismatch negativity. *Clinical Neurophysiology*, *125*, 1604-1617. <http://doi.org/10.1016/j.clinph.2013.12.109>
- Macmillan, N. A., & Creelman, C. D. (2005). *Detection theory: A user's guide, 2nd ed.* *Detection theory: A user's guide, 2nd ed.* Mahwah, NJ, US: Lawrence Erlbaum Associates Publishers.
- Makeig, S., Jung, T. P., Bell, A. J., Ghahremani, D., & Sejnowski, T. J. (1997). Blind separation of auditory event-related brain responses into independent components. *Proceedings of the National Academy of Sciences of the United States of America*, *94*, 10979–84. Retrieved from <http://www.ncbi.nlm.nih.gov/pubmed/9380745>
- Marshall, L., Mölle, M., & Bartsch, P. (1996). Event-related gamma band activity during passive and active oddball tasks. *Neuroreport*, *7*, 1517–20. Retrieved from <http://www.ncbi.nlm.nih.gov/pubmed/8856711>
- Mazaheri, A., & Picton, T. W. (2005). EEG spectral dynamics during discrimination of auditory and visual targets. *Brain Research. Cognitive Brain Research*, *24*, 81–96. <http://doi.org/10.1016/j.cogbrainres.2004.12.013>
- McEvoy, L. K., Pellouchoud, E., Smith, M. E., & Gevins, A. (2001). Neurophysiological signals of working memory in normal aging. *Brain Research. Cognitive Brain Research*, *11*, 363–76. Retrieved from <http://www.ncbi.nlm.nih.gov/pubmed/11339986>
- Micoulaud-Franchi, J.-A., Lopez, R., Vaillant, F., Richieri, R., El-Kaim, A., Bioulac, S., ... Lancon, C. (2015). Perceptual abnormalities related to sensory gating deficit are core symptoms in adults with ADHD. *Psychiatry Research*, *230*, 357–63.

<http://doi.org/10.1016/j.psychres.2015.09.016>

Morlet, D., & Fischer, C. (2014). MMN and novelty P3 in coma and other altered states of consciousness: A review. *Brain Topography*, 27, 467–479.

<http://doi.org/10.1007/s10548-013-0335-5>

Näätänen, R., Jacobsen, T., & Winkler, I. (2005). Memory-based or afferent processes in mismatch negativity (MMN): a review of the evidence. *Psychophysiology*, 42, 25–32. <http://doi.org/10.1111/j.1469-8986.2005.00256.x>

Nader, D. A., & Sanchez, Z. M. (2018). Effects of regular cannabis use on neurocognition, brain structure, and function: a systematic review of findings in adults. *The American Journal of Drug and Alcohol Abuse*, 44, 4–18.

<http://doi.org/10.1080/00952990.2017.1306746>

Nagai, T., Tada, M., Kirihara, K., Araki, T., Jinde, S., & Kasai, K. (2013). Mismatch negativity as a “translatable” brain marker toward early intervention for psychosis: a review. *Frontiers in Psychiatry*, 4, 115. <http://doi.org/10.3389/fpsy.2013.00115>

Niessing, J., Ebisch, B., Schmidt, K. E., Niessing, M., Singer, W., & Galuske, R. A. W. (2005). Hemodynamic signals correlate tightly with synchronized gamma oscillations. *Science*, 309, 948–51. <http://doi.org/10.1126/science.1110948>

Nuechterlein, K.H., Green, M.F. (2006). MATRICS Consensus Cognitive Battery. Los Angeles, MATRICS Assessment, Inc.

O’Donnell, B. F., & Mackie, K. (2014). The mismatch negativity: a translational probe of auditory processing in cannabis users. *Biological Psychiatry*, 75, 428–9.

<http://doi.org/10.1016/j.biopsych.2014.01.015>

Obleser, J., Wöstmann, M., Hellbernd, N., Wilsch, A., & Maess, B. (2012). Adverse

Listening Conditions and Memory Load Drive a Common Alpha Oscillatory Network. *The Journal of Neuroscience*, 32, 12376-12383. Retrieved from <http://www.jneurosci.org/content/32/36/12376.abstract>

Onton, J., Delorme, A., & Makeig, S. (2005). Frontal midline EEG dynamics during working memory. *NeuroImage*, 27, 341–356.  
<http://doi.org/10.1016/j.neuroimage.2005.04.014>

Owen, A. M., McMillan, K. M., Laird, A. R., & Bullmore, E. (2005). N-back working memory paradigm: a meta-analysis of normative functional neuroimaging studies. *Human Brain Mapping*, 25, 46–59. <http://doi.org/10.1002/hbm.20131>

Palomäki, J., Kivikangas, M., Alafuzoff, A., Hakala, T., & Krause, C. M. (2012). Brain oscillatory 4-35Hz EEG responses during an n-back task with complex visual stimuli. *Neuroscience Letters*, 516, 141–145.  
<http://doi.org/10.1016/j.neulet.2012.03.076>

Pasternak, T., & Greenlee, M. W. (2005). Working memory in primate sensory systems. *Nature Reviews. Neuroscience*, 6, 97–107. <http://doi.org/10.1038/nrn1603>

Patrick, G., Straumanis, J. J., Struve, F. A., Nixon, F., Fitz-Gerald, M. J., Manno, J. E., & Soucair, M. (1995). Auditory and visual P300 event related potentials are not altered in medically and psychiatrically normal chronic marijuana users. *Life Sciences*, 56, 2135–40. Retrieved from <http://www.ncbi.nlm.nih.gov/pubmed/7776842>

Poldrack, R. A. (2006). Can cognitive processes be inferred from neuroimaging data? *Trends in Cognitive Sciences*, 10, 59–63. <http://doi.org/10.1016/j.tics.2005.12.004>

Polich, J. (2003). Detection of Change Event-Related Potential and fMRI Findings. *Detection of Change Event-Related Potential and fMRI Findings*. Springer US.

- Polich, J. (2007). Updating P300: an integrative theory of P3a and P3b. *Clinical Neurophysiology*, 118, 2128–48. <http://doi.org/10.1016/j.clinph.2007.04.019>
- Radhakrishnan, R., Wilkinson, S. T., & D'Souza, D. C. (2014). Gone to Pot - A Review of the Association between Cannabis and Psychosis. *Frontiers in Psychiatry*, 5, 54. <http://doi.org/10.3389/fpsyt.2014.00054>
- Raine, A., & Benishay, D. (1995). The SPQ-B: A Brief Screening Instrument for Schizotypal Personality Disorder. *Journal of Personality Disorders*, 9(4), 346–355. <http://doi.org/10.1521/pedi.1995.9.4.346>
- Ramaekers, J. G., Kauert, G., Theunissen, E. L., Toennes, S. W., & Moeller, M. R. (2009). Neurocognitive performance during acute THC intoxication in heavy and occasional cannabis users. *Journal of Psychopharmacology (Oxford, England)*, 23, 266–77. <http://doi.org/10.1177/0269881108092393>
- Rentsch, J., Buntebart, E., Stadelmeier, A., Gallinat, J., & Jockers-Scherübl, M. C. (2011). Differential effects of chronic cannabis use on preattentive cognitive functioning in abstinent schizophrenic patients and healthy subjects. *Schizophrenia Research*, 130, 222–7. <http://doi.org/10.1016/j.schres.2011.05.011>
- Rentsch, J., Penzhorn, A., Kernbichler, K., Plöckl, D., Castro, A. G. De, Gallinat, J., & Jockers-scherübl, M. C. (2007). Differential impact of heavy cannabis use on sensory gating in schizophrenic patients and otherwise healthy controls. *Experimental Neurology*, 205, 241–249. <http://doi.org/10.1016/j.expneurol.2007.02.004>
- Rogalsky, C., Pitz, E., Hillis, A. E., & Hickok, G. (2008). Auditory word comprehension impairment in acute stroke: relative contribution of phonemic versus semantic

factors. *Brain and Language*, 107, 167–9.

<http://doi.org/10.1016/j.bandl.2008.08.003>

- Romanski, L. M., & Goldman-Rakic, P. S. (2002). An auditory domain in primate prefrontal cortex. *Nature Neuroscience*, 5, 15–6. <http://doi.org/10.1038/nn781>
- Rosburg, T., Marinou, V., Haueisen, J., Smesny, S., & Sauer, H. (2004). Effects of lorazepam on the neuromagnetic mismatch negativity (MMNm) and auditory evoked field component N100m. *Neuropsychopharmacology*, 29, 1723–33. <http://doi.org/10.1038/sj.npp.1300477>
- Roser, P., Della, B., Norra, C., Uhl, I., Brüne, M., & Juckel, G. (2010). Auditory mismatch negativity deficits in long-term heavy cannabis users. *European Archives of Psychiatry and Clinical Neuroscience*, 260, 491–8. <http://doi.org/10.1007/s00406-010-0097-y>
- Roser, P., Juckel, G., Rentzsch, J., Nadulski, T., Gallinat, J., & Stadelmann, A. M. (2008). Effects of acute oral Delta9-tetrahydrocannabinol and standardized cannabis extract on the auditory P300 event-related potential in healthy volunteers. *European Neuropsychopharmacology*, 18, 569–77. <http://doi.org/10.1016/j.euroneuro.2008.04.008>
- Rottschy, C., Langner, R., Dogan, I., Reetz, K., Laird, A. R., Schulz, J. B., ... Eickhoff, S. B. (2012). Modelling neural correlates of working memory: a coordinate-based meta-analysis. *NeuroImage*, 60, 830–46. <http://doi.org/10.1016/j.neuroimage.2011.11.050>
- Roux, F., & Uhlhaas, P. J. (2014). Working memory and neural oscillations:  $\alpha$ - $\gamma$  versus  $\theta$ - $\gamma$  codes for distinct WM information? *Trends in Cognitive Sciences*, 18, 16–25.

<http://doi.org/10.1016/j.tics.2013.10.010>

Roux, F., Wibral, M., Mohr, H. M., Singer, W., & Uhlhaas, P. J. (2012). Gamma-band activity in human prefrontal cortex codes for the number of relevant items maintained in working memory. *The Journal of Neuroscience : The Official Journal of the Society for Neuroscience*, *32*, 12411–20.

<http://doi.org/10.1523/JNEUROSCI.0421-12.2012>

Ryttilä-Manninen, M., Fröjd, S., Haravuori, H., Lindberg, N., Marttunen, M., Kettunen, K., & Therman, S. (2016). Psychometric properties of the Symptom Checklist-90 in adolescent psychiatric inpatients and age- and gender-matched community youth. *Child and Adolescent Psychiatry and Mental Health*, *10*, 23.

<http://doi.org/10.1186/s13034-016-0111-x>

Sánchez-Blázquez, P., Rodríguez-Muñoz, M., & Garzón, J. (2014). The cannabinoid receptor 1 associates with NMDA receptors to produce glutamatergic hypofunction: implications in psychosis and schizophrenia. *Frontiers in Pharmacology*, *4*, 169.

<http://doi.org/10.3389/fphar.2013.00169>

Sauseng, P., & Klimesch, W. (2008). What does phase information of oscillatory brain activity tell us about cognitive processes? *Neuroscience and Biobehavioral Reviews*, *32*, 1001–13. <http://doi.org/10.1016/j.neubiorev.2008.03.014>

Scharinger, C., Soutschek, A., Schubert, T., & Gerjets, P. (2017). Comparison of the Working Memory Load in N-Back and Working Memory Span Tasks by Means of EEG Frequency Band Power and P300 Amplitude. *Frontiers in Human Neuroscience*, *11*, 6. <http://doi.org/10.3389/fnhum.2017.00006>

Scherg, M. (1990). Fundamentals of dipole source potential analysis. In *Auditory evoked*

- magnetic fields and electric potentials, Advances in audiology* (Vol. 6, pp. 40–69).
- Schoenberg, M. R., Duff, K., Scott, J. G., & Adams, R. L. (2003). An evaluation of the clinical utility of the OPIE-3 as an estimate of premorbid WAIS-III FSIQ. *The Clinical Neuropsychologist*, *17*, 308–21. <http://doi.org/10.1076/clin.17.3.308.18088>
- Skosnik, P. D., Park, S., Dobbs, L., & Gardner, W. L. (2008). Affect processing and positive syndrome schizotypy in cannabis users. *Psychiatry Research*, *157*, 279–82. <http://doi.org/10.1016/j.psychres.2007.02.010>
- Sneider, J. T., Pope, H. G., Silveri, M. M., Simpson, N. S., Gruber, S. A., & Yurgelun-Todd, D. A. (2008). Differences in regional blood volume during a 28-day period of abstinence in chronic cannabis smokers. *European Neuropsychopharmacology : The Journal of the European College of Neuropsychopharmacology*, *18*, 612–9. <http://doi.org/10.1016/j.euroneuro.2008.04.016>
- Solowij, N., Michie, P. T., & Fox, A. M. (1991). Effects of long-term cannabis use on selective attention: an event-related potential study. *Pharmacology, Biochemistry, and Behavior*, *40*, 683–8. Retrieved from <http://www.ncbi.nlm.nih.gov/pubmed/1806953>
- Solowij, N., Michie, P. T., & Fox, A. M. (1995). Differential impairments of selective attention due to frequency and duration of cannabis use. *Biological Psychiatry*, *37*, 731–9. [http://doi.org/10.1016/0006-3223\(94\)00178-6](http://doi.org/10.1016/0006-3223(94)00178-6)
- Spinks, R., McKirgan, L. W., Arndt, S., Caspers, K., Yucuis, R., & Pfalzgraf, C. J. (2009). IQ estimate smackdown: comparing IQ proxy measures to the WAIS-III. *Journal of the International Neuropsychological Society*, *15*, 590–6. <http://doi.org/10.1017/S1355617709090766>

- Statistics Canada (2018). Table 35-10-0177-01: Incident-based crime statistics, by detailed violations. Retrieved from <https://www150.statcan.gc.ca/t1/tbl1/en/tv.action?pid=3510017701&pickMembers%5B0%5D=1.37&pickMembers%5B1%5D=2.17> 6, Aug19, 2018.
- Steiner, G. Z., Barry, R. J., & Gonsalvez, C. J. (2013). Can working memory predict target-to-target interval effects in the P300? *International Journal of Psychophysiology*, *89*, 399–408. <http://doi.org/10.1016/j.ijpsycho.2013.07.011>
- Stone, J. V. (2002). Independent component analysis: an introduction. *Trends in Cognitive Sciences*, *6*, 59–64. Retrieved from <http://www.ncbi.nlm.nih.gov/pubmed/15866182>
- Sussman, E. S. (2007). A New View on the MMN and Attention Debate: The Role of Context in Processing Auditory Events. *Journal of Psychophysiology*, *21*, 164–175. <http://doi.org/10.1027/0269-8803.21.3.xxx>
- Sussman, E. S., Chen, S., Sussman-Fort, J., & Dinces, E. (2014). The Five Myths of MMN: Redefining How to Use MMN in Basic and Clinical Research. *Brain Topography*, *27*, 553–564. <http://doi.org/10.1007/s10548-013-0326-6>
- Sussman, E. S., & Shafer, V. L. (2014). New perspectives on the mismatch negativity (MMN) component: an evolving tool in cognitive neuroscience. *Brain Topography*, *27*, 425–7. <http://doi.org/10.1007/s10548-014-0381-7>
- Sutherland, M. T., Ross, T. J., Shakleya, D. M., Huestis, M. A., & Stein, E. A. (2011). Chronic smoking, but not acute nicotine administration, modulates neural correlates of working memory. *Psychopharmacology*, *213*, 29–42. <http://doi.org/10.1007/s00213-010-2013-6>

- Thames, A. D., Arbid, N., & Sayegh, P. (2014). Cannabis use and neurocognitive functioning in a non-clinical sample of users. *Addictive Behaviors, 39*, 994–9. <http://doi.org/10.1016/j.addbeh.2014.01.019>
- Theunissen, E. L., Kauert, G. F., Toennes, S. W., Moeller, M. R., Sambeth, A., Blanchard, M. M., & Ramaekers, J. G. (2012). Neurophysiological functioning of occasional and heavy cannabis users during THC intoxication. *Psychopharmacology, 220*, 341–350. <http://doi.org/10.1007/s00213-011-2479-x>
- Todd, J., Whitson, L., Smith, E., Michie, P. T., Schall, U., & Ward, P. B. (2014). What's intact and what's not within the mismatch negativity system in schizophrenia. *Psychophysiology, 51*, 337–47. <http://doi.org/10.1111/psyp.12181>
- Tuladhar, A. M., ter Huurne, N., Schoffelen, J.-M., Maris, E., Oostenveld, R., & Jensen, O. (2007). Parieto-occipital sources account for the increase in alpha activity with working memory load. *Human Brain Mapping, 28*, 785–92. <http://doi.org/10.1002/hbm.20306>
- Uhlhaas, P. J. (2013). Dysconnectivity, large-scale networks and neuronal dynamics in schizophrenia. *Current Opinion in Neurobiology, 23*, 283–90. <http://doi.org/10.1016/j.conb.2012.11.004>
- van Dijk, H., Nieuwenhuis, I. L. C., & Jensen, O. (2010). Left temporal alpha band activity increases during working memory retention of pitches. *The European Journal of Neuroscience, 31*, 1701–7. <http://doi.org/10.1111/j.1460-9568.2010.07227.x>
- Varela, F., Lachaux, J. P., Rodriguez, E., & Martinerie, J. (2001). The brainweb: phase synchronization and large-scale integration. *Nature Reviews. Neuroscience, 2*, 229–

39. <http://doi.org/10.1038/35067550>

- Viola, F. C., Thorne, J., Edmonds, B., Schneider, T., Eichele, T., & Debener, S. (2009). Semi-automatic identification of independent components representing EEG artifact. *Clinical Neurophysiology*, *120*, 868–77. <http://doi.org/10.1016/j.clinph.2009.01.015>
- von Stein, A., & Sarnthein, J. (2000). Different frequencies for different scales of cortical integration: from local gamma to long range alpha/theta synchronization. *International Journal of Psychophysiology*, *38*, 301–13. Retrieved from <http://www.ncbi.nlm.nih.gov/pubmed/11102669>
- Wacongne, C., Labyt, E., van Wassenhove, V., Bekinschtein, T., Naccache, L., & Dehaene, S. (2011). Evidence for a hierarchy of predictions and prediction errors in human cortex. *Proceedings of the National Academy of Sciences of the United States of America*, *108*, 20754–9. <http://doi.org/10.1073/pnas.1117807108>
- Watter, S., Geffen, G. M., & Geffen, L. B. (2001). The n-back as a dual-task: P300 morphology under divided attention. *Psychophysiology*, *38*, 998–1003. <http://doi.org/10.1111/1469-8986.3860998>
- Wechsler, D. (1997). Wechsler Adult Intelligence Scale—3rd ed (WAIS-III): Administration and Scoring Manual. San Antonio, Tex, Psychological Corp.
- Winkler, I., Karmos, G., & Näätänen, R. (1996). Adaptive modeling of the unattended acoustic environment reflected in the mismatch negativity event-related potential. *Brain Research*, *742*, 239–52. Retrieved from <http://www.ncbi.nlm.nih.gov/pubmed/9117400>
- Wong, D., Pisoni, D. B., Learn, J., Gandour, J. T., Miyamoto, R. T., & Hutchins, G. D. (2002). PET imaging of differential cortical activation by monaural speech and

nonspeech stimuli. *Hearing Research*, 166, 9–23. Retrieved from  
<http://www.ncbi.nlm.nih.gov/pubmed/12062754>

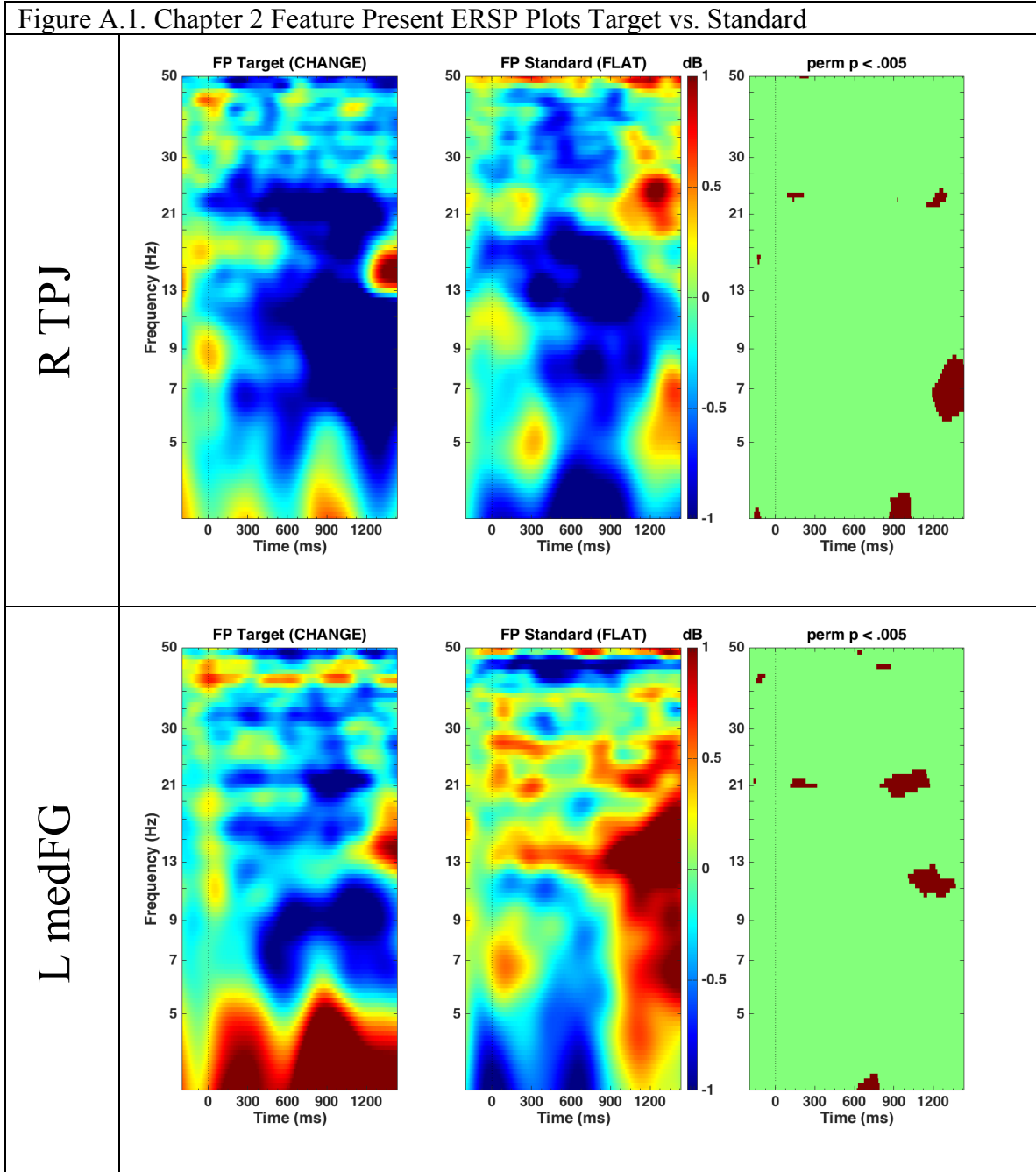
Wronka, E., Kaiser, J., & Coenen, A. M. L. (2012). Neural generators of the auditory evoked potential components P3a and P3b. *Acta Neurobiologiae Experimentalis*, 72, 51–64. Retrieved from <http://www.ncbi.nlm.nih.gov/pubmed/22508084>

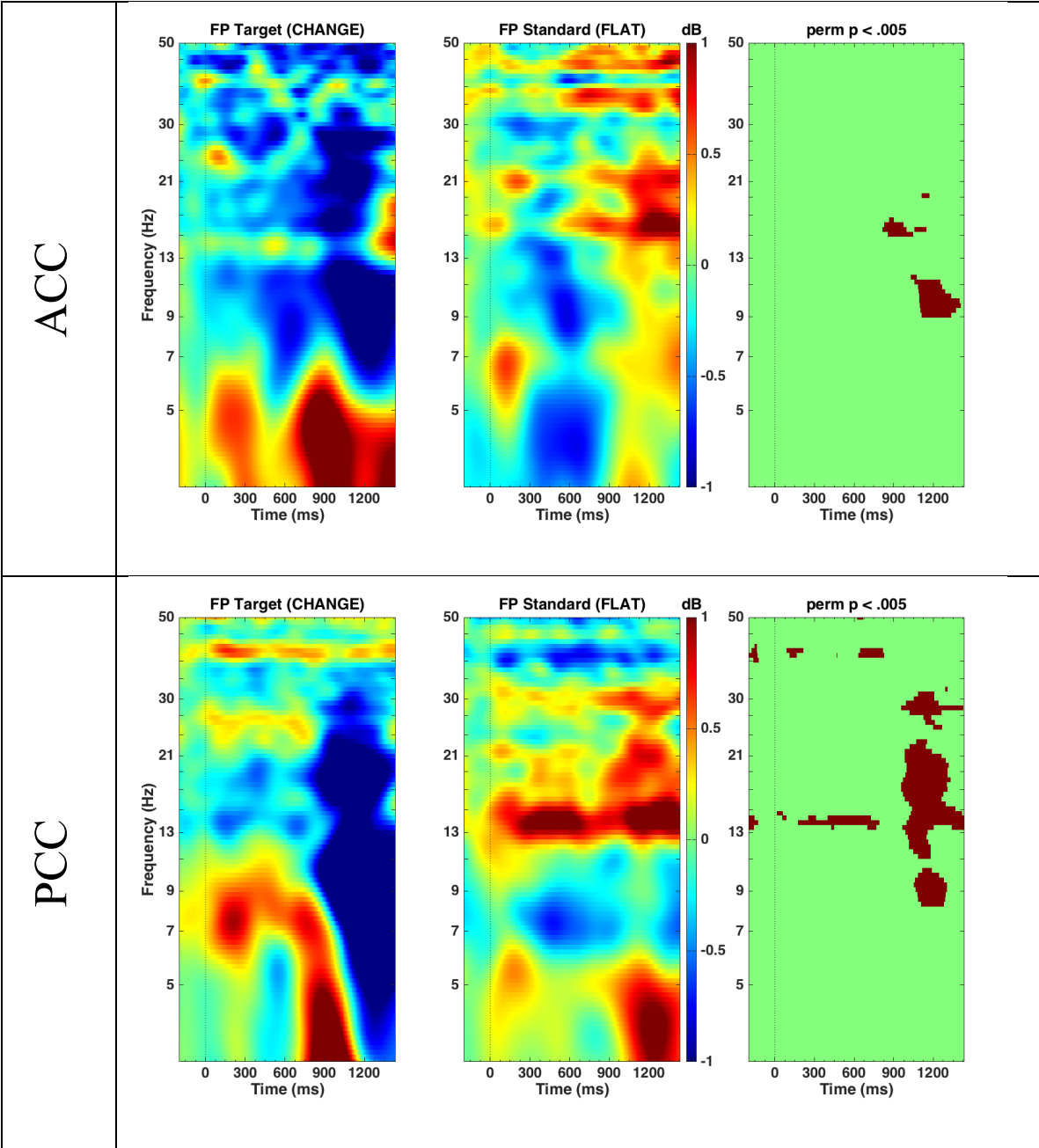
Xia, M., Wang, J., & He, Y. (2013). BrainNet Viewer: a network visualization tool for human brain connectomics. *PloS One*, 8, e68910.  
<http://doi.org/10.1371/journal.pone.0068910>

# Appendices

## Appendix A: Chapter 2 ERSPs for Each ROIs

Figure A.1. Chapter 2 Feature Present ERSP Plots Target vs. Standard





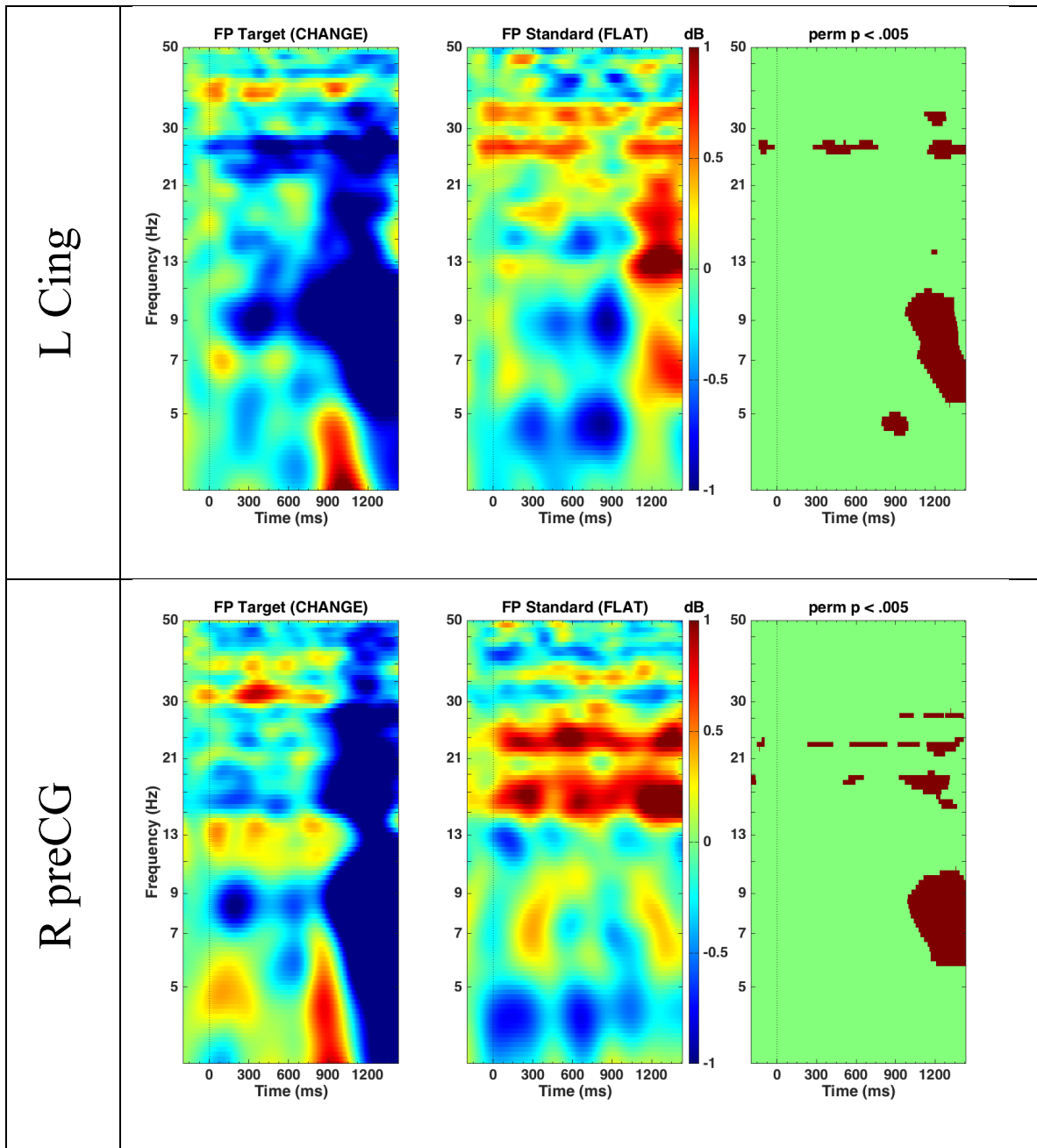
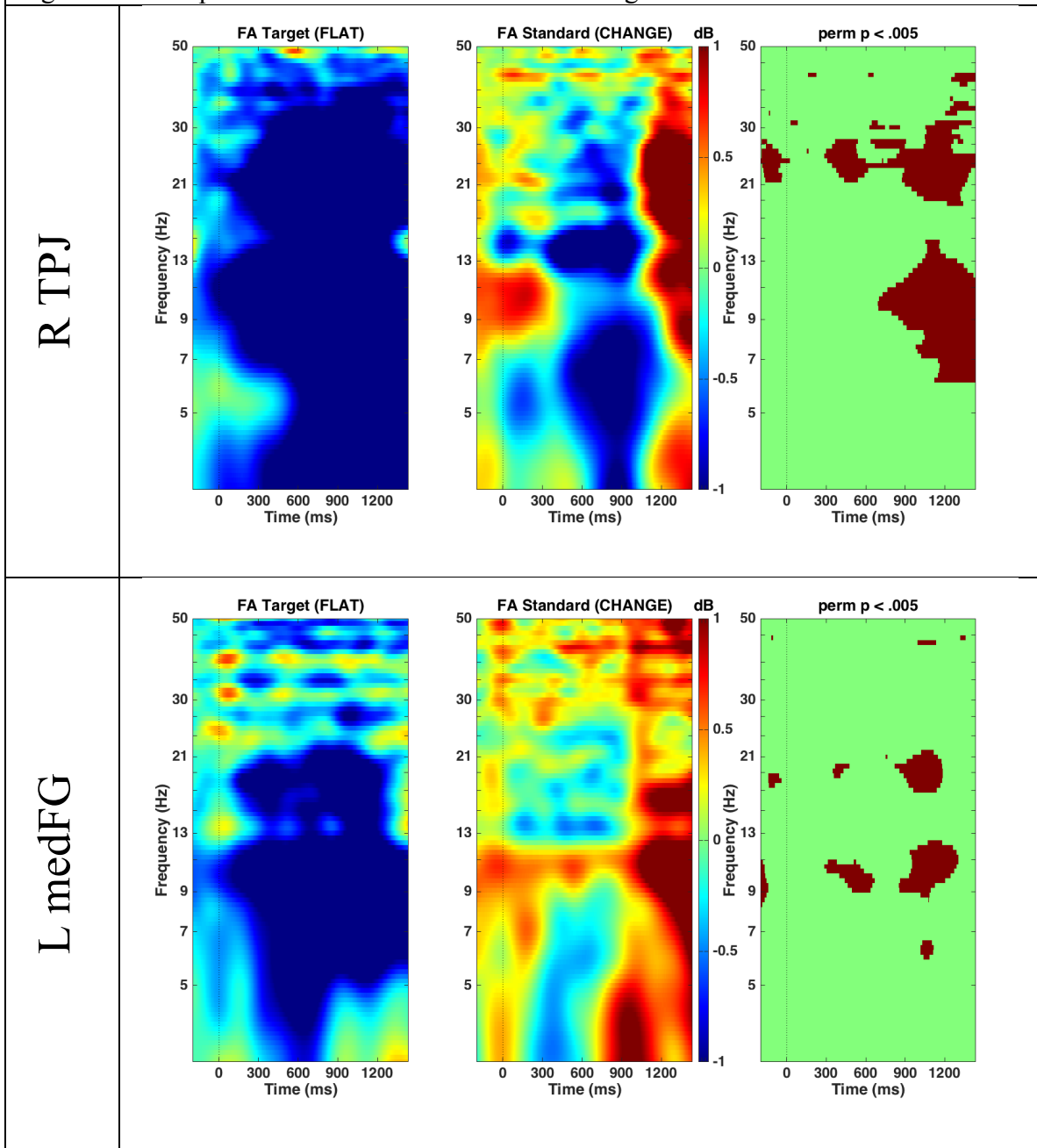
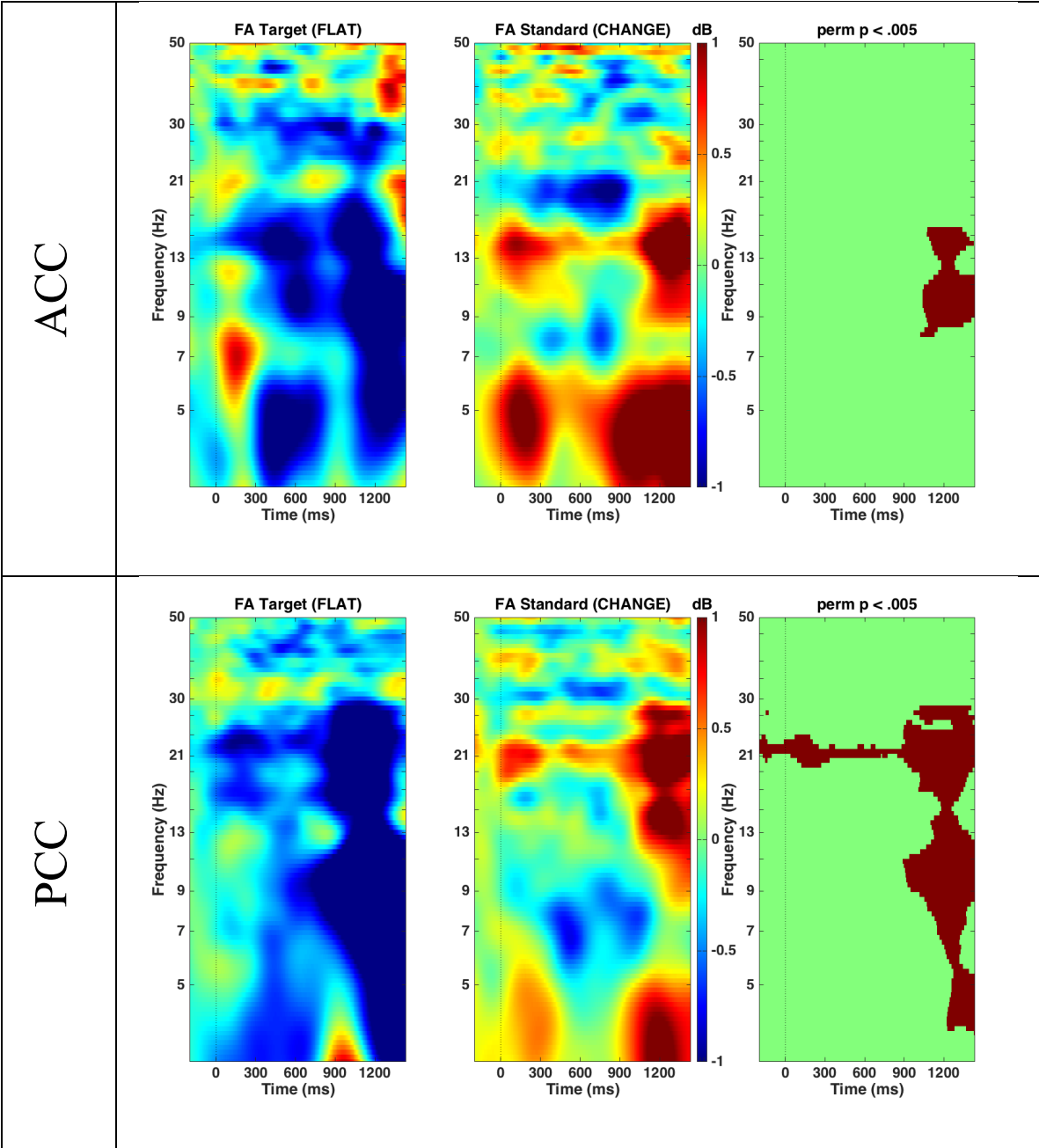


Figure A.1. ERSP (3-50Hz) plots from (-200-1400 ms; onset of 5<sup>th</sup> tone is 600 ms) for each ROI comparing targets and standards in the feature present (FP) condition using a common baseline. Plots are scaled from -1 (blue) to +1 (red) dB. Significance plots (right) represent pairwise comparisons computed using EEGLab permutation statistics ( $p = < .005$ ).

Figure A.2. Chapter 2 Feature Absent ERSP Plots Target vs. Standard





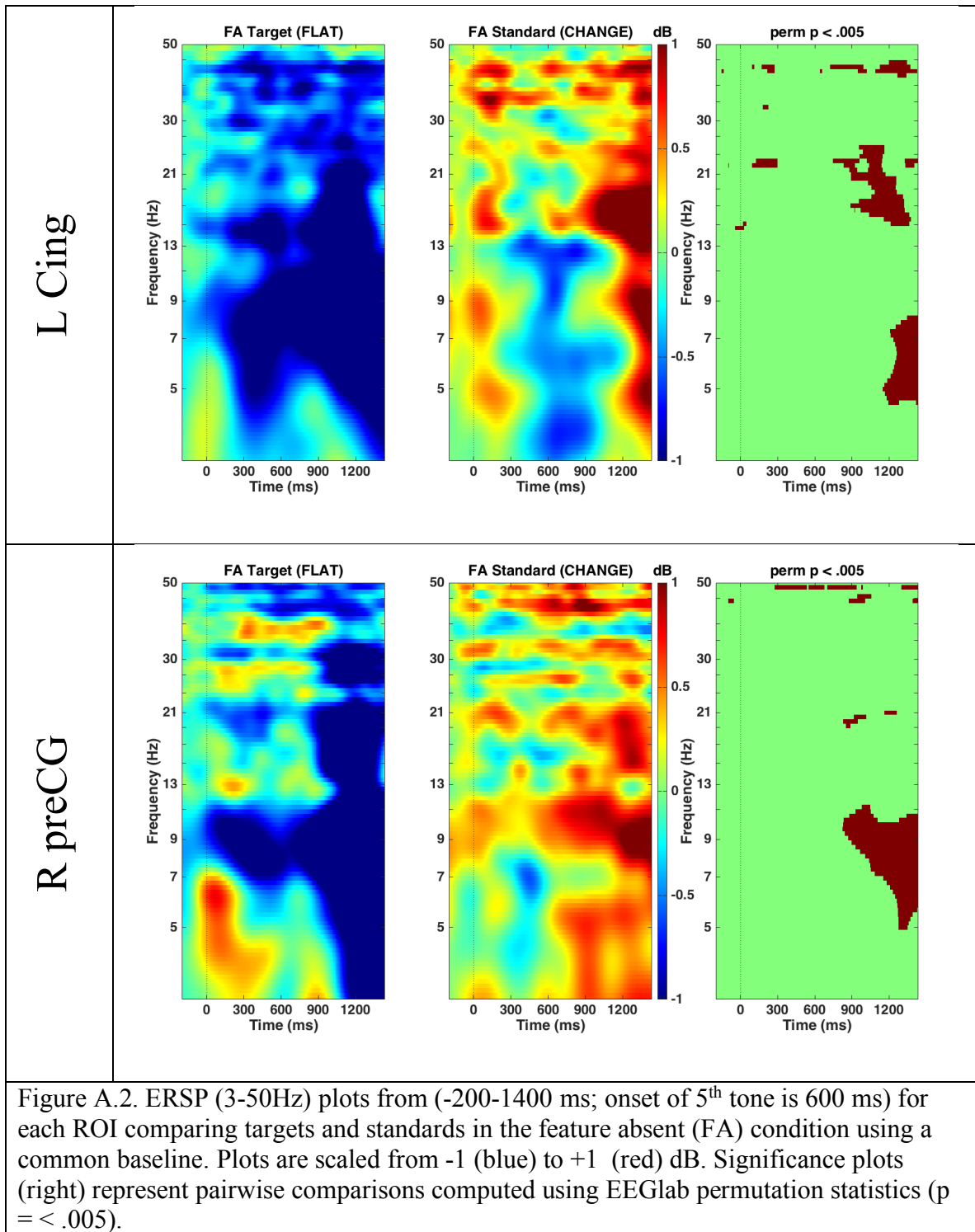
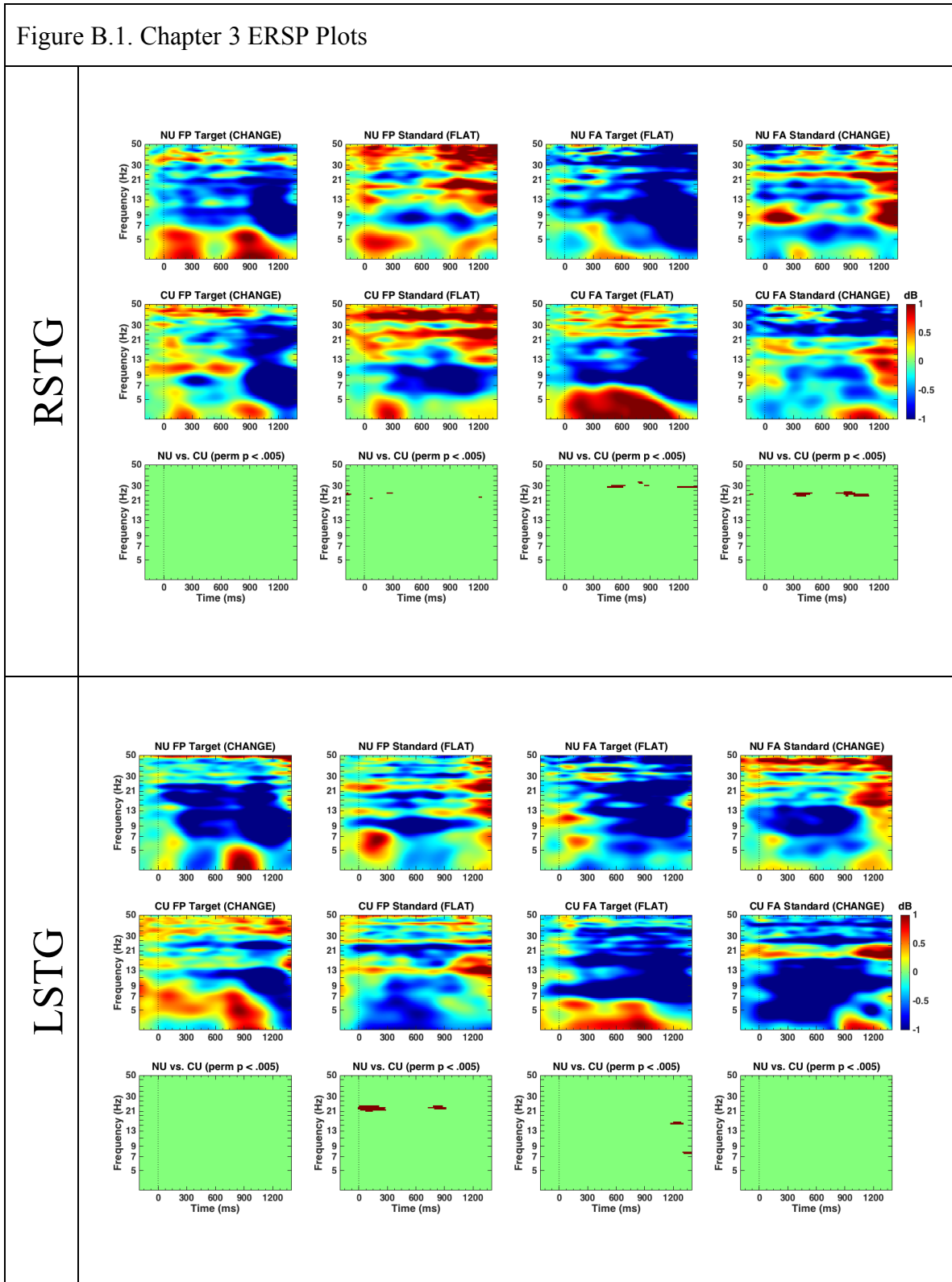


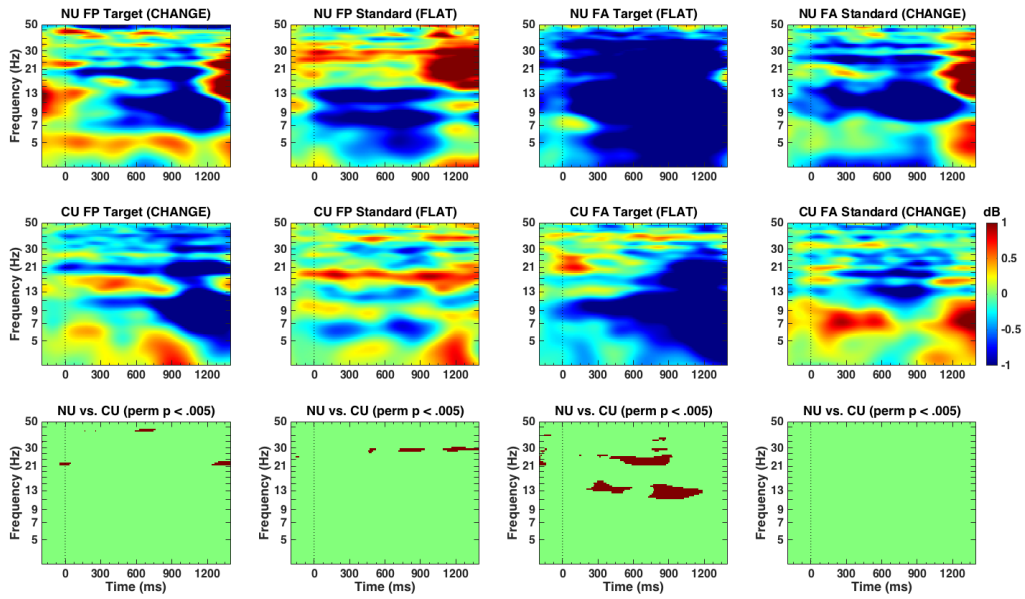
Figure A.2. ERSP (3-50Hz) plots from (-200-1400 ms; onset of 5<sup>th</sup> tone is 600 ms) for each ROI comparing targets and standards in the feature absent (FA) condition using a common baseline. Plots are scaled from -1 (blue) to +1 (red) dB. Significance plots (right) represent pairwise comparisons computed using EEGLab permutation statistics ( $p < .005$ ).

## Appendix B: Chapter 3 ERSP Figures

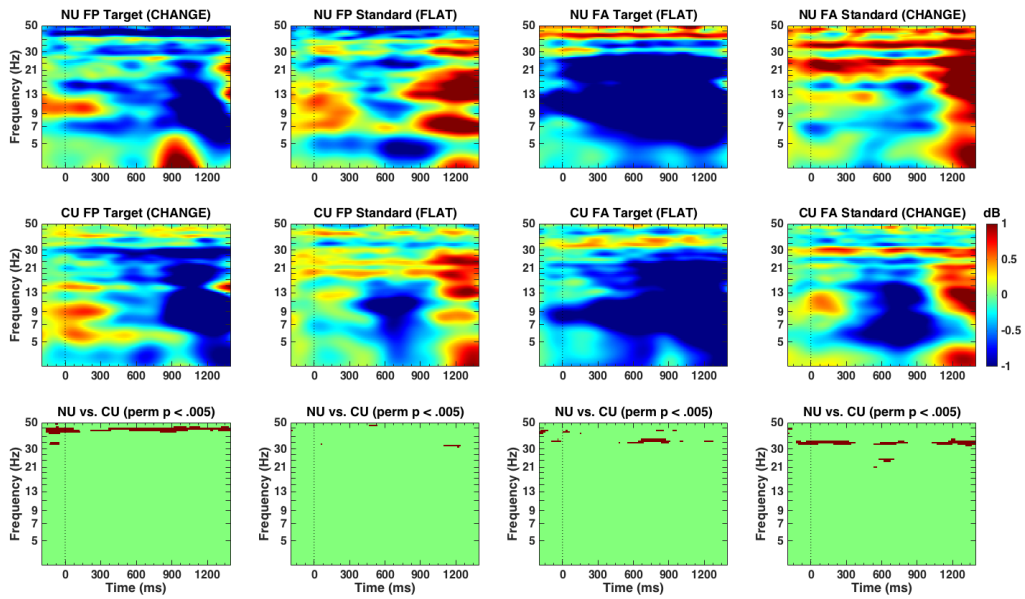
Figure B.1. Chapter 3 ERSP Plots



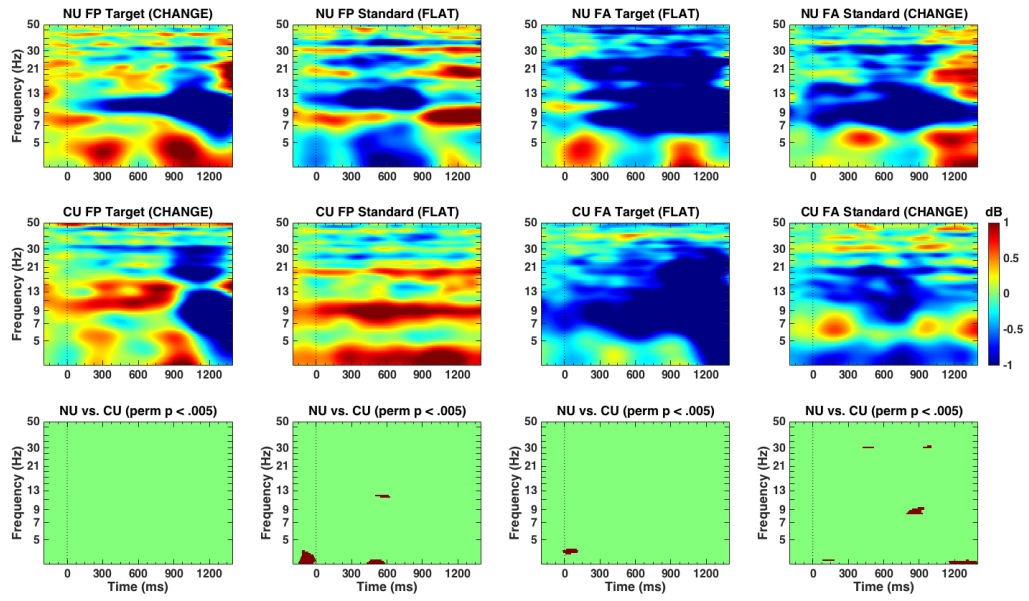
RTPJ



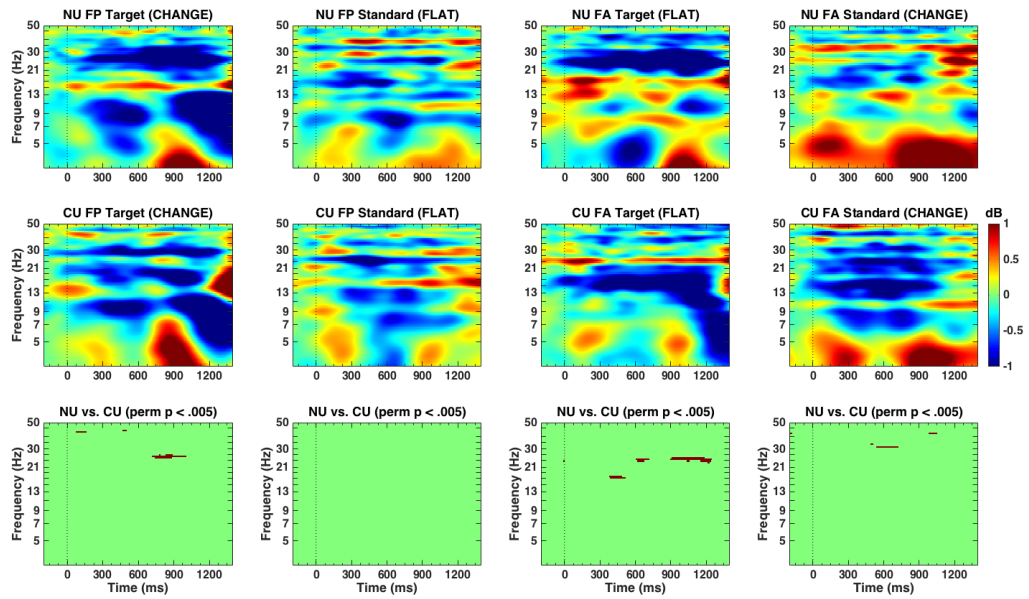
LTPJ



RPCC



LCING



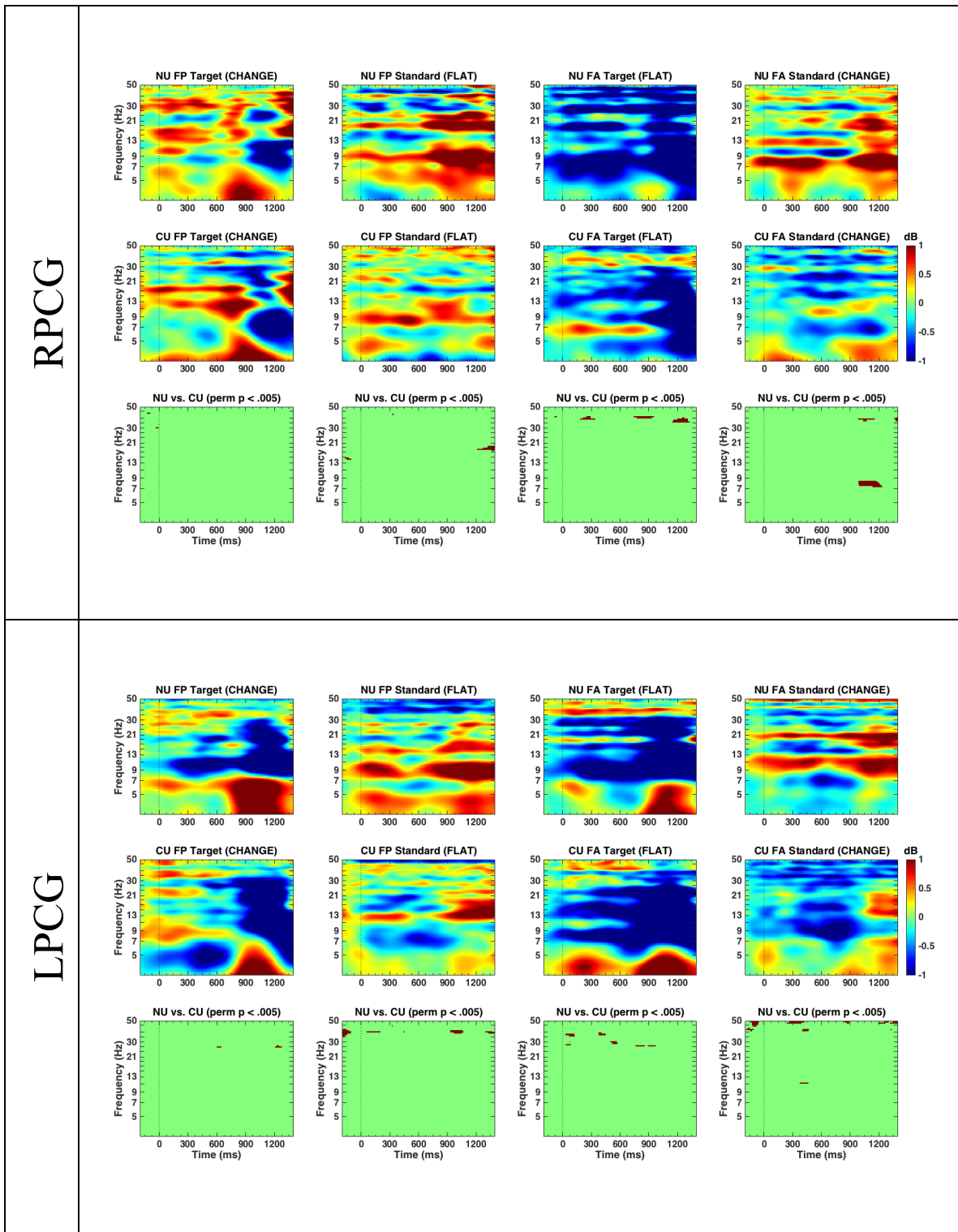
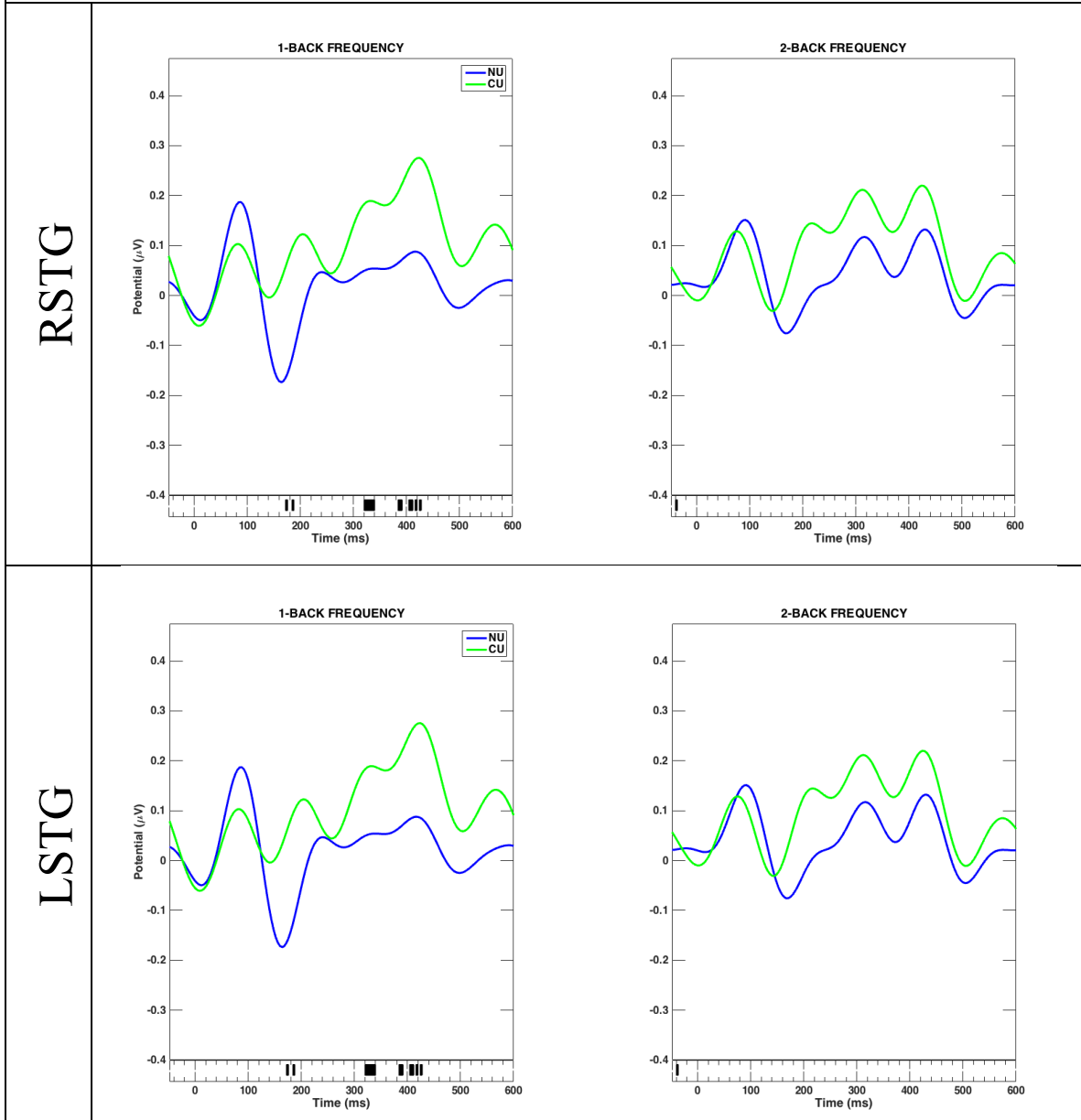
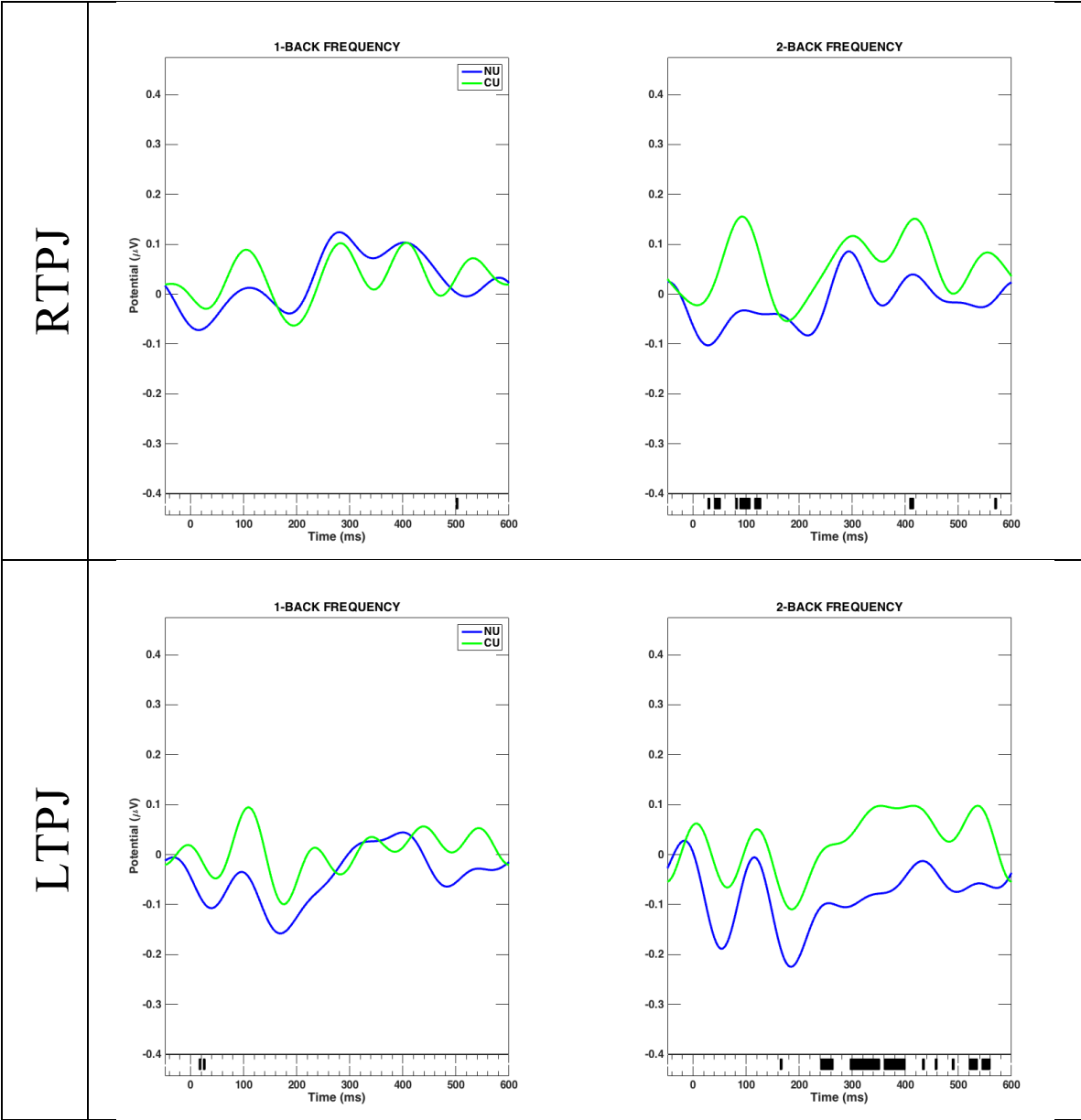


Figure B.1. ERSP (3-50Hz) plots from (-200-1400 ms; onset of 5<sup>th</sup> tone is 600 ms) for each ROI comparing non-users (NU; top) and cannabis users (CU; middle) for targets and standards in both the feature present (FP) and feature absent (FA) conditions. Plots are scaled from -1 (blue) to +1 (red) dB. Significance plots (bottom) represent pairwise comparisons computed using EEGLab permutation statistics ( $p < .005$ ).

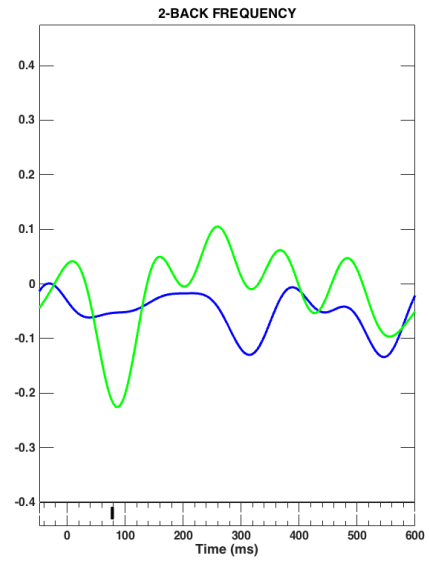
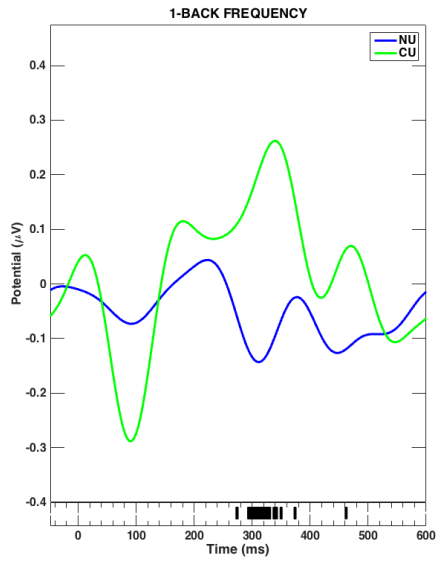
## Appendix C: Chapter 4 ROI ERPs

Figure C.1. ROI ERPS Comparing NU and CU for 1-Back and 2-Back Frequency Match  $n$ -back Task

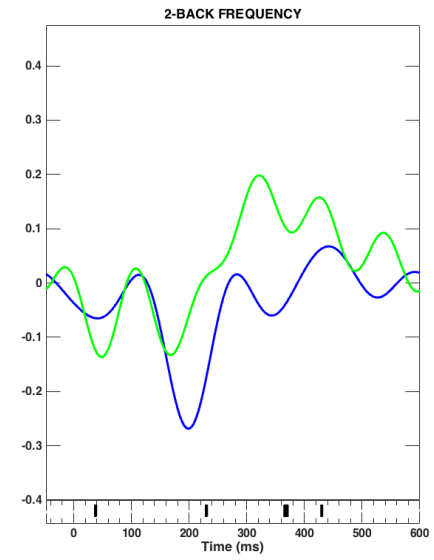
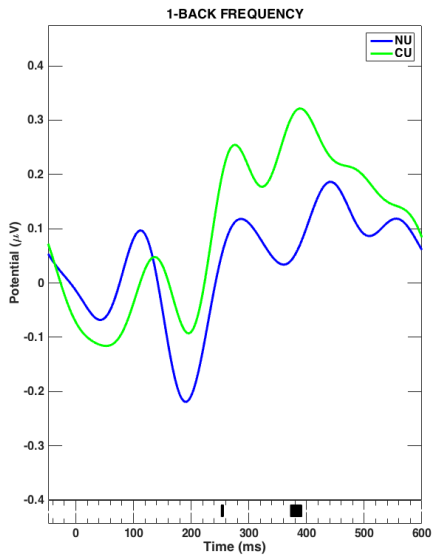


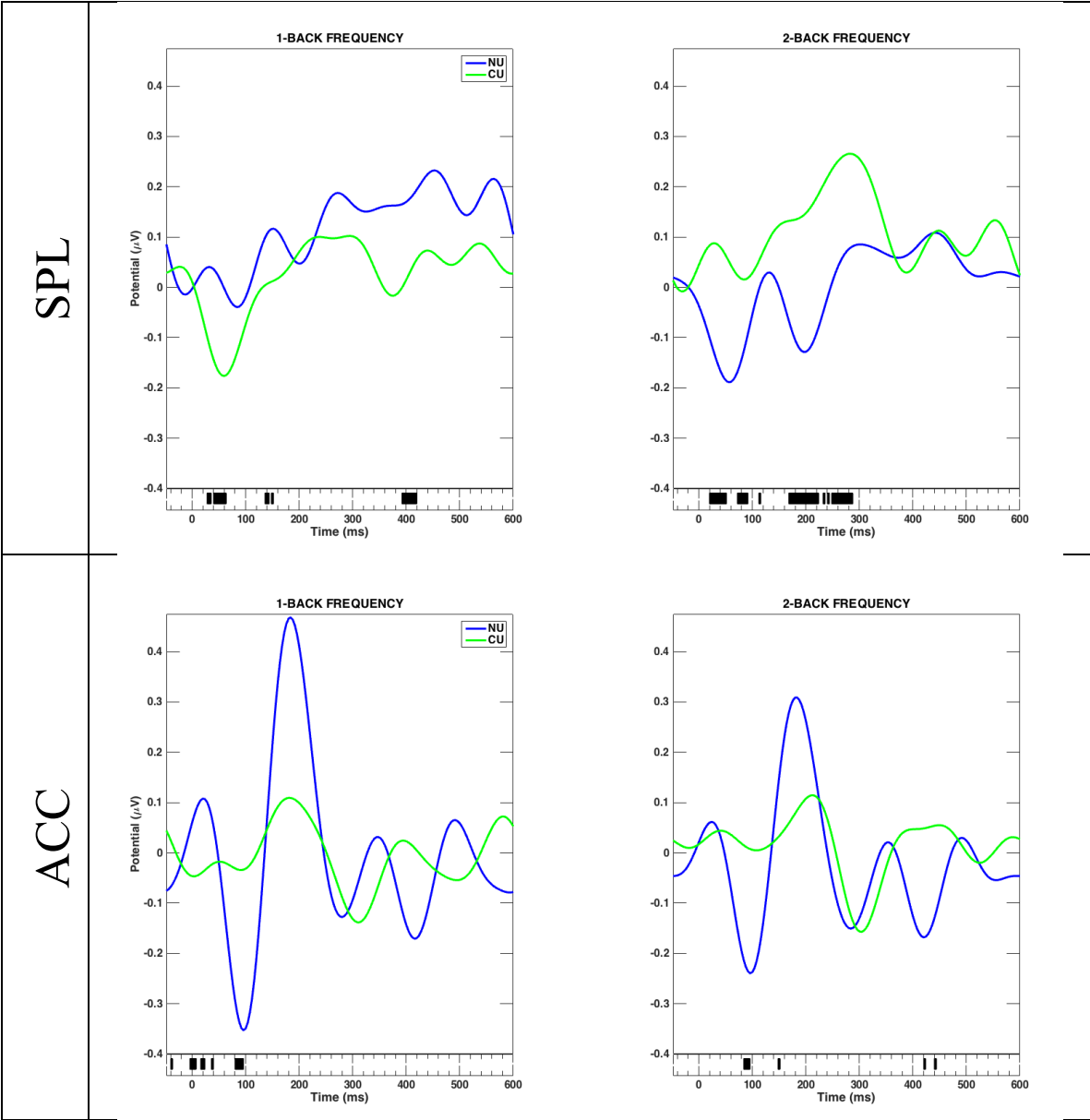


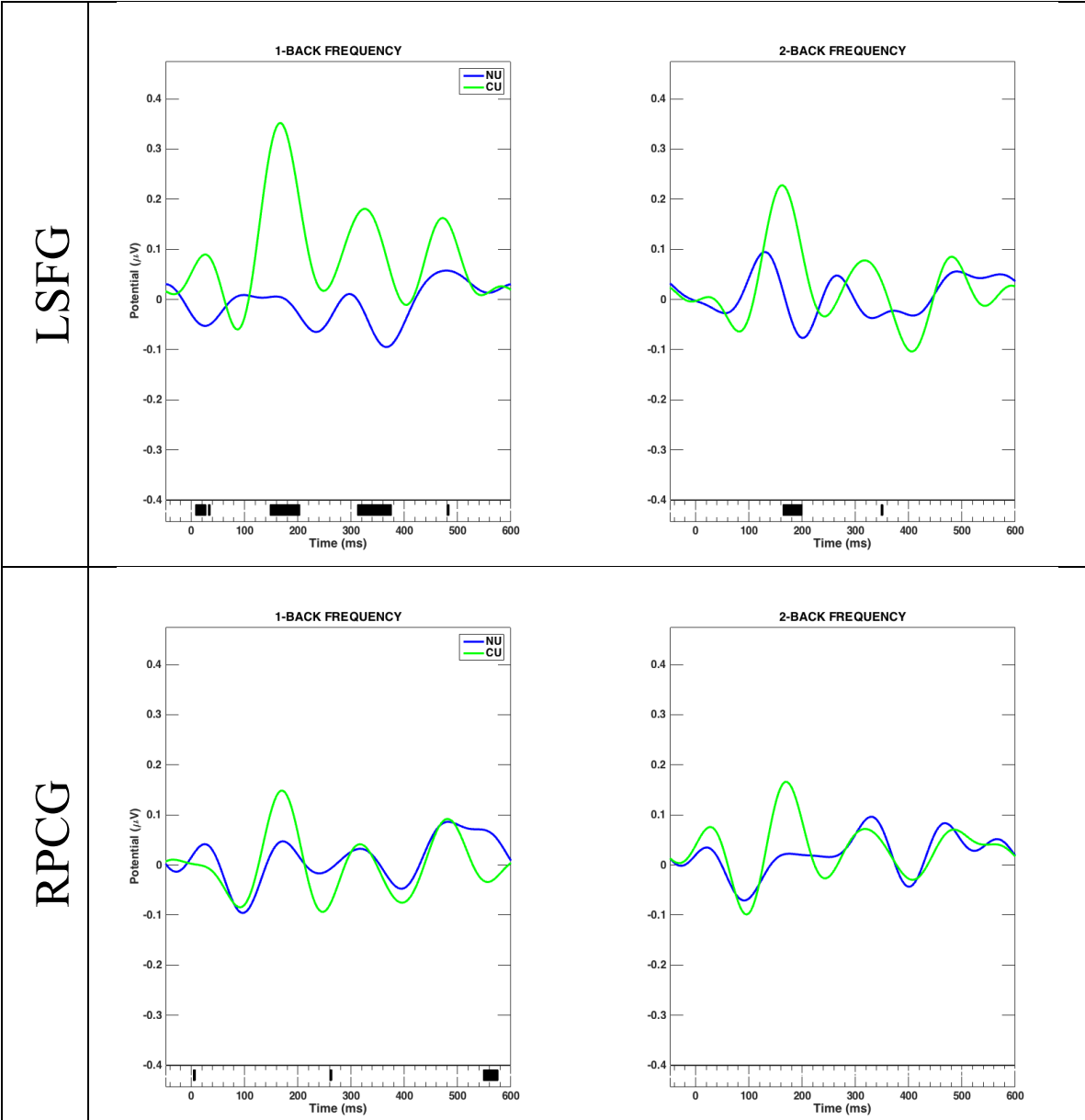
RPFC



PCC







# LPCG

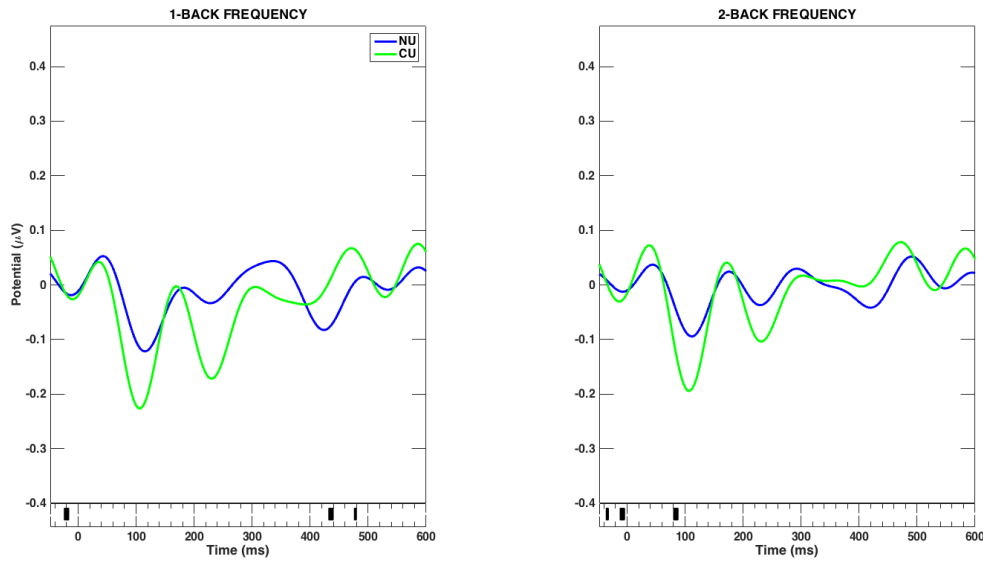
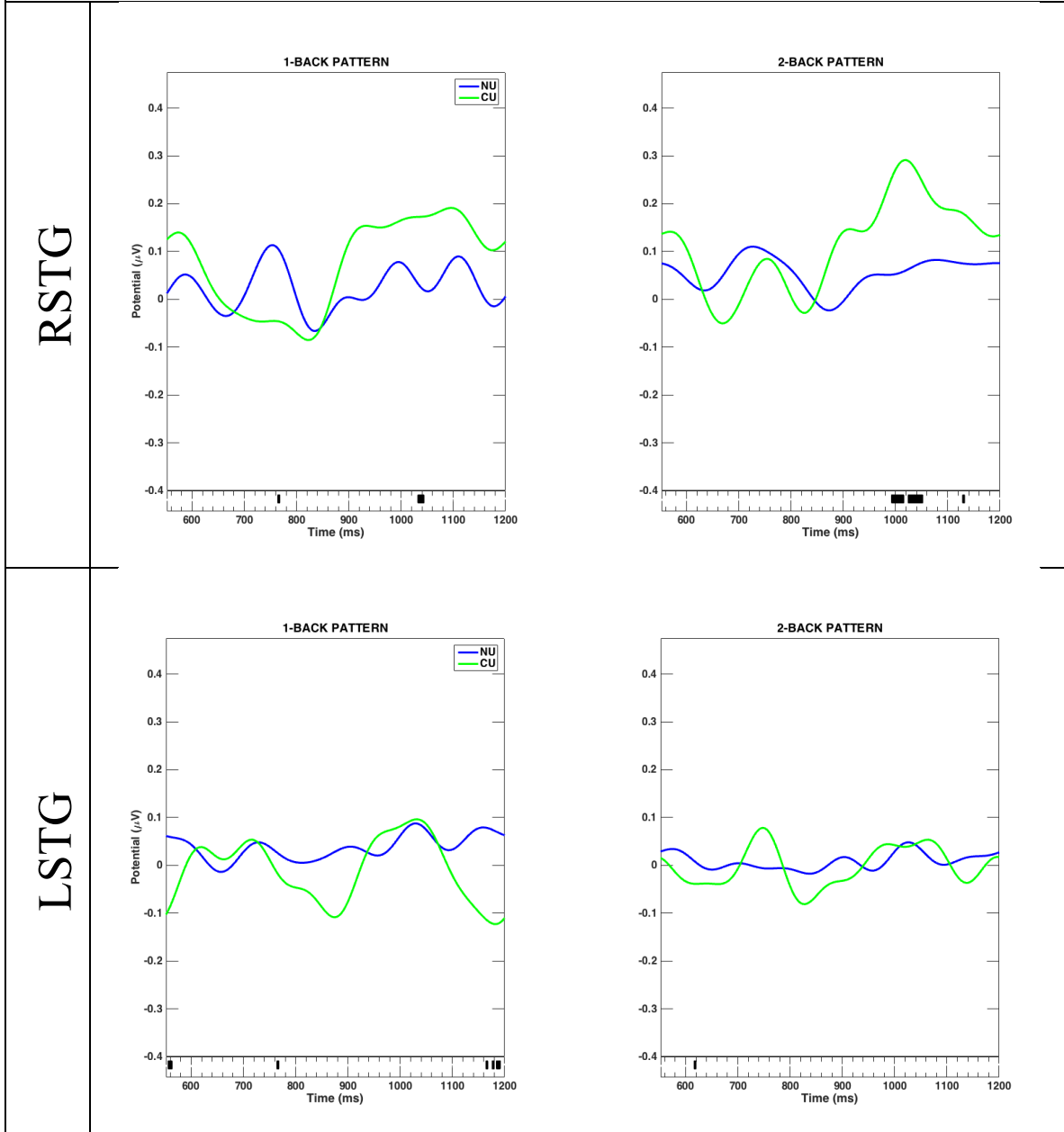
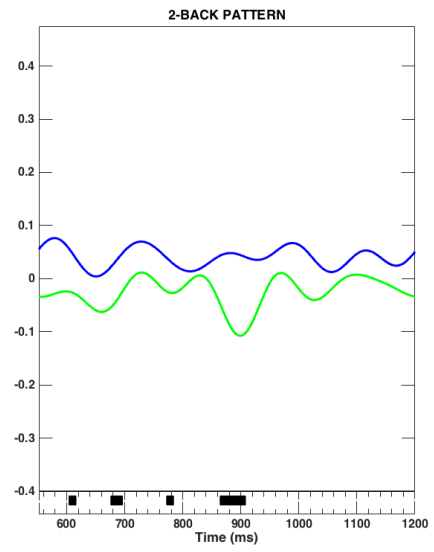
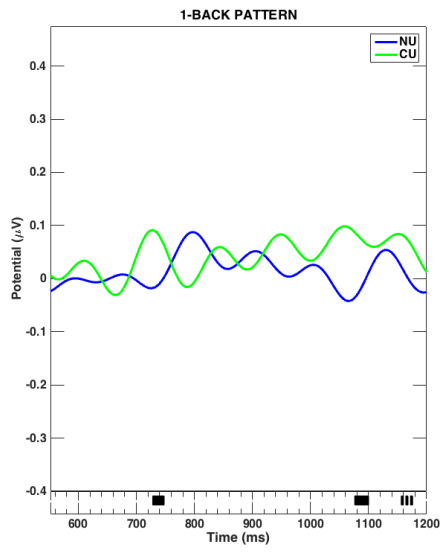


Figure C.1. ROI ERPs of IC activations from -50 to 600 ms comparing non-users (NU; blue) and cannabis users (CU; green) in the frequency match task under low (1-back; left) and high (2-back; right) memory load. Uncorrected pairwise significant group differences are indicated below each plot ( $p < .05$ ).

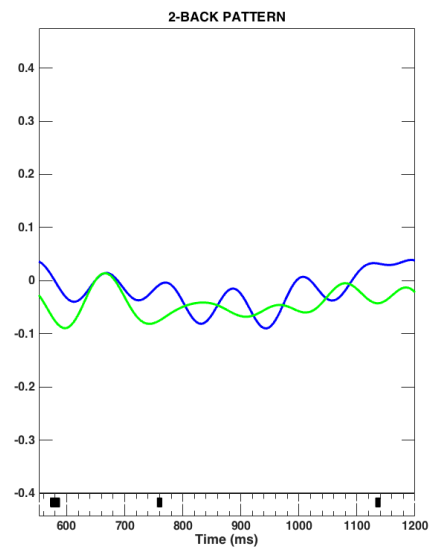
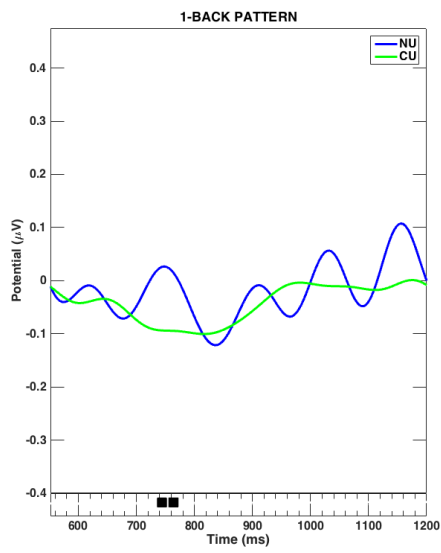
Figure C.2. ROI ERPs Comparing NU and CU for 1-Back and 2-Back Pattern Match  $n$ -back Task



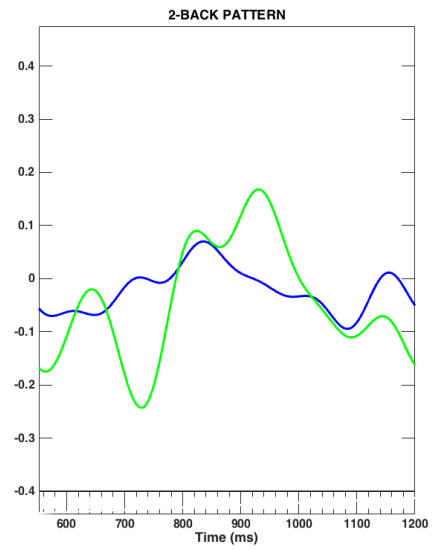
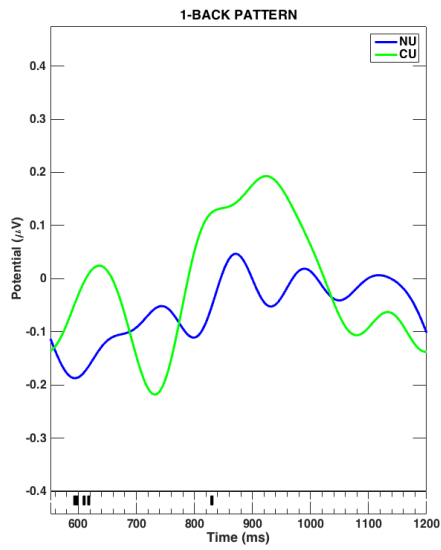
RTPJ



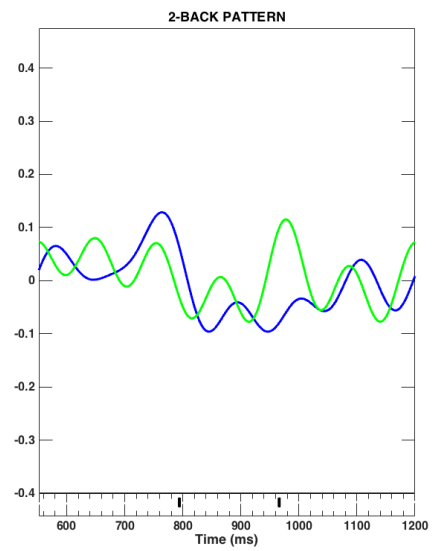
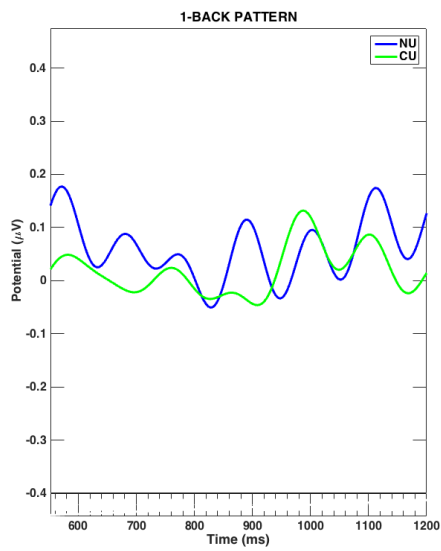
LTPJ

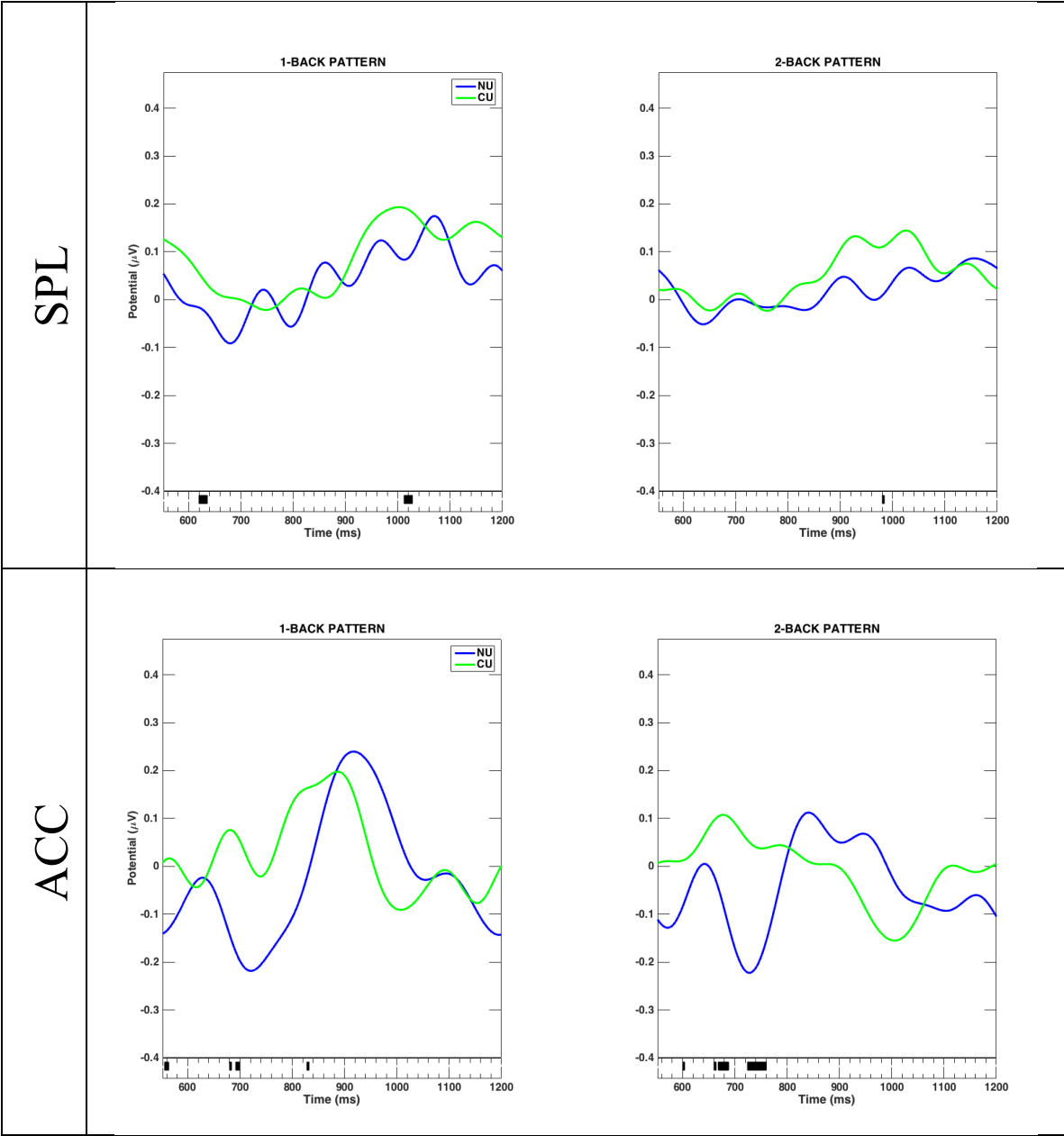


RPFC

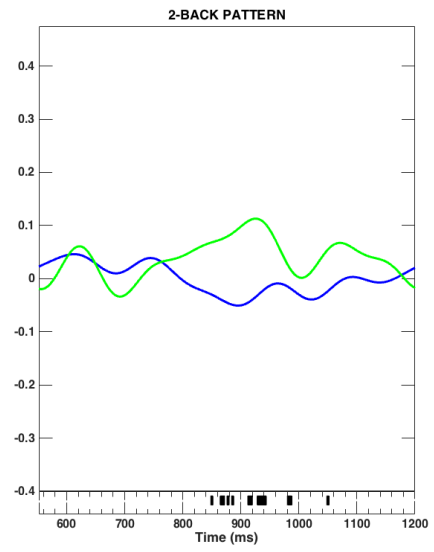
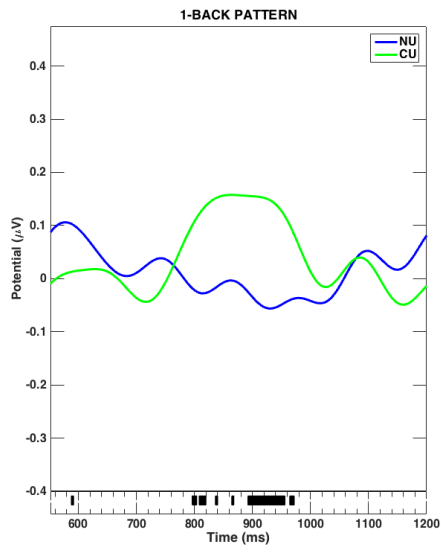


PCC

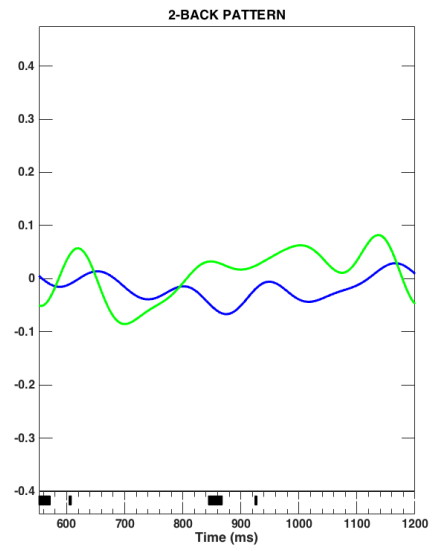
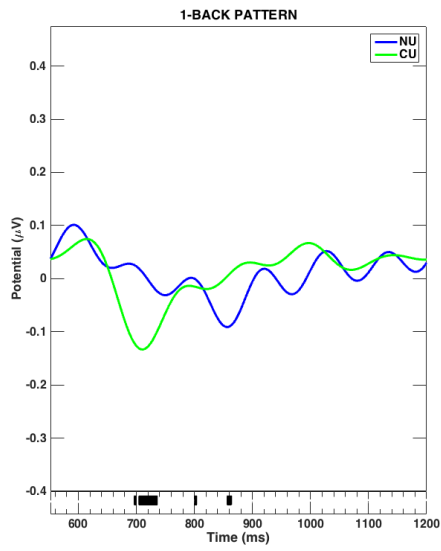




LSFG



RPCG



LPCG

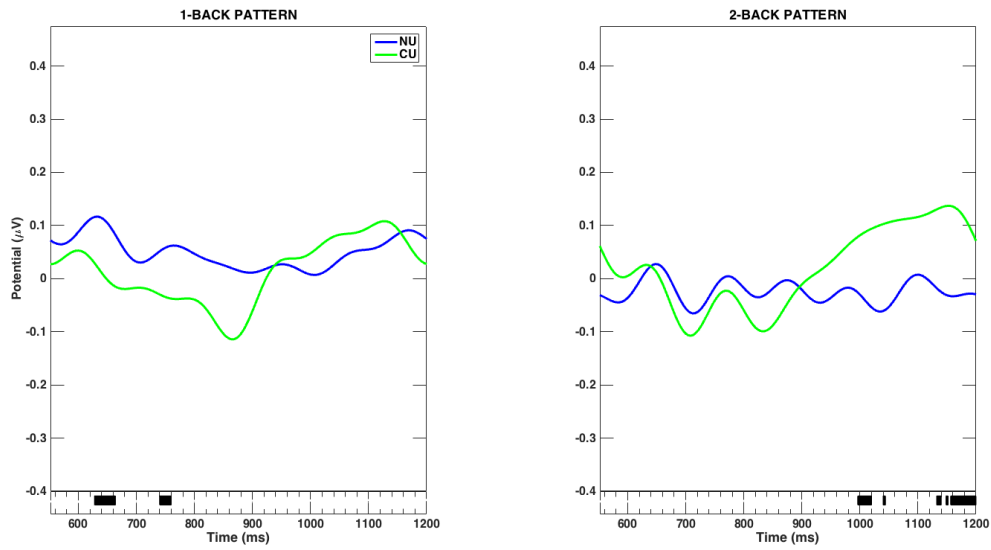


Figure C.2. ROI ERPs of IC activations from 550 to 1200 ms comparing non-users (NU; blue) and cannabis users (CU; green) in the pattern match task under low (1-back; left) and high (2-back; right) memory load. Uncorrected pairwise significant group differences are indicated below each plot ( $p < .05$ ).

## Appendix D: Chapter 5 Correlations

Table D.1. Chapter 5 Spearman Rank Correlations Between MMN and Neuropsychological Measures for Entire Sample (n=57) Across Both Studies

<b>Variables</b>	<b>1</b>	<b>2</b>	<b>3</b>	<b>4</b>	<b>5</b>	<b>6</b>	<b>7</b>	<b>8</b>	<b>9</b>
1. Amplitude <sup>a</sup>	-								
2. Latency <sup>a</sup>	-.078	-							
3. IQ <sup>b</sup>	-.232 <sup>†</sup>	-.088	-						
4. VC <sup>c</sup>	-.199	.116	.726 <sup>***</sup>	-					
5. MR <sup>c</sup>	-.118	-.173	.575 <sup>***</sup>	-.020	-				
6. LNS <sup>d</sup>	.028	.080	.277	.170	.236 <sup>†</sup>	-			
7. CPT-2d <sup>e</sup>	-.051	-.078	.277 <sup>*</sup>	.196	.148	-.033	-		
8. CPT-3d <sup>e</sup>	-.197	-.014	.329 <sup>*</sup>	.399 <sup>**</sup>	.130	.147	.364 <sup>**</sup>	-	
9. CPT-4d <sup>e</sup>	-.213	-.116	.479 <sup>***</sup>	.386 <sup>**</sup>	.276 <sup>*</sup>	.467 <sup>***</sup>	.331 <sup>*</sup>	.473 <sup>***</sup>	-

Table D.1. Spearman rank correlations ( $r_s$ ) between various neuropsychological measures and MMN variables at channel Fz for entire sample. a) Estimated Full-Scale IQ derived by using WAIS-III Matrix Reasoning (MR) and Vocabulary (VC) raw scores combined with demographics (age and education level) according to a regression algorithm (OPIE-3). b) VC, MR, and Letter Number Sequencing (LNS) scores are based upon raw scores derived from each test. c) Scores represent d-prime values for the 2-digit (2d), 3-digit (3d), and 4-digit (4-d) conditions generated automatically by the Continuous Performance Task - Identical Pairs (CPT-IP) software included in the MATRICS battery. \* < .05; \*\* < .01; \*\*\*<.001 and † represents trend significance < .10.